

Analysis of Microbial Diversity in an Extreme Environment: White Island, New Zealand

Raquel Ibáñez-Peral, MSc

A thesis presented to Macquarie University
in fulfilment of the requirements for the degree of
Doctor of Philosophy

Department of Chemistry and Biomolecular Sciences
Division of Environmental and Life Sciences
Macquarie University, Australia

June, 2008

Table of contents

Table of contents	I
Abstract	IX
Statement of candidate	XI
Acknowledgements	XIII
Abbreviations and symbols	XV
CHAPTER I. LITERATURE REVIEW	1
1. Microbial diversity	4
<i>1.1. Origin of early life</i>	4
<i>1.2. Extremophiles</i>	6
<i>1.3. Microbial consortia</i>	8
<i>1.4. Microbial metabolism</i>	8
<i>1.4.1. Sulphur cycling</i>	11
<i>1.4.2. Iron cycling</i>	12
2. Volcanic environments	12
<i>2.1. Geothermal and hydrothermal systems</i>	13
<i>2.2. White Island, New Zealand</i>	13
3. The study of microbial diversity	14
<i>3.1. Culture-independent techniques</i>	14
<i>3.2. Culture-dependent techniques</i>	17
4. Quantum dots	19
<i>4.1. Biological applications of the QDs</i>	21
<i>4.1.1. Cell detection and imaging</i>	21
<i>4.1.2. Gene technology</i>	22
<i>4.1.3. Bacterial, pathogen and toxin detection</i>	23
<i>4.2. QDs and flow cytometry</i>	24
5. Aims of this study	25
CHAPTER II. MATERIALS AND METHODS	27
1. MATERIALS	29
1.1. Chemicals and biochemicals	29
1.2. Reaction kits	30
1.3. Enzymes	30

1.4. Consumables	30
1.5. Laboratory equipment	31
2. METHODS	32
2.1. Buffers and solutions	32
2.2. Sterilisation of reagents	33
2.3. Culture media	33
2.4. Microscopy	34
2.4.1. <i>Light microscopy</i>	34
2.4.2. <i>Fluorescence microscopy</i>	34
2.4.2.1. <i>Fluorochromes</i>	34
2.4.2.2. <i>Epi-fluorescence microscopy</i>	34
2.4.2.3. <i>Confocal laser scanning microscopy</i>	35
2.5. Flow cytometry	36
2.5.1. <i>BD LSI Flow cytometer</i>	36
2.5.2. <i>BD FACS-Calibur Flow cytometer</i>	36
2.5.3. <i>Data acquisition and analysis</i>	37
2.6. Molecular analyses	37
2.6.1. <i>DNA concentration and quantification</i>	37
2.6.1.1. <i>Gel electrophoresis</i>	37
2.6.1.2. <i>Spectrophotometry</i>	38
2.6.2. <i>Polymerase chain reaction (PCR)</i>	38
2.6.3. <i>Sequencing and sequence data analysis</i>	41
2.6.4. <i>Fluorescent in situ hybridisation (FISH)</i>	42
2.6.4.1. <i>Oligonucleotide probes</i>	42
2.6.4.2. <i>Preparation of microscopy slides</i>	43
2.6.4.3. <i>Control organisms</i>	43
2.6.4.4. <i>Preparation of samples</i>	43
2.6.4.5. <i>Hybridisation conditions</i>	44
2.6.4.6. <i>FISH reactions in microcentrifuge tubes</i>	44
CHAPTER III. SAMPLING SITES AND SAMPLING MATERIAL	47
1. INTRODUCTION	48
2. MATERIALS AND METHODS	51
2.1. Sample collection	51
2.2. Sample handling and storage	51
2.3. Physical readings	52
2.4. Chemical analyses	52
3. RESULTS	54

3.1. Description of sampling sites and sample material	54
3.1.1. Site A	55
3.1.2. Site B	56
3.1.3. Site C	56
3.1.4. Site D	57
3.1.5. Site E	57
3.1.6. Site F	58
3.1.7. Site G	59
3.1.8. Site H	60
3.1.9. Site I	60
3.1.10. Site J	61
3.2. Chemical analysis	61
4. DISCUSSION	63
CHAPTER IV. ENRICHMENT CULTURES AND MOLECULAR ANALYSES	67
1. INTRODUCTION	69
2. MATERIALS AND METHODS	72
2.1 Culture media	72
2.1.1. <i>Liquid media</i>	72
2.1.1.1. <i>Acidianus medium</i>	72
2.1.1.2. <i>Diluted nutrient broth medium</i>	72
2.1.1.3. <i>Sulfolobus medium</i>	72
2.1.1.4. <i>Sulfolobus solfataricus medium</i>	73
2.1.1.5. <i>Sediment-extract medium</i>	73
2.1.2. <i>Solid extract agarose-based medium</i>	74
2.2. Cultivation conditions	74
2.2.1. <i>Enrichment cultures</i>	74
2.2.2. <i>Pure cultures</i>	75
2.3. Long-term storage of cultures	75
2.4. Buffers and solutions	75
2.5. Chemical analysis of the sediment-extract	76
2.6. Molecular analyses of enrichment cultures	76
2.6.1. <i>DNA extraction</i>	76
2.6.2. <i>PCR amplification</i>	77
2.6.3. <i>Restriction fragment length polymorphism (RFLP)</i>	77
2.6.3.1. <i>Long-term storage of recombinants</i>	78
2.6.3.2. <i>Extraction of plasmid DNA</i>	78
2.6.4. <i>Sequencing analysis</i>	79
2.6.5. <i>Construction of 16S rDNA consensus sequences</i>	79

2.6.6. <i>Sequence alignments</i>	80
2.6.7. <i>Phylogenetic analyses</i>	80
2.7. Fluorescent <i>in situ</i> hybridisation	81
3. RESULTS	82
3.1. Chemical analysis of the sediment-extract	82
3.2. Enrichment cultures	83
3.3. Molecular analyses of cultured microorganisms	85
3.4. Isolation of pure cultures	91
3.5. FISH	92
4. DISCUSSION	96
4.1. Cultivation of thermo-acidophiles from White Island	96
4.2. Molecular analyses	97
4.3. FISH	100
4.4. Isolation of pure cultures	102
4.5. Chemical analyses	102
4.6. Summary	102
CHAPTER V. OPTICAL AND BINDING CHARACTERISATION OF THE QDs	105
1. INTRODUCTION	107
1.1. Optical properties of the QDs	107
1.1.1. <i>Absorbance characteristics</i>	108
1.1.2. <i>Emission characteristics</i>	108
1.1.2.1. <i>Emission spectra of the QDs</i>	108
1.1.2.2. <i>Quantum yield</i>	109
1.1.2.3. <i>Photo-stability</i>	110
1.2. Physical properties	110
1.3. Surface chemistry of the QDs	112
1.3.1 <i>Types of interactions</i>	112
1.4. Aim	113
2. MATERIALS AND METHODS	115
2.1. Reagents	115
2.1.1 <i>Evitags QDs</i>	115
2.1.2. <i>Qdots™</i>	115
2.1.3 <i>Fluorophores</i>	116

2.1.4. Paramagnetic Dynabeads®	116
2.2. Buffers and solutions	117
2.3. Fluorescence spectrometry	117
2.3.1. Excitation-emission spectrum of Qdot™ 655	117
2.3.2. Excitation-emission spectrum of Hops-Yellow EviTags QDs	117
2.3.3. Molar extinction coefficient	118
2.4. Binding procedures	118
2.4.1. Coupling of thiol-modified probes to amine-modified QDs	118
2.4.2. Washing of Dynabeads® paramagnetic beads	119
2.4.3. Binding of biotinylated QDs to Dynabeads®	119
2.4.4. Binding of biotinylated probes to Dynabeads®	120
2.5. Flow cytometry	120
3. RESULTS	121
3.1. Optical characterisation of the QDs	121
3.1.1. Excitation- emission spectra	121
3.1.2. Molar extinction coefficient	123
3.2. Binding characterisation of the QDs	124
3.2.1. Quantitative method	124
3.2.2. Qualitative method	127
3.3. Binding characterisation of the Dynabeads	128
3.3.1. Fluorescence properties of the Dynabeads	128
3.3.2. Optical behaviour of QDs bound to Dynabeads	130
3.3.3. Binding capacity of the Dynabeads	133
3.3.4. Saturation point of the Dynabeads-probe complexes	136
4. DISCUSSION	138
4.1. Optical properties of the QDs	138
4.2. Binding properties of the QDs	141
4.3. Binding properties of the Dynabeads	141
4.4. Summary	142
CHAPTER VI. APPLICATIONS OF THE QDs	145
1. INTRODUCTION	147
1.1. Aim	147
2. MATERIALS AND METHODS	150

2.1. Reagents	150
2.2. Buffers and solutions	150
2.3. Molecular procedures	151
2.3.1. <i>Deinococcus radiodurans</i>	151
2.3.2. DNA extraction	151
2.3.3. Amplification and analysis of 16S rDNA of <i>D. radiodurans</i>	152
2.3.4. Design of <i>D. radiodurans</i> specific oligonucleotide probes	152
2.3.5. Polymerase Chain Reaction (PCR)	154
2.3.6. Gel electrophoresis analysis	155
2.4. QD-bead complex binding procedures	156
2.4.1. Washing of paramagnetic beads	156
2.4.2. Binding of QD-oligonucleotide amine probe complexes to Dynabeads	156
2.4.3. Binding of complementary oligonucleotide probes to Dynabeads	156
2.4.4. Binding of biotinylated PCR amplicons to Dynabeads	157
2.5. Capture and detection of genomic DNA bound to Dynabeads	157
2.5.1. Direct capture and reporting of gDNA	157
2.5.2. Indirect capture and reporting of gDNA	158
2.5.3. Restriction enzyme digestion of gDNA	159
2.5.3.1. Direct method for capturing digested gDNA	159
2.5.3.2. Indirect method for capturing digested gDNA	160
2.6. Capture and detection of PCR amplicons bound to Dynabeads	160
2.6.1. Alkali treatment for denaturation of PCR amplicons	160
2.6.2. Preparation of target probes modified with QDs	161
2.7. Capture and detection of PCR amplicons bound to QuantumPlex [™] MM beads	161
2.7.1. Calculations of the saturation point of the QuantumPlex [™] MM beads	161
2.7.2. Preparation of QuantumPlex [™] MM beads bound to the capture probe	162
2.7.3. Capturing the non-biotinylated strand of PCR amplicons	162
2.7.4. Evaluation of the bead-based method for the detection of extremophiles	163
2.8. Flow cytometry	164
3. RESULTS	165
3.1. Optimisation of the binding procedures	165
3.1.1. Binding of complementary probes to Dynabeads	165
3.1.2. Binding of biotinylated PCR amplicons to Dynabeads	168
3.1.3. Buffers and incubation times	172
3.2. Bead-based QDs technique for DNA detection	173
3.2.1. Detection of gDNA bound to Dynabeads	173
3.2.2. Detection of digested gDNA bound to Dynabeads	174

3.2.3. <i>Detection of biotinylated PCR amplicons bound to Dynabeads</i>	176
3.2.4. <i>Fluorescent intensity of QDs versus organic dyes</i>	179
3.2.5. <i>Detection of PCR amplicons with QuantumPlex™™ beads</i>	181
3.2.6. <i>Detection of bacterial and archaeal DNA with QuantumPlex™™ beads</i>	184
4. DISCUSSION	188
4.1. Optimisation of the bead-based technique for DNA detection	188
4.2. The bead-based QD technique for DNA detection	189
4.3. Fluorescence detection of QDs versus organic dyes	192
4.4. QDs and FISH	193
4.5. Summary	195
CHAPTER VII. CONCLUDING REMARKS	197
APPENDICES	207
APPENDIX I: QDs as a fluorophore probe for FISH	209
1. Conventional FISH technique	209
2. Non-conventional FISH technique	210
APPENDIX II: BioMag beads	213
APPENDIX III: Hops-Yellow QDs	215
APPENDIX IV: Methods for detection of PCR amplicons bound to the Dynabeads	217
1. Methods	217
1.1. <i>Direct method for labelling PCR amplicons</i>	217
1.2. <i>Indirect method for labelling PCR amplicons</i>	217
1.3. <i>Detection of PCR amplicons with QD525</i>	218
1.4. <i>Blocking the active sites of the QDs with biocytin</i>	218
2. Results	219
2.1. <i>Direct method for labelling PCR amplicons</i>	219
2.2. <i>Indirect method for labelling PCR amplicons</i>	219
2.3. <i>Blocking the active sites of the QDs with biocytin</i>	221
2.4. <i>Modifications in the procedures</i>	222
3. Discussion	223
APPENDIX V: Publications and conference proceedings	225
1. Publications	225
2. Conference proceedings	225

Abstract

White island, the most active volcano in New Zealand, is a poorly studied environment that represents an ideal site for the investigation of acidophilic thermophiles. The microorganisms present on here are continually exposed to extreme environmental conditions as they are surrounded by steamy sulphurous fumaroles and acidic streams. The sediment temperature ranges from 38°C to 104°C whilst maintaining pH values below 3. A survey of the volcanic hydrothermal system of White Island was undertaken in order to gain insights onto the microbial diversity using culture-dependant techniques and molecular and phylogenetic analyses. A novel liquid medium based on “soil-extract” was designed which supported growth of bacterial and archaeal mixed cultures. Molecular analyses revealed that the dominant culturable bacterial species belong to the Bacteroidetes, Firmicutes and α -Proteobacteria groups. Several previously uncultured archaeal species were also present in the mixed cultures. The knowledge gained from these studies was intended to help in the development of a novel microbial detection technique suitable for community analysis.

Conventional molecular techniques used to study microbial biodiversity in environmental samples are both time-consuming and expensive. A novel bead-based assay employing Quantum dots (QDs) was considered to have many advantages over standard molecular techniques. These include high detection speeds, sensitivity, specificity, flexibility and the capability for multiplexed analysis. QDs are inorganic semiconductor nanoparticles made up of crystals about the size of proteins. It has been claimed that the physical and chemical properties of the QDs have significant advantages compared to organic dyes, including brighter fluorescence and resistance to photo-bleaching. Their optical properties facilitate the simultaneous imaging of multiple colours due to their flexible excitation and narrow band emission. Functionalised QDs are able to bind to different biological targets such as DNA, allowing high-throughput analysis for rapid detection and quantification of genes and cells.

The optical and physical characteristics of the QDs as well their interaction with biomolecules are shown to be suitable for the development of a novel bead-based technique able to target the key microbial species and identify them by flow cytometric measurements (FCM). The broad absorption and narrow emission spectra of the QDs, as well as their fluorescence intensity and specificity to target biomolecules, was compared to other organic fluorophores. The potential advantages and limitations of QDs as a fluorophores for biological applications are discussed.

The data acquired during this study provides a broad overview of the microbial diversity and ecology of the volcanically-active hydrothermal systems of White Island and constitutes the baseline for the development of a novel bead-based technique based on QDs.

Statement of candidate

I certify that this thesis contains original work conducted by the author between August 2003 and June 2008. To the best of my knowledge it contains neither material previously published or written by another person for any other institution. Any contribution made to the research by others, with whom I have worked at Macquarie University or elsewhere, is explicitly acknowledged in the thesis.

I also declare that the intellectual content of this thesis is the product of my own work, except to the extent of the acknowledged assistance from others on the project's design, data interpretation or in style, presentation and linguistic expression.

Raquel Ibáñez-Peral

Sydney, June 2008

Acknowledgements

The completion of this thesis would have never been possible without contributions from the following people who helped me to overcome the challenges of this project along with the extraordinary circumstances surrounding it. I would like to thank:

My supervisors **Prof. Peter Bergquist**, **Dr. Belinda Ferrari** and **Prof Malcolm Walter** for the opportunity to work on this project, for their guidance, encouragement, scientific input, linguistic style, professional and personal support throughout my candidature. A special acknowledgement to the **Biotechnology Institute** (Macquarie University) and **Australian Centre for Astrobiology** (Macquarie University) for financial support.

Dr. Moreland Gibbs and **Prof. Ewa Goldys** for their help in designing the quantum dots technique and helping me to understand the physics and molecular concepts behind it.

Dr. Roberto Anitori and **Philip Butterworth** for their assistance in the fieldtrip to White Island, and tireless help and advice in the lab over the duration of my thesis. The **Buttle Family Trust**, owners of White Island, for allowing sampling and the **INGS** team for their assistance during the fieldtrip.

Dr. Ruth Henneberger for her priceless support, advice and help inside and outside university. A special thanks for teaching me the mysteries of fluorescent *in situ* hybridisation and the 1001 reasons why the extraction of DNA, PCR amplification and sequencing would not work.

Debra Birch for her assistance and valued advice on fluorescence microscopy at Macquarie University.

Dr. Jörg Peplies (Ribocon GmbH, Bremen, Germany) for his contribution to the phylogenetics analyses. The **Institute of Geological & Nuclear Sciences Limited**

(Wairakei Analytical Laboratory, New Zealand) and the **National Measurement Institute** (Australian Government, Australia) for the multi-element analyses. **Prince of Wales Hospital** (Australia) for letting me use their BD LSR I flow cytometer in collaboration with **BD Biosciences**.

Everyone in the Australian Centre of Astrobiology, specially **Sarah Chamberlain**, **Jessica Coffey**, **Dr. Stefan Leuko** and **Andrew Simpson** for their friendship in the good-la cucaracha-times and their support in the bad times. I hope one day they would finally be able to say where I am from (Valladolid, not Madrid!).

Everyone in the **EDGE lab** (Macquarie University). Thank you for helping me with all my silly questions and making the lab a great place to work.

Tina Purba-Pajnoo, my Scottish/Indian big sister, for all her support and friendship during the last years. A special thanks for checking my PowerPoint presentations full of strange terms such as “nanometre” and teaching me how to pronounce wavelength.

All my close friends **Mirai Kobayashi**, **Cristina Cobreros**, **Shingo Miyauchi**, **Dr. Ana Rubio**, **Dr. Alex Gupta**, **Ian De Horta** and my favourite “Norwegian” girls **Dr. Miren Castells** and **Eider Zubizarreta**. Your friendship means a lot to me.

This thesis would have not existed without the inspiration, motivation and wholehearted support of my entire family. Muchísimas gracias a mis padres **Carlos Ibáñez-Viloria** y **Maria Peral-Martín** por apoyarme desde el principio en todo, enseñarme a luchar y a pensar por mi misma. Gracias a mi hermanito **Raúl Ibáñez-Peral** por seguir siendo “un incordio” y estar siempre ahí por mí. Gracias al resto de mi familia, sobretodo a mis tios y tias, por todo el cariño incondicional durante estos últimos años. Y gracias a las “chicas de Viana”, amigas de mi madre, por convertirse en un gran apoyo para mi familia. Sin vuestra ayuda, cariño y apoyo la terminación de ésta tesis no habría sido nunca posible. Muchas gracias a todos.

Abbreviations and symbols

Abbreviations

Abbreviation	Meaning	Abbreviation	Meaning
abs	Absolute	MFI	Median fluorescence intensity
approx.	Approximately	M	Molar
CLMS	Confocal laser scanning microscopy	m	Meter
DAPI	4',6-diamidino-2-phenylindol	min	Minutes
DI water	Deionised water	mRNA	Messenger ribonucleic acid
DIC	Differential interface contrast microscopy	nM	Nanomolar
DNA	Deoxyribonucleic acid	μM	Micromolar
ds	Double stranded	nm	Nanometre
EDTA	Ethylenediamine tetra acetate	nov.	Novel
EtBr	Ethidium bromide	OD	Optical density
EtOH	Ethanol	PE	Phycoerythrin
FCM	Flow cytometric measurements	PBS	Phosphate buffer, saline
FITC	Fluorescein isothiocyanate	PCR	Polymerase chain reaction
FISH	Fluorescence <i>in situ</i> hybridisation	pers. comm.	Personal communication
FL	fluorescence	QDs	Quantum dots
FL1	Fluorescence detector 1	R-PE	Derivatised phycoerythrin
FL2	Fluorescence detector 2	rRNA	Ribosomal ribonucleic acid
FL3	Fluorescence detector 3	RT	Room temperature
g	Gram	s	Seconds
GPS	Global positioning system	ss	Single stranded
h	Hour	SSC	Single angle light scatter
kb	Kilobase air	SP	Shortpass filter
kg	Kilogram	sp.	species
l	Litre	UV	Ultra-violet light
LP	Longpass filters	vol	Volume
log	Logarithm	v/v	Volume per volume
		w/v	Weight per volume

Symbols

Symbol	Meaning
Å	Angstrom
°C	Degrees Celsius
ε	Molar extinction coefficient
~	Approximately
® / ™	Registered trademark

This thesis is dedicated to my family, especially to the memory of my mother.

(Dedico ésta tesis a mi familia, en especial a la memoria de mi madre)

“No se está en ningún sitio mejor que en casa”

María Peral-Martín

Chapter I. Literature review

LITERATURE REVIEW

Determining the microbial diversity in extreme environments is one of the outstanding tasks for microbiology. Traditional microbiological techniques have limitations for the identification and characterisation of most microorganisms. Furthermore, physiological and biochemical characterisation of many microorganisms is not possible, as 99% of all microorganisms in nature have not been successfully isolated in pure culture (Amann *et al.* 1995; Rondon *et al.* 1999). Therefore, techniques that complement microbial cultivation approaches are necessary to improve understanding of microbial diversity and its role in ecosystem maintenance.

New revolutionary techniques are replacing conventional methods for the study of microbial diversity. One focus of this study was to develop a bead-based technique that allowed multiplexed, high-throughput analysis for the rapid detection and quantification of genes and cells. Quantum dots (QDs), in combination with detection by flow cytometry, were proposed as a novel diagnostic technique to examine the microbial diversity and ecology of specific hydrothermal environments. White Island, New Zealand's most active volcano, was selected as a model hydrothermal system.

White Island is a poorly studied environment that represents an ideal site for the investigation of extremophiles. A survey of volcanic hydrothermal systems in New Zealand was initiated to gain insights into the phylogenetic diversity of endogenous microorganisms present using culture-dependent and culture-independent molecularly-based analyses. Knowledge of the unique microbial population present in White Island and their specific environmental characteristics will help to create a biological model that may be used to determine the microbial interactions of other similar but unknown environments.

1. Microbial diversity

The microbial world is immense and ubiquitous in both natural and many artificial environments (DeLong 2002). There are more microorganisms per ton of soil (10^{16}) than stars in our galaxy (10^{11}) (Curtis & Sloan 2005). Microorganisms are responsible for maintenance of the biosphere by playing crucial roles in many geochemical processes (Madsen 2005). The largest concentrations and diversity of prokaryotic cells can be found in terrestrial and marine sediments, and soils (Whitman *et al.* 1998; Curtis & Sloan 2004). Despite the importance and ubiquity of microorganisms, the majority of them have not been cultivated and their ecology, physiology and biochemistry remain unknown (DeLong & Pace 2001).

All unicellular microscopic organisms were first placed into the Kingdom Protista (Haeckel 1866). The development of electron microscopy divided these microscopic organisms into cells with a membrane-enclosed nucleus and cells that lack a nucleus. Differences in macromolecules were then used to differentiate cellular life forms further (Zuckerandl & Pauling 1965), and the development of molecular phylogenetics to infer evolutionary relationships between Kingdoms was described in 1977 (Woese & Fox 1977). The study of the small subunit ribosomal RNA contained in all organisms revealed the presence of two types of prokaryotes as unrelated to one another as they were to eukaryotes. This defined the three cellular domains of life: Eukaryota, Bacteria and Archaea (Woese *et al.* 1990). Since then, molecular phylogenetic studies have further defined and amplified these three-domains of life to incorporate new Phyla, Genera and Species (Pace 1997; DeLong & Pace 2001).

1.1. Origin of early life

There have been many theories about the origin of life since phylogenetic studies defined the tree of life. Currently they are two main theories for the origin of life: the “pioneer metabolic theory” where life may have originated on hot, volcanic habitats and the “prebiotic soup” theory based on a cold and oceanic environment (Bada *et al.* 2007). Various models have been proposed on the origin of life on Earth, from a single common ancestor (LUCA) (Fox *et al.* 1980; Woese 1998) to a community of organisms sharing genetic material (Doolittle 2000) or even on another planet (Davies 2001; Cleaves &

Chalmers 2004). A commonly accepted theory is that hydrothermal environments could have been the habitat for early life on Earth (Shock 1996; Nisbet & Sleep 2001).

One method of studying the origin of life is by seeking out regions of contemporary Earth that are similar to what is inferred to have existed when life first began. During the early Archaean period (approximately 3.8 to 2.5 billion years ago) land masses would have been formed predominantly of igneous rocks. The oldest evidence for life on Earth are putative microfossils, biogenic structures and biomarkers preserved in fossilised volcanic structures and hydrothermal systems (Walter 1983; Furnes *et al.* 2004; Allwood *et al.* 2006; Schopf 2006). It has been proposed that the basic organisational unit of life started within hydrothermal environments (Woese *et al.* 1990; Doolittle 2000; Woese 2002), and sulphate and iron reduction were among the earliest metabolic pathways to evolve (Vargas *et al.* 1998; Wagner *et al.* 1998). Therefore, investigating the microbial diversity of such environments may help in the understanding of the origins of early microbial life on Earth (Walter 1983; Walter & Des Marais 1993; Reysenbach & Cady 2001). The geochemical characteristics of volcanic environments have been considered to be analogous to some of the earliest environments on Earth. Volcanic environments are widely distributed on Earth and may be used as model systems to explain the diversity of microbial physiologies and their interactions with the environment (Woese 1998; Herrera & Cockell 2007).

The study of the origin of life on Earth in relation to the possibility of life existing elsewhere in the universe has been a focus of attention in astrobiology (Des Marais & Walter 1999). Astrobiology represents a multidisciplinary combination of all natural sciences as well as space exploration technologies to gain a comprehensive understanding of biological, planetary and cosmic phenomena in relation to the origin, distribution and evolution of life (Des Marais *et al.* 2003). One of the aims of astrobiology is the study of extremophiles, as these microorganisms may have been the precursors of life on Earth and they could have evolved somewhere else in the universe such as on moons like Europa (Rothschild 1990; Chyba & Phillips 2001; Rothschild 2007).

1.2. Extremophiles

The vast biochemical and physiological diversity of microorganisms allows them to grow in a wide range of different habitats. Extremophiles are microorganisms living under extreme conditions such as high or low temperature and pH, high concentrations of salt and pressure, or high levels of radiation (Stetter 1999a; Stetter 1999b; Johnson & Hallberg 2003). The first discoveries of microorganisms growing at high temperatures were in 1866 and 1888 (Brewer 1866; Miquel 1888). These microorganisms, now known as thermophiles, have their growth optimum at 60°C–80°C (Stetter 1996). Hyperthermophiles have been defined to grow fastest at temperatures of 80°C or above, while they are unable to propagate below 60°C (Stetter 1999b). The domain Archaea contains the most hyperthermophilic microbial genera and species described (Blöchl *et al.* 1995; Niederberger *et al.* 2006). To date, the most thermostable specie is *Pyrolobus fumarii* which grows at 113°C (Blöchl *et al.* 1997). However Strain 121 is an archaeon discovered in a hydrothermal vent that is claimed to be able to survive and reproduce at 121°C (Kashefi & Lovley 2003). It has been postulated that Strain 121 is the only known form of life that apparently not only can tolerate such high temperatures, but also is bacteriostatic at 130°C, although these findings are still controversial (Kashefi 2004). It has been hypothesised that the upper limit of life would probably be in the region of 140°C-150°C. Higher temperatures would compromise the work efficiency and maintenance of the biological processes at a molecular level (Cowan 2004).

Acidophiles are microorganisms which are able to live in low pH environments. The first obligatory acidophilic bacterium to be described was *Thiobacillus ferrooxidans* (now *Acidithiobacillus ferrooxidans*) (Temple & Colmer 1951). Since then, acidophiles have been found in many acidic environments (Schleper *et al.* 1995; Edwards *et al.* 2000; Fernández-Remolar *et al.* 2004). The most acidophilic microorganisms known are within the Archaeon genus *Picrophilus* capable of growth at negative pH values as low as -0.2 (Schleper *et al.* 1996). Moreover, microorganisms can be found also in habitats that are extreme for more than one condition. Thermo-acidophilic microorganisms have been found in extremely hot and acidic environments as well as highly acidic environments and those contaminated with heavy metals (Rothschild & Mancinelli 2001; Gonzalez-Toril *et al.* 2003). For example, the genus Crenarchaeota includes microorganisms that tend to

predominate in environments characterised by high temperature and low pH such as hot sulphur springs, where the temperature may be as high as 80°C and the pH as low as 2 (Bosecker 1999; DeLong 2001).

The first report of microorganisms capable of growth at 0°C was in the early 1900s (Schmidt-Nielsen 1902), although psychrophilic bacteria were not defined until 1975 (Moira 1975). These microorganisms are capable of growth below 15°C and can survive at subzero temperatures. Cold environments such as ice shields (Miteva *et al.* 2004), cold waters and frozen lakes (Henneberger *et al.* 2006), dry soils in Antarctica (Cowan *et al.* 2002; Smith *et al.* 2006; Niederberger *et al.* 2008), and sub-glacial sediments or ice (Foght *et al.* 2004) also have been identified as microbial habitats. In cold habitats, such as Antarctica, microenvironments play an important role for microbial survival. The air temperature may be below zero, but on the surface of the rock facing the sun it can reach temperatures up to 20°C (Aislabie *et al.* 2006).

Extremophiles can be found also in saturated salt solutions (Kamekura 1998) and highly alkaline environments (Jones *et al.* 1998). Halophilic microorganisms have been found within saline soils and lakes. *Haloflex mediterranei* has been demonstrated to grow in the presence of 30% sodium chloride (Rodriguez-Valera *et al.* 1983). While alkaliphilic microorganisms grow at high pH of 8.0, they cannot grow at neutral pH. To date, the most alkaliphilic microorganisms found are cyanobacteria that are capable of growth at pH values as high as 13 (Horikoshi 1990; Pikuta *et al.* 2007). Some extremophiles are able to tolerate high levels of radiation and the presence of heavy metals (Ferreira *et al.* 1999; Nies 1999), such as *Deinococcus radiodurans*, the first radioresistant bacterium found (Raj *et al.* 1960), and *Thermococcus gammatolerans* which is a sulphur-reducing archaeon capable of resisting 30 kGy of γ -irradiation (Edmond *et al.* 2003).

Extremophiles and their products have potential biotechnological applications in industrial, agricultural and medical areas. Studies into cold adaptation have identified a broad range of cellular products like cold-active enzymes (Gerday *et al.* 2000; Cavicchioli *et al.* 2002), metabolic cofactors and ether-linked lipids (Patel & Sprott 1999). Halophilic microorganisms growing in highly saline environments have been found to produce polymers, enzymes and compatible solutes that may be valuable for biotechnology

(Ventosa & Nieto 1995). In addition, enzymes from thermophilic and extremely thermophilic microorganisms are of interest in biotechnological applications due to their thermo-stability and resistance to heat (Bergquist *et al.* 1987; Bragger *et al.* 1989; Coolbear *et al.* 1992; Cowan 1992) such as hyperthermophilic xylanases (Bergquist *et al.* 2001; Bergquist *et al.* 2002) and proteases (Cowan *et al.* 1987; Coolbear *et al.* 1988; McHale *et al.* 1991).

1.3. Microbial consortia

The association of two or more microorganisms results in their complementary activities being more efficient compared to either of those microorganisms alone. In consortia, microorganisms gain benefits as illustrated by feedback reactions which occur, for example, between chemolithotrophic and heterotrophic acidophiles resulting in cross-feeding (Spiegelman *et al.* 2005; Rawlings 2005)

Interactions between thermo-acidophilic microorganisms in their natural environment have been studied previously (Johnson 1998). Obligatory acidophilic protozoa have been observed to predate mesophilic heterotrophic and chemolithotrophic bacteria (McGinness & Johnson 1992; Johnson & Rang 1993). Mutualism between thermo-acidophilic microorganisms has also been observed, for example, by feedback reactions during cycling of iron, where the interactions of ferrous-oxidising chemolithotrophs (using iron as electron donor) and ferric-reducing heterotrophs (using iron as electron acceptor) result in both partners gaining benefits (Hallmann *et al.* 1992; Johnson *et al.* 1993; Johnson & Roberto 1997). The association of two or more acidophilic microorganisms that results in their complementary activities being more efficient in terms of product formation (synergism) than by either microorganism alone has been described on several occasions, mostly in the context of enhanced mineral oxidation by mixed populations (Norris 1990).

1.4. Microbial metabolism

Microbial diversity can be classified depending on the source of energy a microorganism requires for growth, including the temperature, acidity and atmospheric conditions of the habitat. Photoautotrophic microbes can assimilate CO₂, producing complex organic

compounds by photosynthesis. The majority of them are eukaryotic micro-algae, and include filamentous and unicellular forms and diatoms (Gyure *et al.* 1987; Lopez-Archilla *et al.* 2001). Heterotrophic microorganisms are adept scavengers and require organic compounds as a source of carbon which is obtained from dead organic matter derived from inputs of the living soil biomass, like the carbon originating as leakage or lysis products from autotrophic acidophiles (Kletzin *et al.* 2004). Photoheterotrophs assimilate organic carbons to obtain energy from light. Chemoautotrophic (lithotrophic) microorganisms use CO₂ as their sole source of carbon while chemoheterotrophic microorganisms require organic compounds. However, both of them obtain their energy from the oxidation and reduction of inorganic compounds like elemental sulphur, nitrate, H₂, H₂S, NH₃ and various metals such as oxides and sulphides (Pronk *et al.* 1991; Kelly *et al.* 1997; Kelly 1999).

In relation to temperature, only archaeal hyperthermophilic microorganisms have been found growing at temperatures above 100°C (Bosecker 1997; Huber, *et al.* 2000b). Moderately thermal environments (40-60°C) normally are inhabited by Euryarchaeota and Gram-positive bacteria (Johnson 1998; Kinnunen & Puhakka 2004) such as *Sulfobacillus sp.* (Hallberg & Johnson 2001; Johnson & Hallberg 2003). Mesophilic conditions (20-40°C) are generally dominated by Gram-negative bacteria (autotrophs and heterotrophs). However, there are some exceptions, such as *Sulfobacillus disulfidooxidans*, a mesophilic spore-forming Gram-positive eubacterium which uses pyrite and elemental sulphur as sole energy sources to grow heterotrophically on various organic substrates (Dufresne *et al.* 1996).

The oxidation and reduction of different oxidation states of sulphur and iron are some of the most important energy-yielding reactions for microorganisms living in volcanic hot springs, solfataras and submarine hydrothermal vents, including heterotrophic, mixotrophic and chemolitho-autotrophic, carbon-fixing species (Hallberg & Johnson 2001).

Metabolic pathways based on sulphur and iron are believed to have been the earliest to evolve and many of these processes have been extensively studied over the past decade (Vargas *et al.* 1998; Wagner *et al.* 1998; Johnson 2001). Whilst most acidophiles

conventionally have been considered to be obligatory aerobes, there is increasing evidence that many isolates are facultative anaerobes and they are able to couple the oxidation of organic or inorganic electron donors to the reduction of ferric iron. Common abiotic spontaneous reactions between inorganic sulphur and iron compounds feed the environment with protons and different oxidation states of both iron and sulphur that can be used by the microorganisms as an energy source. Despite the knowledge gained so far, many aspects of these cycles and their impact on biochemical processes remain unclear (Madsen 2005).

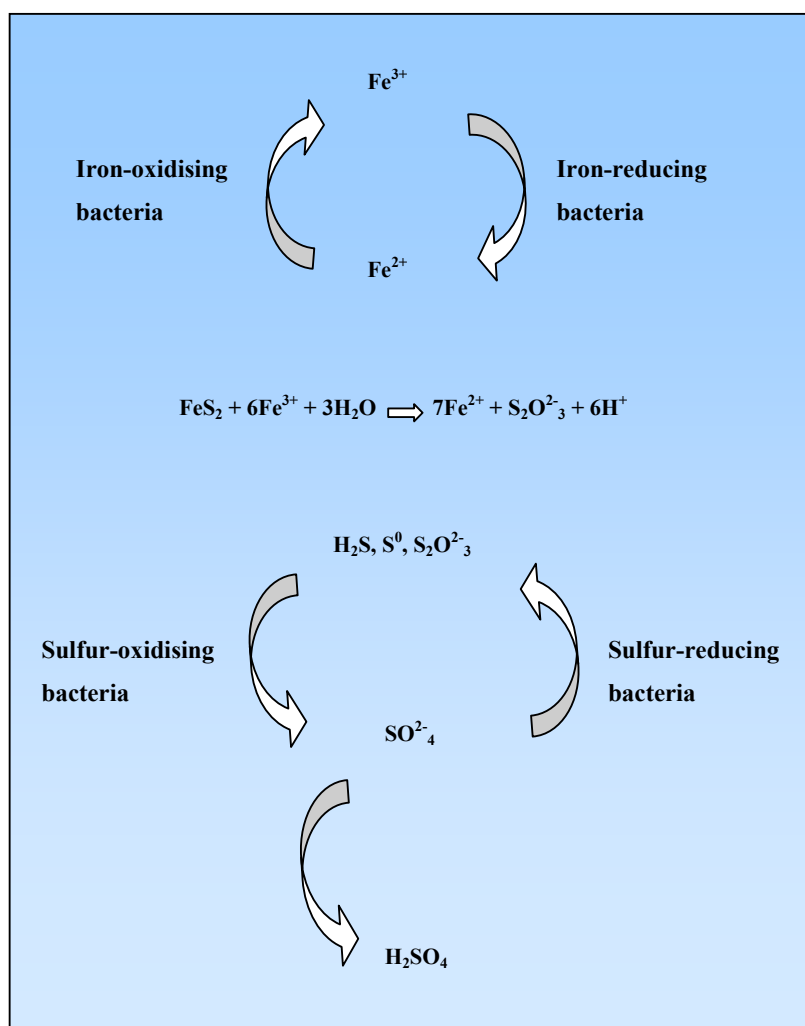


Figure 1.1. Schematic representation of the metabolic physiologies of thermo-acidophilic microorganisms. Common abiotic spontaneous reactions between inorganic sulphur and iron compounds, such as pyrite, feed the environment with protons. Different states of oxidation of both iron and sulphur can be used by various microorganisms for their metabolic processes.

1.4.1. Sulphur cycling

Within sulphur- and sulphide-rich environments, utilisation and cycling of sulphur species plays a major role in energy production and the maintenance of the microbial community (Habicht & Canfield 1996; Douglas & Douglas 2001). Elemental sulphur and sulphur components are highly abundant in volcanic environments where the emitted gases contain high amounts of sulphur dioxide (SO₂) and hydrogen sulphide (H₂S) (Montegrossi *et al.* 2001). The microbial community structure of sulphur-rich habitats is influenced by the prevalent environmental conditions of the specific habitat (Elshahed *et al.* 2003). Sulphur acts as a significant electron donor and acceptor in numerous bacterial metabolic pathways (Jorgensen 1982; Jorgensen 1994; Prescott *et al.* 1996).

Sulphur oxidation, where sulphur compounds are present in the environment from geological sources or as products of metabolic activities from other microorganism, are performed by prokaryotes of the domains Archaea and Bacteria (Lane *et al.* 1992; Friedrich *et al.* 2005). Aerobic sulphur oxidation of Archaea appears to be restricted to members of the order *Sulfolobales*, a group of thermo-acidophilic microorganisms commonly found in terrestrial hydrothermal environments (Stetter 1989; Friedrich *et al.* 2001). On the other hand, sulphur is oxidised by a diverse group of aerobic-chemotrophic and anaerobic-phototrophic bacteria (Kelly *et al.* 1997; Friedrich *et al.* 2001; Friedrich *et al.* 2005).

The reduction of sulphate to sulphide has been demonstrated as occurring in extremely acidic environments (Gyure *et al.* 1990; Langdahl & Ingvorsen 1997) as well as in freshwater and marine aquatic systems, hypersaline cold environments and hot springs (Jorgensen *et al.* 1992; Knoblauch *et al.* 1999; Fishbain *et al.* 2003; Scholten *et al.* 2005). Sulphur reduction has been observed in many different species of bacteria (Fuseler *et al.* 1996), while the reduction of sulphate appears limited to the genus *Archaeoglobus* within the archaeal domain (Kletzin *et al.* 2004).

1.4.2. Iron cycling

Pyrite (FeS_2) is the most abundant of all sulphidic minerals and the largest physical reservoir is in the Earth's crust, where sulphur and iron are found (Silverman 1967). Pyrite, in presence of moisture and air, oxidises spontaneously, generating ferrous iron and sulphites that can be used as electron donors for iron and sulphur oxidisers (Stumm & Morgan 1981; Diaby *et al.* 2007). The cycling of iron compounds is closely connected to the sulphur cycle as many acidophilic iron-oxidising microorganisms use reduced sulphur compounds as substrates (Lane *et al.* 1992; Hallberg & Johnson 2001).

The oxidation of ferrous iron (Fe^{2+}) to ferric iron (Fe^{3+}) normally occurs spontaneously in oxic environments. However, this reaction is highly pH dependant and it is not spontaneous under acidic conditions. Microorganisms take advantage of the accumulation of ferrous iron in acidic environments to obtain energy (Okibe & Johnson 2004). Moderately thermophilic iron-oxidising acidophilic microorganisms have highly versatile metabolic capabilities as they may grow as autotrophs, heterotrophs, mixotrophs or chemolitho-heterotrophs (Bridge & Johnson 1998; Bacelar-Nicolau & Johnson 1999).

The microbial reduction of ferric iron under acidic conditions has received little attention in comparison to the oxidation of ferrous iron (Pronk & Johnson 1992; Küsel *et al.* 2002). Many acidophilic heterotrophic bacteria possess the ability to reduce ferric iron since their natural environments are invariably iron-rich (Johnson & McGinnes 1991; Küsel *et al.* 2002). Reduction of ferric iron by some strains of mesophilic heterotrophic acidophiles has been found to be more rapid and extensive when the bacteria are grown under (micro)aerobic conditions than when they are grown under anaerobic conditions (Johnson & McGinnes 1991). Some acidophilic microorganisms are able to catalyse ferrous iron oxidation in a low pH environment, regenerating ferric iron, and also can generate sulphuric acid via oxidation of elemental sulphur and reduced inorganic sulphur compounds (Baker & Banfield 2003; Johnson & Hallberg 2003).

2. Volcanic environments

A volcano is an opening, or rupture, in a planet's surface or crust, which allows hot, molten rock, ash and gases to escape from below the surface (Scarth 1994). Volcanic

activity involves the extension of rock, tending to form mountains or features like mountains over a period of time (Simkin 1993). However, volcanoes can also form large piles of lava on the ocean floor or small cylindrical cones on the land (Simkin & Siebert 2000).

2.1. Geothermal and hydrothermal systems

Minor volcanic features without the emission of lava are called geothermal systems. The high temperatures associated with volcanic activity result in both surface and subsurface geothermal or hot spring systems (Barns *et al.* 1994; Herrera & Cockell 2007). Geothermal features which contain a natural reservoir of water, groundwater or meteoric water are called hydrothermal systems (Nisbet & Sleep 2001). Volcanic regions are mostly acidic metal-rich environments associated with geothermal activities and hydrothermal systems (Johnson 2001). These habitats are characterised by heterogeneous conditions with wide variations of temperatures and acidity gradients and high concentrations of metals which support a high biodiversity of extremophiles (Keller & Zengler 2004; Curtis & Sloan 2005).

Hydrothermal systems presently occur in terrestrial and marine environments as a direct result of plate tectonic movements (Reysenbach & Cady 2001). Microbial diversity has been studied from sediments and chimney structures of deep-sea vent systems (Schrenk *et al.* 2003; Takai *et al.* 2003), terrestrial hot springs (Atkinson *et al.* 2000; Baker *et al.* 2001; Anitori *et al.* 2002), geothermal spring waters (Norris *et al.* 2002; Hetzer *et al.* 2007) and volcanic environments such as Mount Hood, US (Henneberger 2008).

2.2. White Island, New Zealand

White Island is the most active volcano in New Zealand, located in the Bay of Plenty, 50 km off the coast of the North Island at the north-eastern end of the Taupo Volcanic Zone (Scott *et al.* 1995). It is an andesitic composite volcano that has a sub-aerial extent of about 3.5 km² and hosts an extensive acidic hydrothermal system lined with fumaroles and acidic lakes (Giggenbach & Sheppard 1989; Houghton & Naira 1991; Mongillo & Wood 1995; Nishi *et al.* 1996; Wardell *et al.* 2001).

The island has been built up by continuous volcanic activity and steam release over the past 150,000 years (Black 1970). Craters and fumaroles on the island continually emit gases at rates of several hundred to several thousand tonnes per day (Wardell *et al.* 2001). Acidic gases combine with water in the steam to form acid droplets. Hot springs discharge on the floor of the main crater, forming the subaerial expression of a long-lived acidic hydrothermal system related to the deeper magmatic system of the volcano (Cole *et al.* 2000). The locus of eruptive activity is changeable and over the years there have been numerous such vents, with the formation of craters (Clark 1970; Mongillo & Wood 1995). Further details on the geological history of White Island are found in Chapter III.

The microbial diversity of White Island is largely unknown. To date, there is only one published study reporting the presence of α - and β -Proteobacteria, Firmicutes and eukaryotic algae in acid stream water of White Island (Donachie *et al.* 2002). Despite the fact that Archaea are the most hyperthermophilic and acidophilic microorganisms normally found in hydrothermal sulphur-rich environments, archaeal species were not found in that study.

3. The study of microbial diversity

3.1. Culture-independent techniques

The development of molecular biological methods has revolutionised the field of environmental microbiology by allowing the analysis of microbial diversity without the need to isolate individual species (Olsen *et al.* 1986; Hugenholtz *et al.* 1998a). Techniques such as the application of universal primers for direct PCR amplification of diverse 16S RNA genes from total community DNA combined with cloning and sequencing technologies, have generated a vast quantity of data that has redefined the microbial diversity (Woese 1987; Pace 1997; Gans *et al.* 2005). Such studies have demonstrated for example, the high diversity of thermo-acidophiles in many habitats like the Tinto River in Spain (González-Toril *et al.* 2003; Lopez-Archilla *et al.* 2004; Hallberg *et al.* 2006).

The study of the ribosomal RNA operon, typically the small subunit (16S gene) and the less widely used 5S rRNA, have been the most common molecules used for the

determination of prokaryotic diversity and phylogeny (Woese & Fox 1977; Fox *et al.* 1980; Woese *et al.* 1990; Saul *et al.* 1993) due to its ubiquity and slow rate of evolution (Woese 1998; Woese 2002). Environmental sequencing projects targeting 16S rDNA have revealed a large number of new phylotypes previously undetectable by culture-dependent techniques (Ward *et al.* 1990a; Barns *et al.* 1996; DeLong & Pace 2001; Tringe *et al.* 2005).

Culture-independent techniques normally are based on PCR amplification of DNA extracted from environmental samples. These techniques include the ribosomal intergenic spacer analysis (RISA), denaturing gradient gel electrophoresis (DGGE), temperature gradient gel electrophoresis (TGGE), single-strand conformation polymorphism (SSCP), random amplified polymorphic DNA (RAPD) and amplified ribosomal DNA restriction analysis (ARDRA) (Kirk *et al.* 2004; Zhong & Cai 2004; Fierer & Jackson 2006). Although these techniques have allowed the study of microbial diversity from many habitats, these procedures have several limitations, becoming inefficient for the detection of certain populations of microorganisms. The extraction of community genomic DNA from environmental samples represents the initial step for most culture-independent techniques. The extraction efficiency can be influenced by various factors and strongly depends on the characteristic of the samples (Krsek & Wellington 1999). For example, the DNA extraction from acidic sulphur-rich environments such as White Island has many difficulties as the high content of heavy metals and minerals that strongly bind to the nucleic acids, and the acidity of the sample not only increases the binding of the DNA to the clay minerals but also decreases the amount of extracted DNA, as nucleic acids are easily degraded by depurination under acidic conditions (Frostegard *et al.* 1999; Miller *et al.* 1999; Roh *et al.* 2006; Henneberger 2008).

Sequence-based analyses of microbial communities also can be influenced by several factors such as contaminants and artefacts which may occur during PCR amplification having significant impact on the resulting data and leading to misinterpretation of the results obtained (Tanner *et al.* 1998; Klappenbach *et al.* 2001; Rossello-Mora & Amann 2001; Acinas *et al.* 2005; Osborne *et al.* 2005). Different approaches have been developed to improve detection and resolution of amplified DNA fragments. These include length heterogeneity PCR (LH-PCR) (Ritchie *et al.* 2000) and terminal restriction fragment

length polymorphism (T-RFLP) (Marsh 1999). However, variables that affect the efficiency of culture-independent techniques for the study of microbial diversity of unknown habitats, such as genome size or the number of the rRNA operons present in the different microorganisms, cannot be estimated and the accuracy of the resulting data cannot be confirmed (Farrelly *et al.* 1995)

Fluorescent *in situ* hybridisation (FISH), as a culture-independent technique, allows simultaneous visualisation, identification, enumeration and localisation of individual microbial cells in their natural habitat. FISH also provides insights into community structure and diversity, spatial distribution, and abundance of specific types of microorganisms (DeLong *et al.* 1989; Amann *et al.* 1990b; Amann *et al.* 1995). FISH has been used to visualise uncultured microorganisms from a wide range of environments (Eilers *et al.* 2000; Gonzalez-Toril *et al.* 2003), as well as to study microbial communities and biofilms (Bond *et al.* 2000a; Daims *et al.* 2001a; Ferrari *et al.* 2006). For example, a microbial community comprising novel archaeal and bacterial species living in the cold sulphurous marsh water of Sippemauer Moor (Germany) were discovered to form strings of pearls-like morphologies using FISH (Rudolph *et al.* 2001).

FISH relies on the use of fluorescently-labelled oligonucleotide probes which hybridise specifically to complementary target sequences within an intact target cell. The most commonly used target molecule for FISH is the 16S rRNA because of its genetic stability, its domain structure with conserved and variable regions and its high copy number (Woese 1987). Oligonucleotide probes can be designed at a taxonomic level according to the region of the rRNA targeted (Amann *et al.* 1995) and new probes targeting different phylogenetic levels are constantly being designed (Amann & Ludwig 2000; Nercessian *et al.* 2004; Rusch & Amend 2004) allowing assignation of the targeted microorganism to a phylogenetic group (Amann *et al.* 1990b). However, FISH also has many limitations. The most common problem is autofluorescence of the microorganisms themselves or autofluorescence of sample detritus such as soil and minerals particles which interferes with target cell detection (Moter & Gobel 2000; Bertaux *et al.* 2007). Low fluorescent signal from the fluorescent probes is another limitation which may be a consequence of the insufficient permeabilisation of cell walls using standard fixation protocols, poor accessibility of rRNA for the probes or low ribosomal content of the cells due to

decreased metabolic activity (Poulsen *et al.* 1993; Bhatia *et al.* 1997). Several modifications and new technologies have been reported to overcome the limitations of FISH, such as the use of polynucleotide probes with multiple fluorescent labels and the use of peptide nucleic acids (DeLong & Taylor 1999; Stender *et al.* 1999; Zimmermann *et al.* 2001). These techniques have allowed the detection, for example, of marine plankton previously undetectable with standard oligonucleotide probes (DeLong & Taylor 1999; Pernthaler *et al.* 2003). In addition, catalysed reporter deposition (CARD)-FISH results in increased signal intensity compared to traditional FISH (Schönhuber *et al.* 1997) allowing, for example, clear signal detection above the autofluorescent background in certain cyanobacteria (Pernthaler *et al.* 2002). Although these new technologies can represent useful tools for the detection and identification of microorganisms in environmental communities, these modifications are associated with high costs and are time-consuming compared to traditional FISH (Wagner *et al.* 2003).

3.2. Culture-dependent techniques

Nonculturable microorganisms represent one of the most pressing problems currently associated with microbial ecology (Zengler *et al.* 2002; Leadbetter 2003). Most of the microorganisms occurring in a nature, in principle, should be culturable, as between 50%-90% of the bacterial cells in natural samples appear to be metabolically active (Fry 1990; Bartscht *et al.* 1999). At present, 52 phyla have been delineated, of which only 26 have cultivated representatives (Rappe & Giovannoni 2003). The intensive application of molecular techniques to describe microbial diversity in natural environments is yielding a large amount of data as indicated by the large number of sequences available in the public databases (Baker *et al.* 2003; Baker & Cowan 2004; Ludwig *et al.* 2004). However, comparisons between classical culture-dependent and molecular methods have revealed that only a small fraction, about 1% of the prokaryotic diversity, appears to be amenable to culture (Amann *et al.* 1995; Hugenholtz *et al.* 1998a; Rappe & Giovannoni 2003) and less than 0.1% of archaeal species have been cultivated from soil (Bintrim *et al.* 1997).

Cultivation and subsequent isolation of microorganisms in pure culture is required to gain a comprehensive understanding of microbial physiology, their interaction with one another in their environment and to provide access to genes encoding metabolic pathways

which may be dispersed throughout the genome (Palleroni 1997; Keller & Zengler 2004; Schleifer 2004; Green & Keller 2006). Traditional culturing approaches are based on complex nutrient-rich media that supply excessive amounts of nutrients to the system as the specific requirements of many uncultured microorganisms are unknown. However, these approaches allow the enrichment of faster-growing microorganisms that are capable of colony or biofilm formation (Amann *et al.* 1995; Saul *et al.* 1999; Leadbetter 2003; Ferrari *et al.* 2004). These organisms are not necessarily the most abundant species in the environmental samples, but their fast growth allows them to out-compete other microorganisms present in the culture (Saul *et al.* 1999). Microorganisms may be difficult to cultivate for diverse reasons such as lack of necessary symbionts or nutrients, excess of inhibitory compounds, incorrect combinations of temperature, pressure or atmospheric gas composition, accumulation of toxic waste products from their own metabolism leading to slow growth rate or rapid dispersion from colonies (Caruge *et al.* 2004). In addition, the microbial compositions of the enrichment cultures are also influenced by the concentration of inoculum as the cultures resulting from inoculation at low concentration seem to be dominated by species that have superior growth capabilities in that medium, while high concentrations of inoculum result in cultures of those species whose growth was inhibited when using a lower concentration of inoculum (Jackson *et al.* 1998).

No single method or medium is suitable for the cultivation of the majority of microorganisms from environmental samples (Green & Keller 2006). Laboratory techniques for successful cultivation and isolation of environmental microorganisms are required to mimic and reproduce the specific nutritional and physical conditions of their natural habitat (Kaeberlein *et al.* 2002). Novel techniques and culture media have been developed to address these issues (Frohlich & Konig 2000; Bruns *et al.* 2003). Cultivation and isolation of new microorganisms has been achieved by the use of media with low concentrations of nutrients containing polymeric growth substrates and long incubation times (Eilers *et al.* 2000; Cannon & Giovannoni 2002; Sait *et al.* 2002; Stevenson *et al.* 2004; Davis *et al.* 2005). For example, diluted nutrient broth has been used successfully to isolate novel soil bacteria microorganisms within the divisions *Actinobacteria*, *Acidobacteria*, *Proteobacteria* and *Verrucomicrobia* (Janssen *et al.* 1997; Janssen *et al.* 2002).

Many environments are very complex with respect to their chemical composition and physical parameters. These environments are difficult to reproduce under laboratory conditions. However, novel techniques have been developed to mimic the natural habitat and supply the media with the essential trace elements, such as the use of sterilised sample material (Alef 1995; Anitori & Bergquist 2006) and *in situ* chambers and membrane systems which allow the direct uptake of nutrients from the environment and the exchange of metabolites (Reysenbach *et al.* 2000; Kaeberlein *et al.* 2002; Moissl *et al.* 2003; Svenning *et al.* 2003; Ferrari *et al.* 2005). For example, ubiquitous microorganisms, such as the SAR11 clade found in nearly every pelagic marine bacterioplankton community studied by culture-independent techniques, was not cultured successfully and isolated until low-nutrient media based on sterilised natural sea water was used (Rappe *et al.* 2002).

Despite these developments, the majority of microorganisms remain to be cultured and isolated. Detailed analyses of the environmental parameters of the habitat to be studied can provide valuable information required for mimicking the natural conditions and develop novel culture-dependant techniques.

4. Quantum dots

Quantum dots (QDs) are highly luminescent inorganic colloidal semiconductor nanocrystals. They were initially prepared in 1982 for investigation of surface kinetics, where it was found that the quantum yield of the nanocrystals was sensitive to the concentration of surface-absorbed species that can undergo reduction (Rossetti & Brus 1982). The first reports describing the use of QDs as fluorescent labels for biomolecules were published in 1998 (Bruchez *et al.* 1998; Chan & Nie 1998). Since then, interest in their applications has increased enormously, ranging from cell imaging to analytical chemistry (Jaiswal *et al.* 2004; Bruchez 2005; Dubertret 2005; Medintz *et al.* 2005; Parak & Pellegrino 2005).

QDs are considered to be the most promising nanomaterials emerging in biotechnology with potential applications in a broad range of medical and biological techniques (Chen 2008). The diverse potential applications of QDs are attributed to their unique properties as fluorophores (Dabbousi *et al.* 1997; Mattoussi *et al.* 2000; Bailey & Nie 2003; Lim

2003). The physical and chemical properties of QDs confer significant advantages over traditional dyes, such as brighter fluorescence (Wu *et al.* 2003; Lee *et al.* 2004; Xiao & Barker 2004) and resistance to photo-bleaching (Jaiswal *et al.* 2003; Ballou *et al.* 2004; Hoshino *et al.* 2004b). Their unique optical properties include flexible excitation coupled with narrow emission spectra that enables simultaneous multiplexed detection and imaging using a single light source (Dabbousi *et al.* 1997; Mattoussi *et al.* 2000; Lim 2003). Additionally, the surface of the QDs can be functionalised to target a wide range of molecules, enabling their application in many biological techniques (Zhang *et al.* 2007).

In comparison, conventionally-used organic fluorescent dyes for biological applications have several limitations such as photo-bleaching, as they cannot fluoresce continuously for extended periods of time (Chan *et al.* 2002), relatively broad emission spectra that can easily overlap with the emission of other fluorophores (Sharma *et al.* 2006) and defined excitation wavelengths (Shapiro 1977; DeLong *et al.* 1989; Amann *et al.* 1990b; Veal *et al.* 2000). The emission–excitation spectra of organic fluorophores often is susceptible to changes in the local chemical environment and the background fluorescence sometimes may overcome the low fluorescent signal derived from organic dyes, resulting in an inability to distinguish them from the background signal (Sharma *et al.* 2006).

Table I.1: Comparison between QDs and organic fluorophores

	QDs	Organic fluorophores*	References
Excitation	Very broad. UV light can excite any size of QDs	Narrow excitation spectra	(Jaiswal & Simon 2004; Ozkan 2004)
Emission bandwidth	20-40 nm	50-100 nm	(Jaiswal & Simon 2004; Bruchez 2005)
Fluorescence lifetime	10-40 ns	Few ns	(Alivisatos <i>et al.</i> 2005)
Photo-stability[†]	Stable for over 14 h	Fluorescein photobleaches completely in 20 min	(Jaiswal <i>et al.</i> 2003)
Molar extinction coefficient^{††}	$\sim 10^5\text{--}10^6 \text{ M}^{-1} \text{ cm}^{-1}$	10-100 times smaller	(Ozkan 2004)

* Exemplified by fluorescein.

[†] Photo-stability upon constant illumination with a 50 mW, 488 nm laser.

^{††} Molar extinction coefficient for CdSe QDs.

4.1. Biological applications of the QDs

4.1.1. Cell detection and imaging

The photo-stability of the QDs has allowed them to be used for a wide range of applications in live cell labelling, organelle tracking and selective intracellular delivery (Dahan *et al.* 2003; Jaiswal *et al.* 2003; Hoshino *et al.* 2004a; Michalet *et al.* 2005; Delehanty *et al.* 2006) as well as imaging of entire subcellular structures (Kim *et al.* 2004; Yamamoto *et al.* 2007), detection and targeting of specific cells (Weng *et al.* 2006) and tracking cells over long periods of time (Hoshino *et al.* 2004b; Garon *et al.* 2007). For example, QDs conjugated with polyclonal anti-mouse antibodies used in immunofluorescent detection of three-dimensional confocal analysis of p-glycoprotein was found to be 420-fold more resistant to photo-bleaching than its labelling with conventional organic fluorophores such as fluorescein isothiocyanate (FITC), R-phycoerythrin and Alexa Fluor 488 (Sukhanova *et al.* 2004).

The resistance to metabolic degradation and bleaching in combination with high quantum yields of the QDs confer advantages for *in vivo* targeting and imaging of cells over organic dyes (Akerman *et al.* 2002; Ballou 2005; So *et al.* 2006). For example, cancer cells and mouse tissues have been detected successfully with QDs (Ballou *et al.* 2004; Gao *et al.* 2004). Multiple compartments and specific antigens such as the membrane protein erbB2 (Her2), microtubules, actin and nuclear antigen have been labelled with QDs in both live and fixed cells and in tissue sections, demonstrating their photo-stability and superior sensitivity compared with organic dyes (Wu *et al.* 2003; Zhang *et al.* 2008).

Active receptors from the cell surface have been tracked for the first time using QDs on vesicular trafficking and fusion of living cells by endocytosis (Lidke *et al.* 2004; Giepmans *et al.* 2005; Howarth *et al.* 2005). The signal of the QDs in those studies was monitored continuously for long periods of time up to 60 min (Lidke & Arndt-Jovin 2004).

External labelling with QDs has been proven to be relatively simple, but intracellular delivery of QDs has many limitations due to the final size of the QD complexes in

comparison with organic fluorophores (Dahan *et al.* 2003). Several methods have been used to deliver QDs into the cytoplasm for staining of intracellular structures such as microinjection techniques to label embryos for fluorescent labelling of cellular proteins (Dubertret *et al.* 2002; Rieger *et al.* 2005). Although the uptake of QDs into cells via both endocytic and non-endocytic pathways has been demonstrated, it normally results in only an endosomal localisation (Hanaki *et al.* 2003; Jaiswal *et al.* 2003).

4.1.2. Gene technology

The fact that several QDs can be excited by the same excitation source is highly valuable for multiplexing and high-throughput screening of multiple targets simultaneously (Chan *et al.* 2002). QDs conjugated to oligonucleotide sequences have been used to bind DNA or mRNA (Gerion *et al.* 2002; Crut *et al.* 2005; Liang *et al.* 2005; Mahtab *et al.* 2007). Some of the results found in those studies when targeting QDs to small sequences of oligonucleotides suggested that QDs could be used to produce more efficient assays, requiring smaller quantities of DNA, than traditional techniques, for example, in nucleotide polymorphism assays (Xu *et al.* 2003). In addition, the study of single DNA molecules using conventional DNA staining agents has the drawbacks of photo-bleaching over time and changes in the electrostatic, structural and mechanical properties of the DNA (Kabata *et al.* 1993). Alternatively, the use of QDs for the study of single DNA molecules in the absence of DNA-binding organic fluorophores has overcome these issues, resulting in a 60% successful detection frequency (Crut, *et al.* 2005).

Molecular beacons or hairpins have been designed to conjugate QDs to different molecules such as DNA or oligonucleotides for detection by fluorescence resonance energy transfer (FRET), resulting in a high sensing responsiveness (Williard *et al.* 2001; Zhou *et al.* 2005; Medintz *et al.* 2006; Algar & Krull 2007; Wang *et al.* 2008). FRET involves the transfer of fluorescence energy from a donor particle to an acceptor whenever the distance between the donor and the acceptor result in an increase in the acceptor's emission intensity (Riegler & Nann 2004). QDs linked to DNA probes have been reported to be able to detect 50 copies or less of target DNA by FRET (Zhang *et al.* 2005).

4.1.3. Bacterial, pathogen and toxin detection

Traditionally, the detection of pathogenetic bacteria has been done using organic fluorophores and luminescent enzymes such as luciferase (Loessner *et al.* 1996). However, these fluorophores have two major limitations: sensitivity and rapidity due to low signal-to-noise ratio, and low photo-stability. The use of QDs instead of organic fluorophores for bacterial and pathogen detection has been reported to overcome some of these issues. For example, QDs conjugated to phages has provided the specific detection of as few as 10 bacterial cells per millilitre, with a 100-fold amplification signal over background in 1 h (Edgar *et al.* 2006).

The first use of QDs for bacterial labelling was reported by Kloepfer *et al.* (Kloepfer *et al.* 2003). QDs have been used since for labelling, detection and quantification of *Mycobacterium bovis* (Otsuka *et al.* 2004), *Escherichia coli* O157:H7 (Su & Li 2004; Li *et al.* 2006), *Salmonella enterica* (Yang & Li 2005; Yang & Li 2006), *Cryptosporidium parvum* and *Giardia lamblia* (Lee *et al.* 2004), *Listeria monocytogenes* (Tully *et al.* 2006) and human oral bacteria in biofilms (Chalmers *et al.* 2007). Simultaneous multiplexed labelling of both *C. parvum* and *G. lamblia* using QDs as immunofluorescent fluorophores was reported to have a high signal-to-noise ratio, with better photo-stability and brightness compared with two commonly used staining kits (Zhu *et al.* 2004). However, mixed results have been reported when using QDs for bacterial and pathogen detection. For example, immunofluorescence staining of *Cryptosporidium* with QDs, compared to organic fluorophores such as FITC, Alexa Fluor 488 and phycoerythrin, revealed that non-specific binding to detrital particles by the QDs was significantly higher than organic fluorophores and the fluorescent signal was up to 35 times less than organic fluorophores (Ferrari & Bergquist 2007).

Recently, it has been reported that there are several pitfalls regarding the use of QDs for biological applications, such as blinking and quenching effects which may reduce their potential (Jaiswal & Simon 2004). Moreover, despite the large list of potential biological applications described, the use of QDs on a large scale in many areas replacing conventional tools is still far away. Full characterisation of their physical, optical and chemical properties still remains unclear and their commercial development still may need

appropriate regulations (Azzazy *et al.* 2007). Toxicity of the QDs is becoming a big concern in recent years, especially for applications involving *in vivo* imaging and therapy, as it is unknown if the core of the QDs made of CdSe would have harmful effects on living cells after exposure over extended periods of time (Shiohara *et al.* 2004; Pinaud *et al.* 2006). Therefore, a comprehensive study of the characteristics of the QDs is still needed.

4.2. QDs and flow cytometry

Flow cytometry is a technique for counting, examining and sorting cells and particles suspended in a stream of fluid (Shapiro 1986). The basis of the flow cytometer is a jet of isotonic sheath fluid into which samples are injected at a controlled rate, creating a laminar flow of cells or particles that move in single file into the cytometer (Shapiro *et al.* 1998). One or more laser beams are directed onto the stream of fluid, illuminating a single particle at any given time. If the cells or particles of interest are naturally fluorescent or have been fluorescently-labelled, they will emit light. The signals resulting from the interaction between the cells or particles with the light are detected using a photomultiplier tube and their optical properties are collected and measured on a computer (Shapiro 1993; Wood 1998). The amount of light scattered can provide information on the internal structure of cells as well as their shape, size, granularity and fluorescence (Schwartz *et al.* 1998; Shapiro 2001). Three parameters are generally measured: forward scatter (FCS) which correlates with the cell volume; the side scatter (SSC) which depends on the inner complexity of the cell or particle; and fluorescence (FL) (Shapiro 1986; Shapiro 2004). The detectors, filters and the light source vary depending of the flow cytometer used (van den Engh & Stokdijk 1989; Roederer 2001). Some flow cytometers are capable of sorting cells or particles from the main fluid stream while collecting their optical characteristics (Fulwyler 1980; Britten & Murphy 1986; Shapiro 2000; Ibrahim & van den Engh 2003; Ibrahim & van den Engh 2007).

Flow cytometry has been widely used in many applications and scientific fields from clinical techniques to environmental microbiology (Page & Burns 1991; van den Engh 1993; Porter *et al.* 1997; Ferrari *et al.* 2000; Morgan *et al.* 2004). In addition, flow cytometry has been used in combination with FISH for identification and estimation of

microorganisms from mixed microbial communities (Amann *et al.* 1990a; Wallner *et al.* 1993; Simon *et al.* 1995; Wallner *et al.* 1995). FISH has also been used in combination with cell sorting for the isolation of microorganisms, detection of DNA sequences in nuclei and quantification of chromosome-specific DNA (Trask *et al.* 1985; Trask *et al.* 1988; Kalyuzhnaya *et al.* 2006).

Multicolour optical coding using QDs offers important advantages that are not possible with conventional dyes in applications for microsphere-based analyses in environmental microbiology. Up to now, there have been only isolated reports of QD applications for flow cytometric analyses (Abrams & Dubrovsky 2007). For example, QDs have been used for bacterial and pathogen detection in combination with flow cytometry (Edgar *et al.* 2006; Ferrari & Bergquist 2007). Moreover, the multiplexing capabilities of the QDs have been used to analyse the phenotype of multiple antigen-specific T-cell populations as the QDs were able to resolve up to 17 different fluorescence emissions (Chattopadhyay *et al.* 2006).

5. Aims of this study

The first aim of this thesis is to do a survey of the microbial diversity and ecology of White Island using culture-dependant and molecular-based techniques in order to obtain a general picture of the extremophilic microorganisms present within this sulphur-rich hydrothermal system.

The second aim of this thesis is to describe, develop and optimise a novel bead-based technique to detect specific DNA sequences from environmental samples using quantum dots in combination with flow cytometry. The technique was aimed to provide a rapid and highly sensitive method to determine the key microbial species present within a specific habitat such as White Island.

Chapter II. Materials and Methods

1. MATERIALS

1.1. Chemicals and biochemicals

All chemicals were supplied by Sigma[®] - Aldrich (St. Louis, USA) except those chemicals and biochemicals described in Table II.1

Table II.1: Suppliers of chemicals and biochemicals.

Chemical	Supplier
Agar, bacteriological	Oxoid, Basingstoke (UK)
Agarose I, biotech grade	AMRESCO Inc., Solon (USA)
Ammonium sulfate	Riedel-de Haën, Seelze (Germany)
Boric acid	AMRESCO Inc., Solon (USA)
Calcium Nitrate-4-hydrate	Riedel-de Haën, Seelze (Germany)
Chloroform	Univar, Ajax Finechem, Seven Hills (Australia)
Citifluor A1	Citifluor Ltd, London (UK)
Citifluor AF-3	Citifluor Ltd (UK)
EDAC (1-Ethyl-3-(3-dimethyl-aminopropyl)carbodiimide Hydrochloride)	Pierce, Rockford, IL (USA)
Ethanol	Univar, Ajax Finechem, Seven Hills (Australia)
EDTA, anhydrous	AMRESCO Inc., Solon (USA)
Formamide, deionised	AMRESCO Inc., Solon (USA)
Gelatine	Oxoid, Basingstoke (UK)
IPTG (Isopropyl- β -D-thiogalactoside)	Progen Biosciences, Archerfield (Australia)
Isopropanol	Biolab Ltd., Auckland (New Zealand)
Molecular biology grade H ₂ O	Eppendorf AG, Hamburg (Germany)
Nucleotides (dATP,dGTP,dCTP,dTTP)	GE Healthcare, Buckinghamshire (UK)
Paraformaldehyde	Riedel-de Haën, Seelze (Germany)
Phenol, buffer saturated	AMRESCO Inc., Solon (USA)
SDS (Sodium Dodecyl Sulfate)	AMRESCO Inc., Solon (USA)
Sodium Chloride	Univar, Ajax Finechem, Seven Hills (Australia)
Tris (hydroxymethyl) aminomethane (Tris base)	AMRESCO Inc., Solon (USA)
Tris (hydroxymethyl) aminomethane hydrochloride (Tris/HCl)	AMRESCO Inc., Solon (USA)
Yeast Extract	Oxoid, Basingstoke (UK)
X-gal (5'-Bromo-4-Chloro-3-Indolyl- β -D-Galactoside)	Progen Biosciences, Archerfield (Australia)
1kb DNA ladder, Generuler™	Fermentas Life Sciences, St. Leon-Rot (Germany)

1.2. Reaction kits

Table II.2: General molecular biology reaction kits.

Reaction kit	Supplier
Original TA Cloning [®] Kit	Invitrogen, Carlsbad (USA)
QIAprep Spin Miniprep Kit	Qiagen GmbH, Hilden (Germany)
QIAquick PCR Purification Kit	Qiagen GMBH, Hilden (Germany)
Wizard <i>Plus</i> SV Minipreps DNA purification system	Promega (Madison, USA)

1.3. Enzymes

Table II.3: General molecular biology enzymes.

Enzyme	Supplier
AmpliTaq Gold [®] DNA polymerase, including reaction buffer and MgCl ₂ solution	Applied Biosystems, Foster City (USA)
BigDye [®] Terminator, sequencing RR100, v3.01, including reaction buffer	Applied Biosystems, Foster City (USA)
<i>Dde</i> I, including reaction buffer	New England Biolabs, Inc. (Ipswich, USA)
<i>Bsu</i> RI Endonuclease, including reaction buffer	Fermentas Life Sciences, St. Leon-Rot (Germany)
<i>Hin</i> fI Endonuclease, including reaction buffer	Fermentas Life Sciences, St. Leon-Rot (Germany)
<i>Hin</i> P1I, including reaction buffer	New England Biolabs, Inc. (Ipswich, USA)
Lysozyme	Boehringer Mannheim (Germany)
Mutanolysin	Sigma [®] -Aldrich, St. Louis (USA)
<i>S. griseus</i> protease	Sigma [®] -Aldrich, St. Louis (USA)
RNAase A	Sigma [®] -Aldrich, St. Louis (USA)

1.4. Consumables

Table II.4: General consumables used throughout this thesis.

Consumable	Supplier
Cover slips, 22x22 mm and 24x50 mm	Menzel-Gläser, Braunschweig (Germany)
Diagnostic slides, 6-well epoxy-resin mask	Paul Marienfeld GmnH & Co. KG, Lauda-Königshofen (Germany)
Glassware (bottles, beakers, measuring cylinders)	SCHOTT AG, Mainz (Germany)
Microcon centrifugal filter devices regenerated cellulose 3.000 MWCO	Millipore, Billerica (USA)
Microcon centrifugal filter devices regenerated cellulose 100.000 MWCO	Millipore, Billerica (USA)
Microscopy slides, JIA 7101 WT	Sail Brand (China)
Petri dishes	Sarstedt AG & Co., Nümbrecht (Germany)
Phase Lock Gel [®] light, 2 ml and 15 ml	Eppendorf AG, Hamburg (Germany)
Pipette tips, Pagoda [™]	Labcon, Petaluma (USA)
Pipette tips, Diamond [®] D10	Gilson, Middleton (USA)
pH indicator strips	Sigma [®] -Aldrich, St., Louis (USA)

Quartz cells 10 mm (capacity 3 ml)	Hellma GmbH & Co., Müllheim (Germany)
Reaction tubes, 0.5 ml and 1.5 ml	Sarstedt AG & Co., Nümbrecht (Germany)
Reaction tubes, PCR, 0.2 ml	Sarstedt AG & Co., Nümbrecht (Germany)
Reaction tubes, PP 15 ml and 50 ml	Greiner Bio-One, Frickenhausen (Germany)
Toothpicks	Alpen Products Pty. Ltd., Brookvale (Australia)
UVette [®] cuvette	Eppendorf AG, Hamburg (Germany)

1.5. Laboratory equipment

Table II.5: General laboratory equipment.

Equipment	Supplier
Balance, BP310S	Sartorius AG, Göttingen (Germany)
Biofuge pio, bench top centrifuge	Heraeus, Hanau (Germany)
BioPhotometer	Eppendorf AG, Hamburg (Germany)
Centrifuge, Eppendorf 5415R, cooling	Eppendorf AG, Hamburg (Germany)
Centrifuge, Eppendorf 5417C	Eppendorf AG, Hamburg (Germany)
Centrifuge, Sigma 3-18K	SIGMA Laborzentrifugen GmbH, Osterode (Germany)
Centrifuge, Sigma 6K15	SIGMA Laborzentrifugen GmbH, Osterode (Germany)
Chemilmager [™] 4400 digital imaging system	Alpha Innotech, San Leandro (USA)
Gel-electrophoresis system, Mini-Sub Cell GT	Bio-Rad Laboratories, Hercules (USA)
GeneAmp PCR System 2400	Perkin Elmer, Walham (USA)
Hybridisation oven, Hybaid	Termo Fisher Scientific, Waltham (USA)
Hybridisation oven, ProBlot 12S	Labnet International Inc., Edison (USA)
Laboratory incubator	Thermoline, Smithfield (Australia)
Mastercycler gradient	Eppendorf AG, Hamburg (Germany)
Milli-Q [®] Ultrapure Water Purification System	Millipore, Billerica (USA)
Minispin plus, bench top centrifuge	Eppendorf AG, Hamburg (Germany)
Incubator, shaking, Bionline	Edwards Instrument Company, Sydney (Australia)
pH meter, SyrScan 500	Activon Inc., Beaver Dam (USA)
Vortex mixer	Ratek, Wadhurst (Australia)
Water bath	Thermoline, Smithfield (Australia)

2. METHODS

2.1. Buffers and solutions

Reagents were dissolved in ultra-pure H₂O; ionic and organic components were removed through filtration (0.22 µm pore size) with the Milli-Q[®] Ultrapure Water Purification System. Buffers and solutions not listed in Table II.6 are described in specific chapters.

Table II.6: Buffers and solutions.

Sodium phosphate buffer	0.2 M Na ₂ HPO ₄ /NaH ₂ PO ₄ . 0.2 M solutions of both phosphates were prepared separately. Na ₂ HPO ₄ was titrated against NaH ₂ PO ₄ until the desired pH value was reached
1xPBS (Phosphate buffered saline)	130 mM NaCl and 10 mM Phosphate buffer (pH 7.2)
Tris/HCl	1 M Tris base. pH adjusted to the desired value with concentrated HCl prior to autoclaving
EDTA, pH 8	250 mM EDTA, disodium salt. EDTA dissolved in H ₂ O. pH adjusted with 5 N NaOH
TE buffer	10 mM Tris/HCl (pH 8) and 1 mM EDTA (pH 8)
TBE buffer (10x)	0.9 M Tris base, 0.89 M Boric acid and 40 ml of 0.5 M EDTA (pH 8) were combined. The 10x solution was diluted 1:10 in deionised H ₂ O prior to use
FISH hybridisation buffer	0.9 M of NaCl, 100 mM Tris-HCl (pH 7.2), 35% formamide (v/v) and 0.1% of sodium dodecyl sulfate (SDS)
FISH washing buffer	100 mM Tris-HCl (pH 7.2), 0.18 M NaCl and 0.1% of SDS (v/v)

Table II.7: General solutions

Loading dye, Type III (6x)	0.25% (v/v) Bromophenol blue, 0.25% (v/v) Xylene cyanol and 30% Glycerol
30% Paraformaldehyde stock solution	1.5 g of Paraformaldehyde, 3.3 ml of H ₂ O MilliQ water, 15 µl of 5 M of NaOH, 1.65 ml of 3xPBS, and 10-15 µl of 2 M HCl. Paraformaldehyde was mixed with H ₂ O and NaOH and

	heated to 60°C until clear. After cooling to RT, 3xPBS was added and pH adjusted to 7 with HCl. After filtration through a cellulose filter, the solution was stored at 4°C for up to 7 days
Nucleotide mixture	10 µl of each: dATP, dCTP, dGTP, dTTP into 360 µl of molecular biology grade H ₂ O
SDS buffer	20 mM Tris/HCl (pH 7.8), 1 M NaCl, 1 mM EDTA and 0.02% SDS
6 x SSC	0.09 M Sodium citrate and 0.9 M NaCl. Final pH adjusted to 7 using concentrated HCl
50 x Denhardt's Mix	1% (w/v) of Ficoll, 1% (w/v) of Polyvinyl pyrrolidone (PVP) and 1% (w/v) of Bovine Serum Albumen (BSA). The solution was filtered using 0.22 µm pore filters and stored at -20°C

2.2. Sterilisation of reagents

Liquid solutions: culture media, buffer and stock solutions were steam-sterilised by autoclaving for 20 min at 121°C and 200 kPa pressure.

Solid items: glassware, sampling tools, pipette tips, reaction tubes and plastic bottles were autoclaved for 40 min under the same conditions as the liquid solutions.

Organic or heat-sensitive inorganic solutions were sterilised by filtration through cellulose-acetate filters (0.2 µm pore size).

2.3. Culture media

Table II.8: General media used for cultivation.

LB Broth	Tryptone	1% (w/v)
	Yeast extract	0.5% (w/v)
	NaCl	1% (w/v)
LA Agar	Tryptone	1% (w/v)
	Yeast Extract	0.5% (w/v)
	NaCl	1% (w/v)
	Agar, Bacteriological	15% (w/v)

2.4. Microscopy

2.4.1. Light microscopy

The phase contrast Olympus BH-2 light microscope (Olympus Corporation, Japan) equipped with oil objective A100 PL 1.30 160/0.17 was used to monitor microbial growth.

2.4.2. Fluorescence microscopy

Fluorescence microscopes are used to study the properties of organic or inorganic substances using the phenomenon of fluorescence and phosphorescence. The basis of a fluorescence microscope is to illuminate a sample at a specific wavelength which is absorbed by the fluorophore, causing the emission of light at a longer wavelength than the excitation light. Fluorescence microscopes are equipped with emission filters to separate the illumination light from the emitted light of the fluorophore, excitation filters and dichronic mirrors. The light source is usually a xenon arc lamp or mercury-vapour lamp.

2.4.2.1. Fluorochromes

Table II.9: General fluorochromes used throughout this thesis. Fluorochromes were supplied by Invitrogen Corporation (Australia).

Fluorochrome	Maximum excitation	Maximum emission	Application
Alexa Fluor 488	488 nm	519 nm	FISH
FITC	488 nm	520 nm	FISH
Cy3	552 nm	565 nm	FISH
DAPI	358 nm	461 nm	Staining ds DNA
Rhodamine Green	502 nm	527 nm	FISH

2.4.2.2. Epi-fluorescence microscopy

The excitation light of an epi-fluorescent microscope is passed from above through the objective and then onto the sample instead of passing first through the sample. In a conventional epi-fluorescence microscope, a short wavelength light is reflected by a

chromatic reflector through the objective and bathes the whole of the specimen in fairly uniform illumination. The chromatic reflector has the property of reflecting short wavelength light and transmitting longer wavelength light. Emitted fluorescent light from the specimen passes straight through the chromatic reflector to the eyepiece.

Epi-fluorescence microscopy was performed with an Olympus BH2-RFC microscope (Olympus Corporation, N.Y., USA) with a universal condenser for Nomarski differential interference contrast (DIC) and a mercury burner for broad band excitation (Olympus BH2-RFL-T3). The microscope was equipped with a 100x oil immersion objective with numeric aperture 1.3 (A100 PL 1.30 oil 160/0.17). The microscope features dichronic mirrors with different sets of excitation and barrier filters which reflect short radiation wavelengths towards the objective to illuminate the specimen, while passing longer wavelengths (selection of filters in Table II.10). Images were obtained and processed using a Nikon DXM 1200F digital camera (Nikon Corporation, Tokyo, Japan) and Nikon ACT-1 software package v.2.62.

Table II.10: Filter set used in the epi-fluorescence microscope.

Fluorochrome	Dichroic mirror	Excitation filter	Emission filter
Alexa Fluor 488, Rhodamine Green, FITC	DM500	20 BP 490	17 O 515
Cy3	DM570	20 BP 545	17 O 590
DAPI	DM400	20 UD 1	17 < 420

2.4.2.3. Confocal laser scanning microscopy

Confocal laser scanning microscopy (CLSM) is a technique used to increase micrograph contrast and/or to reconstruct three-dimensional images by using a spatial pinhole to eliminate out-of-focus light or flare in specimens that are thicker than the focal plane (Sugita & Tenjin 1993).

CLSM was performed using an Olympus FluoView 300 (Olympus Corporation, Japan) equipped with an inverted microscope with a universal condenser (Olympus IX70) and three lasers (Melles Griot, Carlsbad, USA): Argon laser (488 nm excitation wavelength),

Helium Neon green laser (543 nm excitation wavelength) and a Helium Neon red laser (633 nm excitation laser). Samples were examined using a 100x oil immersion objective with numeric aperture 1.35. Images were obtained and processed using Olympus software Fluoview v.4.3.

Table II.11: General characteristics of the confocal laser scanning microscope.

Fluorochrome	Excitation wavelength	Filter
Alexa 488	488 nm – Argon laser	BA 510 IF and BA530 RIF
Cy3	543 nm – HeNe laser	BA 510 IF

2.5. Flow cytometry

All samples were placed in BD Falcon™ Round Bottom tubes (BD Biosciences, Sydney, Australia) for analyses by flow cytometry.

2.5.1. BD LSI Flow cytometer

BD LSR I (BD Biosciences, Sydney, Australia) is a modified 6 colour, 4 laser flow cytometer. The primary laser was an argon-ion 488 nm with 20 mW power output. The second laser was a Helium-cadmium 325 nm (UV) laser with 8mW power output, the third was a Helium-Neon 633 nm (red) 17 mW power output laser and the fourth laser was a 594 nm (yellow) Helium-Neon. This instrument was housed in a facility at the Prince of Wales Public Hospital (Sydney, Australia). The detectors used were side scatter (SSC), FL3 with 620SP as steering optics and 670LP as a filter and FL4 with 510LP as steering optics, and the filter 660/13 nm.

2.5.2. BD FACS-Calibur Flow cytometer

Flow cytometric analysis was performed using a BD FACS-Calibur flow cytometer equipped with a 488 nm air-cooled argon-ion laser for excitation (BD Biosciences). Sheath fluid consisted of diluted Osmosol (Lab Aids Pty Ltd, Narrabeen, NSW, Australia).

The detectors used were: side scatter (SSC) with the voltage set at 150 V: forwards scatter (FSC) E00. Fluorescence detectors, FL1, FL2 and FL3 varied between fluorophores. Green fluorescence (FITC, Alexa Fluor 488, QD525 and QD535) was detected using FL1, 530/30 nm band-pass filter and 474 V. Orange fluorescence (R-PE and QD585) was detected using FL2, 585/42 nm band-pass at 520 V filter and red fluorescence (QD680) using FL3, 650 nm long-pass filter at 520 V. Regular instrument calibration was carried out using two-colour BD Calibrate™ beads as recommended by the manufacturer.

Unlabeled Dynabeads were used for instrument setup using a portion (normally 10 µl) of washed unlabelled Dynabeads diluted in 300 µl BW buffer. Unlabeled Dynabeads were analysed on a bivariate dot-plot of FSC channel versus SSC channel thresholding on FSC. As single colour detection only was being analysed, compensation was set at zero. A data file containing 2,000 events was collected for all analyses.

2.5.3. Data acquisition and analysis

The data generated by the flow cytometer was plotted as one or two parameter histograms. A one-parameter histogram is a graph of cells or particles counted on the y-axis and the measurement parameter on the x-axis. A two parameter histogram or bivariate dot-plot is a graph representing two measurement parameters, on the x- and y-axes, and cell or particle count height on a density gradient (Pinkel & Steen 1982). Data analysis was carried out with CellQuest software (BD Biosciences, Sydney, Australia) and processed using the program WinMDI v.2.8 available on the World Wide Web (<http://facs.scripps.edu/software.html>).

2.6. Molecular analyses

2.6.1. DNA concentration and quantification

2.6.1.1. Gel electrophoresis

PCR products and genomic DNA were analysed by gel electrophoresis. In all procedures, unless it is stated otherwise, 5 µl of sample was mixed with 2 µl of loading dye (6x) and

run on a 1% agarose gel (w/v). Each gel was prepared in 1xTBE buffer containing 5 µg EtBr/100 ml. The gel was subjected to electrophoresis for 30 min at 100 V in 1xTBE buffer containing 50 µg EtBr/l. After electrophoresis, the gel was visualised under UV excitation using a Chemilmager 4400 digital imaging system (Alpha Innotech, San Leandro, USA). GeneRuler 1 kb DNA ladder or 1kb DNA ladder plus were used as DNA standards to determine fragment sizes and estimate product yields.

2.6.1.2. Spectrophotometry

Spectrophotometry is a simple method to quantify ds-DNA, ss-DNA and RNA. An absorbance ratio of 260 nm and 280 nm gives an estimate of the purity of the solution. Pure DNA and RNA solutions have OD₂₆₀/OD₂₈₀ values of 1.8 and 2.0 respectively. However, this method is not useful for small quantities of DNA or RNA (<1 µg/ml). A ratio less than 1.8 indicates that there may be proteins and/or other UV absorbers in the sample, in which case the DNA requires another precipitation and washing step. A ratio higher than 2.0 indicates the samples may be contaminated with chloroform or phenol and should be precipitated with ethanol. For all readings, the following procedure was followed unless stated otherwise: the ds- or ss-DNA sample was diluted 1:20 times in TE buffer or sterile Milli-Q H₂O with a final volume of 100 µl. The equipment was calibrated using 100 µl of TE buffer or sterile Milli-Q H₂O as a blank. Clean UVette[®] cuvettes were used for all measurements.

2.6.2. Polymerase chain reaction (PCR)

Polymerase chain reaction (PCR) amplification of 16S ribosomal RNA genes was carried out using the primers described in Table II.12.

Table II.12: 16S rRNA gene specific primers for PCR amplification. All primers were synthesised and purified by Sigma-Genosys (Sigma-Aldrich Pty. Ltd., Castle Hill, Australia). The primers were dissolved in sterile TE buffer to a final concentration of 100 µM and stored at -20°C. The position of the primers indicates the position relative on the *E. coli* 16S rRNA gene (Brosius *et al.* 1978).

Primer	Position*	Sequence 5' → 3'	Specificity	Reference
PB36	11-30	AGR GTT TGA TCM TGG CTC AG	Bacteria	(Saul <i>et al.</i> 1993)
PB38	1534-1551	GKT ACC TTG TTA CGA CTT	Universal	(Bell <i>et al.</i> 2002)
1406uR	1390	ACG GGC GGT GTG TRC AA	Universal	(Lane 1991)
16SR2	1125-1146	GCG CTC GTT GCG GGA CTT AAC C	Bacteria	(Sunna & Bergquist 2003)
16SF1	539-560	TGC CAG CAG CCG CGG TAA TAC G	Bacteria	(Sunna & Bergquist 2003)
ASF	334	CGA GGC CCT ACG GGG CGC A	Archaea	Saul, pers. comm.
ASR	1398	GTG TGC AAG GAG CAG GGA C	Archaea	Saul, pers. comm.
Arch21F	21	TTC CGG TTG ATC CYG CCG GA	Archaea	(DeLong <i>et al.</i> 1989)
1044aF	1044	GAG AGG WGG TGC ATG GCC G	Archaea	(Burggraf <i>et al.</i> 1994)
pCR21F	/	GCC GCC AGT GTG CTG GA	Vector pCR [®] 2.1	Anitori, pers. comm.
pCR21R	/	GTG ATG GAT ATC TGC AGA	Vector pCR [®] 2.1	Anitori, pers. comm.
M13F	/	GTT TTC CCA GTC ACG A	Vector pCR [®] 2.1	Invitrogen
M13R	/	GGA AAC AGC TAT GAC CAT G	Vector pCR [®] 2.1	Invitrogen

Table II.13: Specific amplification conditions for individual primer combinations.

Target gene	Forward primer	Reverse primer	Anneal. Temp.*	Cycles	Positive control
Bacterial 16S rRNA	PB36	PB38	50°C	30/35	<i>E. coli</i>
Bacterial 16S rRNA	PB36	1406uR	50°C	30/35	<i>E. coli</i>
Archaeal 16S rRNA	ASF	ASR	55°C	30/35	<i>Archaeoglobus fulgidus</i>
Archaeal 16S rRNA	ASF	1406uR	55°C	30/35	<i>A. fulgidus</i>

* Annealing temperature

† Polymerisation time

All the reactions were prepared using aerosol filter tips and 0.2 µl reaction tubes or 96-well plates. The total volume of the PCR reactions was 50 µl. The DNA template volume for the PCR reaction was calculated depending on its concentration (10-100 ng) and added to the mixture after the PCR reaction master-mix was prepared (Table II.14).

Table II.14: PCR reaction mixtures for bacterial and archaeal 16S rDNA amplification.

Component	Bacterial 16S rRNA	Archaeal 16S rRNA
Sterile Milli-Q water	26.8 – 30.8 µl	28.8 – 32.8 µl
10x Taq buffer	5 µl	5 µl
MgCl ₂ solution (25 mM)	6 µl	4 µl
dNTP mix (2.5 mM each)	5 µl	5 µl
Forward primer (10 mM)	1 µl	1 µl
Reverse primer (10 mM)	1 µl	1 µl
AmpliTaq Gold polymerase (5 U/µl)	0.2 µl	0.2 µl
DNA template (10 – 100 ng)	1 – 5 µl	1 – 5 µl

All experiments included a negative control without DNA and a positive control containing purified bacterial DNA (*E. coli*) or archaeal DNA (*Archaeoglobus fulgidus*). Table II.15 describes the general PCR amplification protocol.

Table II.15: PCR amplification protocol.

Steps	Time	Temperature for bacterial PCR	Temperature for archaeal PCR	Number of cycles
Initialising	15 min	94°C	94°C	1
Denaturing	30 s	94°C	94°C	30 - 35
Annealing	30 s	50°C	55°C	
Polymerisation	2 min	72°C	72°C	
Final elongation	5 min	72°C	74°C	1
Hold	∞	4°C	4°C	

The resulting PCR amplicons were purified using the QIAquick PCR Purification Kit. The final products were stored at 4°C until further use.

2.6.3. Sequencing and sequence data analysis

Amplified genomic DNA or recombinant 16 S rRNA genes in plasmids were sequenced by the chain-termination method using BigDye Terminator (v3.01, Applied Biosystems, Foster City, USA) and the bacterial 16S RNA specific primers or the vector-specific primers described above (Table II.12).

Table II.16: Sequencing reaction.

Reagents	Volume
Plasmid DNA or PCR product	350 – 500 ng or 100 – 150 ng (respectively)
5x sequencing buffer	1.5 µl
BigDye Terminator	1 µl
Primer (3.2 pmol/µl)	1 µl
H ₂ O	Add to 20 µl

Table II.17: Standard protocol for sequencing reactions.

Steps	Time	Temperature	Number of cycles
Denaturing	10 s	96°C	25
Annealing	5 s	50°C	
Polymerisation	4 min	60°C	
Hold	∞	4°C	

The products obtained after the sequencing reaction (Table II.17) were cleaned and precipitated using different protocols depending on the analysis facility used for sequencing. Products to be analysed at the Automated DNA Analysis Facility, University of New South Wales (Sydney, Australia) were transferred to clean 1.5 ml reaction tubes. The products were mixed with 16 µl of sterile Milli-Q H₂O and 64 µl of EtOH (99%) and vortexed briefly. After incubation at RT for 45 min and centrifugation for 45 min (16,000 rpm, 4°C, Sigma 3-18K) the supernatant was removed completely. The pellets were washed in 250 µl of 70% (v/v) EtOH and centrifuged for 10 min. The supernatant was discarded and the pellets dried for several min at 70°C. Sequencing reactions were analysed using an ABI-Prism 96-capillary 3730DNA Analyser (Applied Biosystems).

Products to be analysed at the DNA Analysis Facility, Macquarie University (Sydney, Australia) were mixed with 4 µl of 3 M NaOAc (pH 5) and 12 µl of sterile Milli-Q H₂O. The products were transferred to 0.5 ml Eppendorf tubes and mixed with 64 µl of EtOH (95%). After incubation at RT for 10-15 min and centrifugation for 20 min (13,000 rpm, Sigma 3-18K), the supernatant was removed completely. The pellets were washed as described above and the final sequencing reactions were analysed using an ABI-Prism 377 Sequencer (Applied Biosystems).

2.6.4. Fluorescent *in situ* hybridisation (FISH)

2.6.4.1. Oligonucleotide probes

Oligonucleotide probes were synthesised and purified by MWG-Biotech AG (Ebersberg, Germany) and Sigma-Proligo (Sigma-Aldrich Pty., Castle Hill, Australia). Lyophilised probes were dissolved in 100 µl of sterile TE buffer. Stocks solutions were stored at -80°C. Working solutions were diluted in sterilised Milli-Q water to a final concentration of 50 ng/µl and stored at -20°C. Domain-specific probes generally were used as mixtures, called EubMix (Eub338I, 50 ng/µl and Eub338II/III, 100 ng/µl) and ArchMix (Arch344, arch915 and Arch1060, 50 ng/µl each). EubMix was labelled with Alexa Fluor[®] 488, while ArchMix was labelled with Cy3. Euk502 was modified with a biotin group at the 5' position (Table II.18).

Table II.18: Binding position, sequence and specificity of oligonucleotide probes.

Oligo-nucleotide	Position*	Sequence 5' → 3'	Specificity	Reference
Eub338I	338	GCT GCC TCC CGT AGG AGT	Bacteria	(Amann <i>et al.</i> 1990a)
Eub338II/III	338	GCW GCC ACC CGT AGG TGT	Bacteria	(Amann <i>et al.</i> 1990a)
Arch344	344	TTC GCG CCT GST GCR CCC CG	Archaea	(Moissl <i>et al.</i> 2003)
Arch915	915	GTG CTC CCC CGC CAA TTC CT	Archaea	(Stahl & Amann 1991)
Arch1060	1044	GGC CAT GCA CCW CCT CTC	Archaea	(Moissl <i>et al.</i> 2003)
Euk502	502**	ACC AGA CTT GCC CTC C	Eucarya	(Alm <i>et al.</i> 1996)

* Position relative to the *E. coli* 16S rRNA gene

** Position relative to the *E. coli* 18S rRNA gene

2.6.4.2. Preparation of microscopy slides

Diagnostic glass slides with a 6-well epoxy-resin mask (Paul Marienfeld GmbH & Co, KG, Lauda-Königshofen, Germany) were cleaned by several washes with detergent followed by rinsing with deionised water and wiping with acetone. After air-drying, slides were briefly dipped into hot gelatine solution (0.1% gelatine, 0.01% KCr (SO₄)₂ w/v) at approximately 70°C. The slides were dried at RT in a vertical position. Coated slides were stored in a dust-free environment for up to one year.

2.6.4.3. Control organisms

Microbial strains used as a positive control for FISH were the bacterium *E. coli* (bacteria) and the euryarchaeon SM1 (Moissl *et al.* 2003). *E. coli* strain DH5 α was purchased from Life Technologies (Invitrogen, Carlsbad, USA). *E. coli* was grown in LB broth medium at 37°C with shaking at 250 rpm under aerobic conditions. Microbial growth was monitored by light microscopy and cell numbers were estimated and recorded as cells per field of view. To subculture actively growing cultures, 250-200 μ l was transferred aseptically to 15-20 ml of fresh media (1:100 dilution). Fixed SM1 euryarchaeon was kindly provided by Dr. Ruth Henneberger (Macquarie University, Australia).

2.6.4.4. Preparation of samples

Actively growing microbial cultures of control organisms and samples were fixed by adding 1/10 volume of 30% (w/v) paraformaldehyde stock solution directly to the culture (end concentration 3% (w/v)). After incubation at RT for 1 h or at 4°C overnight, the cells were centrifuged for 10 min and the supernatant was removed completely. The cell pellet was resuspended in 1 ml of 1 x PBS, centrifuged for 10 min and the supernatant discarded. This step was done twice and the final pellet was resuspended in 25-50 μ l of 1 x PBS (end concentration of cells approx. 10⁸/ml). Finally, one volume of 100% EtOH was added to the samples and the fixed cells were stored at -20°C.

2.6.4.5. Hybridisation conditions

A portion of a fixed culture (10-50 μ l) was spotted onto the wells of pre-treated microscope slides without scratching the slide's surface. After air-drying, the cells were dehydrated in an increasing ethanol series (50%, 80% and 99% (v/v) in H₂O) for 3 min each. The slides were dried at RT and then, 8 μ l of FISH hybridisation buffer was applied to each well. The slides were placed horizontally in 50 ml hybridisation chambers (reaction tubes with screw caps containing moist tissues). After pre-hybridisation for 15 min at 46°C, the slides were placed on a preheated pad or heating block (37°C) and the probes added to each well. 50 ng of each probe was applied to the control cultures, and 50-100 ng of each probe was used for the samples. The slides were subsequently hybridised for 4 h at 46°C. Approximately 3 ml of preheated (48°C) FISH washing buffer was used to briefly rinse the slides before they were placed in 50 ml reaction tubes containing the same buffer. The slides were washed for 15 min at 48°C (rotating, 100 rpm), rinsed with cold, deionised water and air-dried in the dark. For DNA-specific counterstaining, 10 μ l of DAPI solution (1 ng/ml in 0.01 M Tris/HCl, pH 7.2) was applied to each well and incubated in a moist chamber for 5 min. The slides were washed, dried, mounted and stored as described earlier. Positive controls for every probe or probe mixture were included in each hybridisation reaction.

2.6.4.6. FISH reactions in microcentrifuge tubes

FISH reactions using 1.5 ml Eppendorf microcentrifuge tubes instead of microscope slides were performed on *E. coli* (control organism) in experiments carried out using quantum dots as fluorophores. The hybridisation conditions were the same as described earlier except Eppendorf tubes were used instead of slides. A portion (5 μ l) of pre-fixed *E. coli* cells were transferred into clean 1.5 ml Eppendorf tubes. The cells were dehydrated in an increasing ethanol series (50%, 80% and 99% (v/v) in H₂O). 50 μ l of each concentration was added to the tubes and incubated for 1 min followed by centrifugation for 3 min at 5,000 rpm. The supernatant was discarded after each step. After dehydration, the pellet was resuspended in 50 μ l of FISH hybridisation buffer (0.25% of SDS, 20% Formamide, 0.9M of NaCl and 10 mM of Tris-HCl pH 7.2) and incubated at 46°C for 15 min in the water bath. 2 μ l of each probe was added followed by another incubation step at 46°C for

3 h. After incubation, the tubes were centrifuged for 5 min at 13,000 rpm. Pellets were resuspended in 50 μ l of pre-heated FISH washing buffer (0.23 M NaCl, 10 mM Tris-HCl pH 7.2 and 0.25% SDS) and incubated at 48°C for 15 min. Another centrifugation step was necessary for 5 min at 13,000 rpm and then, supernatant was discarded. The pellets were resuspended in 50 μ l of TE buffer pH 8. The final products were spotted onto non-treated glass microscopy slides prior to analysis.

Chapter III. Sampling sites and sampling material

1. INTRODUCTION

White Island is the summit of a large (16 by 18 km) submarine volcano which has accreted from the sea floor at 300 m to 400 m depths. Its active subaerial caldera has a vent located below sea level (Houghton & Naira 1991). The volcano is isolated from the sea water by chemically-sealed zones that confine a long-lived acidic hydrothermal system, within a sequence of fine-grained volcanoclastic sediment and ash (Figure III.1.A). It is an andesitic composite volcano which has a sub-aerial extent of about 3.5 km² and hosts an extensive acidic hydrothermal system lined with fumaroles and acid lakes (Giggenbach & Sheppard 1989; Houghton & Naira 1991; Mongillo & Wood 1995; Nishi *et al.* 1996; Wardell *et al.* 2001).

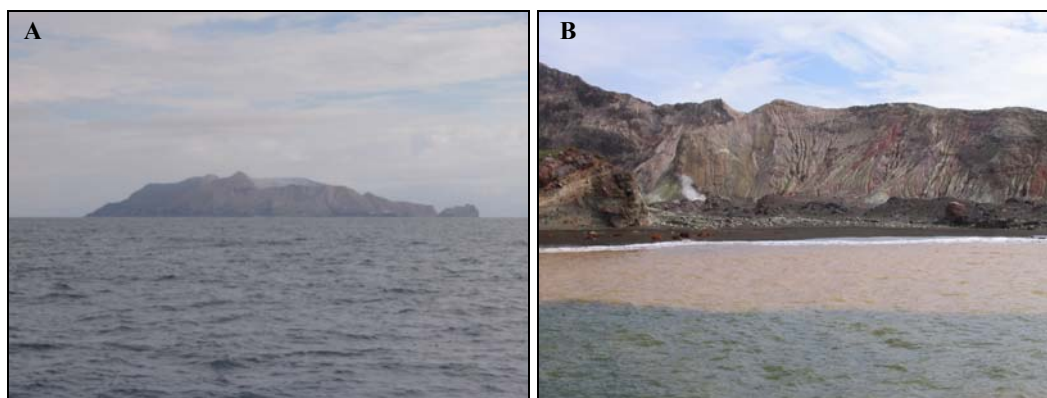
The volcano has a history of frequent small phreatic and phreatomagmatic eruptions, interrupting long intervals of continuous intense fumarolic and hydrothermal activity (Cole & Nairn 1975; Cole *et al.* 2000; Shane *et al.* 2006). Trace-metal distribution in marine sediments around the island indicates that hydrothermal activity has been sustained for at least 10,000 years, presumably driven by a deep magmatic body beneath the volcano (Black 1970; Cole 1981; Giggenbach & Sheppard 1989). The main crater was formed by the collapse of three overlapping subcraters in prehistoric times. In September 1914, the southwest corner of the high crater wall collapsed to produce a hot avalanche at the eastern end of the crater, burying 11 mine workers and the sulphur mine infrastructure.

Noisy Nellie crater was formed in 1947 during an explosive ash eruption (Clark 1970). During 1976 and 1982 there was high volcanic activity in White Island (Houghton *et al.* 1989; Houghton & Nairn 1989a; Houghton & Nairn 1989b; Houghton & Nairn 1989c). Eruptions were caused by the rise of magma beneath the volcano (Christoffel 1989) and the main crater collapsed in 1978 (Clark & Otway 1989; Nairn & Houghton 1989). During 1979-1980, eruptions occurred less frequently as the magma withdrew to deeper levels (Houghton *et al.* 1983). During the volcanic activity from 1976-1982 about 10 million cubic metres of volcanic ash were deposited on the island and offshore

(Giggenbach & Sheppard 1989). Small eruptions during 1983 and 1984 were the only activity prior to a large eruption sequence which occurred from a new vent in the wall of the main crater in 1986. Ash eruptions in 1986 were followed in 1987 by an explosion which threw blocks over the main crater floor. Ash emission was almost continuous into 1988 with occasional larger explosions ejecting blocks of lava. Donald Duck crater was formed in 1988 and the main crater was enlarged by a collapse during a period of heavy rainfall in 1990 (Scott *et al.* 1995).

White Island has had significant eruptions every few years. These are continuing, with several months of ash emission occurring in mid-2000 (Hurst *et al.* 2004). The craters and fumaroles on the island continually emit gases at rates of several hundred to several thousand tonnes per day. The gases are mostly steam, carbon dioxide and sulphur dioxide, with small quantities of chlorine and fluorine. Acid gases combine with water in the steam to form acid droplets and precipitates.

At present, the central subcrater contains the Donald Mount fumaroles, the Noisy Nellie and Donald Duck craters and fumaroles (Figure III.1, C). The western sub-crater is host to most of the surface expression of present-day volcanic hydrothermal activity. Most of the present main crater floor lies less than 30 m above sea level. The currently active vent is a deep pit, at present covered by an enlarging acid lake (Figure III.1, D) filling at approximately 1.5 m per month since spring 2003 as a result of condensation of volcanic gases rising from the submerged vent (Moon *et al.* 2005).



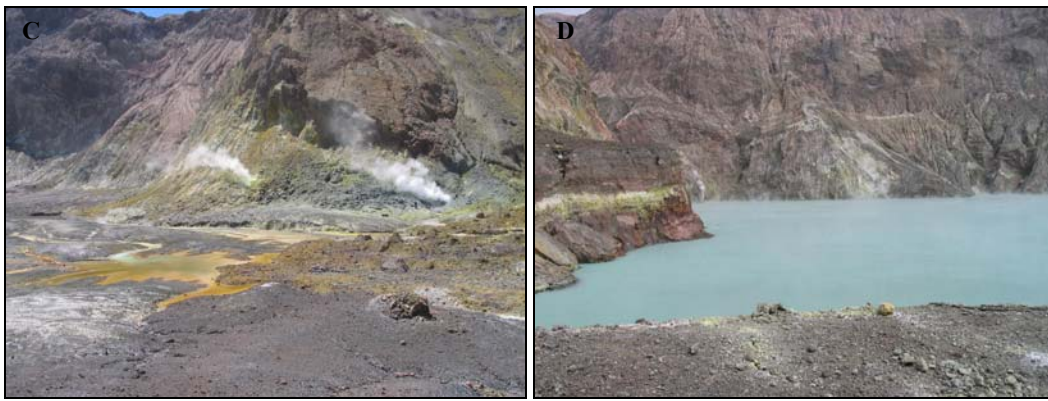


Figure III.1: A: White Island. B: Crater Bay. C: Hydrothermal systems of White Island. D: Main crater.

The geology of the island is of andesite-dacite composition, and includes a complex arrangement of lava flows, breccias, agglomerates, and unconsolidated beds of ash and tuff containing lava blocks (Black 1970). Further details on the geology and geochemical characteristics of White Island can be found in Chapter I.

The aim of this chapter is to describe the sediment and water samples collected from White Island. Ten different sampling sites from the western sub-crater of White Island were selected for microbiological and molecular biological analyses. A detailed description of individual sampling sites, as well as chemical and physical data, was made to obtain a general picture of the environmental characteristics of White Island.

2. MATERIALS AND METHODS

2.1. Sample collection

White Island has a very dynamic hydrosystem environment with regular crater eruptions which change the topography, land surfaces and acid stream courses. For this study, ten different locations from the hydrothermal systems present on White Island were selected in 2004. Sample material was collected aseptically using sterile spatulas and spoons. Sampling equipment was sterilized by soaking with 4% (w/v) sodium hypochlorite for 15–30 min followed by rinsing with sterile MilliQ water prior to autoclaving (II.2.2). All samples were collected using a new sterile tool and fresh latex gloves to avoid cross-contamination between sampling sites.

Water samples were collected in 100 ml or 250 ml sterile tubes using sterile spoons. Multiple sediment samples from representative areas were taken from the surface in bulk by excavating a small hole up to 4 cm deep without separating the surface material and the deeper material to ensure homogeneity of sampling and to recover representative material from the site. Samples were collected in 250 ml or 50 ml sterile tubes. Each location site was sampled at different physical locations with respect to local heterogeneity and portions were collected for physical and chemical analyses and for culturing microorganisms. Additionally, 1 kg of sediment was collected from each sample site for the preparation of the sediment-extract to be used for microbial cultivation purposes.

2.2. Sample handling and storage

Water and sediment samples were placed on ice after collection and kept at 4°C in the dark during transportation to Australia for further processing. For long-term storage, a portion of each sample was mixed with 8% of sterile glycerol (v/v) and immediately frozen by inserting the tubes into 100% ethanol plus dry ice. Revco medium was used also for long-term storage of samples. Revco medium contained: 3.73 g KCl, 0.81 g MgCl₂ x 6 H₂O and 50% glycerol (v/v) with the final pH adjusted to 3.3. A portion of sample material of 1 ml was mixed with 1 ml of sterile Revco medium and frozen immediately as

described earlier. Frozen samples were stored at -80°C. Sample material for chemical analyses was frozen at -20°C within 24 h of collection.

2.3. Physical readings

Physical readings of individual sample sites were taken along with photographs of the general areas and the sampling sites prior- and post-collection. The location of sample sites were determined via Global Positioning System (GPS 12XL, Garmin™, Olathe, USA).

Temperature measurements from the surface of the sample sites and the sample material were performed using a digital thermometer with stainless steel probe (Checktemp-1, HANNA® Instruments, Woonsocket, USA). For surface temperature readings, the probe was held directly onto the surface until a stable reading was obtained. The probe was pushed a few centimetres under the ground to measure temperatures below the surface. Several readings were taken at all sample sites to obtain an average value. Temperatures from the gas steam emitted by the fumaroles were taken with the same thermometer.

Surface pH values were taken with a digital handheld pH probe (ExStick™ PH110, EXTECH® Instruments, Waltham, USA). The pH probe was calibrated following the manufacturer's manual before taking new measurements at the different locational sites with compensation for temperature. The probe was placed directly onto the sediment sample material until a stable value was displayed. After each reading, the probe was cleaned with deionised water and re-calibrated. A second reading was taken using pH indicator strips for moist sediment samples and water samples.

2.4. Chemical analyses

Multi-element analyses of sample material collected from sample site J was done by X-ray spectrometry at the Institute of Geological & Nuclear Sciences Limited (Wairakei Analytical Laboratory, Taupo, New Zealand). Ammonia was determined with 2 M KCl extraction by flow injection analysis (FIA). Chloride was determined by a potentiometric method (APHA 4500-CI D 20th Edition 1998). Conductivity was measured with a conductivity meter (APHA 2510 B 20th Edition 1998). Nitrate nitrogen, phosphorus, sulphite (SO₃) and sulphate were measured by ion chromatography (APHA 4110-B 20th

Edition 1998). Sulphide (total as H₂S) was determined by the methylene blue method (APHA 4500-S2 D 20th Edition 1998). Total organic carbon was determined by catalytic oxidation and IR detection (APHA 5310 B 20th Edition 1998).

3. RESULTS

3.1. Description of sampling sites and sample material

A total of ten different sites from White Island were sampled. Samples were taken from the active hydrothermal system situated between the main crater (1978) and the Crater Bay. Sampling sites are marked in red in Figure III.2 (sites A, B, C, D, E, F, G, H and I). Exact positions, temperatures and pH readings from each sampling site are summarised in Table III.1. Multiple samples were recovered from each location site at more than one representative area.

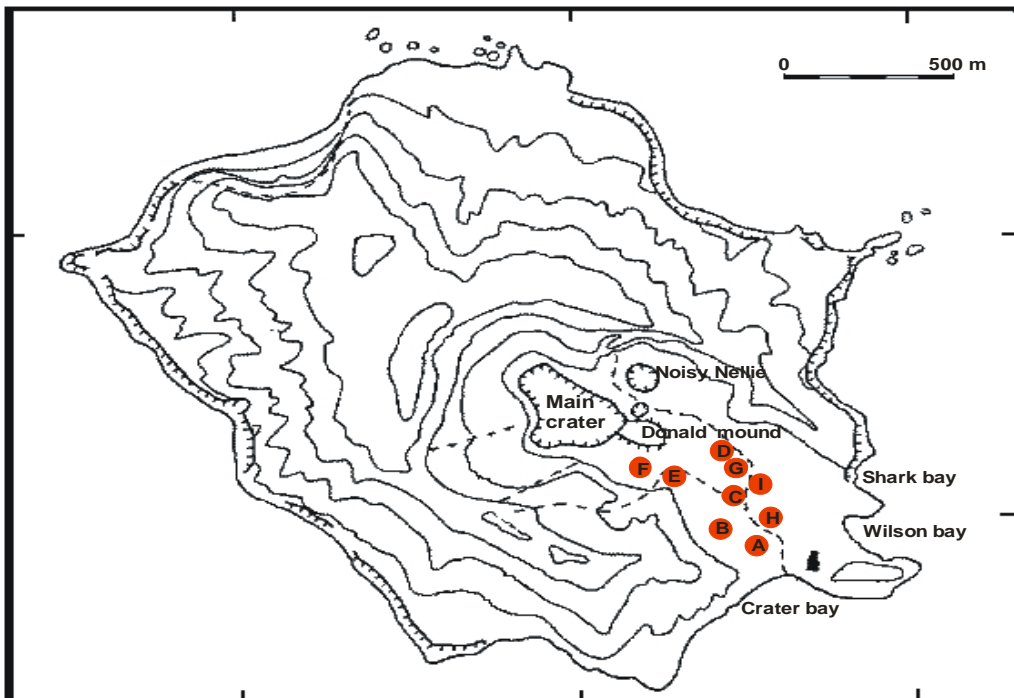


Figure III.2: Simplified topographic map of White Island showing the main crater, Noisy Nellie crater and Donald Mound. Sampling sites are indicated in red.

Table III.1: Position, temperature and pH readings of each sampling site selected on White Island.

Site	Position	Surface temperature	pH
A	E 2880274 / N 6400130	97.6°C	2.01
B	E 2880332 / N6400339	38.7°C	3.5
C	E 2880426 / N 6400290	72°C	3.05
D	E 2880417 / N 6400102	74.5°C	3.6
E1	E 2880518 / N 6399916	62°C	3.8
E2	E 2880518 / N 6399916	93°C	3.32
F	E 288024 / N 6400056	50°C	2.8
G	E 2880408 / N 6400315	63°C	2.02
H	E 2880438 / N 6400078	44.7°C	3.2
I	E 2880504 / N 6399977	42°C	2.5

3.1.1. Site A

Site A was located near Crater Bay off an acidic water stream surrounded by white and yellow deposits around the borders (Figure III.3). Below a thin crust, the ground was white-grey dense clay formed by small particle size. The temperature of the running water was 68°C while the surface was at 97.6°C. Samples were collected from 4 different sites at this location. Sediment samples were collected from this site using sterile spoons and spatulas and transferred to 2 sterile tubes of 250 ml each and 2 sterile tubes of 50 ml each. The average pH of the sediment was 2.01.



Figure III.3: Sample site A.

3.1.2. Site B

Site B consisted of a mud surface surrounded by several small fumaroles of approximately 1 cm in diameter (Figure III.4). The surface had grey and white deposits with some orange spots. Under the hard and dry surface there was wet grey mud formed by small particles. The temperature of the surface was 38.7°C. Samples were collected from 4 different sites at this location site. Two samples were taken from the surface and the other two samples from underneath the surface. Samples were taken using sterile spatulas and transferred into one sterile tube of 250 ml and three sterile tubes of 50 ml. The average pH of the sediment surface was 3.5.



Figure III.4: Sampling site B.

3.1.3. Site C

Site C was a bubbling pool of water found in the acid stream with clear running water (Figure III.5). Samples were collected from 5 different sites at this location. Sediment and water samples were collected from this site location and transferred into one sterile tube of 250 ml and four sterile tubes of 50 ml each. The sediment consisted of black, white, brown and orange sediments. The temperature of the water was 72°C and the average pH was 3.05.



Figure III.5: Sampling site C.

3.1.4. Site D

Site D was a water pool with high iron precipitation and red and yellow deposits around the borders (Figure III.6). Yellow sediments were found underneath the thin surface crust. Samples were collected from 7 different sites at this location site. Sediment and water samples were collected from this location and transferred into two sterile tubes of 250 ml each and 5 sterile tubes of 50 ml each. The average temperature was 74.5°C and the pH was 3.6.

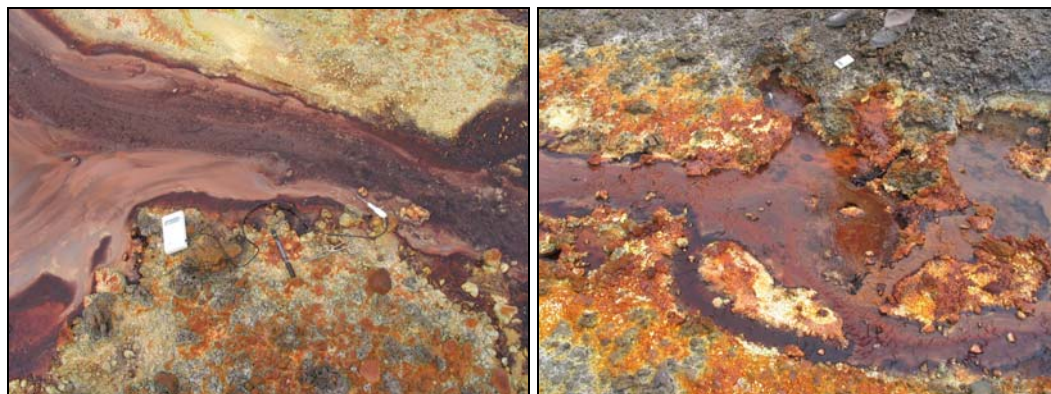


Figure III.6: Sampling site D.

3.1.5. Site E

Site E1 was a small water pool, about 5 cm deep, with leaks of gas forming bubbles (Figure III.7.A). The water within the pool was clear. The borders of the holes from which

steam was issuing contained black precipitate. There were orange-red deposits around the edges of the pool. Samples were collected from 7 different sites at this location. Water and sediment samples were collected from this site location and transferred into 50 ml sterile tubes. The temperature of the surface near the water was 62°C while the water was at 58°C. The average pH was 3.8.

Site E2 was located in front of location E1 (Figure III.7.B). This site consisted of a black pool of water with strong gas leaks forming big bubbles. The pool was approximately 50 cm deep. Five water samples from the pool were collected into 50 ml sterile tubes. The temperature was at 93°C and the average pH was 3.32.

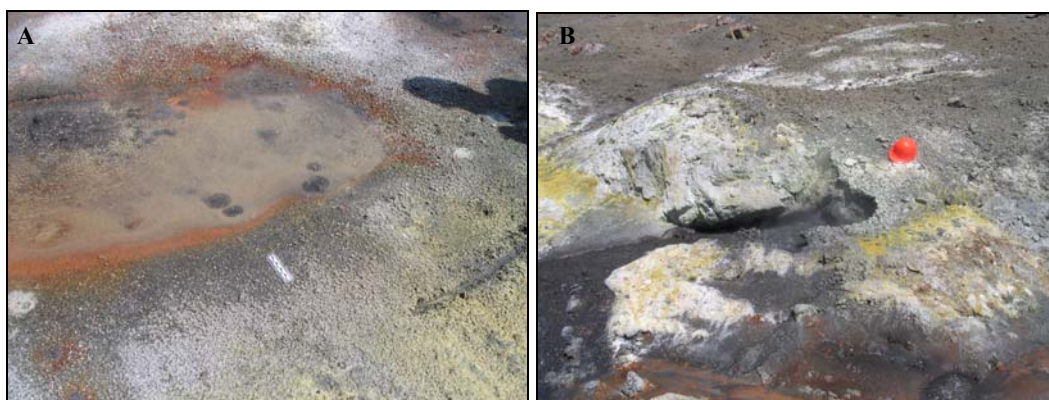


Figure III.7: A: Sampling site E1. B: Sampling site E2.

3.1.6. Site F

Site F consisted of a small fumarole of approximately 10 cm high. Sulphurous steam was being released from the fumarole as well as a small stream of black water (Figure III.8). Samples were collected from 6 different sites at this location. Samples were collected from the sediment and the stream water surrounding the fumarole and transferred into 50 ml sterile tubes. The temperature at surface was at 50°C while the temperature of the steam was at 97°C. The average pH of both the sediment and the water was 2.8.



Figure III.8: Sampling site F.

3.1.7. Site G

Site G consisted of sediment surrounded by small fumaroles at approximately 5 metres apart (Figure III.9). The surface was a hard crust containing white, yellow and orange deposits. Below the surface there was moist pale grey sediment made up of small particles. The average temperature was at 63°C and the pH was 2.02. Samples were collected from 5 different locations at this site. Sediment samples were collected and transferred into 50 ml sterile tubes.



Figure III.9: Sampling site G.

3.1.8. Site H

Site H consisted of a small stream of acidic water containing dark red deposits (Figure III.10). Green and white slimes were also present within the water. The stream was surrounded by dark red, yellow and white precipitates. Samples were taken from the green slime, and from yellow and red precipitates within the stream. Samples were collected from 5 different sites at this location. Sediment samples were taken from the borders of the stream and transferred into 50 ml sterile tubes. Below a thin crust of deposits, dark grey clay made up of small particles was found. The average temperature of the sediment was at 44.7°C and the pH was 3.2.



Figure III.10: Sampling site H.

3.1.9. Site I

Site I consisted of a stream of clear acidic water (Figure III.11). Samples were collected from 5 different sites at this location. Water samples were collected from this location as well as from sediment samples at the borders and transferred into 50 ml sterile tubes. The average temperature of the water and sediments was at 42°C. The pH of the sediments was 2.5 while the pH of the water was 1.5.



Figure III.11: Sample site I.

3.1.10. Site J

Site J was the same acidic water stream as described for sampling site I but located approximately 7 metres south of site I (Figure III.12). Samples were collected from 5 different sites at this location. Water and sediment samples were taken from this location and transferred into 50 ml sterile tubes. The average temperature for sediment and water samples was at 47.7°C. The pH of the water was 1.62, while the pH of the sediments was 2.6.



Figure III.12: Sample site J.

3.2. Chemical analysis

Site J was chosen as a control sampling site for undertaking the chemical analysis. Multi-element analysis of sediment collected from site J revealed high amounts of magnesium,

aluminium, silicon, sulphur and iron. A detailed list of the multi-element analysis and analytical report from White Island sediment is shown in Table III.2 and Table III.3.

Table III.2: Multi-element analysis of sediment from White Island.

Element	Value (weight %)	Element	Value (weight %)
Sodium	1.42	Iron	5.50
Magnesium	4.43	Nickel	0.011
Aluminium	5.20	Copper	0.007
Silicon	25.5	Zinc	0.006
Phosphorus	0.071	Rubidium	0.004
Sulphur	2.84	Strontium	0.013
Chlorine	0.917	Yttrium	0.002
Potassium	0.980	Zirconium	0.008
Calcium	5.94	Titanium	0.378
Titanium	0.378	Chromium	0.028
Manganese	0.093		

Table III.3: Analytical report of sediment from White Island.

Element	mg/g (dry wet)
Ammonia	0.015
Chloride	6.4
Nitrate (as N)	< 0.002
Phosphate (as P)	< 0.004
Sulphate	3.8
Sulphide	< 0.0001
Total organic carbon	< 0.5

The total organic carbon and nitrogen were very low, while iron and sulphur contents were very high in the samples analysed from White Island. Elements such as chloride, silicon, sulphate, magnesium, aluminium and calcium contents were also very high while nitrate and phosphate were very low.

4. DISCUSSION

The aim of this chapter was to provide a general picture of the geothermal and environmental characteristics of White Island as an active hydrothermal system for the habitat of thermo-acidophiles. Knowledge of the specific characteristics of the environment will help to understand the composition of the microbial populations and their interactions with the habitat in future studies.

Volcanic activity at White Island is caused by a large body of hot magma deep beneath the island (Cole *et al.* 2000). Water from hydrothermal systems such as White Island is heated around the magma reservoirs located underneath the volcanic area. As the water rises through the crust, chemical reactions take place with the surrounding rocks, enriching the water with elements such as chloride, sulphate, carbonate and soluble metals (Scarth 1994). Vapour is formed when the water reaches a level where the pressure is low enough for boiling, allowing it to ascend through rock fissures and fractures until it reaches the surface, forming hot springs and fumaroles emitting steam and gases (Clark 1970). The volcanic gases react with the surface rocks if cooled to around 100°C, generating sulphur deposits by the condensation of sulphur dioxide and hydrogen sulphide (Montegrossi *et al.* 2001). These deposits were observed to form yellow crystals around the margins of fumaroles of White Island. Minerals, metals and salt crystals also dissolved in the hydrothermal fluids can be redeposited at the surface. These coloured deposits, such as red iron precipitates, formed the visible precipitates observed at White Island within the springs and around the fumaroles. The gases rising towards the ground surface also heat the groundwater at shallow depths beneath the crater floor, consequently increasing the temperature at the surface of the volcano. The surface temperatures measured from the sampling sites were extremely variable between 38°C to 97°C.

Redox reactions between atmospheric oxygen or surface water and the volcanic gases and fluids results in the formation of acids (Scarth 1994; Goff & Janik 2000). The sediment analysed from White Island consisted of high deposits of heavy metals. Iron, sulphur,

chloride, silicon, magnesium, aluminum and calcium were the principal elements found in the sediment. It is not surprising to find these minerals in high concentration as they are generally found in the vapour released by volcanic fumaroles. For example, chloride normally is found in the steam of fumaroles of volcanoes such as White Island in the form of hydrogen chloride (HCl) which is very soluble in condensing water droplets and it promotes the acidity of the habitat (Symonds *et al.* 1994). Sulphate is a salt of sulphuric acid (SO_4^{2-}) which occurs as microscopic particles such as aerosols also resulting from volcanic activity, increasing the acidity of the atmosphere and forming acid water. Silicon is also normally found in volcanic environments, forming crystalline structures such as sand, quartz and clay minerals resulting from breakdown of the rocks due to hydrothermal heat and acidity (Goff & Janik 2000).

Although the outlet temperatures of the fumaroles in White Island range from 100°C to 700°C (Giggenbach & Sheppard 1989), the temperature readings from the sampling sites reached up to 98°C. However, the temperature from volcanic gases released by large fumaroles was not measured due to the danger and health risk associated with these regions. The gas discharge in White Island has been described to be made up of two source components: a primary “magmatic” component high in SO_2 , rising rapidly and directly from the underlying magma, and a secondary “hydrothermal” component rising slowly from a two-phase, saline brine-vapour envelope surrounding the magmatic system (Giggenbach 1987). It has been suggested that the entire volcanic system of White Island is fed by a common magmatic source unaffected by secondary processes causing the addition or removal of a significant amount of CO_2 , N_2 or Ar at shallow levels (Giggenbach 1986; Cole *et al.* 2000). The gases are mostly steam, carbon dioxide and sulphur dioxide, with small quantities of chloride and fluoride. Reduced gases (H_2 and H_2S) are chemically oxidised when approaching the surface (White *et al.* 1971).

The organic carbon and nitrogen levels measured were very low, indicating a low content of biomaterial. Sample site J was chosen as a representative location at White Island for undertaking chemical analyses due to its acidic water stream and yellow, orange, white and green sediments deposited on the borders of the stream. Chemical analyses from all the sites examined at White Island would have allowed future statistical correlation between the presence of specific phylotypes and the chemical properties of the sites.

However, the cost of analyses prevented a more expansive account of the sediment composition.

The environmental conditions in which microorganisms grow have a direct influence on their metabolic pathways and physiologies. For example, the high amounts of S^0 and sulphur compounds generated on White Island are sources of both electron acceptors and electron donors for a wide range of autotrophic and heterotrophic microorganisms living in this environment and helping to maintain the redox equilibrium (Johnson 1998; Kletzin *et al.* 2004). The oxidation of sulphur by acidophilic organisms normally uses elemental sulphur, sulphide (S^{2-}) and thiosulphate ($S_2O_3^{2-}$) as substrates, leading to the formation of sulphuric acid and consequently increasing the acidity of the environment (Parker & Prisk 1953; Lettl *et al.* 1981; Kelly 1982; Hedderich *et al.* 1999). On the other hand, the SO_4^{2-} reduction leads to the formation of sulphides in the environment and, under anaerobic conditions, Fe^{3+} and SO_4^{2-} are reduced to Fe^{2+} and HS^- (Devereux *et al.* 1989; Devereux & Boddy 1993). These reactions form a black precipitate of ferrous sulphide which can react further to form a number of sulphide minerals. In consequence, the reduction process increases the pH of the system (Küsel *et al.* 2001). The average pH from the sampling sites measured of White Island ranged from 2.01 to 3.8.

Chapter IV. Enrichment cultures and molecular analyses

1. INTRODUCTION

Thermally- and chemically-extreme habitats in volcanically active areas have been revealed to host a vast microbial diversity (Seeger *et al.* 1993). Such habitats include submarine hydrothermal vents (Sievert *et al.* 2000), hot springs and hydrothermal systems (Atkinson *et al.* 2000; Meyer-Dombard *et al.* 2005; Kvist *et al.* 2007) and active volcanoes (Gomez-Alvarez *et al.* 2007; Losekann *et al.* 2007; Henneberger 2008). Culture-independent techniques have revealed a wide range of diverse thermo-acidophilic microorganisms in these environments where the conditions are so extreme that it was considered that life could not exist (Ward *et al.* 1990b; Rothschild & Mancinelli 2001). A molecular phylogenetic survey carried out in hot springs from Yellowstone National Park found 54 distinct bacterial sequences types of which 30% of them were unaffiliated with any previously recognised bacterial division (Hugenholtz *et al.* 1998b). Similar surveys carried out in deep-sea hydrothermal vent environments showed a great microbial diversity where the majority of them appeared to be uncultivated and unidentified archaeal species (Takai & Horikoshi 1999).

However, culture-independent techniques alone are inadequate for the study of environmental microbial diversity as the sequences obtained from 16S rRNA gene libraries of natural bacterial communities frequently contain many novel sequences, which often do not match with the sequences of cultivated strains from the same samples (Suzuki *et al.* 1997; Felske *et al.* 1999). Moreover, cultivation of microorganisms is required to gain a comprehensive understanding of the microbial physiologies, the interaction of microbes with one another in their environment and to provide access to genes encoding metabolic pathways which may be dispersed throughout the genome (Keller & Zengler 2004). Most microorganisms in the environment are recalcitrant to growth using traditional cultivation methods, which employ complex media as the specific growth requirements of many uncultured microorganisms are unknown (Leadbetter 2003; Ferrari *et al.* 2004). No single method or medium is suitable for the cultivation of the majority of microorganisms from environmental samples as they prefer stable, nutrient-poor

environments (Green & Keller 2006). It is essential to understand the physical and chemical characteristics of each particular environment being studied in order to develop a cultivation method which can simulate the natural habitat (Ferrari *et al.* 2005). Thermo-acidophilic microorganisms inhabiting acidic geothermal environments have been difficult to cultivate due to their fastidious requirements (Johnson 1995). Therefore, there is a need to improve traditional techniques with new and novel approaches. Several cultivation techniques have been developed in recent years to mimic the natural habitat which have resulted in the successful cultivation of microorganisms from diverse phyla (Frohlich & Konig 2000; Reysenbach *et al.* 2000; Kaeberlein *et al.* 2002; Svenning *et al.* 2003).

Although White Island represents an ideal location for the study of thermophilic acidophilic microorganisms, this habitat has been poorly studied. The first description of the microbial communities in a stream of acidic hydrothermal waters on White Island was reported in 2002 (Donachie *et al.* 2002). Culture-independent techniques based on 16S rRNA gene libraries from community DNA revealed the presence of α - and β -Proteobacteria, green-sulphur bacteria, and uncultured Firmicutes. The same bacterial groups were represented in enrichment cultures based on previously defined media to support the growth of heterotrophic bacteria such as marine broth, and TA medium designed for acidophilic Archaea. *Cyanidium caldarium*, two Firmicutes and an acidophilic α -Proteobacteria, *Acidiphilum cryptum*, were obtained in pure cultures through repeated transfers on nutrient media. However, archaeal species were not found in that study despite the fact that Archaea are the most hyperthermophilic and acidophilic microorganisms normally found in hydrothermal sulphur-rich environments (Stetter 1999a).

This chapter focuses on the cultivation and isolation of thermo-acidophiles from the volcanically-active sediments of White Island. Several different conventional liquid media were used for cultivation purposes. The lack of success using standard methods led to the development of a new liquid medium based on a sediment-extract which mimicked the natural habitat and supplied the essential metabolic trace elements required for microbial growth. Molecular analyses revealed that the dominant culturable bacterial species present in the mixed cultures belonged to the Bacteroidetes, Firmicutes and α -Proteobacteria groups. Several previously uncultured archaeal species from the Euryarchaeota and

Crenarchaeota phyla were also present. Pure isolates were recovered using a novel low pH agarose-based solid medium based upon sediment-extract.

Microorganisms live in complex communities and networks that interact with each other and their natural habitats (Watnick & Kolter 2000). Fluorescent *in situ* hybridisation (FISH) supplied evidence to support the hypothesis that the existence of microbial consortia and their inherent interactions with sediment particles provide the interface for microbial metabolic interactions. An introduction to the FISH technique can be found in Chapter I.

2. MATERIALS AND METHODS

2.1 Culture media

2.1.1. Liquid media

Four different liquid media traditionally used for the cultivation of thermo-acidophilic microorganisms were tested. Liquid media recipes were obtained from the German Resource Centre for Biological Material, DMSZ (www.dsmz.de).

2.1.1.1. *Acidianus* medium

This medium was based on one previously developed for the cultivation of *Acidianus brierleyi* (DSMZ, medium 150). It contained: $(\text{NH}_4)_2\text{SO}_4$ (3 g), $\text{K}_2\text{HPO}_4 \times 3 \text{H}_2\text{O}$ (0.5 g), $\text{MgSO}_4 \times 7 \text{H}_2\text{O}$ (0.5 g), KCL (0.1 g), $\text{Ca}(\text{NO}_3)_2 \times 4 \text{H}_2\text{O}$ (0.01 g), yeast extract (0.4 g), and elemental sulphur (10 g) in 980 ml of dH₂O. The pH was adjusted to 3 using 5M H₂SO₄. The medium and yeast extract solution were autoclaved (120°C for 20 min) separately, and mixed after the sterilisation procedure. The final medium was stored at 4°C.

2.1.1.2. Diluted nutrient broth medium

This medium consisted of Difco Nutrient Broth (Sigma-Aldrich, Australia) at a concentration of 0.4%. The pH was adjusted to 3 at RT with 5M H₂SO₄ prior to autoclaving (120°C for 20 min). The final medium was stored at 4°C.

2.1.1.3. *Sulfolobus* medium

This medium was developed previously for the cultivation of *Sulfolobus spp.* (DSMZ, medium 88). It contained: KH_2PO_4 (0.28 g), $(\text{NH}_4)_2\text{SO}_4$ (1.30 g), $\text{MgSO}_4 \times 7 \text{H}_2\text{O}$ (0.25 g), $\text{CaCl}_2 \times 2 \text{H}_2\text{O}$ (0.07 g), $\text{FeCl}_3 \times 6 \text{H}_2\text{O}$ (0.02 g), $\text{MnCl}_2 \times 4 \text{H}_2\text{O}$ (1.80 mg), $\text{Na}_2\text{B}_4\text{O}_7 \times$

10 H₂O (4.50 mg), ZnSO₄ x 7 H₂O (0.22 mg), CuCl₂ x 2 H₂O (0.05 mg), Na₂MoO₄ x 2 H₂O (0.03 mg), VoSO₄ x 2 H₂O (0.03 mg), CoSO₄ (0.01 mg), and yeast extract (1 g) in 1 L of dH₂O. The pH was adjusted to 3.5 at RT with 5M H₂SO₄ prior to autoclaving (120°C for 20 min) and stored at 4°C.

2.1.1.4 *Sulfolobus solfataricus* medium

This medium was developed previously for the cultivation of *Sulfolobus solfataricus* (DMSZ, medium 182). It contained: yeast extract (2.00 g), KH₂PO₄ (3.10 g), (NH₄)₂SO₄ (2.50 g), MgSO₄ x 7 H₂O (0.20 g), and CaCl₂ x 2 H₂O (0.25 g) in 1 L of dH₂O. The pH was adjusted to 3.5 at RT with 5M H₂SO₄ prior to autoclaving (120° C for 20 min) and stored at 4°C.

2.1.1.5 Sediment-extract medium

Sediment-extract was prepared by mixing 250 g of sediment collected from White Island from each of the different sampling sites with 2 L of MilliQ water. The mixture was boiled for two hours with occasional stirring. The boiled extract was cooled for 30 min to allow settlement of large rock particles. Smaller particles in the solution were then removed by filtration using Miracloth paper filters (EMB Biosciences Inc., La Jolla.). The final sediment-extract was autoclaved at 121°C for 50 min and stored at 4°C.

Liquid sediment-extract medium contained KH₂PO₄ (0.28 g), (NH₄)₂SO₄ (1.30 g), MgSO₄ x 7 H₂O (0.25 g), CaCl₂ x 2 H₂O (0.1 g), AlCl₃ (0.1 g) and yeast extract (1 g) in 798ml of dH₂O. The solution was sterilised (120°C for 20 min), cooled, and then supplemented with 1 ml (500 mM) of FeCl₃ x 6 H₂O (previously sterilised by filtration through a 0.22 µm filter) and 1 ml of trace elements: MnCl₂ x 4 H₂O (900 mg), Na₂B₄O₇ x 10 H₂O (2.25 mg), ZnSO₄ x 7H₂O (110 mg), CuCl₂ x 2 H₂O (25 mg), Na₂MoO₄ x 2 H₂O (15 mg), VoSO₄ x 2 H₂O (15 mg), elemental sulphur (1 g) and CoSO₄ (5 mg) in 500 ml of dH₂O. Finally, 200 ml of sediment-extract and 5 g of elemental sulphur were added to the solution. The final pH was adjusted to 3 and stored at 4° C.

2.1.2 Solid extract agarose-based medium

The solid medium was modified from a washed agarose/yeast extract (WAYE) medium developed previously to facilitate growth of oligotrophic and heterotrophic acidophiles from environmental samples (Johnson 1995). It was prepared as follows (per L of medium): solution A contained KH_2PO_4 (0.28 g), $(\text{NH}_4)_2 \text{SO}_4$ (1.30 g), $\text{MgSO}_4 \times 7 \text{H}_2\text{O}$ (0.25 g), $\text{CaCl}_2 \times 2 \text{H}_2\text{O}$ (0.1 g), AlCl_3 (0.1 g) and yeast extract (0.5 g) in 650 ml of MilliQ water with the final pH adjusted to 3. The solution was sterilised (120°C for 15 min). Solution B was a non-acidified solution of distilled water-washed agarose. 9 grams of agarose (Sigma type 1) was soaked for 30 min in 1 L dH₂O with continuous stirring. The suspension was allowed to settle for 15 min. Most of the water was removed by decanting and the remaining bulky agarose suspension centrifuged. The supernatant was discarded and the agarose particles were re-suspended in 250 ml of dH₂O and the solution sterilised. Solution C consisted of 100 ml of sediment-extract from White Island (IV.2.1.1.5). Solutions A and B were sterilised (120°C for 15 min) and combined with solution C when cool. The final medium was supplemented with 500 mM of $\text{FeCl}_3 \times 6 \text{H}_2\text{O}$ and 1 ml of trace elements (as explained above) sterilised by filtration through a 0.22 µm filter. Finally, after sterile addition of the supplements, the medium was dispensed onto Petri plates.

2.2. Cultivation conditions

2.2.1. Enrichment cultures

For enrichment of microorganisms directly from the environment, approximately 0.5 g of sample material was transferred aseptically to test tubes containing 10 ml of liquid media. Cultures were incubated aerobically at 37°C and/or 60°C, with shaking (100 rpm). Microbial growth was monitored by light microscopy. To subculture actively growing cultures, 500 µl was transferred aseptically to fresh media.

2.2.2. Pure cultures

Solid low pH agarose-based plates supplemented with sediment-extract were inoculated with 500 μ l of each liquid medium culture and incubated aerobically at 37°C and 60°C for up to 7 days. Single colonies were picked and streaked onto fresh plates to obtain pure cultures. This step was repeated up to 4 times in order to obtain pure cultures which were confirmed by light microscopy.

2.3. Long-term storage of cultures

Actively growing cultures and subcultures were mixed with 10% DMSO (v/v) or 6% betaine (v/v) or 10 % glycerol (v/v) and immediately frozen at -80°C. Frozen stocks were slowly thawed on ice for recovery of cultures, transferred to fresh, liquid medium and incubated under suitable conditions. The concentrations of DMSO, betaine and glycerol were determined empirically by observing recovery and successful subculturing after storage at -80°C for several weeks.

2.4. Buffers and solutions

General buffer and solutions are described in Chapter II.

Table IV.1: General buffers and solutions.

XS buffer	1% potassium ethyl xanthogenate (w/v), 800mM of ammonium acetate, 100 mM of Tris-HCl pH 7.4, 20 mM of EDTA pH 8 and 1% of SDS (w/v). Buffer was kept at -20°C in the dark after autoclaving and discarded after 2 weeks
Potassium acetate	4 M potassium acetate
Phenol/Chloroform/Isoamylalcohol (25:21:1)	Chloroform/isoamylalcohol (CIAA) at 24:1. Saturated phenol buffer was mixed with CIAA (24:1) in a ratio of 1:1 at least 1 h prior to use and stored protected from light
TER buffer	10 mM Tris-HCl pH 7.4, 1 mM EDTA pH 8 and 100 mg/ml of RNAase A
Ampicillin solution	100 mg/ml of Ampicillin. Ampicillin was dissolved in H ₂ O, sterilised by filtration and stored at -20°C
X-Gal solution	20 mg/ml of X-Gal. X-Gal was dissolved in dimethylformamide and stored at -20°C after filter sterilisation

IPTG solution

5 mg/ml of IPTG. IPTG was dissolved in H₂O and stored at -20°C after filter sterilisation

2.5. Chemical analysis of the sediment-extract

Multi-element analysis to detect trace elements and heavy metals from the sediment-extract used to supplement the liquid and solid medium was carried out by mass spectrophotometry at the National Measurement Institute (Australian Government, Australia).

2.6. Molecular analyses of enrichment cultures

2.6.1. DNA extraction

After 3 months of cultivation, genomic DNA was extracted from 4 ml of each enriched liquid culture using a modified XS buffer DNA extraction method (Tillett & Neilan 2000). Between 5 to 20 ml of actively growing culture was centrifuged for 30 min (5,000 rpm). Cell pellets were resuspended in 50 µl of TER buffer and mixed with 70 µl of fresh XS buffer. The mixture was vortexed at full speed for up to 5 min followed by incubation at 65°C for 2 h with occasional mixing by hand every 30 min. After incubation, tubes were vortexed for 10 s and placed on ice for 10–15 min. After centrifugation (10 min at 10,000 rpm in a bench-top centrifuge or 30 min at 5,000 rpm in a Sigma 6K15 swing-out rotor 11150/13420), the supernatant was transferred to a PhaseLock Gel light tube and mixed with 1 volume of phenol/CIAA (25:24:1) by 5 min of vigorous shaking. The tube was centrifuged for 5 min (3,000 rpm, 15°C) and the aqueous layer transferred to a fresh 1.5 ml Eppendorf tube. 1 volume of 100% cold Isopropanol (-20°C) and 1/10 volume of 4 M potassium acetate were added and mixed gently. DNA was precipitated for 30 min at -80°C or at -20°C overnight followed by a centrifugation step at 16,000 rpm (45 min, 4°C, Sigma 3-18K rotor 12154-H). The supernatant was discarded and the pellet washed once in 1 ml of 70% EtOH. The dried pellet was resuspended in 50 – 250 µl of TE buffer depending on the concentration of DNA obtained.

2.6.2. PCR amplification

Polymerase chain reaction amplification of 16S ribosomal RNA genes was carried out as described in Chapter II.2.6.2, using universal bacterial primers (PB36 and PB38) and the universal archaeal primers (ASF and ASR). DNA extracted from both enriched and pure cultures was used as the template (diluted up to 1:100). PCR products were analysed by 1% gel electrophoresis and visualised and documented under UV excitation using a Chemilmager 4400 digital imaging system (II.2.6.1).

2.6.3. Restriction fragment length polymorphism (RFLP)

Restriction fragment length polymorphism (RFLP) analyses were carried out on amplified DNA. Amplified PCR products were ligated with the pCR2.1 vector using the TA Cloning Kit (Invitrogen, Australia), following the manufacturer's instructions. Ligation was performed overnight at 14°C. Competent *E. coli* strain DH5 α cells were transformed with the ligated vector according to the manufacturer's protocol. Transformant cells were plated on LB agar plates: 600 ml of LA agar supplemented with 600 μ l of X-Gal (40 mg ml⁻¹), 480 μ l of IPTG (100 mM) and 600 μ l of ampicillin (100 mg l⁻¹). X-Gal, IPTG and ampicillin were added to molten LA agar at approximately 50°C and then 20 ml was poured onto individual Petri dishes. After solidification, the plates were stored at 4°C. Inoculated plates were incubated overnight at 37°C. Blue-white screening on the plates was used as a selective marker for successful ligation and transformation. White colonies (transformant cells) were picked with sterile toothpicks and transferred into a standard PCR reaction with the vector-specific primers pCR21F and pCR21R (II.2.6.2). After transferring the colonies into the PCR reaction mix, the toothpicks were subsequently streaked onto numbered segments of fresh supplemented LB plates, as described earlier, for incubation overnight at 37°C. Plates were then stored at 4°C. PCR reactions were prepared on ice according to the following protocol, using aerosol filter tips and 0.2 μ l reaction tubes. Each PCR reaction contained 0.1 μ l of AmpliTaq Gold DNA polymerase (5 U/ μ l), 2.5 μ l of 10x Taq Buffer, 2.5 μ l MgCl₂ (25 mM), 2.5 μ l of dNTPs mixture (2.5 mM of each dNTP), 0.5 μ l of pCR 21F (10 mM) as forward primer, 0.5 μ l of pCR 21R (10 mM) as reverse primer and 10.9-15.7 μ l of sterile MilliQ water to make a final volume of 25 μ l. The DNA template was added at 0.2-5.0 μ l. Each cycle was composed of

10 min at 94°C, 30 s at 94°C, 30 s at 50°C, 2 min at 72°C and 5 min at 72°C. After 30 cycles, the reactions were stored at 4°C. 5 µl of each PCR reaction was analysed on a 1% agarose gel. Only products showing the correct insertion size were used for further analyses.

Restriction enzyme digestions of the PCR products were carried out according to the manufacturer's protocols using 0.25 µl *Hinf*I and 0.25 µl *Bsu*RI restriction endonucleases added to each PCR product (20 µl), followed by incubation at 37°C for approximately 4 h. Digested DNA was mixed with DNA loading buffer and run on 3% (w/v) agarose gel at 90 V for up to 90 min. DNA was visualised using ethidium bromide staining and documented as described previously (II.2.6.1). The patterns were compared to each other, and recombinants with identical patterns were grouped into ribotypes (preliminary operational taxonomic units, OTUs). A representative recombinant of each ribotype was selected for sequencing and phylogenetic analysis.

2.6.3.1 Long-term storage of recombinants

Selected recombinants for sequencing were transferred to 10 ml of LB broth containing 0.1 mg/ml of ampicillin (II.2.3). After incubation at 37°C for 12-14 h with shaking at 250 rpm, 2 ml of each culture was transferred to a sterile reaction tube and centrifuged at 13,000 rpm for 10 min. The supernatant was discarded and the cell pellets were resuspended thoroughly in 1 ml of 50% (v/v) glycerol in LB broth and immediately stored at -80°C.

2.6.3.2. Extraction of plasmid DNA

Plasmid DNA from liquid recombinants cultures (IV.2.6.3.) was extracted with the QIAprep Spin Miniprep Kit or the Wizard *Plus* SV Miniprep DNA purification system following the manufacturer's instructions. The concentration of extracted plasmid DNA was determined via absorbance at 260 nm with a Biophotometer.

2.6.4. Sequencing analysis

Recombinant 16S rRNA genes in plasmids were sequenced by the chain-termination method using BigDye Terminator v3.01 (Applied Biosystems, Foster City, USA) and the vector-specific primers M13F or M13R (Table II.12). Sequencing reactions were prepared as follows: 350-500 ng of plasmid DNA or 100-150 ng of PCR product, 1.5 µl of 5x sequencing buffer, 1 µl of BigDye Terminator v3.01, 1 µl of primer (3.2 pmol/µl) and sterile MilliQ water up to 20 µl. The sequencing program is described in Table IV.2.

Table IV.2: Standard protocol for sequencing reaction.

	Time	Temperature	Number of cycles
Denaturing	10 s	96°C	25
Annealing	5 s	50°C	
Polymerisation	4 min	60°C	
Hold	∞	4°C	

The products obtained were transferred into clean 1.5 ml Eppendorf tubes and mixed with 16 µl of sterile MilliQ H₂O and 64 µl of 99% EtOH and vortexed briefly. The reactions were incubated at RT for 45 min followed by centrifugation at 4°C for 45 min at 16,000 rpm (Sigma 3-18K, rotor 12154-H). The supernatant was removed completely and the pellets were washed with 250 µl of 70% EtOH (v/v) and centrifuged for 10 min. The supernatant was discarded and the pellets were dried for several minutes at 70°C. Sequencing reactions were analysed at the Automated DNA Analysis Facility for Sequencing (School of Biotechnology and Biomolecular Sciences, University of New South Wales, Australia) using an ABI Prism 96-capillary 3730 DNA Analyser (Applied Biosystems) (II.2.6.3).

2.6.5. Construction of 16S rDNA consensus sequences

Sequence fragments were assembled and edited using the *Vector NTI Advance* software package (Invitrogen, Carlsbad, USA).

Consensus 16S rDNA sequences (1024 – 1033 bp for archaeal and 1482 – 1497 bp for bacterial) were compared to datasets from GenBank (National Centre for Biotechnology

Information, NCBI) (Altschul *et al.* 1997) using the BlastN algorithms megablast and discontinuous megablast. These programs identify regions of local similarity between sequences (<http://www.ncbi.gov/BLAST/>) for preliminary phylogenetic placement.

All consensus sequences were analysed for the presence of possible chimeric artefacts, using the programs Bellerophon (<http://foo.maths.uq.edu.au/~huber/bellerophon.pl>) (Huber *et al.* 2004) and Chimera-Check RDP (Cole *et al.* 2003) (<http://rdp8.cme.msu.edu/cgis/chimera.cgi?su=SSU>). Putative chimeric sequences were confirmed by alignments with possible parent sequences and excluded from further analyses.

2.6.6. Sequence alignments

Multiple sequence alignments of non-chimeric consensus sequences were performed with ClustalX (Thompson *et al.* 1997), ClustalW (Thompson *et al.* 1994) and Vector NTI Advanced software package. The aligned sequences were compared with each other and sequence similarities were calculated over the full length of the recombinant genes. The recombinants were assigned to phylotypes (operational taxonomic units, OTUs) based on sequence similarities of $\geq 99\%$ (McCaig *et al.* 1999; Singleton *et al.* 2001).

2.6.7. Phylogenetic analyses

The recombinant 16S rDNA gene sequences obtained were analysed using the ARB software package (Ludwig *et al.* 2004). They were added to the latest SSURef dataset of the SILVA database project (www.arb-silva.de; release 1.4 from February 2007) containing 137,788 quality-checked and aligned nearly full-length small subunit rRNA sequences. The sequences were aligned automatically according to the SILVA reference alignment using the Fast Aligner of the ARB_EDIT tool, followed by manual correction taking into account the secondary structure of the rRNA molecule and positional variability of the alignment positions. To identify the tentative phylogenetic position of the sequences obtained, they were initially added to the main navigation tree provided with the SILVA database according to parsimony criteria without changing the overall tree topology as allowed by the “quick add” function of ARB. Based on this classification,

subsets of sequences of appropriate quality and representing the groups harbouring the sequences plus reference groups were chosen from the SILVA SSU database for *de novo* tree reconstruction.

The phylogenetic trees presented were reconstructed based on distance-matrix (ARB neighbour joining) and maximum-likelihood analysis for bacteria and archaea, respectively, using filters excluding highly variable positions of the alignment. Tree topologies were evaluated by various tree reconstruction algorithms including maximum-parsimony analyses and by exclusion of filters to test overall stability of the branching patterns. For distance-matrix analysis, which was less computationally intense compared to the other methods, extended sub-datasets were used (up to several hundred sequences) to evaluate tree topology. The sequences from this study were added subsequently to the trees as described above. For a better overview, only 16S rDNA sequences from this study plus selected reference sequences were displayed on the trees.

2.7. Fluorescent *in situ* hybridisation

For fixation, 1ml of liquid culture was fixed with 110 µl of 30% paraformaldehyde and prepared following the procedures described in Chapter II.2.6.4.4. Fixed samples were then spotted onto pre-cleaned microscope slides (II.2.6.4.2) and hybridised to the probes (II.2.6.4.5). Finally, the slides were rinsed with cold dH₂O, dried and mounted in Citifluor AF-1 (Citifluor Ltd, London, United Kingdom).

The rRNA-targeted oligonucleotides used for FISH were a combination of universal bacterial and archeal probes. The bacterial probes were Eub338, Eub388-II and Eub388-III 5' labelled with Alexa488. The archeal probes were ARCH344, ARCH1060 and ARCH915 5' labelled with Cy3 (II.2.6.4.1). All probes were supplied by Sigma-Aldrich (Sydney, Australia). Samples were observed by fluorescence microscopy using appropriate filters for Alexa 488 and Cy3 visualisation (II.2.4.2).

3. RESULTS

3.1. Chemical analysis of the sediment-extract

Multi-element analysis from the sediment-extract used to supplement the culture medium was performed to gain a better understanding of its composition in relation to the environmental sediment samples collected from White Island. The analysis revealed that the sediment-extract had similar analytical composition to the sediment collected from White Island (III.3.2), including the presence of numerous trace elements in small quantities and high amount of magnesium, aluminium, silicon, sulphur and iron (Table IV.3).

Table IV.3: Multi-element analysis of sediment-extract.

<1 ug/L	1-10 ug/L	10-50 ug/L	50-100 ug/L	100-500 ug/L	500ug-1 mg/L	1-5 mg/L	>5 mg/L
Antimony	Beryllium	Arsenic	Barium	Caesium	Strontium	Lithium	Aluminium
Germanium	Bismuth	Cerium	Yttrium	Chromium		Rubidium	Boron
Gold	Cadmium	Cobalt		Copper		Sulphite	Calcium
Holmium	Dysprosium	Neodymium		Nickel			Iron
Iridium	Erbium	Phosphorus		Zinc			Magnesium
Lead	Europium	Scandium					Manganese
Lutetium	Gadolinium	Titanium					Potassium
Mercury	Gallium	Vanadium					Silicon
Molybdenum	Hafnium						Sodium
Niobium	Samarium						Sulphur
Palladium	Thallium						Chloride
Platinum	Thorium						Ammonia
Rhodium	Ytterbium						Sulphate
Ruthenium	Zirconium						Nitrate
Selenium							
Silver							
Tantalum							
Tellurium							
Terbium							
Thulium							
Tin							
Tungsten							
Uranium							

3.2. Enrichment cultures

Standard liquid media were used to obtain enrichment cultures from representative sediment samples from all the location sites examined at White Island, including *Acidianus* medium, *Sulfolobus* medium, *Sulfolobus solfataricus* medium, and diluted nutrient broth medium at low pH. These liquid media were designed for the cultivation of acidophiles and thermophiles. Growth was observed by light microscopy after 5 days cultivation at 37°C and 60°C. These cultivation temperatures were chosen in order to discriminate between mesophilic and thermophile microorganisms. 37°C was chosen to simulate the cooling experienced as the result of distance from the geothermal source. Higher incubation temperatures were not possible due to the lack of suitable equipment and glassware.

All cultures were observed every 3-4 days by phase contrast microscopy and details of the morphologies of the microorganisms were recorded. Consecutive subcultures were carried out after approximately 10 days of incubation. A general reduction of cell yield in subcultured samples was observed for all standard liquid media used for cultivation after approximately 4 weeks from the first inoculation, as observed by phase contrast microscopy. The lack of sustainable cultures may be caused by the limited amounts of the essential minerals and trace elements require for microbial growth. As a control, the standard liquid media without inocula were used as a negative control, confirming that there were no contamination issues. Actively growing cultures were stored for the long-term using DMSO, betaine and glycerol before subculturing into fresh media.

A sediment-extract medium was formulated as a result of the lack of suitable growth in standard media. Sediment from all sample sites of White Island was used to prepare the sediment-extract supplement. The medium was inoculated with sediment collected from all the sampling sites and incubated in aerobic conditions at 37°C and 60°C. Growth was observed by light microscopy after 2 days of incubation. All positive cultures at 37°C and their subcultures contained diverse morphotypes of cells, dominated by rod-shaped cells with different shapes and lengths (Table IV.4). In some cases, the rods appeared as short chains or as small clusters. Irregular small cocci were also detected at both culture temperatures. Repeated subculturing in the sediment-extract medium resulted in sustained growth for the length of the study (3 months). Microbial growth from locations C and E2

were not obtained. These sites consisted of small pools of water with strong gas leakage that resulted in a bubbling black solution. Cultures from locations E1, F and G seemed to have a higher cell number and a more diverse population of microorganisms than cultures from other locations.

Table IV.4: Morphologies of microorganisms cultured in sediment-extract medium after the first inoculation and after subculturing for the ninth time.

Sample	Enrichment at 37°C		Enrichment at 60°C	
	1 st Inoculation	9 th Subculture	1 st Inoculation	9 th subculture
A	Rods (diff. shapes / lengths)	Rods (diff. shapes / lengths)	Small cocci	Small cocci
B	Rods (diff. shapes / lengths)	Rods (diff. shapes / lengths)	-	-
C	-	-	-	-
D	Rods (diff. shapes / lengths)	Rods (diff. shapes / lengths)	Rods (diff. shapes / lengths)	Rods (diff. shapes / lengths)
E1	Rods (diff. shapes / lengths); irregular cocci	Rods (diff. shapes / lengths); irregular cocci	Rods (diff. shapes / lengths); irregular cocci	Rods (diff. shapes / lengths); irregular cocci
E2	-	-	-	-
F	Small rods (diff. shapes); cocci	Small rods (diff. shapes); cocci	Small cocci	Small cocci
G	Rods (diff. shapes / lengths); irregular cocci	Rods (diff. shapes / lengths); irregular cocci	Rods (diff. shapes / lengths); irregular cocci	Rods (diff. shapes / lengths); irregular cocci
H	Rods (diff. shapes / lengths)	Rods (diff. shapes / lengths)	Rods (diff. shapes / lengths)	Rods (diff. shapes / lengths)
I	Rods (diff. shapes / lengths); flagellated rods; diatoms	Rods (diff. shapes / lengths); flagellated rods; diatoms	Rods (diff. shapes / lengths); diatoms	Rods (diff. shapes / lengths); diatoms
Blank	-	-	-	-

-: No cells observed.

The sediment-extract used to supplement the medium contained small particles with similar sizes to the microorganisms cultured (Figure IV.1). Therefore, unequivocal cell counts of the enriched cultures could not be made. Although the cells could not be distinguished from the minerals, sometimes they were found to be detached and were isolated, allowing clear resolution of their morphology. In these cases, the reflection of

light under phase contrast microscopy aided in the identification of the cells. As a control, the medium without inoculum was used as a negative control and it was confirmed that there were no microorganisms growing naturally from the sediment-extract.



Figure IV.1: Sediment-extract from White Island used to supplement the medium.

3.3. Molecular analyses of cultured microorganisms

Molecular techniques were used to characterise the microbial diversity present in the cultured microorganisms obtained using the liquid sediment-extract medium. Due to time limitations, only three locations were selected for molecular analyses. Locations E1, F and G were selected as being the most representative features of White Island and provided diverse microbial populations as identified by light and confocal microscopy.

DNA was extracted from enrichment cultures from the three locations at 37°C and 60°C using the modified XS buffer method. Molecular analyses were carried out with all the sequences obtained to investigate the evolutionary relatedness among the microorganisms cultured (Table IV.5).

Table IV.5: 16S rDNA sequence analyses of microorganisms cultivated from White Island samples. Several previously uncultured bacterial and archaeal species from diverse lineages were identified growing in liquid sediment-extract media from the three sites studied.

Sample Site	Temperature	Representative sequence ^a	Best BLAST match database (accession no.)	% Sequence identity	Closest described microorganisms (accession no., % identity)	NBCI accession no.
E	37°C	E377	Uncultured bacterium clone fig7 16S ribosomal RNA gene, partial (DQ303265.1)	99%	<i>Acidiphilium angustum</i> (D30772.1, 95%)	EF555310
		E371	<i>Alicyclobacillus acidocaldarius</i> gene for 16S rRNA, strain:DSM 455 (AB059665.1)	99%	NA	
		E376	Uncultured bacterium clone SK968 16S ribosomal RNA gene, partial sequence (DQ834220.1)	98%	<i>Acidicaldus organivorans</i> (AY140238.1, 96%)	EF555309
		E378	<i>Alicyclobacillus tolerans</i> 16S ribosomal RNA gene, partial sequence (AF137502)	99%	NA	
		E374	Uncultured archaeon clone SK320 16S ribosomal RNA gene, partial sequence (DQ179006.3)	98%	NA	EF555308
F	37°C	F371	Uncultured archaeon clone ASL32 16S ribosomal RNA gene, partial sequence (AF544222)	99%	<i>Thermoplasma acidophilum</i> (M38637.1, 93%)	EF555320
		F372	<i>Alicyclobacillus tolerans</i> 16S ribosomal RNA gene, partial sequence (AF137502)	99%	NA	
G	37°C	G371	<i>Acidiphilium</i> sp. YA-1 partial 16S rRNA gene, strain YA-1 (AM176777.1)	100%	<i>Acidiphilium organovororum</i> (D30775.1, 98%)	EF555329
		G372	<i>Alicyclobacillus tolerans</i> 16S ribosomal RNA gene, partial sequence (AF137502)	99%	NA	

E	60°C	E601	<i>Alicyclobacillus acidocaldarius</i> gene for 16S rRNA (AB060166.1)	99%	NA	
		E606	<i>Thermaerobacter</i> sp. C4-1 16S ribosomal RNA gene, partial sequence (AY094621.1)	95%	<i>Thermaerobacter subterraneus</i> (AF343566.1, 93%)	EF535316
		E604	<i>Alicyclobacillus tolerans</i> 16S ribosomal RNA gene, partial sequence (AF137502)	99%	NA	
		EF602	Uncultured archaeon clone HHA3 16S ribosomal RNA gene, partial (DQ523826.1)	99%	<i>Thermoplasma acidophilum</i> (M38637.1, 93%)	EF535318
	F602	<i>Sulfolobacillus acidophilus</i> gene for 16S rRNA (AB089842.1)	99%	NA		
	F608	Uncultured thermal sediment bacterium clone YNPFFP6 16S ribosomal RNA gene, partial sequence (AF391987.1)	95%	<i>Thermoanaerobacter siderophilus</i> (AF120479.1, 97%)	EF535328	
	F601	<i>Alicyclobacillus acidocaldarius</i> gene for 16S rRNA (AB060166.1)	99%	NA		
	F604	<i>Thermoplasma volcanium</i> 16S ribosomal RNA gene, partial sequence (AF339746.1)	97%	NA	EF535324	
	F605	<i>Thermoplasma volcanium</i> 16S ribosomal RNA gene, partial sequence (AF339746.1)	97%	NA	EF535325	
	EF602	Uncultured archaeon clone HHA3 16S ribosomal RNA gene, partial (DQ523826.1)	99%	<i>Thermoplasma acidophilum</i> (M38637.1, 93%)	EF535318	
F607	Uncultured archaeon clone 16S ribosomal RNA gene (DQ383358)	99%	<i>Sulfolobus tokodaii</i> (BA000023.2, 94%)	EF535327		
F606	Uncultured thermal sediment archaeon clone YNPFFA23 16S ribosomal RNA gene, partial sequence (AF391991.1)	98%	NA	EF535326		
F	60°C					

Bacterial and archaeal phylogenetic trees were generated from the sequences obtained from the recombinant libraries. The bacterial phylogenetic tree revealed a diverse range of microorganisms belonging to the phyla Bacteroidetes, α -Proteobacteria and Firmicutes (Figure IV.2). Microorganisms from the α -Proteobacteria phylum were only found in cultures at 37°C from locations E and G (Table IV.5). They were relatively close to *Acidocaldus organivorans* with 96% sequence identity, *Acidiphilium organovorum* with 98% similarity and 95% sequence identity to *Acidiphilium angustum* (Table IV.5). *Sulfobacillus acidophilus* was found in both F and G locations in cultures at 60°C only. The most closely related microorganism to E606 was *Thermaerobacter subterraneus* with 93% sequence identity, while the remaining matches belonged to previously uncultured microorganisms from hydrothermal systems (Table IV.5). Both sequences F608 and G602 were most closely related to previously uncultured microorganisms from thermal sediment environments and they had 97% similarity to *Thermoanaerobacter siderophilus*. *Alicyclobacillus tolerans* and *Alicyclobacillus acidocaldarius* were both present in cultures at 37°C and 60°C from locations E and F (Table IV.5). The only cultured sample found that belonged to the *Bacteroidetes* phylum was G605 present in location G.

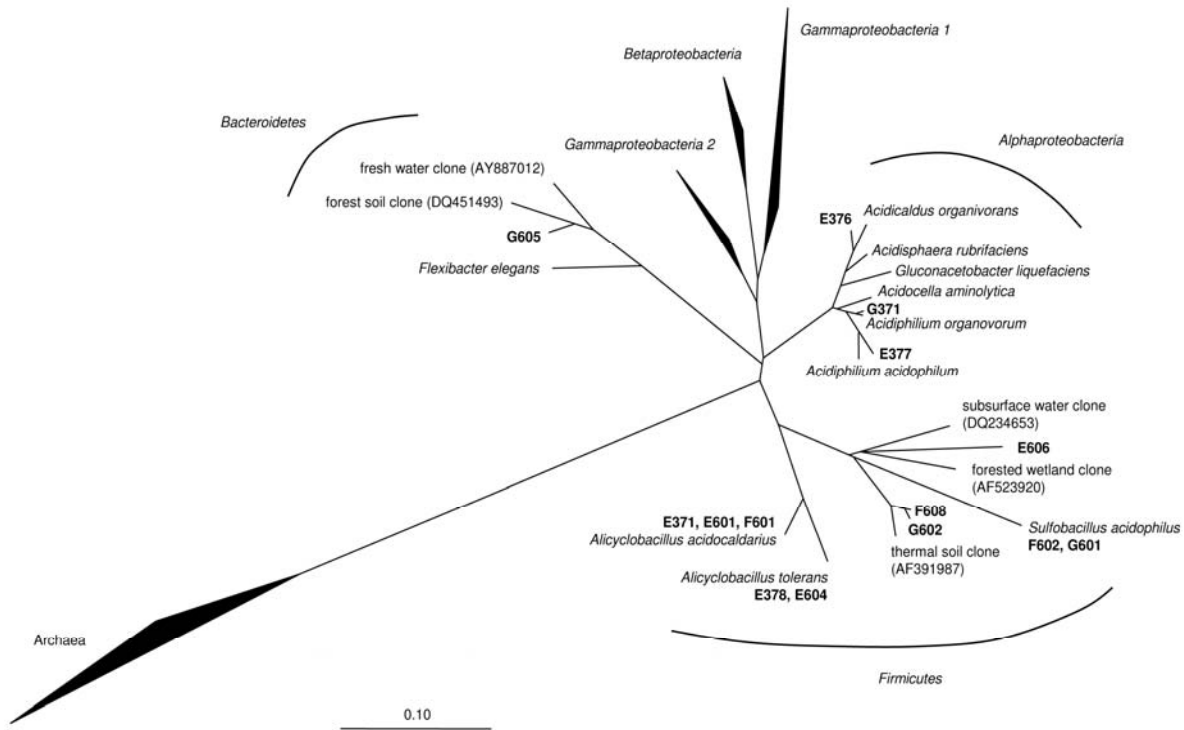


Figure IV.2: Maximum likelihood phylogenetic tree of 16S rRNA gene sequences from bacterial sequences of volcanically-active sediments of White Island microorganisms cultured using sediment- extract media. For each recombinant sequence the next relative is shown (in the case of uncultivated organisms accession numbers are indicated in brackets). The bar indicates 10% estimated sequence divergence.

Evidence for the presence of previously uncultured archaeal isolates from the Euryarchaeota and Crenarchaeota Phyla were found in cultures from the three locations analysed (Figure IV.3). The Euryarchaeota sequences were related to the genus *Thermoplasma*. Sequences F605 and F604 both showed 97% similarity to *Thermoplasma volcanium* but the sequences were still significantly different to *Thermoplasma acidophilum*. F371 had 99% sequence similarity to an uncultured microorganism previously found in acid mine-drainage environments, while EF607 had 99% sequence identity to a previously uncultured microorganism from a bioleaching reactor. Although EF602 and F371 were allocated to separate sites in the tree, both sequences showed 93% identity to *Thermoplasma acidophilum*. Crenarchaeota were more diverse; G603 belonged to a large group of uncultured Crenarchaeota previously identified from hot springs with 96% sequence similarity to *Ignicoccus pacificus*. Sequences F607 and G604 belonged to the family Sulfolobales. Sequence F607 had high similarity to an uncultured archeon related to *Sulfolobus tokadaii*, while G604 had 93% similarity to *Sulfolobus*

acidocaldarius. Sequences F606 and E374 belonged to another large group of uncultured Crenarchaeota identified from hot springs which have very low similarity to any previously described microorganisms from these habitats.

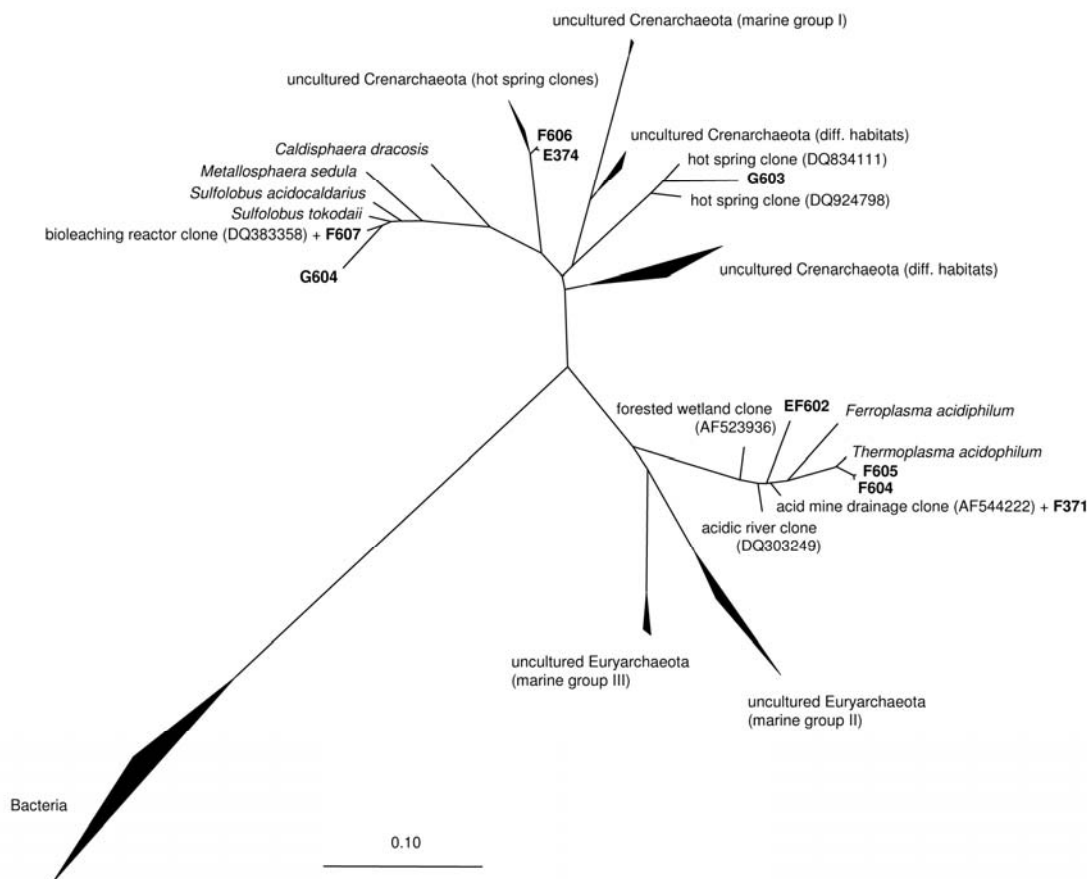


Figure IV.3: Evolutionary distance of 16S rDNA archeal sequences of representative isolates microorganisms cultured using sediment-extract media from volcanically-active sediments of White Island. For each sequence the nearest relative is shown (in the case of uncultivated organisms accession numbers are indicated in brackets). The bar indicates 10% estimated sequence divergence.

3.4. Isolation of pure cultures

Isolation of microorganisms from mixed cultures present in the liquid sediment-extract medium was achieved through the formulation of a new solid agarose plate medium (Figure IV.4). This medium was supplemented with sulphur and sediment-extract from White Island. The medium designed was able to solidify at low pH and retain its water content for up to 7 days, enabling the formation of small white colonies at both 37°C and

60°C. Sub-culturing was then carried out to obtain the isolates in pure cultures at both temperatures.

Molecular analyses were carried out on 2 purified isolates obtained using solid agarose-based plates incubated at 60°C from location F. The sequence information revealed that the isolates had above 99% sequence identity to *Alicyclobacillus acidocaldarius* and *Sulfobacillus acidophilus* (Isolates F602 and F601). Both microorganisms were rod-shaped and spore-forming as determined by light contrast microscopy.

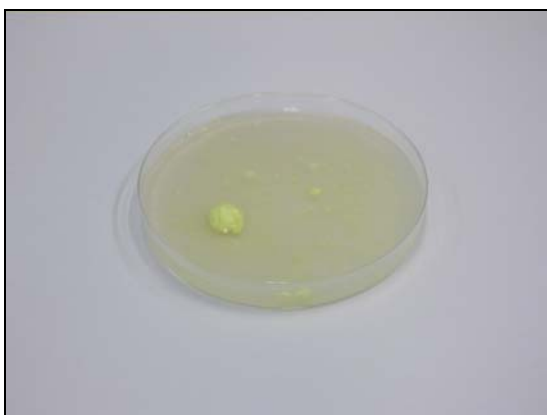


Figure IV.4: Solid agarose plate supplemented with sulphur and sediment-extract from White Island.

3.5. FISH

Fluorescent *in situ* hybridisation was used to study the microbial interaction between the microorganisms cultured in the sediment-extract medium. FISH was performed with domain-specific probes to assign the microorganisms to either Archaea or Bacteria. The controls for FISH were *E. coli* and archaeon SM1 stained with Alexa Fluor 488 and Cy3 respectively (Figure IV.5).

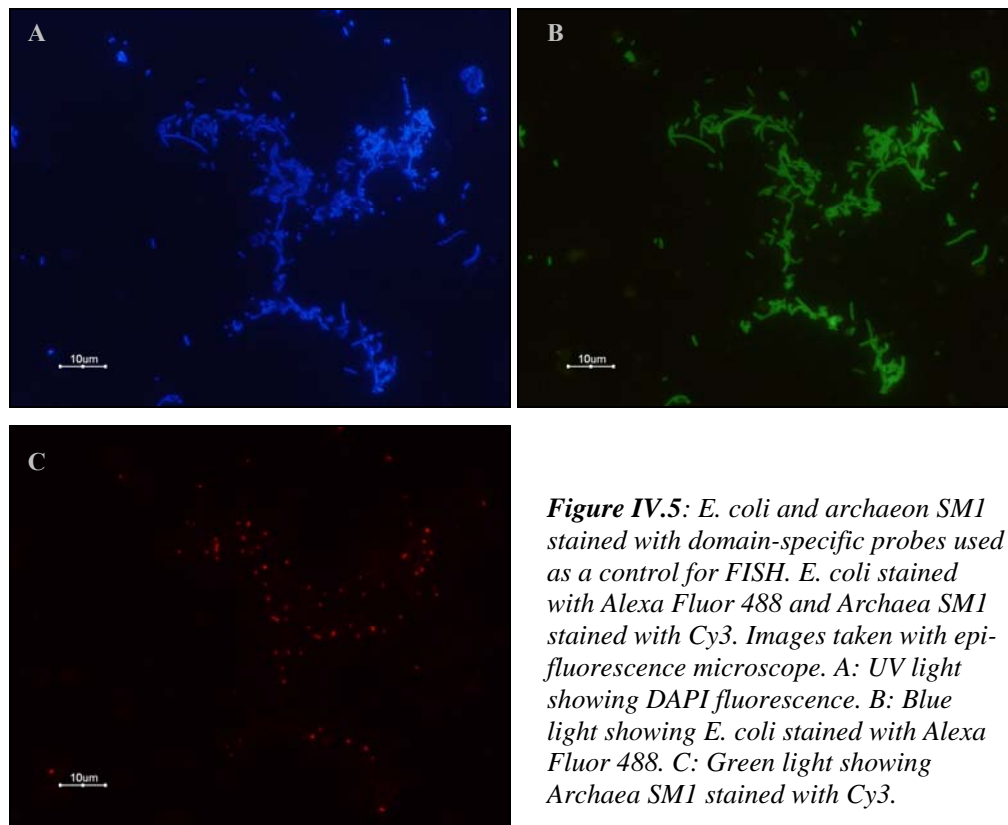


Figure IV.5: *E. coli* and archaeon *SM1* stained with domain-specific probes used as a control for FISH. *E. coli* stained with Alexa Fluor 488 and Archaea *SM1* stained with Cy3. Images taken with epi-fluorescence microscope. A: UV light showing DAPI fluorescence. B: Blue light showing *E. coli* stained with Alexa Fluor 488. C: Green light showing Archaea *SM1* stained with Cy3.

Initial experiments with FISH using epi-fluorescence microscopy revealed high levels of background autofluorescence resulting from the minerals present in the sediment-extract (Figure IV.6). The minerals also showed non-specific binding to the FISH probes. The strong background from the sample material interfered with the ability to distinguish microorganisms from minerals. To avoid the background autofluorescence, the samples were visualised using a confocal microscope instead of the commonly used epi-fluorescence microscope.

High concentrations of formamide were required during the hybridisation step for FISH, to decrease non-specific binding of fluorescent probes to the minerals present in the medium and to optimise the probe specificity. Although 35% formamide was found to be the optimum concentration to balance the problem of auto-fluorescence background and the integrity of the microorganism's cell wall, the minerals still showed high levels of fluorescence difficulting the differentiation of microbial cells under the epi-fluorescence microscope (Figure IV.6). Higher concentrations of formamide promoted the loss of the integrity of the cell walls.

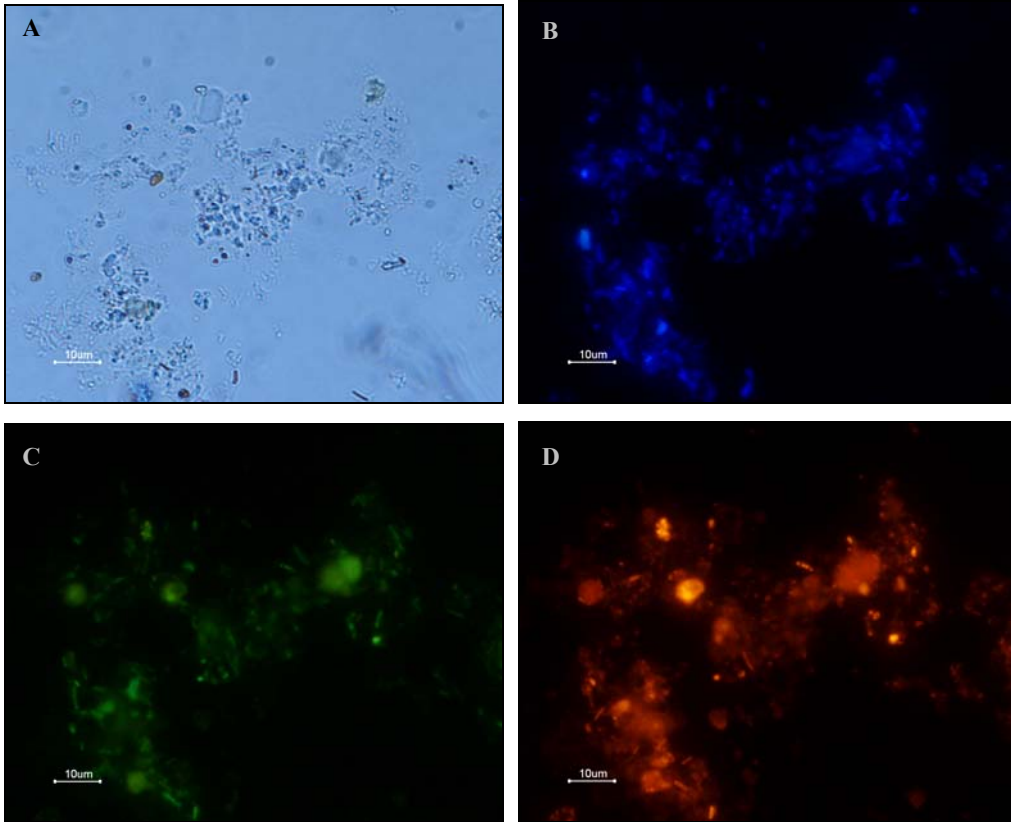


Figure IV.6: FISH images by epi-fluorescence microscopy of enrichment cultures from location site G growing at 60°C. A: DIC. B: UV light. C: Blue light. D: Green light.

Confocal microscopy was used to avoid the autofluorescence background by applying point illumination and a pinhole in an optically conjugate plane to result in the detection of fluorescence only in the focal plane (Figure IV.7).

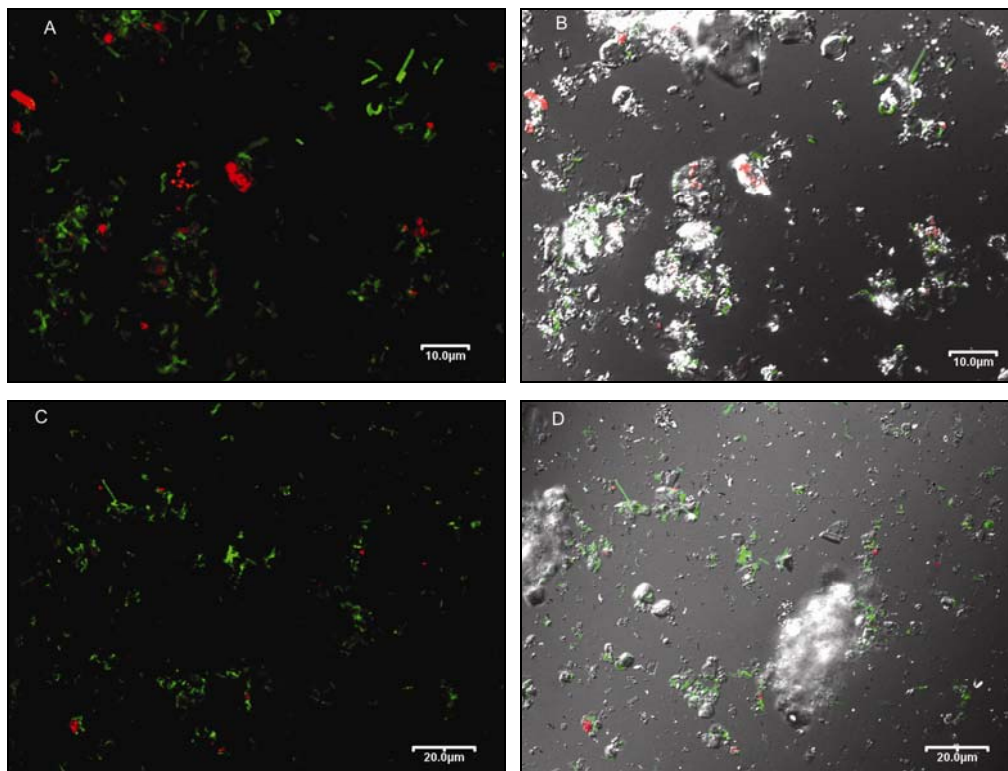


Figure IV.7: FISH images by confocal microscopy of enrichment cultures from location F and G at 60°C. All two-colour images reveal mixed populations of both Archaea –Cy3 (red) and Bacteria –Alexa Fluor 488 (green). Figures A and B belong to sample site F. Figures C and D belong to sample site G. Figures B and D show differential interference microscopy images combined with their respective fluorescence staining to demonstrate particulate and microbial interactions in liquid sediment-extract medium.

Bacterial microorganisms were stained with Alexa Fluor 488 (green) while archaeal microorganisms were stained with Cy3 (red). Both Bacteria and Archaea were observed as small communities attached to the minerals present in the medium in all cultures (Figure IV.7).

The enrichment cultures of the three locations analysed by confocal microscopy consisted of approximately 70% Bacteria and 30% Archaea when the cultures were cultivated at 60°C. Archaeal species were not uniformly present in cultures incubated at 37°C, except for sample site E where Archaea were observed to account for 9% of the population. These results reflected the culturable representatives of the microbial communities of White Island at the three locations studied.

4. DISCUSSION

4.1. Cultivation of thermo-acidophiles from White Island

Initially, various traditional media used for the cultivation of thermo-acidophilic microorganisms were tested (Johnson 1995). Cultivation using these conventional media was unsuccessful as the cultures were not sustainable over time, despite light microscopy revealing that growth was present initially. Volcanic sediment, when used as an inoculum, contains not only microbial life but also limited amounts of the essential minerals and chemical compounds require for microbial growth. These trace elements, initially present in the culture media when sediment was as an inoculum, were progressively diluted after serial sub-culturing. As a consequence, microbial growth initially observed in every traditional medium tested was not sustainable over time as the natural resources were not longer available.

Here, a new liquid medium based upon the utilisation of sediment-extract was formulated to ensure the availability of essential trace elements required for microbial growth over longer periods of time. Soil-extract has been known, since the late 1940s, as a valuable constituent of media for the growth of many bacteria where studies revealed that cultures isolated from soil-extract agar were unable to grow in liquid media without the presence of soil-extract (Lochhead & Chase 1943; Taylor 1951; Johnson 1995). However, the use of soil-extract in liquid or solid media has not been widely applied to the cultivation of microorganisms.

The lack of successful cultivation in standard media could be also explained by the lack of sediment particles which support the indispensable microbial metabolic pathways or by the nature of the microbial consortia (Spiegelman *et al.* 2005). Traditionally, microbiologists use complex transparent media to assist in the optical observation of microbial growth. The sediment-extract developed for cultivation purposes in this study was turbid due to the presence of high concentrations of minerals and small particles. This turbidity presumably enabled the necessary interactions between microorganisms and

sediment particles. This factor may be crucial for maintaining growth. The attachment of cells to specific minerals, such as ferrous iron sulphate crystals, is hypothesised to be significant for cycling of iron and sulphur (Druschel *et al.* 2004). Microbial communities of the order *Thermoplasmatales* have been found previously to be in direct contact with pyrite or ferrous-iron solutions (Druschel *et al.* 2004). Additionally, microorganisms typically form an exopolysaccharide (EPS) layer when they adhere to the surfaces of minerals (Sand *et al.* 1995) but not when they are growing as planktonic cells (Devasia *et al.* 1993). It is within this EPS layer that biooxidation reactions take place more rapidly and efficiently than when microorganisms are growing as planktonic cells (Gehrke *et al.* 1998; Rohwerder *et al.* 2003; Rawlings 2005).

4.2. Molecular analyses

The first step for molecular analyses is the extraction of genomic DNA from the samples. This step may be influenced by a variety of different factors. It has been reported that low yields of DNA are due to the adsorption of DNA to clay and quartz particles, especially under acidic conditions (Khanna & Stotzky 1992; Franchi *et al.* 1999). An enzymatic lysis protocol (described in Chapter VI.2.3.2) was used initially to extract the genomic DNA from the enrichment cultures resulting in very low yields of DNA. This result could be explained by the loss of activity of the enzymes (Lysozyme, Mutanolysin, RNAaseA and a protease from *S. griseus*) due to the low pH values present in the liquid media. For this reason, extraction of DNA was carried out using a chemical lysis method, resulting in adequate DNA yields for further analyses.

In addition, PCR amplification can be influenced by various factors such as primer mismatches, annealing temperature, or number of amplification cycles and differential amplification of different rRNA genes from mixed template DNAs producing artefacts (Reysenbach *et al.* 1992; Osborne *et al.* 2005). Variations in genome size or numbers of copies of the rRNA operon in the different microorganisms can also introduce bias (Farrelly *et al.* 1995). Those variables and their influences on PCR amplification cannot be estimated in analyses of unknown environmental samples and cultures. The choice of primers and the number of amplification cycles is crucial when amplifying unknown DNA (Suzuki & Giovannoni 1996). For this reason universal primers were used in this study to allow a match for a wide variety of microorganisms. However, universal primers may also

underestimate or overlook the total microorganisms present in the sample (Farris & Olson 2007). In order to obtain the best coverage of the microbial diversity of unknown samples, several extraction methods and primers for PCR amplification would be necessary. However, such analyses are time-consuming and expensive and became a limiting factor for their use in this study.

Various acidophilic, mesophilic and moderately thermophilic sulphur- and iron-metabolising species were identified from the enrichment cultures. Several of the amplified bacterial and archaeal sequences represented novel phylotypes or showed closest matches to previously uncultured or unidentified organisms (Table IV.5).

The diversity of the bacteria cultured was similar at all three locations studied from White Island. Phylogenetic analyses revealed that all α -Proteobacteria cultured were most closely related to previously uncultured microorganisms (Figure IV.2). As expected, α -Proteobacteria, which are traditionally mesophilic (optimal temperature range from 20 to 40°C), were only found in cultures growing at 37°C. The rest of the bacteria cultured were moderate thermophiles (Johnson *et al.* 1998). Phylotypes from α -Proteobacteria found in the enrichment cultures were closely related to *Acidiphilum angustum* and *Acidiphilum organovorum*. These microorganisms are acidophilic iron-reducers found in acidic metal-rich environments (Johnson & McGinness 1991; Dopson *et al.* 2003; Roling *et al.* 2006; Rowe *et al.* 2007). The third phylotype from α -Proteobacteria found in cultures from location site E was closely related to *Acidicaldus organivorans* (Johnson *et al.* 2006).

Three major groups were found from the *Firmicutes* division. Members from the genus *Sulfobacillus* include endospore-forming, rod-shaped aerobic Gram-negative, moderately thermophilic, acidophilic bacteria that obtain energy by oxidising ferrous iron, elemental sulphur and sulphide minerals (Golovacheva & Karavaiko 1978; Norris *et al.* 1996b; Johnson *et al.* 2003; Bogdanova *et al.* 2006). Isolates of *Sulfobacillus spp.* have been obtained previously from a range of thermal acidic environments and the uncultured and unclassified members of this group have also been found in acidic habitats, such as geothermal areas, self-heating mine-waste spoils and commercial mineral-processing operations (Golovacheva & Karavaiko 1978; Bond *et al.* 2000a; Kinnunen *et al.* 2003; Kinnunen & Puhakka 2004; Diaby *et al.* 2007). *Sulfobacillus acidophilus* was identified

from enrichment cultures growing at 60°C of two locations. Two members from the genus *Alicyclobacillus* were identified from enrichment cultures from the three locations examined. *A. tolerans*, previously classified as *Sulfobacillus thermosulfidooxidans* (Karavaiko *et al.* 2005), and *A. acidocaldarius* are both moderately thermophilic acidophiles and Gram-positive spore-forming bacteria (Darland & Brock 1971; Wisotzkey *et al.* 1992; Yokota *et al.* 2007) previously found from acidic soils and mines (Kinnunen *et al.* 2003; Groenewald *et al.* 2008). The rest of the phylotypes found from the division *Firmicutes* belonged to previously unidentified microorganism closely related to *Thermoaerobacter* and *Thermoanaerobacter* species.

Although Bacteroidetes are widely distributed in many environments including sediments, they are not normally found in acidic geothermal habitats (Fierer *et al.* 2007). In this study, one bacterial isolate belonging to the Bacteroidetes phylum was cultivated which was closely related to an uncultured bacterium from forest soils (Tsai *et al.* 2007).

Volcanic regions and hydrothermal systems featuring high temperatures and acidity levels are preferred habitats for archaeal species (Stetter 1999b). Archaea were detected in almost all the samples analysed (Table IV.5). Unlike Bacteria, most archaeal phylotypes were novel and/or showed closest matches to uncultured microorganisms. The phylotypes were clustered within three orders of acidophiles commonly found in acidic volcanic environments, the Crenarchaeal *Sulfolobales* and *Desulphurococcales*, and the Euryarchaeal *Thermoplasmatales* (Figure IV.3). The *Sulfolobales* represent a group of thermophilic acidophilic organisms that show facultative or obligate chemolithoautotrophic growth on sulphur and sulphur compounds and they have been found in a wide range of volcanic environments (Segerer *et al.* 1993; Atkinson *et al.* 2000). *Sulfolobales* phylotypes from previously uncultured microorganisms were detected in enrichment cultures from location F and G growing at 60°C. They were closely related to *S. acidocaldarius* and *S. tokodaii* isolated from similar environments (Chen *et al.* 2005; Kvist *et al.* 2005; Hetzer *et al.* 2007; Kvist *et al.* 2007). One phylotype from location site G growing at 60°C was closely related to *Ignicoccus pacificus* from the *Desulphurococcales* order. *I. pacificus* was firstly found living in marine hydrothermal vents (Huber *et al.* 2000a). This microorganism is able to live at temperatures from 70°C up to 98°C while reducing elemental sulphur to hydrogen sulphide to gain energy.

Ignicoccus ssp. have also been found living in symbiosis with nanoarchaea (Huber *et al.* 2002).

The third group of archaeal phylotypes identified clustered within the order *Thermoplasmatales*, genus *Thermoplasma*. These phylotypes were found in locations F and E. *Thermoplasma* species are thermo-acidophiles that grow at high temperatures and low pH values. They have been found also to require organic material for their growth (Cowan 2000; Huber & Stetter 2000). The phylotypes were closely related to *T. acidophilum* and *T. volcanium*. Both microorganisms are thermophilic heterotrophic prokaryotes. *T. acidophilum* has been found to grow at 55°C-60°C and at pH values from 0.5 to 4 in self-heating coal-refuse piles and solfatara fields (Brock 1978; Cowan 2000) while *T. volcanium* can grow at 33°C-67°C and pH values from 1-4 (Kawashima *et al.* 2000; Simmons & Norris 2002).

Despite the fact that many of the phylotypes found in the enrichment cultures were closely related to previously uncultured microorganisms, their specific physiology and metabolic properties could only be determined accurately unless they were isolated and characterised individually. Further molecular analyses undertaken directly from the sediment collected in White Island would help to increase the knowledge of the microbial diversity present in volcanically-active sediments compared to the cultured microbial diversity obtain from this study.

4.3. FISH

Microbial cell staining with specific fluorescent oligonucleotide probes used in FISH allowed the detection and enumeration of microorganisms in their natural habitat (DeLong *et al.* 1989; Amann *et al.* 1992; Amann *et al.* 1995; Brand *et al.* 2000). Epi-fluorescence microscopy is a common technique for bio-imaging and fluorescence analysis of numerous samples (Klepner & Pratt 1994). Epi-fluorescence microscopy was used to analyse the cultured microbial communities of White Island by FISH. However, background fluorescence of the sediment and non-specific binding of fluorescence probes to minerals did not allow clear detection of hybridised microbial cells. Small inorganic particles and clay minerals with high affinity to nucleic acid probes interfered with the analysis of microorganisms by epi-fluorescent microscopy, despite the latest

improvements in FISH and fluorescent molecular probes (Moter & Gobel 2000; Caracciolo *et al.* 2005).

Confocal microscopy can reduce interference from non-specific background fluorescence, allowing FISH studies in environmental samples (Caldwell *et al.* 1992; Bloem *et al.* 1995). Three-dimensional reconstructions of the specimen allows the analysis of spatial distribution and microbe-surface interactions while reducing background autofluorescence of the minerals (DeLeo *et al.* 1997). Images obtained using confocal microscopy revealed that the majority of the microorganisms detected were associated with the sample particles (Figure IV.7). The confocal microscope constructs an image by pointing the light along one focal plane. Therefore, microbial cells situated above or below the plane scanned cannot be detected, resulting in a potential underestimation of cell numbers (Li *et al.* 2004). Semiautomatic and automated methods based on confocal and epi-fluorescence microscopy have been developed to count cells in environmental samples (Pernthaler *et al.* 2003; Zhou *et al.* 2007). However, for reliable statistical analyses and accurate cell counts, several hundreds of cells need to be present in the analysed area and the cells need to be relatively evenly distributed throughout the sample (Daims *et al.* 2001b). These automated methods were not compatible with the cultured samples from this study as the microorganisms were not evenly distributed and in many cases they were present in very low numbers. In addition, cells often cannot be eluted from soil and sediment samples due to strong adsorption to mineral surfaces or trapping within micropores (Li *et al.* 2004). Nycodenz density gradient centrifugation was briefly tested with cultured microorganisms for extraction of the cells (Ford & Rickwood 1982). However, no cells were recovered from the samples, probably due to the strong interaction with the minerals. Flow cytometry represents another commonly applied method to enumerate microbial cells within environmental samples (Wallner *et al.* 1993; Vives-Rego *et al.* 2000). However, difficulties in distinguishing microorganisms from the abundant fluorescent mineral particles present in the media made it impossible to obtain accurate cell counts of the samples in this study.

FISH results were inconclusive and further work will be required to overcome these problems. For example, the use of CARD-FISH could increase the signal intensities enabling a better detection of cells associated with fluorescent minerals (Schönhuber *et al.*

1997). In addition, the fluorescent background produce from non-specific binding of FISH probes to the minerals could be reduced by the use of molecular beacons (Lenaerts *et al.* 2007).

4.4. Isolation of pure cultures

Low pH agarose plates are usually difficult to handle, as acidic salts destroy the capacity of agarose to solidify and form a gel (Manning 1975). An agarose-based medium was developed which required the removal of any soluble constituents and organic material which may inhibit the growth of thermo-acidophilic microorganisms. The resulting solid medium was then supplemented with the same sediment-extract as supplied to the liquid medium, which provided not only the essential nutrients for microbial growth but also the acidic environment required for thermo-acidophiles. During the solidification of the agarose, precipitation of sulphites and iron was observed which may have helped the plates retain more water at higher temperatures compared to conventional agar plates.

The microorganisms isolated in pure culture using sediment-extract agarose were identified as being *Alicyclobacillus acidocaldarius* and *Sulfobacillus acidophilus* (Table IV.5). *S. acidophilus* has been described previously as an acidothermophilic ferrous- iron- and mineral-sulphide oxidising bacterium able to grow autotrophically, mixotrophically and heterotrophically (Norris *et al.* 1996b). *Alicyclobacillus ssp.* can be found in similar habitats to *Sulfobacillus ssp.* which are often rich in metals and metal sulphide minerals (Simbahan *et al.* 2004).

4.5. Chemical analyses

Multi-element analyses of the sediment-extract were carried out to gain a better understanding of its composition and superiority over standard media. The results showed that the sediment-extract contained high concentrations of magnesium, sulphur, sulphate, sulphite, iron and nitrate (Table IV.3). These elements and radicals are known to be used as sources of energy for many thermo-acidophilic microorganisms (Huber *et al.* 2000b).

4.6. Summary

This study represents the first description of the microbial communities of acidic volcanically-active sediments of White Island. It is not surprising to find that the

microbial communities cultured from White Island are related to the *Sulfobacillus*, *Alicyclobacillus* and *Acidiphilum* groups. *Sulfobacillus* spp. species as they oxidise reduced sulphur compounds such as sulphite, hydrogen sulphide and elemental sulphur to obtain energy, generating sulphates and sulphuric acid (Norris *et al.* 1996b; Johnson *et al.* 2005; Bogdanova *et al.* 2006). The sulphates are then used by sulphur-reducing bacteria, such as *Alicyclobacillus* spp., to obtain energy, generating hydrogen sulphide and sulphites that can then be re-used by the sulphur-oxidising bacteria (Bridge & Johnson 1998; Simbahan *et al.* 2004). This results in mutually beneficial cross-feeding interactions. In the same way, iron-oxidising bacteria such as *Acidiphilum* spp. utilise ferrous iron to obtain energy, while generating ferric iron, which can then be used by iron-reducing bacteria, a process which regenerates the ferrous iron (Johnson *et al.* 1979; Wichlacz *et al.* 1986).

This study also reports the presence of Archaea species in the hydrothermal systems of White Island for the first time. Most of the archaeal phylotypes detected were novel or showed closest matches to previously uncultured microorganisms.

The microbial communities found from the sediments of White Island appeared to be different from the communities described previously from the acidic waters (Donachie *et al.* 2002). Although the analyses undertaken on acidic waters also revealed the presence of α -Proteobacteria and Firmicutes species, only *Acidiphilum* species was found to be in common with the microbial population found from the sediments in this thesis. The rest of the microorganisms described were placed into different phyla. In addition, enrichment cultures from acidic waters were not obtained at cultivation temperatures up to 60°C (Donachie *et al.* 2002). In contrast, a wide range of microbial diversity was found from the enrichment cultures of sediment samples cultivated at that temperature (Table IV.5). Moreover, neither molecular analyses nor the microbiological methods undertaken on acidic stream waters revealed the presence of Archaea species.

The presence of sediment particles in the sediment-extract liquid media may have conferred a substantial advantage over conventional media for the cultivation of environmental microorganisms as it provided the essential nutrients for their growth and the physical support for their associated microbial interactions. The limited success

achieved when attempting to obtain diverse acidophilic microorganisms in pure culture, compared to the diversity found in the liquid media, may be due to a number of factors such as the presence of inhibitory materials like organic compounds or soluble oligo- and mono-saccharides within the gel formed by the hydrolysis of the agarose under acidic conditions (Johnson 1995), or the need for the microorganisms to grow in consortia (Kaeberlein *et al.* 2002).

Further investigation into the physiology of thermo-acidophilic microorganisms found in White Island may provide a better understanding of the microbial interactions and the essential roles that the very different species play in the environment (Lazaroff *et al.* 1982; Bridge & Johnson 1998).

Chapter V. Optical and binding characterisation of the QDs

1. INTRODUCTION

This chapter records an examination of the chemical, optical and physical properties of Quantum dots (QDs) for their use in environmental samples. It provides characterisation of the fluorescent properties of QDs in comparison to traditional organic fluorophores and discusses their future applications in flow cytometry through evaluation of their excitation-emission spectra and their binding to paramagnetic beads using standard instrumentation.

1.1. Optical properties of the QDs

QDs have unique optical properties over traditional fluorophores as they can be excited by broad excitation wavelengths while emitting narrow fluorescent emission maxima, combined with photo-stability and longer decay lifetimes.

Table V.1: Glossary of terms.

Terms	Definition
Bandgap	An intrinsic property of semiconductors and refers to the energy difference between the valence band and the conduction band.
Blinking	The property of a fluorophore where it switches between fluorescent and non-fluorescent states.
Exciton Bohr radius	An exciton refers to the electron-hole pair created in a semiconductor when an electron is promoted from the valence band to the conduction band and leaves a hole behind. Exciton Bohr radius is the physical distance between the separated electron and hole.
Fluorescence excited state lifetime	Lifetime of a fluorescent molecule is measured as the time lapse in which the fluorescence intensity decays to 1/e of the initial value
Fluorescence lifetime	The time the molecules remain in the excited state before emitting a photon
Molar extinction coefficient	A measure of how strongly a compound absorbs light at a certain wavelength.
Passivation	A chemical process by which the core of the QD is surrounded by another material with a larger optical bandgap (the shell)

Quantum yield	The ratio of the number of photons emitted by the fluorophore to the number absorbed
Stokes Shift	The Stokes Shift is measured by the distance or energy (wavelength) between the excitation peak and emission peak maxima

1.1.1. Absorbance characteristics

The broad excitation properties of the QDs result from their ability to absorb light at all wavelengths shorter than their emission maxima (Evanko 2006). This unique characteristic allows different colours of QDs to be excited by a single common light source allowing multiplex analyses of more than one target from a single sample (Figure V.2). In contrast, the absorbance band of organic fluorophores is narrow and usually spectrally close to the light emitted, resulting in the need for various excitation light sources (Figure V.1). The high Stokes Shift of the QDs (hundreds of nanometres) compared to organic dyes (~ 15-30 nm) and the larger molar extinction coefficients (Table V.1) allow QDs to absorb light more efficiently than organic fluorophores.

1.1.2. Emission characteristics

1.1.2.1. Emission spectra of the QDs

The size of QDs is related directly to their fluorescent emission characteristics (Jaiswal & Simon 2004; Bruchez 2005). The narrow, symmetrical emission spectra of the QDs make the detection of multiple colours possible without spectral overlap or cross-talk (Azzazy *et al.* 2007). In contrast, the emission spectra of organic fluorophores are narrow, making efficient collection of the emitted light difficult due to scatter, auto-fluorescence and the need for precise optical filters (Figure V.1).

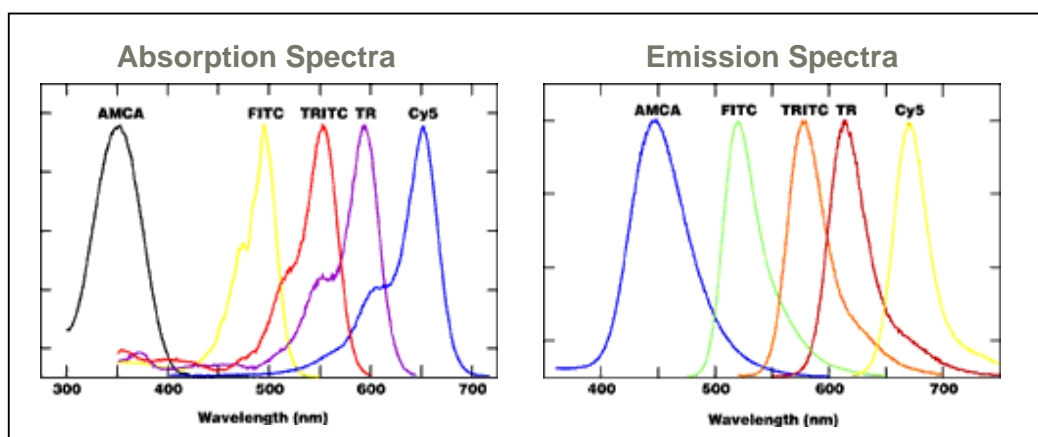


Figure V.1: Absorption and emission spectra of conventional organic dyes showing their narrow absorption coupled with broad emission spectra.

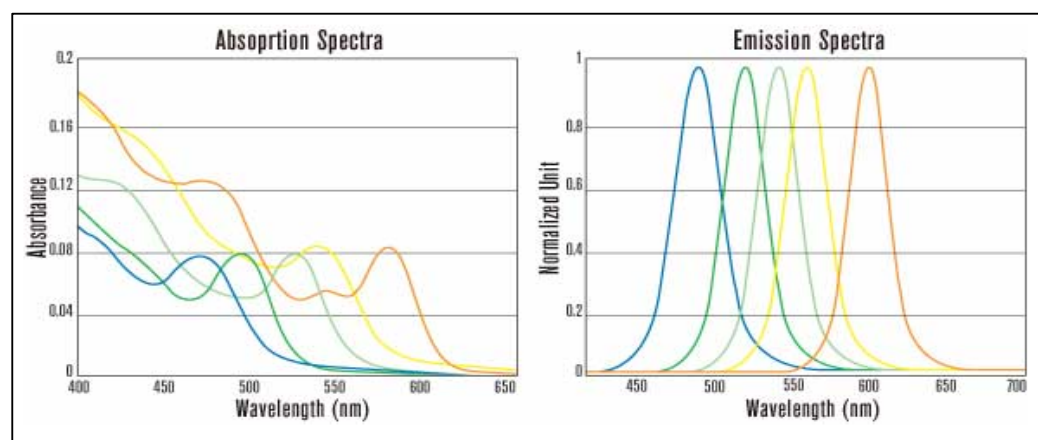


Figure V.2: Absorption and emission spectra of commercial QDs showing their broad absorption coupled with narrow emission spectra. Information extracted from the user manual supplied by Quantum Dots Corporation.

1.1.2.2. Quantum yield

Quantum yield (Table V.1) is defined as the ratio of light emitted to light absorbed by the fluorescent material (Wang *et al.* 2008). The quantum yield of QDs is generally over 50% (Sharma *et al.* 2006), making them efficient with regards to conversion of the excitation light into emission. It has been reported that cadmium selenide (CdSe) QDs exhibit quantum yields ranging from 40% to 90% (Azzazy *et al.* 2007). The quantum yield of a fluorophore usually decreases after conjugation to other molecules. However, QDs have been claimed to retain their high quantum yields even after conjugation to biological affinity molecules (Wu *et al.* 2007b).

1.1.2.3. Photo-stability

The photo-stability of QDs leads to longer fluorescence lifetimes, increased brightness and resistance to photo-bleaching over traditional organic fluorophores (Wu *et al.* 2003; Zhelev *et al.* 2004; Medintz *et al.* 2005; Michalet *et al.* 2005). Photo-bleaching is a process in which the molecular structure of a fluorophore is altered irreversibly as a result of the absorption of light, thus rendering it non-fluorescent (Weng & Ren 2006). Organic fluorophores are bleached progressively by the light sources used to excite them. Although a wide range of photo-stability has been observed in various fluorescent dye molecules, their stability does not approach that observed for QDs (Weng & Ren 2006). Studies on the photo-stability of QDs have reported that even, under conditions of intense illumination, little if any degradation of fluorescence is observed (Dahan *et al.* 2003; Jaiswal *et al.* 2003; Ballou *et al.* 2004; Lidke *et al.* 2004). This increased photo-stability also results in QDs exhibiting longer fluorescence lifetimes (in the order of 10-50 ns), allowing them to be distinguished from auto-fluorescent background with increased sensitivity (Bruchez *et al.* 1998; Smith & Nie 2004; Alivisatos *et al.* 2005).

1.2. Physical properties

QDs are semiconductor nanocrystals composed of atoms from II-IV or III-V groups elements such as cadmium selenide (CdSe), cadmium telluride (CdTe), indium phosphide (InP) and indium arsenide (InAs) (Alivisatos 1996; Michalet *et al.* 2001). These nanocrystals are capped with a protective shell of an insulating semiconductor material or wide-bandgap to protect surface atoms from oxidation and other chemical reactions which may reduce the overall quantum yield (Michalet *et al.* 2005). After capping, it is necessary to make the nanocrystals water-soluble to facilitate their conjugation or binding to biomolecules. Several methods have been described, including: derivatising their surface with mercaptoacetic acid or silica overcoat (Chan & Nie 1998; Yang *et al.* 2004); encapsulating them in phospholipid micelles (Dubertret *et al.* 2002); or by coating them with an amine-modified poly(acrylic acid) (Wu *et al.* 2003).

Commercially-available QDs used for biological applications are complex multi-layered structures, typically composed of three different layers with a final size similar to large proteins (10-20 nm) (Figure V.3).

- **1. Core:** The core is normally composed of CdSe. It determines the optical properties of the final QD.
- **2. Core-shell:** The core is commonly passivated (Table V.1) with a semiconducting inorganic outer-shell of zinc sulphide (ZnS). This prevents the contamination of the core material and improves the optical properties of the nanocrystal by reducing photochemical bleaching while increasing the quantum yield (Hines & Guyot-Sionnest 1996; Michalet *et al.* 2005). The core-shell ranges between 3 to 10 nm and defines the fluorescent emission of the QDs.
- **3. Polymer layer:** The surface of the core-shell is covalently attached to a layer of an organic ligand. This layer makes the QDs water-miscible (Wu *et al.* 2007b). The outer part of the polymer layer is hydrophilic and functionalised with carboxylic acid derivatives. This enables functional groups, such as proteins or chemical compounds, to be integrated into the QDs which allow specific binding to the desired target (Michalet *et al.* 2005).

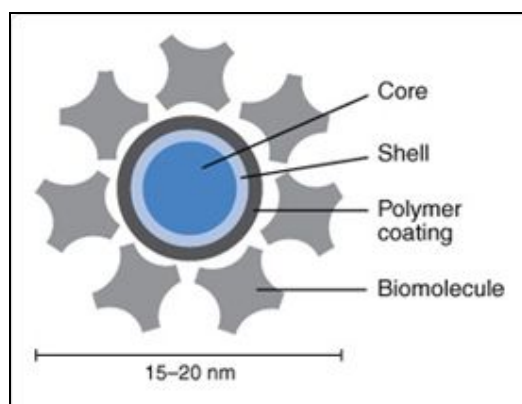


Figure V.3: Schematic representation of a single QD (<http://www.invitrogen.com>).

The optical, electronic and chemical properties of the QDs are ruled by the small size of the nanocrystal. The diameters of semiconductor nanocrystals are smaller than their exciton Bohr radius (Table V.1), resulting in the phenomenon known as the “quantum confinement effect” (West & Halas 2003; Arya *et al.* 2005). QDs absorb photons when the excitation energy exceeds the bandgap, leaving the holes behind and resulting in the creation of an electron-hole pair (exciton). During this process, electrons are promoted from the valence band to the conduction band. The absorption has an increased probability at higher energies (shorter wavelengths) and results in a broadband absorption spectrum.

When the exciton returns to a lower energy level, a narrow, symmetric energy-band emission occurs (True & Gao 2007).

1.3. Surface chemistry of the QDs

QDs are considered to be negatively charged owing to molecules absorbed on their surface (Mattoussi *et al.* 2000). The surface chemistries of QDs are designed to include functional groups such as amine (-NH₂), carboxyl (-COOH) or mercapto (-SH) molecules that enable direct conjugation of the QDs to biomolecules.

QDs have been successfully coupled to biomolecules, such as transferrin, immunoglobulin G, biotin, streptavidin, avidin and nucleic acids (Bruchez *et al.* 1998; Chan & Nie 1998; Dubertret *et al.* 2002; Goldman *et al.* 2002; Kloepfer *et al.* 2003; Mansson *et al.* 2004). These conjugates are luminescent probes that bind with specificity and sensitivity to a variety of targets.

1.3.1 Types of interactions

In this study, two different types of chemical interactions were used to bind QDs to the molecular probes: a covalent interaction, and a non-covalent biological interaction. For the covalent interaction, amine-modified QDs were conjugated to the thiol-modified molecular probes using the cross-linker reagent EDC (1-ethyl-3-(3-dimethylaminopropyl)carbodiimide) (Figure V.4). EDC reacts with the thiol group of the molecular probe to form an active intermediate. This intermediate then is attracted to the primary amine (-NH₂) group of the QDs, forming a stable covalent bond between them. To increase the yield, a second reagent N-hydroxysulfosuccinimide (Sulfo-NHS) was added to form a more stable active ester intermediate (Taylor *et al.* 2000).

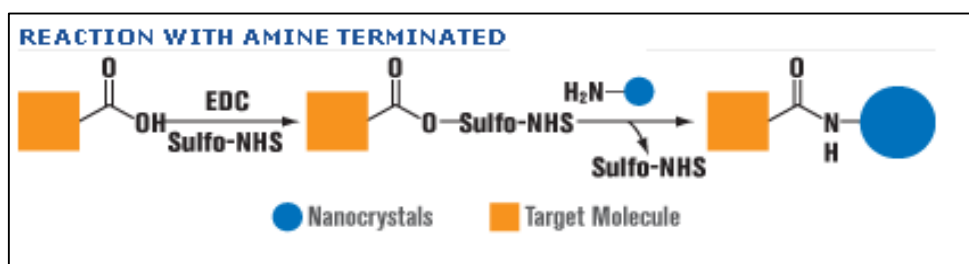


Figure V.4: Schematic chemical reaction of QDs functionalised with amine groups to the thiol groups of molecular probes using EDC and Sulfo-NSH as cross-linkers.

The non-covalent biological interaction was used to bind streptavidin-modified QDs to biotin-modified molecular probes. The avidin-biotin binding is the strongest known non-covalent biological interaction between protein and ligand (Goldman *et al.* 2002). Avidin is a glycoprotein found in egg white and contains four identical subunits each of which is capable of binding with one molecule of biotin. Biotin (Vitamin H) is a relatively small molecule found in tissue and blood and can be easily bound with protein molecules without significantly altering their biological activity (Bayer & Wilcheck 1980; Bagwe *et al.* 2003; Kampani *et al.* 2007).

1.4. Aim

The aim of this chapter was to characterise the optical properties of the QDs and their binding characteristics to molecular probes and paramagnetic beads. For this purpose, the excitation–emission profiles of two different species of QDs were characterised using fluorescence spectrophotometry and the binding capacity of the QDs to molecular probes was investigated by quantitative and qualitative methods. The quantitative method was based upon the absorbance spectra of QDs in solution compared to the absorption of QDs bound to the molecular probes as measured by spectrophotometry. The qualitative method was based on the difference between QDs in solution and QDs bound to the molecular probe as determined by electrophoretic analysis.

Dynabeads are paramagnetic beads selected as a platform for the binding of QDs due to their smooth spherical shape and their suitable size for flow cytometric analysis. The properties of the Dynabeads and optical behaviour of the QDs after binding to the Dynabeads were investigated. The binding characteristics of Dynabeads, including their detection limits, was analysed and the procedures to bind QDs and molecular probes

modified with fluorescein isothiocyanate (FITC) were established and confirmed by epifluorescence microscopy and flow cytometry.

2. MATERIALS AND METHODS

2.1. Reagents

2.1.1 EviTags QDs

Hops-Yellow CdSe/ZnS EviTags QDs (Evident Technologies Inc., Australia) were functionalised with amine groups. Table V.2 describes their general characteristics.

Table V.2: General characteristics of Hops-Yellow amine EviTags.

Characteristics	Hops-Yellow amine EviTags QDs
Emission Peak	560 ± 10 nm
Typical FMHM	< 30 nm
Suggested excitation wavelength	< 450 nm
First excitation peak	~ 555 nm
Concentration	~ 4nmol/ml (4x10 ⁶ mol/L) solvent in DI water (0.25 mg/ml)
Nanoparticle size	30 – 50 nanometres
pH stability	6 – 10
Temperature stability	4 – 25°C
Photo-stability under imaging conditions	75 mi

2.1.2. Qdots™

CdSe/ZnS Qdots™ (Quantum Dot Corp., CA, USA) were functionalised either with biotin or streptavidin groups. Quantum Dot Corp. is now part of Invitrogen (Carlsbad, CA, USA). Qdots™ were supplied in suspension with 50 mM borate (pH 8.3). Table V.3 describes the general characteristics of the QDs used in this study.

Table V.3: General characteristics of Qdots™.

Characteristics	Qdot™ 525	Qdot™ 535	Qdot™ 585	Qdot™655	Qdot™ 680
Colour	Yellow	Yellow	Orange	Red	Red
Emission max	525 nm	535 nm	585 nm	655 nm	680 nm
Conjugate	Streptavidin	Streptavidin	Streptavidin	Biotin	Streptavidin
Concentration	1 µM	2 µM	2 µM	2 µM	1 µM
Supplier	Invitrogen	Invitrogen	Invitrogen	Quantum Dot Corp.	Quantum Dot Corp.

2.1.3 Fluorophores

Fluorescent-dye conjugates to streptavidin were purchased from Invitrogen (Sydney, Australia).

Table V.4: Characteristics of fluorescent dye conjugates to streptavidin.

Fluorophore	Maximum excitation	Maximum Emission	Concentration
Fluorescein (FITC)	494 nm	518 nm	2 mg/mL solution in PBS, pH 7.2, 5mM sodium azide
Alexa Fluor® 488	495 nm	519 nm	NA
R-PE*	496, 546, 565† nm	578 nm	1 mg/mL solution in 0.1 M sodium phosphate, 0.1 M NaCl, 2 mM sodium azide, pH 7.5

* Streptavidin R-Phycoerythrin

† Multiple excitation peaks

2.1.4. Paramagnetic Dynabeads®

Dynabeads M-280 streptavidin are super-paramagnetic polystyrene beads of 2.8 µm in diameter (Dyna® Biotech Pty Ltd, Australia). They were supplied as a suspension containing 6.7×10^8 Dynabeads per ml (10 mg/ml), dissolved in phosphate-buffered saline (PBS), pH 7.4. The binding capacity of the beads as indicated by the manufacturer was: 1 mg of Dynabeads binds to 200 pmol of biotinylated oligonucleotide (single stranded).

2.2. Buffers and solutions

All buffers and solutions were autoclaved for 20 min at 121°C and 200 kPA pressure. For general buffers and solutions refer to Chapter II.

Table V.5: Description of buffers and solutions.

Binding Wash buffer (BW buffer)	10 mM Tris/HCl (pH 7.5), 2.0 M NaCl and 1 mM EDTA
BioMag buffer	20 mM Tris (pH 7.8), 1 M NaCl, 1mM EDTA and 0.02% Triton x-100
QD incubation buffer	2% BSA in 50 mM borate with 0.05% sodium azide. Final pH 8.3
Piranha solution	3:1 mixture of sulphuric acid and 30% hydrogen peroxide. Used to clean lab instruments from free DNA or RNA. A fresh solution was made and mixed before application. First, H ₂ SO ₄ was applied followed by H ₂ O ₂ in a Pyrex container inside a hood. After 1-2 min, the solution was aspirated and the material was washed with autoclaved Milli-Q water several times

2.3. Fluorescence spectrometry

2.3.1. Excitation-emission spectrum of Qdot™ 655

Fluorescence measurements of Qdot™ 655 (QD655) were performed on a Perkin Elmer Luminescence Spectrometer LS 50B (Rowville, Victoria, Australia) equipped with a xenon discharge lamp. QD655 were diluted (1:1500) into dH₂O in 10 mm Quartz cells (Hellma, NY, USA). The excitation spectrum was scanned between 310 nm and 490 nm. The emission spectrum was scanned between 500 nm and 700 nm at 1500 mm⁻¹/sec scan speed.

2.3.2. Excitation-emission spectrum of Hops-Yellow Evitags QDs

Fluorescence measurements of Hops-Yellow Evitags QDs were performed on a Beckman DU® 650 UV/VIS spectrophotometer (Beckman Coulter, Inc. Fullerton, USA) which operates in the wavelength range of 190 to 1100 nm and has a bandwidth of <1.8 nm. A portion (10 µl) of Hops-Yellow QDs (0.25 mg/ml) was diluted in 500 µl 1 x PBS buffer and sterilised by filtration through 0.22 µm Millipore filters. The sample was placed in 1

ml Quartz cuvettes and analysed. The emission spectra of Hops-Yellow QDs were obtained between the 200-600 nm at 600 nm/min scan-speed wavelength at RT using the scan program and the standard pre-installed software (Beckman Coulter, USA).

2.3.3. Molar extinction coefficient

Absorption and reflection spectra measurements of both Hops-Yellow Evitags QDs and molecular probes were collected using a Varian Cary 5 double-beam spectrophotometer (Varian, Inc., Palo Alto, USA). The samples were scanned between 400 to 700 nm wavelength range at 0.5 nm intervals, with a $60 \text{ nm}\cdot\text{min}^{-1}$ scanning rate at RT. The results were processed using the standard software v.02 incorporated in the spectrophotometer. The molecular probe used was DeinoFam (further details of the molecular probes are found in VI.2.3.4), an oligonucleotide modified with thiol at the 5' end. Prior to analyses, 3 ml Quartz cuvettes (Hellma, NY, USA) were cleaned with Piranha solution to remove any organic residues. One cuvette was used as a blank for all measurements and contained 2 ml of autoclaved MilliQ water sterilised by filtration. Hops-Yellow QDs and DeinoFam probes were diluted separately in autoclaved MilliQ water sterilised by filtration. Then, 100 μl of Hops-Yellow QDs (0.25 mg/ml) were conjugated to 25 μl of DeinoFam probe (5 μM) following the protocol described below (V.2.4.1).

2.4. Binding procedures

All procedures involving the use of QDs or organic fluorophores were carried out in darkness to avoid exposure to light. The final products were kept at 4°C in the dark for less than 24 h until further analysis.

2.4.1. Coupling of thiol-modified probes to amine-modified QDs

Two thiol-modified probes were used for binding to Hops-Yellow QDs. DeinoFam was a thiol-modified probe designed to hybridise to specific regions of the 16S rRNA sequence of *D. radiodurans*. QDLinker was a poly-A probe with a biotin modification at the 5' end and thiol modification at the 3' end (further details and descriptions of the probes are found in VI.2.3.4).

For activation, 450 μl of 1xPBS, 25 μl of DeinoFam or QDLinker probe (0.1 mM) and 25 μl BMPA (N- β -Maleimidopropionic acid, 200 mM) were combined, followed by incubation for 2 h at RT. Microcon centrifugal filter devices (3000 MWCO) were used as indicated in the user's manual to remove the excess of BMPA from the solution. Then, a portion (70 μl) was transferred to a fresh 1.5 ml Eppendorf tube including 270 μl of dH_2O , 50 μl of 10xPBS, 100 μl of amine modified Hops-Yellow QDs and 10 μl of EDC at a final concentration of 100 mg/ml (the interaction between amine and thiol groups was explained in V.1.3.1). The solution was incubated at RT for up to 2 h, and then 500 μl of 1 M Tris pH 7.4 were added to quench the conjugation reaction. Excess unbound probes were removed using Microcon centrifugal devices (100,000 MWCO). These filters discriminate between free probes and QDs. The final product was resuspended in 120 μl of 1 x PBS and stored at 4°C.

2.4.2. Washing of Dynabeads[®] paramagnetic beads

Dynabeads[®] M-280 Streptavidin paramagnetic beads were used for all the binding procedures at a stock concentration of 10 mg/ml. A portion of bead solution (depending of its application) was placed into fresh 1.5 ml Eppendorf tubes and placed in 1.5 ml Dynal MPC[™] Magnet (Invitrogen, Mount Waverley, Australia) for 1-2 min to separate the beads from the original solvents and preservatives. The supernatant was removed carefully by aspiration with a pipette without removing the tube from the magnet. The tube was then removed from the magnet and BW buffer was added along the inside of the tube where the beads had been collected. The beads were resuspended in the same volume of BW buffer as the initial volume taken from the vial stock solution to keep the concentration of the beads constant. The washing step was repeated up to 3 times.

2.4.3. Binding of biotinylated QDs to Dynabeads[®]

Generally, for all experiments unless stated otherwise, a portion (100 μl) of washed Dynabeads was transferred to a fresh 1.5 ml Eppendorf tube. Then, portions of 5 μl of the washed Dynabeads were distributed to 1.5 ml test-tubes and resuspended in 200 μl of BioMag Buffer. Qdot[™] 655 QDs was diluted 1:1000 in Qdot incubation buffer. Binding of QDs to the Dynabeads was carried out by incubating the reaction at RT for 2 h with

gentle rotation or occasional mixing by gently tapping the tubes. Following the incubation period, unbound QDs were removed from the solution by washing the beads twice with 100 μ l of BW buffer using the magnet. Finally, the QD-bead complexes were resuspended in 300 μ l of BW buffer and stored in the dark at 4°C for no more than 24 h until further analysis.

2.4.4. Binding of biotinylated probes to Dynabeads®

Biotinylated probes used in this thesis are described in Chapter VI.2.3.4. Generally, for all experiments unless stated otherwise, a portion (5 μ l) of washed Dynabeads was transferred into 1.5 ml Eppendorf tubes and resuspended in 200 μ l of BW buffer. Biotinylated probes (100 μ M) were diluted (1:1000) in sterile MilliQ water. Binding of biotinylated probes to Dynabeads was carried out as above (V.2.4.3). After conjugation, the samples were washed twice with 100 μ l of BW buffer and resuspended in 300 μ l of BW buffer. Dynabeads bound to the probes were stored at 4°C in the dark up to 24 h until further analysis.

2.5. Flow cytometry

FCM was carried out as described in Chapter II.2.5. Data analysis was carried out using CellQuest software (BD Biosciences, Sydney, Australia). For data analysis, FL1 and FL3 histograms were created by gating the events falling within the defined region (R1). The peak generated by each of the samples of probe-bead complexes were analysed in the FL1 histogram and the median value recorded. Samples of QDs-bead complexes were analysed on the FL3 histogram and the median value recorded. The analysis program WinMDI version 2.8 was used for all data presentation of CellQuest data files and was obtained by downloading it from the *World Wide Web* (<http://facs.scripps.edu/software.html>).

3. RESULTS

3.1. Optical characterisation of the QDs

3.1.1. Excitation- emission spectra

The excitation-emission spectra of two different types of QDs, Hops-Yellow Evitags and QD655, were analysed by fluorescence spectroscopy.

The excitation-emission spectrum of QD655 was analysed between 310 nm to 490 nm by using a luminescence spectrometer (V.2.3.1). The emission spectrum was detected between 500 nm to 700 nm. The maximum fluorescence emission exhibited was at 655 nm for all excitation wavelengths examined (Figure V.5). The results indicated that QD655 remained fluorescent under all the excitation wavelengths examined. However, the intensity of the peak varied depending on the excitation wavelength used with a significant decrease observed at longer wavelengths. A 4-fold increase in fluorescence intensity was observed at short excitation wavelengths (UV = 320 nm) compared with longer excitation wavelengths (488 nm).

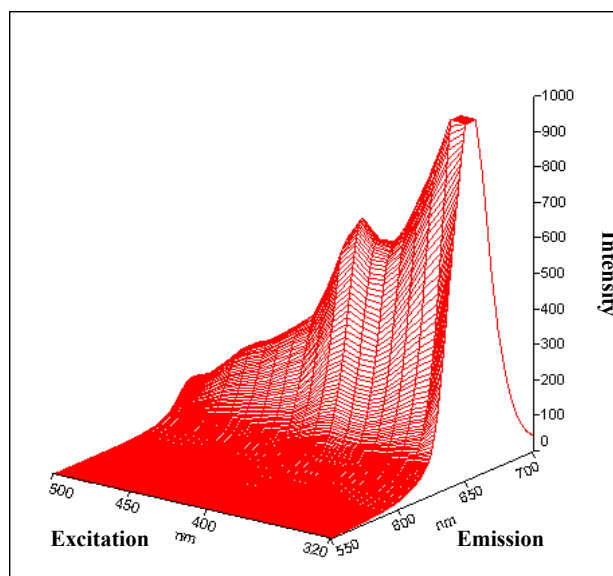


Figure V.5: Excitation-emission spectrum of QD655. Y-axis; fluorescent intensity in arbitrary units (a.u). X-axis: excitation wavelengths from 320 nm to 500 nm. H-axis: emission wavelengths detected from 550 nm to 700 nm.

The excitation-emission spectrum of Hops-Yellow QDs was then analysed by luminescence spectrophotometry (V.2.3.2). The excitation-emission spectrum was obtained between 200-600 nm wavelengths (Figure V.6) and the fluorescence emission peak was observed at 560 nm for all the excitation wavelengths examined. The intensity of the peak varied depending on the excitation wavelength used, with a significant decrease observed at longer wavelengths. Hops-Yellow QDs remained fluorescent at all the excitation wavelengths examined.

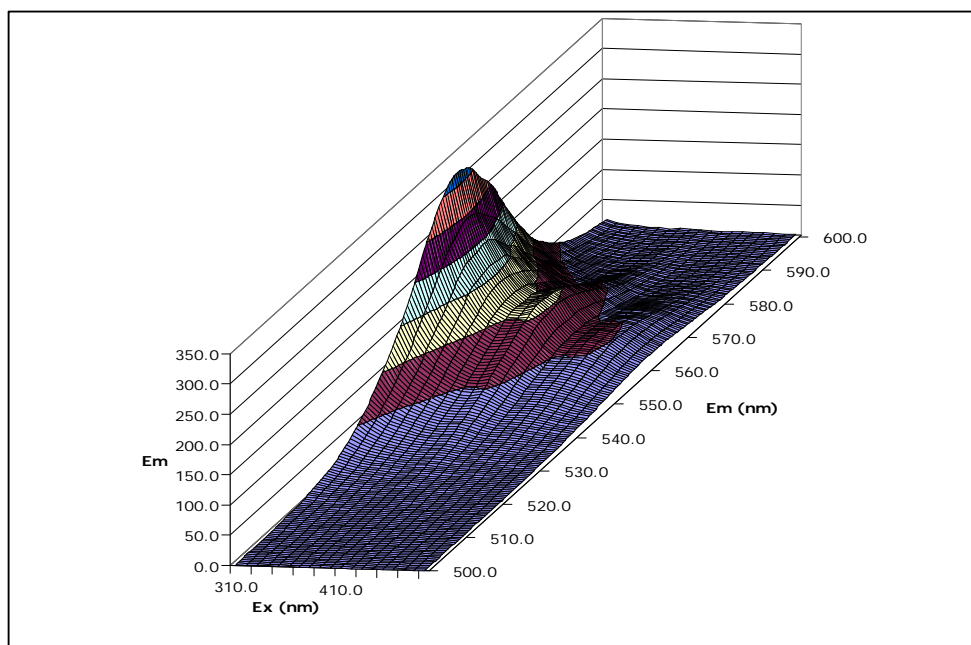


Figure V.6: Excitation-emission spectrum of Hops-Yellow QDs. Y-axis: fluorescent emission in arbitrary units (a.u). X-axis: excitation wavelengths from 310 nm to 500 nm. H-axis: emission wavelengths detected from 500 nm to 600 nm.

Both QDs studied have absorbance spectra that increase dramatically in the blue portion of their emission. Despite the broad absorbance, the emission wavelength is independent of the excitation wavelength, so whether exciton was at 600 nm or at 310 nm, the shape of their emission spectra remains the same, while the intensity is approximately 4-fold higher with short excitation wavelengths. The absorption spectra of the QDs appear as a series of overlapping peaks that get larger at shorter wavelengths, each peak corresponding to an energy transition between discrete electron-hole (exciton) energy levels. QDs did not absorb light that has a wavelength longer than that of the first exciton peak, also termed the

absorption onset. The wavelength of the first peak, and all of the subsequent peaks, was a function of the composition and size of the QDs.

The peak emission wavelength was a Gaussian bell-shaped for both QDs studied and it occurred at a slightly wavelength than the lowest energy exciton peak.

3.1.2. Molar extinction coefficient

The molar extinction coefficient (molar absorptivity) is a measure of how strongly a chemical absorbs light at a given wavelength. It is an intrinsic property of the chemical. The absorbance (A) of a sample is dependent on the pathlength (l) and the concentration (c) of the species via the Beer-Lambert law ($A = \epsilon cl$). Molar absorptivity represents the corrected absorption value for comparing the spectra of different compounds and determining the relative strength of light-absorbing factors.

The molar extinction coefficient of QDs was not provided by the manufacturer at this stage of the project. The absorbance of Hops-Yellow QDs (Table V.6) from 400 nm to 700 nm excitation wavelengths was measured by spectrophotometry (V.2.3.3). Absorbance usually ranges from 0 (no light at that particular wavelength is absorbed) and 1 (90% of the light at that wavelength is absorbed). The energy exciton peak or absorption onset of Hops-Yellow QDs was at 560 nm.

Table V.6: Series of Hops-Yellow QDs concentrations and their absorbance in arbitrary units (a.u.) as measured by spectrophotometry.

Sample number	Concentration (nmol/ml)	Absorbance at 560 nm (a.u.)
1	0.53	0.53
2	0.4	0.43
3	0.32	0.37
4	0.26	0.32
5	0.22	0.3
6	0.2	0.27
7	0.17	0.25
8	0.16	0.24
9	0.14	0.23
10	0.13	0.22

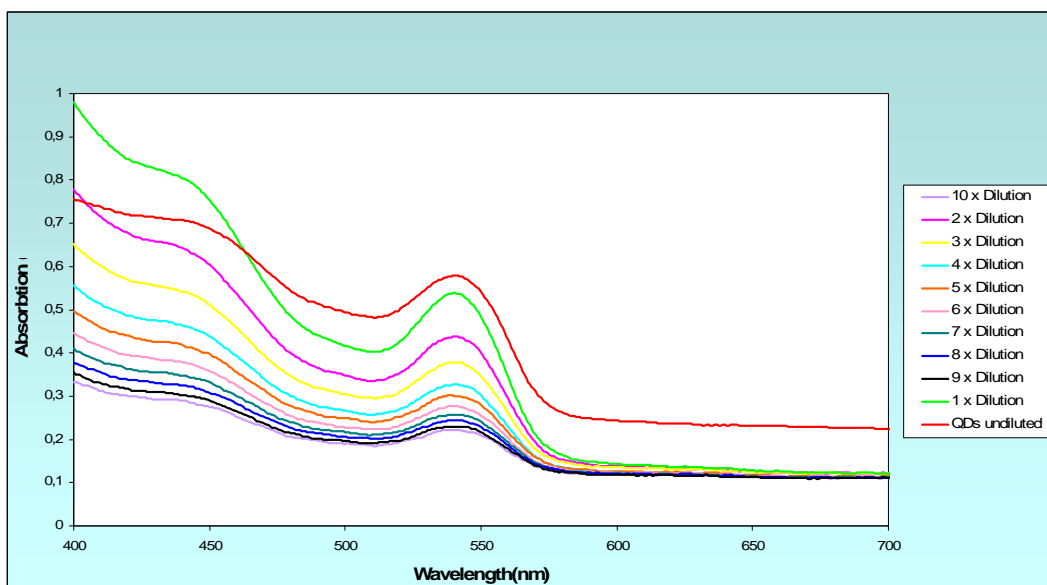


Figure V.7: Absorption spectra of the different concentrations of Hops-Yellow QDs (Table V.6) using excitation wavelengths from 400 to 700 nm. The absorption was measured in arbitrary units (a.u.). The absorption onset was at 560 nm.

The absorption onset for all samples was at 545 nm (Figure V.7). Following the Beer-Lambert law ($A = \epsilon cl$), the molar extinction coefficient (ϵ) could be calculated as $A / (c (400 \text{ mol/L}) * 1 (1 \text{ cm}))$. Therefore, $\epsilon = 0.001 \text{ mol}^{-1} \text{ cm}^{-1}$.

3.2. Binding characterisation of the QDs

Quantitative and qualitative methods were designed to investigate the number of molecular probes that could be attached to a single QD.

3.2.1. Quantitative method

A quantitative method to study the number of molecular probes that could be bound to a single QD was designed based on the absorption spectra of both the QDs and the probes. The absorbance of a sample is proportional to the number of absorbing molecules (molar concentration) that interact with the light beam. QDs have a specific absorption onset depending on the size of their core. The QDs and the molecular probes used exhibit different spectral signatures. Hypothetically, when studying the absorbance spectra of QDs bound to the probes, two distinct peaks should be observed; one peak corresponding to the absorption onset or energy exciton peak of QDs and a second peak, corresponding

to the absorption of the probes. From the spectral signatures it should be possible to quantify the number of probes bound per QD.

The absorption spectra of Hops-Yellow QDs as shown in Figure V.7 indicated that the absorbance of Hops-Yellow QDs increased at shorter excitation wavelengths and the energy exciton peak was at 545 nm.

The absorption spectrum of a molecular probe (DeinoFam) was investigated by spectrophotometry (V.2.3.3). The absorption peak of the probe was at approximately 269 nm (Figure V.8).

Table V.7: Absorption measurements of two concentrations of DeinoFam obtained by spectrophotometry.

Sample number	DeinoFam concentration (μM)	Absorbance at 260 nm (a.u.)
1	3.96	0.5228
2	1.96	0.2502

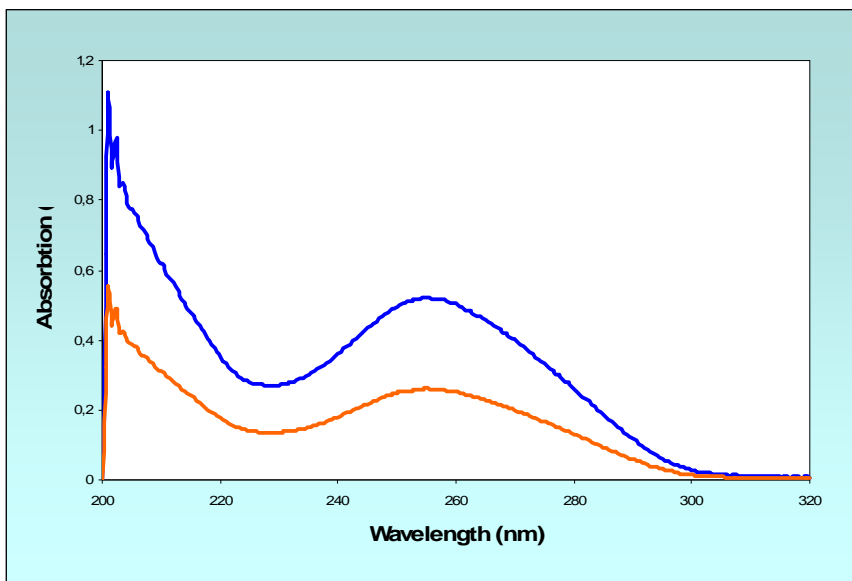


Figure V.8: Absorption spectra of two different concentrations of DeinoFam probe (Table V.7). Sample 1: Blue line. Sample 2: Orange line. X-axis: excitation wavelengths from 200 nm to 320 nm. Y-axis: absorption values obtained at every excitation wavelength in arbitrary units (a.u.).

Hops-Yellow QDs were bound to DeinoFam probes by the covalent interaction using EDC as the cross-linker (Figure V.4) (V.2.4.1). The subsequent absorption spectrum of the complexes was observed by spectrophotometry (V.2.3.3).

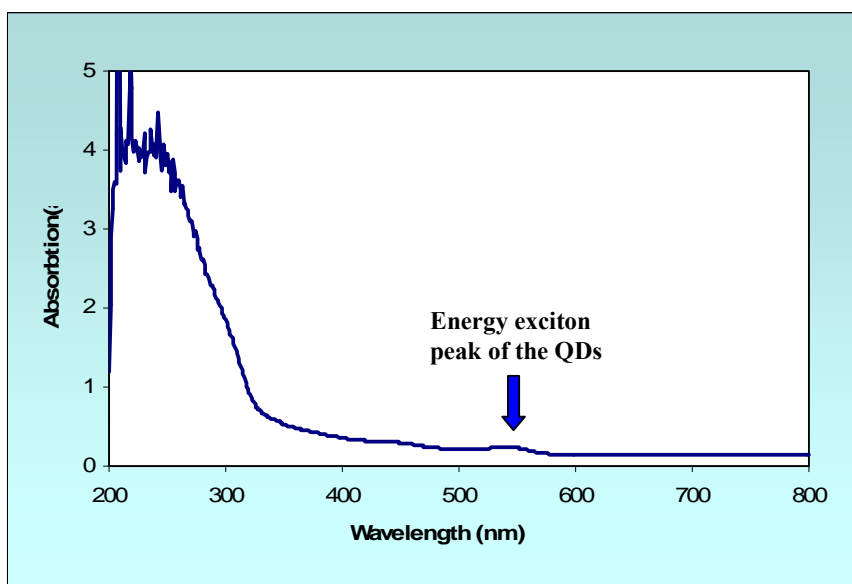


Figure V.9: Absorption spectrum of Hops-Yellow QDs bound to DeinoFam probe. X-axis: excitation wavelengths from 200 nm to 320 nm. Y-axis: absorption values obtained at every excitation wavelength in arbitrary units (a.u.)

Under optimal conditions, the absorption spectra of both free and bound QDs should be zero on the y-axis between the wavelengths of 600 nm to 700 nm indicating no absorption of the light (Figures V.7 and V.9). However, the absorption spectra obtained from free QDs revealed background noise at that region (Figure V.7). Even at low concentrations of QDs, the background noise did not decrease, indicating that the noise was not affected by the buffers used during the procedure, but by another unknown factor.

The absorption spectrum of Hops-Yellow QDs with bound molecular probe resulted in a unique spectral signature (Figure V.9). In theory, two distinct peaks, one from the QDs energy exciton peak and a second one from the probe should be distinguishable in the spectrum observed. The energy exciton peak of Hops-Yellow QDs was observed to be at 540 nm while the absorption peak of the probe was observed at 269 nm. The absorption spectrum of the QDs increased at shorter wavelengths. Although the absorption of QDs alone were not studied in the 200-300 nm range, it could be predicted that their absorption would continue increasing in that range resulting from the background noise observed in Figure V.9. This background noise made it impossible to distinguish any distinct peak in this range.

3.2.2. Qualitative method

Gel electrophoresis was used as a qualitative method to determine the successful binding of QDs to molecular probes.

The size and the negative charge of the surface of the QDs made them suitable for gel electrophoretic analysis. Unbound QDs run faster through the gel as compared to QDs bound to molecular probes. The binding of several probes to the surface of a single QD made them larger, and consequently they migrated more slowly than single QDs in agarose gel. Typical results from the gel electrophoretic analysis of QDs bound to oligonucleotide probes are shown below (Figure V.10).

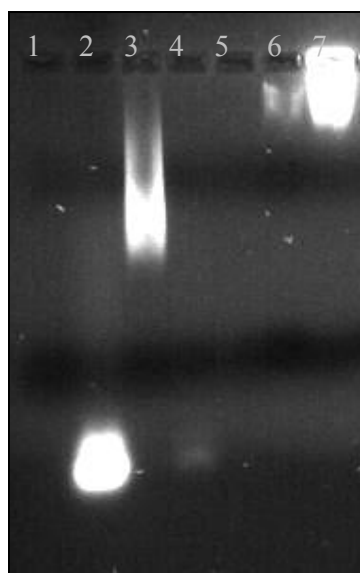


Figure V.10: Unbound QDs, oligonucleotide probes and QDs bound to the probes running on a 1% agarose gel.

Bands:

- 1 – Blank (no sample)
- 2 – Probes
- 3 – QDs
- 4 – First waste fraction after binding QDs to the probes
- 5 – Second waste fraction after binding QDs to the probes
- 6 – QDs bound to the probes
- 7 – QDs bound to the probes (loaded in the gel at higher concentration)

The size of unbound QDs allowed them to run successfully on an agarose gel (Figure V.10, band 3). QDs bound to the probes were considerably larger and consequently ran more slowly on the gel (Figure V.10, bands 6 and 7). The waste fractions were also analysed to ensure that both QDs and probes had not been separated during the binding procedures. The first waste fraction (Figure V.10, band 4) showed the presence of a small concentration of unbound probes. The second waste fraction did not show any unbound probes or QDs (Figure V.10, band 5).

3.3. Binding characterisation of the Dynabeads

3.3.1. Fluorescence properties of the Dynabeads

Fluorescent microscopy analysis of unlabelled Dynabeads revealed a low level of autofluorescence under all excitation wavelengths examined (Figure V.11).

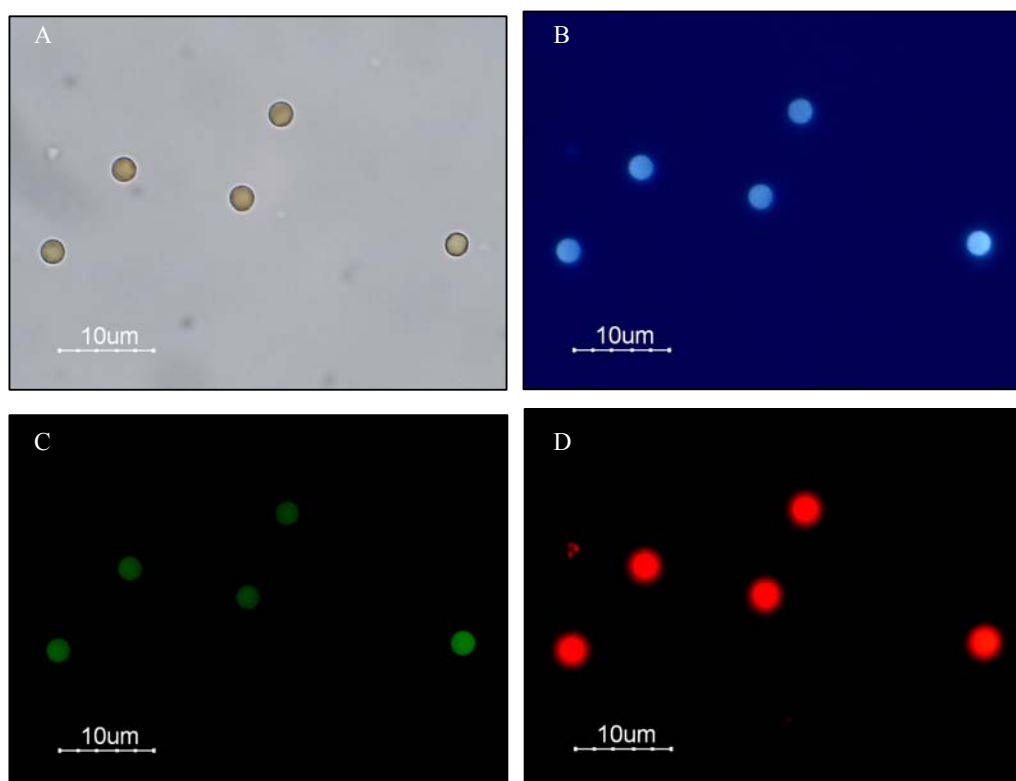


Figure V.11: Background autofluorescence of unlabelled Dynabeads under epi-fluorescence microscopy. A: DIC. B: UV light. C: Blue light. D: Green light.

QD655 (0.6 pmol) were bound directly to Dynabeads (5 μ l, 10 mg/ml) by the biotin-streptavidin interaction (V.2.4.3). The influence of background noise from the Dynabeads after binding to QDs was investigated by epi-fluorescence microscopy. Despite the background autofluorescence of unlabelled Dynabeads, a significant increase in red fluorescence was observed at all wavelengths examined by epi-fluorescence microscopy after binding to QD655 (Figure V.12). This demonstrated both the success of the binding procedures used and the broad excitation spectra of QDs. No clustering of fluorescence on

the surface of the beads was observed, indicating that the QDs had not agglomerated as had been observed using other binding methods (Appendix II: BioMag beads).

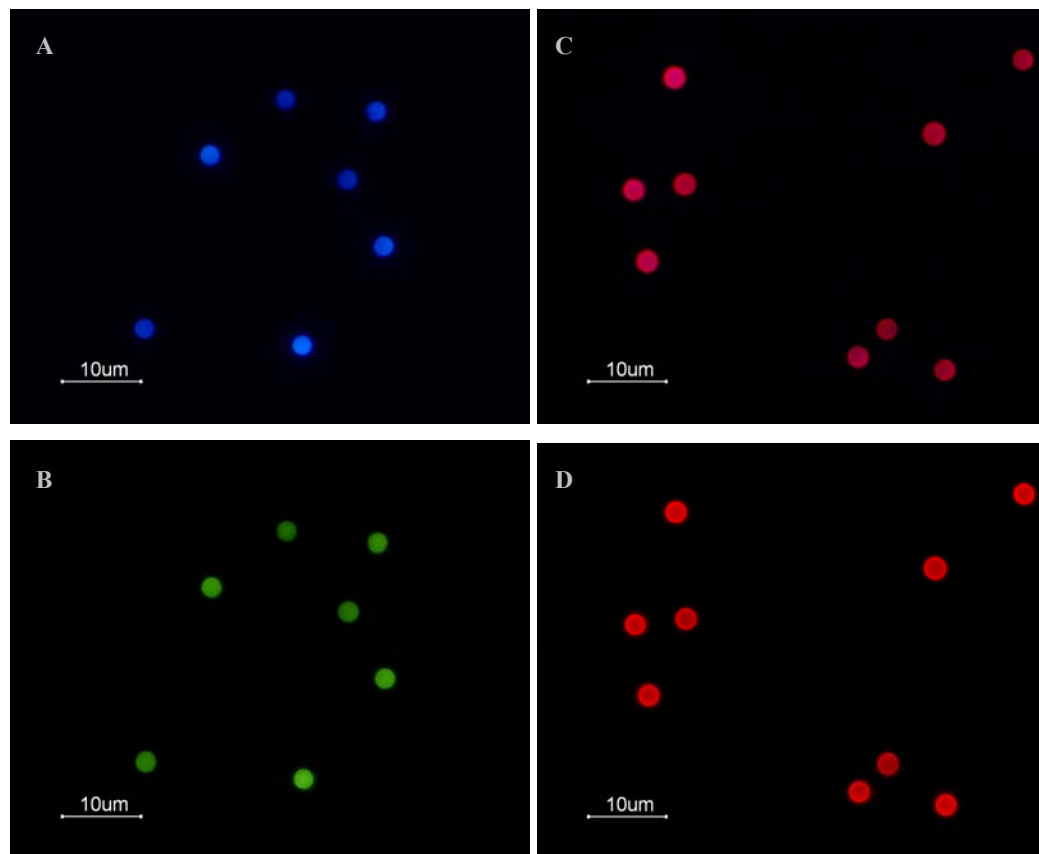


Figure V.12: Unlabelled Dynabeads and Dynabeads bound to QD655 observed by epi-fluorescence microscopy. A: Unlabelled Dynabeads under UV light. B: Unlabelled Dynabeads under blue light. C: Dynabeads labelled with QD655 under UV light. D: Dynabeads labelled with QD655 under blue light.

Dynabeads prior to and after binding to QD655 were also analysed by the BD-FACS Calibur flow cytometer and the median fluorescence intensity (MFI) measured. Dynabeads bound to QD655 exhibited a substantial increase in the intensity of the fluorescent signal in FL3 (MFI: 199) compared to unlabelled Dynabeads (MFI: 10). This increase in fluorescence indicated positive binding between the QDs and the Dynabeads (Figure V.13). The background fluorescence of the Dynabeads did not seem to affect the fluorescence emission of the QD655-Dynabeads complexes.

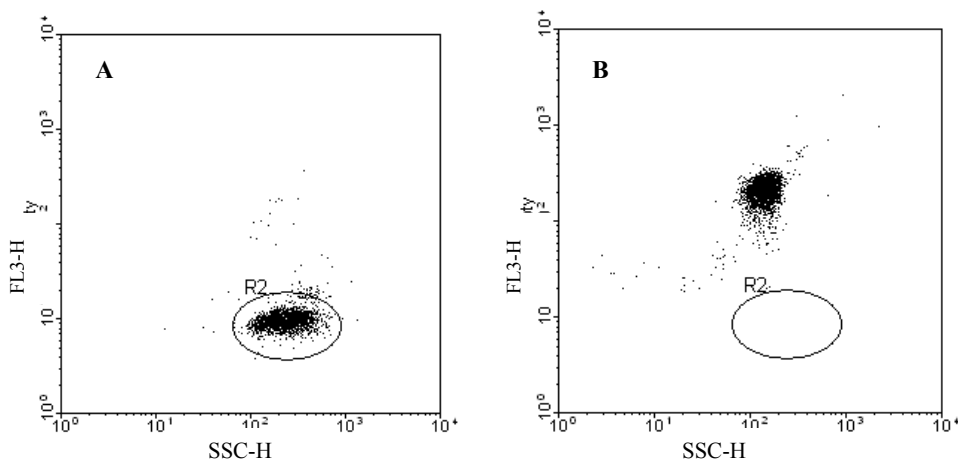


Figure V.13: Flow cytometric analysis of Dynabeads bound to QD655. Bivariate dot-plots defining log FL3 channel (y-axis) versus log SSC channel (x-axis) A; Unlabelled Dynabeads. A circular region (R2) was defined around the unlabelled Dynabeads. B; Dynabeads bound to QD655. Observed is a significant increase in fluorescence emission by Dynabeads which confirmed binding to QD655.

3.3.2. Optical behaviour of QDs bound to Dynabeads

The optical behaviour of QD655 after binding to Dynabeads was investigated using a BD LRS I flow cytometer (II.2.5.1) incorporating blue- and UV-light excitation wavelengths.

Different concentrations of QD655 (Table V.8) were bound to Dynabeads by the biotin-streptavidin interaction (V.2.4.3). Figure V.14 represents the binding of several QDs to a single Dynabead.

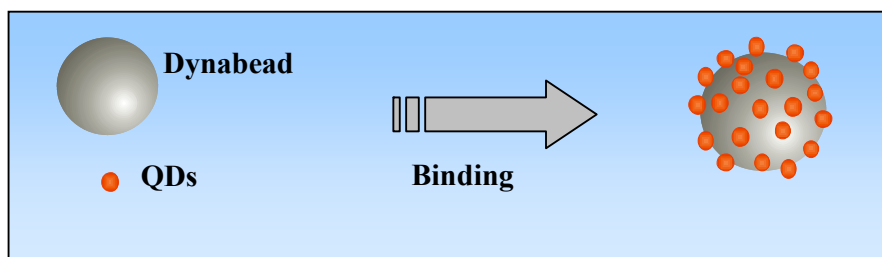


Figure V.14: Schematic representation of Dynabeads labelled with QD655 by the biotin-streptavidin interaction.

Table V.8: Dilutions of QD655 bound to Dynabeads by the biotin-streptavidin interaction.

Sample number	Line colour in the Figures V.15 and V.16	Concentration of QD655	Volume of Dynabeads (10 mg/ml)
1	Green	0.001 pmol	5 μ l
2	Pink	0.01 pmol	5 μ l
3	Blue	0.2 pmol	5 μ l
4	Orange	0.3 pmol	5 μ l
5	Dark blue	0.4 pmol	5 μ l
6	Yellow	0.5 pmol	5 μ l
7	Light blue	0.6 pmol	5 μ l
8	Red	0.8 pmol	5 μ l

Unlabelled Dynabeads were used as a negative control to set up the parameters on the flow cytometer. The fluorescent signal of a sample was considered positive when it was detected above 10^1 on the axis of the channel detector, indicating the successful binding of QD655 to the Dynabeads.

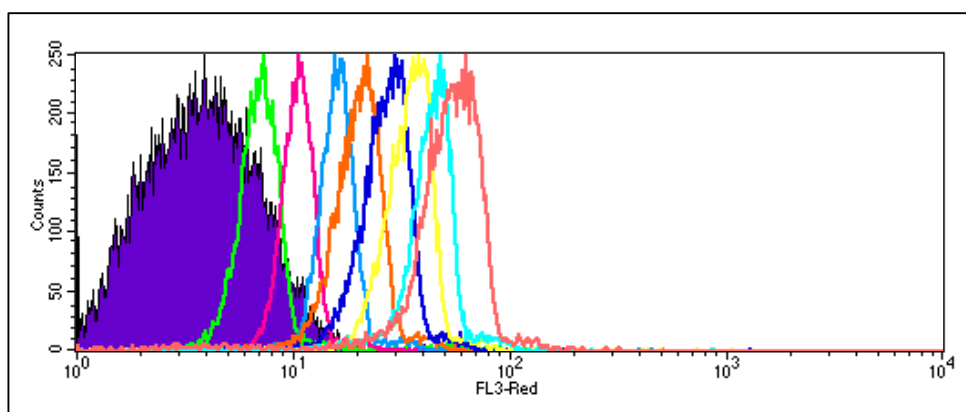
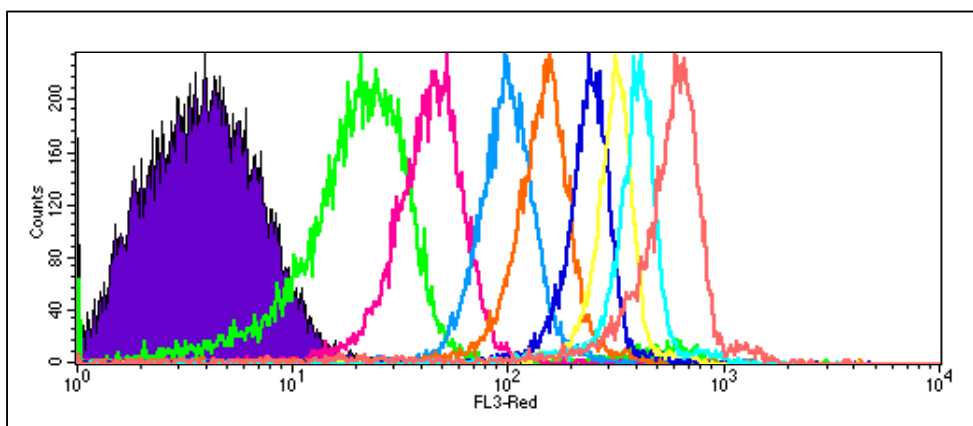


Figure V.15: Flow cytometric analysis. Histogram of different concentrations of QD655 bound to Dynabeads. X-axis represents the fluorescent signal in arbitrary units detected by the FL3 channel. Y-axis represents the number of particles counted per reaction. The excitation wavelength was 488 nm (blue light).



Legend Figure V.15 and V.16:

- Purple curve:** Blank (unlabelled Dynabeads)
- Green line:** 0.001 pmol of QD655
- Pink line:** 0.01 pmol of QD655
- Blue line:** 0.2 pmol of QD655
- Orange line:** 0.3 pmol of QD655
- Dark blue line:** 0.4 pmol of QD655
- Yellow line:** 0.5 pmol of QD655
- Light blue line:** 0.6 pmol of QD655
- Red line:** 0.8 pmol of QD655

Figure V.16: Flow cytometric analysis. Histogram of different concentrations of QD655 bound to Dynabeads. X-axis represents the fluorescent signal in arbitrary units detected by FL3 channel. Y-axis represents the number of particles counted per reaction. The excitation wavelength was 325 nm (UV light).

The results indicated a substantial increase in the fluorescent signal of all samples when UV light (325 nm) was used as an excitation source instead of blue light (488 nm) (Figures V.15 and V.16). The results showed that 0.01 pmol of QD655 bound to the Dynabeads (Figure V.15, pink line) were needed to obtain a positive result when they were excited with blue light (488 nm). However, only 0.001 pmol of QD655 bound to the Dynabeads (Figure V.16, green line) were needed to obtain a positive result under UV excitation. This result confirms the increase in the fluorescent signal of QDs observed under UV excitation, previously described when analysing unbound QDs by spectrophotometry (Figure V.5).

3.3.3. Binding capacity of the Dynabeads

The binding capacity of the Dynabeads to molecular probes was calculated mathematically and experimentally by comparing the fluorescent signal from known concentrations of FITC molecules bound to the Dynabeads (Figure V.17). FITC is a conventional organic fluorophore normally used for flow cytometric analysis. A modified poly-A probe (LinkerFITC) with a biotin group at the 3' end and FITC at the 5' end was used to label Dynabeads (V.5.4.4).

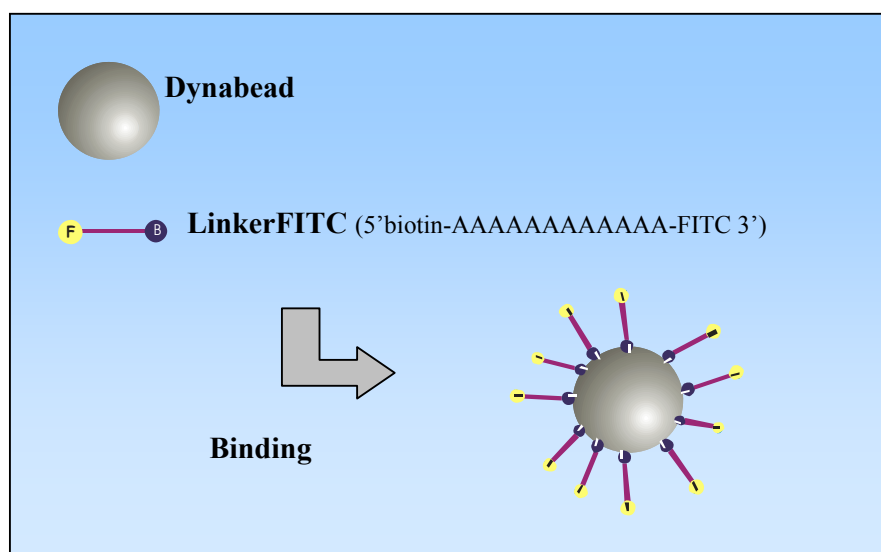


Figure V.17: Schematic representation of LinkerFITC (biotinylated probe modified with FITC) bound to Dynabeads by the biotin-streptavidin interaction.

Calculations were performed to estimate the concentration of biotinylated probes that could be bound to the Dynabeads, which were provided in a suspension at a concentration of 10 mg (6.7×10^8 beads) per ml. As indicated by the manufacturers, 1 mg (100 μ l) of Dynabeads is expected to bind to 700 pmol of free biotin or 200 pmol of biotinylated oligonucleotide probe (single stranded). Therefore, 5 μ l of Dynabeads in suspension should bind to 10 pmol of biotinylated probes.

If 10 mg of the Dynabeads in suspension contains 6.7×10^8 beads, then 100 μ l (1 mg) contains 6.7×10^7 beads. Therefore, 6.7×10^7 beads should bind to 200-700 pmol of biotin or to 1.204×10^{14} - 4.216×10^{14} molecules of biotin. Therefore, 1 bead binds 1.044×10^{-5} -

2.98×10^{-6} pmol (1,794,705-6,287,490 molecules) of biotin depending of whether the biotin is free or covalently-linked to the oligonucleotide.

Avogadro's number: $6.0227 \times 10^{23} \text{ mol}^{-1} = 1 \text{ mol}$ contains 6.02257×10^{23} molecules
 $= 1 \text{ pmol}$ contains 6.02257×10^{11} molecules

The binding capacity of the Dynabeads was confirmed experimentally by binding known concentrations of a biotinylated probe modified with FITC to Dynabeads. Several concentrations of LinkerFITC (100 μM) were bound to a constant concentration of Dynabeads (V.2.4.3) as described in Table V.9. The data was analysed on bivariate dot-plots of SSC versus FL1.

Table V.9: Concentrations of LinkerFITC bound to Dynabeads.

Sample number	Volume of LinkerFITC	Concentration of LinkerFITC	Molecules per sample	Volume of Dynabeads (10 mg/ml)
1	1 μl	1 pmol	6.0225×10^{11}	5 μl
2	2 μl	2 pmol	1.2045×10^{12}	5 μl
3	3 μl	3 pmol	1.806×10^{12}	5 μl
4	4 μl	4 pmol	2.409×10^{12}	5 μl
5	5 μl	5 pmol	3.011×10^{12}	5 μl
6	6 μl	6 pmol	3.6135×10^{12}	5 μl
7	7 μl	7 pmol	4.215×10^{12}	5 μl
8	8 μl	8 pmol	4.818×10^{12}	5 μl
9	9 μl	9 pmol	5.420×10^{12}	5 μl
10	10 μl	10 pmol	6.0225×10^{12}	5 μl
11	11 μl	11 pmol	6.624×10^{12}	5 μl
12	12 μl	12 pmol	7.227×10^{12}	5 μl
13	13 μl	13 pmol	7.829×10^{12}	5 μl
14	14 μl	14 pmol	8.4313×10^{12}	5 μl
15	15 μl	15 pmol	9.033×10^{12}	5 μl

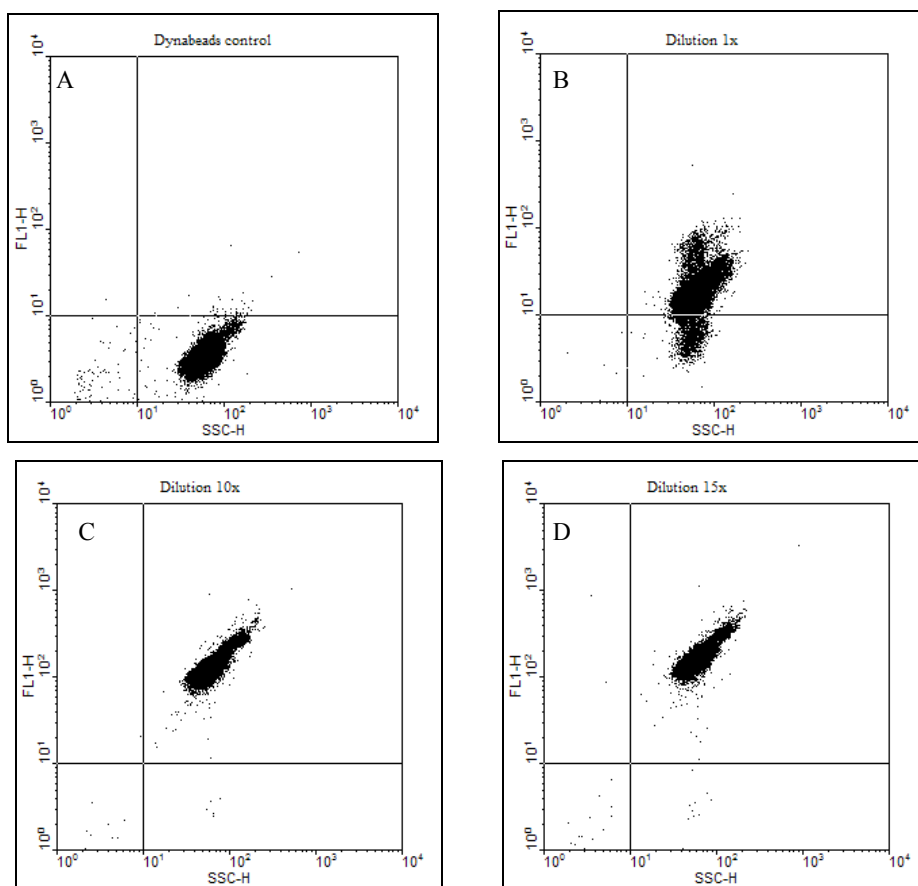


Figure V.18: Flow cytometric analysis of LinkerFITC bound to Dynabeads. Bivariate dot-plots defining log FLI channel (y-axis) versus log SSC channel (x-axis) A: Unlabelled Dynabeads. B: Dynabeads bound to 1 pmol of LinkerFITC. C: Dynabeads bound to 10 pmol of LinkerFITC. D: Dynabeads bound to 15 pmol of LinkerFITC.

The fluorescent signal of the Dynabeads was observed to increase with increasing concentrations of LinkerFITC bound to them (Figure V.18). The MFI values did not increase from samples 10 to 15, indicating that the saturation point of the Dynabeads was reached when 10 pmol of LinkerFITC were added to the binding reaction. This result confirmed the mathematical calculations previously made: 5 μ l (10 mg/ml) of Dynabeads in suspension bound to a maximum of 10 pmol of biotinylated probes.

3.3.4. Saturation point of the Dynabeads-probe complexes

The saturation point of the Dynabeads varies depending of the size of the target molecule. The binding capacity of the Dynabeads labelled with QD655 and FITC molecular probes was compared using the BD FACS-Calibur flow cytometer.

Dynabeads were labelled with QD655 by the biotin-streptavidin interaction (V.2.4.3). The fluorescent signal of the Dynabeads labelled with both fluorophores, FITC and QD655, was analysed by flow cytometry and the MFI values collected (Figure V.19).

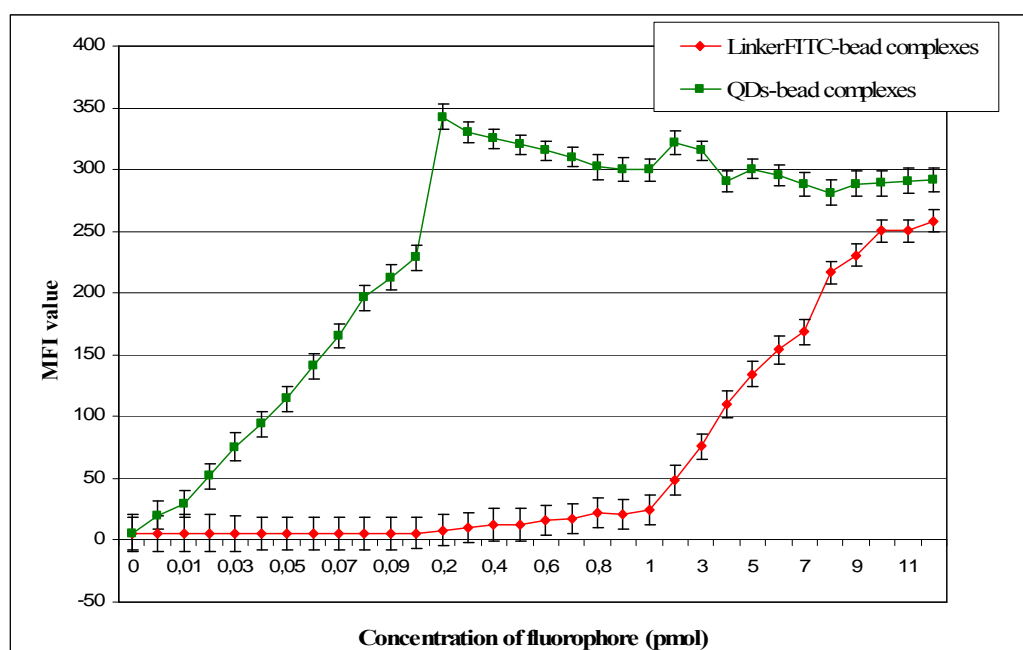


Figure V.19: Fluorescent intensity of Dynabeads labelled with QD655 and FITC measured as MFI values by flow cytometry. X-axis: Concentration of QD655 and LinkerFITC in pmoles bound to Dynabeads (5 μ l, 10 mg/ml, per reaction). Y-axis: Median value of each sample. QD655 was analysed using the FL3 channel while FITC was analysed using the FL1 channel of the BD FACS-Calibur flow cytometer.

The MFI value of each sample was obtained by defining a rectangular region around the centre of the main fluorescing population of Dynabeads. Once the region was defined, the MFI value was obtained from that region using the CellQuest software. The maximum binding capacity of beads for oligonucleotides probes, as indicated by the product data sheet, was 200 pmol of biotinylated oligonucleotides per one milligram of beads (DynaL Biotech) or 10 pmol of biotinylated probe per 5 μ l of Dynabeads stock solution.

Moreover, the binding capacity of Dynabeads appeared to be different for the two fluorophores examined.

Dynabeads labelled with QD655 were observed to reach the maximum binding capacity at significantly lower concentrations than that observed for FITC (Figure V.19). The fluorescent signal of the Dynabeads bound to QD655 increased exponentially until they reached their saturation point (0.2 pmols). However, LinkerFITC bound to the beads confirmed the stated bead commercial binding capacity as the maximum fluorescent intensity was observed at 10 pmols of LinkerFITC per 5 μ l of beads (Figure V.18).

The MFI value of each reaction showed that Dynabeads bound to QD655 could be clearly discriminated above the negative control at amounts QDs as low as 0.01 pmol (Figure V.19). By comparison, the minimum amount required to clearly detect Dynabeads bound to LinkerFITC above the negative control was at a much higher concentration of 0.3 pmol.

4. DISCUSSION

4.1. Optical properties of the QDs

Commercially-available QDs have been described as highly fluorescent particles with very broad excitation, and narrow and symmetric emission spectra which enable a variety of colours to be excited by a single excitation. Although they have been used in a large number of biological applications, their behaviour has yet to be fully characterised. Moreover, commercial QDs are not spectroscopically standardised and their characterisation has not been completed (Jamieson *et al.* 2007). Their properties can be influenced by details of their synthetic history (Tonti *et al.* 2004; Wu *et al.* 2007b). Therefore, in this study the physical and optical properties of two types of commercial QDs were investigated by measuring their fluorescence emission over a wide range of excitation wavelengths.

The excitation and emission spectra properties of QD655 and Hops-Yellow QDs in solution were studied. The fluorescent intensity of the QDs decreased 4-fold when examined at short excitation wavelengths of 320 nm (UV light) compared to longer wavelengths of 490 nm (blue light) (Figures V.5 and V.6). Additionally, the fluorescent intensity of QD655 bound to the Dynabeads by the biotin-streptavidin interaction was found to be 2-fold brighter when excited with UV light over blue excitation (Figures V.15 and V.16) instead of the 4-fold difference found for unbound QDs. Therefore, it was concluded that approximately 50% of the fluorescent emission was lost when the QDs were bound to the Dynabeads.

The broad absorption spectra observed for the QDs were in accordance with the broad absorption spectra reported previously (Dabbousi *et al.* 1997). However, there is an anomalous dependence of quantum yields on the excitation wavelengths, especially at less than 420 nm. This phenomenon has also been reported recently (Wu *et al.* 2007a). This effect is probably due to the size heterogeneity and the semiconductor properties of the QDs (Wu *et al.* 2007b). The fluorescent emission of semiconductor nanocrystals is due to

radiative recombination of excited electron-hole pairs. QDs absorb photons when the excitation energy slightly exceeds the band gap of the core material. During this process, the electrons are promoted from lower to higher energy levels, leaving holes behind. Shorter excitation wavelengths (UV light) possess higher energy than long excitation wavelengths (blue light). Thus the electrons are promoted to comparatively higher energy levels when they are excited with shorter excitation wavelengths. At such higher energies the density of the final electron states is high and so is the probability of electron excitation, whereas for lower excitation energy this probability is lower. In both cases, the electron-hole pair re-emits at the same lowest possible energy (the longest wavelength, in this case 655 nm) but with different probabilities, reflecting the different probabilities of excitation. These varying probabilities explain why QDs are comparatively brighter at short excitation wavelengths (Wu *et al.* 2007a).

The photo-stability of the QDs has been reported to be influenced by several parameters such as pH, temperature and ionic buffers. A range of buffers were tested during the binding procedures of QDs to molecular probes and paramagnetic beads in the following chapter VI (VI.3.1.3). Buffers with a high pH helped to maintain the fluorescence of the QDs better than buffers close to neutral values (Figure VI.11). This phenomenon has been reported in the literature recently, indicating that the fluorescent intensity of QDs decreased linearly by 90% with pH decreasing from 8.0 to 5.0 and could not be restored by adding OH⁻ (Yu *et al.* 2007). The sensitivity of the QDs' photoluminescence to pH might be explained as a function of their surface modification and effects on exciton trap sites (Gao *et al.* 1998; Zhang *et al.* 2003). Possibly the shell does not completely cover the core of the QDs, and the added H⁺ can pass through the shell layer, partially destroying the core. Ionic buffers have been also found to degrade the fluorescent signal of the QDs (Boldt *et al.* 2006). The signal loss when QDs are subjected to high concentrations of cations in solution could be due to the slow degradation of surface ligands and coatings, leading to surface defects and fluorescence quenching (Hess *et al.* 2001; Manna *et al.* 2002).

Temperature also influenced the fluorescence intensity of the QDs. Photo-stability of the QDs remained stable at room temperature but it decreased when the temperature was increased over 50°C (data not shown). An effect of temperature on the QDs has been

reported recently where approximately 25% of fluorescent intensity was found to decrease when the temperature increased from 20°C to 50°C (Liu *et al.* 2006; Yu *et al.* 2007). This effect may have been attributed to variation in the particle size of QDs. It is known that the wavelength of fluorescence depends on the bandgap and thus on the size of the QD (Murray *et al.* 2000; Qu & Peng 2002).

Size heterogeneity of the QDs may be another significant contributor to the observed variation in the quantum yield of the QDs (Wu *et al.* 2007b). Recent studies showed that photo-excitation of QD585 in the wavelength window between 420 and 500 nm yielded a uniform quantum efficiency, while QD525 within the same spectral window showed more pronounced anomalies, even leading to blinking (Ozkan 2004; Wu *et al.* 2007a). Blinking is caused by charge trapping and untrapping at surface defects during excitation, and results in an alternation of bright and dark states during which no photons are emitted (Michalet *et al.* 2001). QDs with smaller core sizes, such as QD525, have been observed to be more unstable and unreliable than QDs with higher core sizes.

The molar extinction coefficient is a measure of how strongly a compound absorbs light at a certain wavelength. The molar extinction coefficient of Hops-Yellow QDs used for the preliminary experiments was unknown. Therefore, it was calculated via the Beer-Lambert law. The molar extinction coefficient was found to be $0.001 \text{ M}^{-1} \text{ cm}^{-1}$ at 560 nm. In comparison, the molar extinction coefficient of organic fluorophores such as FITC has been reported elsewhere to be 7.69×10^4 to $8.80 \times 10^4 \text{ M}^{-1} \text{ cm}^{-1}$ at 520 nm (DeRose & Kramer 2005). The results obtained in this study were in contradiction to recently published reports claiming the molar extinction coefficient of QDs to be 10–100 times greater than conventional fluorophores (Leatherdale *et al.* 2002; Ozkan 2004; Azzazy *et al.* 2007).

Several factors may have influenced the determination of the molar extinction coefficient such as purity of the solutions and the spectrophotometer calibration (DeRose & Kramer 2005). Hops-Yellow QDs were functionalised with amine groups which are organic compounds with at least one amine ($-\text{NH}_2$) group attached. It has been reported that solvent polarity and pH can effect the absorption spectra of organic compounds such as amine (van Dalen *et al.* 1970). In addition, the molecular probes were modified with thiol

groups in order to allow covalent attachment to the QDs. Thiol groups may be photocatalytically-oxidised making the QDs photochemically unstable and, consequently, losing their absorption efficiency (Aldana *et al.* 2001). Photooxidation of the thiol groups also may form a micelle-like structure around the QDs, causing agglomeration which also may influence the kinetics and the photo-stability of the QDs (Ozkan 2004). Therefore, an accurate measurement of the molar extinction coefficient of QDs depends of their purity and composition. Further development of QDs synthesis is needed in order to obtain high-quality photostable QDs.

4.2. Binding properties of the QDs

A single QD has approximately 7 active groups on its surface (as indicated by the manufacturer). Quantitative and qualitative methods were designed to confirm this information by calculating the number of molecular probes that could be attached to a single QD. Spectrophotometric analyses were used to study the absorption spectrum of QDs bound to molecular probes (Figure V.9). However, the broad absorption spectra of the QDs resulted in high background noise at low wavelengths, making it impossible to detect any distinctive peak and allow estimation of the number of probes bound per QD by spectrophotometry. Although gel electrophoresis could not provide an accurate number of probes bound to the QDs, these analyses were useful in verifying the binding procedures (Figure V.10).

4.3. Binding properties of the Dynabeads

The binding capacity of the Dynabeads was found to be different for QDs over organic dyes. LinkerFITC bound to Dynabeads confirmed the commercial binding capacity indicated by the manufacturer (Figure V.18). As the maximum binding capacity was reached in accordance with the maximum fluorescence observed by flow cytometry, it was inferred that the FITC molecules were not in sufficiently close proximity on the bead's surface to transfer energy to each other. Therefore, bead saturation by LinkerFITC did not contribute to fluorescence-quenching due to FRET (fluorescence resonance energy transfer).

In contrast, the maximum fluorescence intensity of QDs-bead complexes was observed to be at significantly lower concentrations than observed for FITC (Figure V.19). This

reduction may be explained in terms of steric hindrance of fluorophore binding. The final size of commercial QDs is approximately 20 nm, while FITC is approximately 12 Å. This 15-fold increase in size could severely affect probe binding. In addition, this phenomenon may potentially have significant consequences for many biological and biomedical applications where the samples studied have low binding capacities for active targets, consequently making them undetectable by flow cytometry.

The capability of the QDs for specific target detection, coupled with lower detection limits and greater multiplexed capability using single light sources, has been suggested to offer significant advantages over conventional organic dyes (Horejsh *et al.* 2005). However, the results found in this study revealed that the binding capacity of the QDs is considerably lower than organic dyes and thus may substantially reduce their capacity for target detection.

Although the fluorescent signal of QD655 appeared to be higher than FITC, a comparison between the fluorescent intensity of QD655 versus FITC could not be quantified. QD655 was detected in the FL3 channel of the flow cytometer while FITC was detected in the FL1 channel. For comparative purposes both fluorophores should have been analysed under the same channel and experimental settings. The apparent brightness of QD655 over FITC could be due to the core size of the QDs since the quantum yield of the QDs is dependant on the core size. Red QDs have bigger core sizes than yellow QDs, and consequently their quantum yield would be expected to be higher.

4.4. Summary

Anomalies in the physical and optical characteristics of QDs observed in this study potentially could lead to difficulties when using them in biological applications. Many fundamental characteristics of their surface chemistry and physicochemical properties in varying situations still need to be investigated. Some important technical problems remain, particularly in defining and characterising the surface-coating chemistry. This aspect could be controlled to develop a coating which provides minimal non-specific binding, whilst maintaining stability, avoiding oxidation and tolerating the salt concentrations found in cells and biological solutions. QDs should also maintain strong

fluorescence without bleaching, quenching, or blinking. Further analyses to study the binding characteristics of the QDs are still required.

Chapter VI. Applications of the QDs

1. INTRODUCTION

Several bead-based QDs techniques have been described for flow cytometric assays. The majority of these methods have focused on embedding beads with different amounts of QDs for the detection of biomolecules. For example, polystyrene beads have been embedded previously with different amounts of QDs, and each bead surface was modified with various biomolecules to target specific DNA sequences from the sample (Han *et al.* 2001; Wang *et al.* 2006) or for multiplex assays (Gao & Nie 2003; Xu *et al.* 2003; Gao & Nie 2004; Cao *et al.* 2006). Although, these reports have demonstrated the utility of QDs as an indicator in bead-based flow cytometry assays, the potential applications and advantages of QDs as fluorophores to label specific targets for flow cytometric analyses still remains to be investigated.

1.1. Aim

The overall aim of this part of the project was to design a bead-based technique which targeted specific sequences of DNA using QDs for detection by flow cytometry.

The small size of QDs prevented the analysis of the quantum yield of a single QD by flow cytometry. Therefore, commercial paramagnetic beads were used as a surface platform to bind high numbers of targeted sequences. Paramagnetic beads were covalently coupled with a monolayer of functional groups such as streptavidin or carboxylic groups, allowing the interaction with suitably modified molecular probes. The paramagnetic material of the beads allows them to be attracted to a magnetic field, facilitating the separation of the bead-molecule complex from the rest of the molecules in solution with a magnet. Therefore, unbound molecules were simply washed away preventing non-specific binding and agglomeration issues.

The desired sequences of DNA were captured on beads and labelled with QDs using specific molecular probes as linkers. A capture probe modified with biotin or carboxylic groups was used to hybridise to the DNA while binding the paramagnetic beads by the streptavidin-biotin interaction. A target probe was used to hybridise to the DNA while

labelling the DNA with the QDs or other fluorophores for comparative purposes (Figure VI.1).

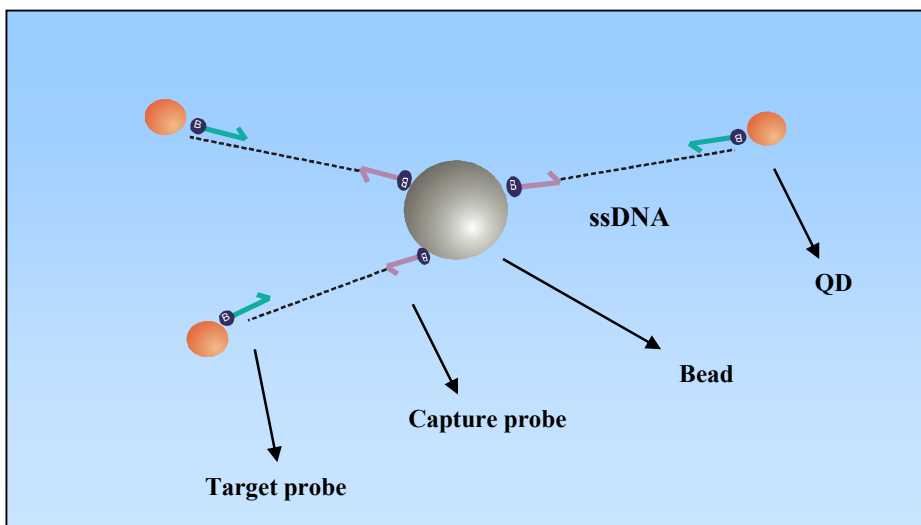


Figure VI.1: Diagram of the bead-based QDs technique for DNA detection. It represents the hybridisation of the capture and target probes to the DNA and binding to the paramagnetic beads.

Commercially-available functionalised QDs were used to develop the bead-based technique. QDs were functionalised with streptavidin or amine groups (Chan *et al.* 2002; Parak & Pellegrino 2005). Details and characteristics of commercial QDs were discussed in Chapter V.

Prior to developing the bead-based technique, preliminary experiments were undertaken to detect modified PCR amplicons of *D. radiodurans* labelled with different fluorophores, such as FITC, bound to the paramagnetic beads. These experiments set the basis and background knowledge necessary for the full development of the technique.

The bead-based QD technique was designed initially to label and detect genomic DNA (gDNA) from *D. radiodurans*. However, the difficulties found when working with gDNA led to the amplification of small segments of DNA by PCR. Specific capture and target probes were designed to label the PCR fragments. Two types of paramagnetic beads were selected as a platform for capturing the labelled PCR amplicons: Dynabeads and QuantumPlex™ beads.

The bead-based QD technique was aimed to be applied to study the microbial diversity of environmental samples, such as the sulphur-rich acidic volcanic hydrosystems of White Island. Two main applications of the technique were anticipated for this project: first, screening of the environmental DNA to detect the key microbial species by flow cytometric analyses; and secondly, targeting and isolation of specific microorganisms from the environment for further analyses.

2. MATERIALS AND METHODS

2.1. Reagents

The QuantumPlex™ Carboxyl kit (Bangs Laboratories Inc., Fishers, IN, USA) consisted of five populations of uniform super-paramagnetic microspheres (~6 µm in diameter) incorporating different intensities of Starfire Red™ fluorescent dye. The beads were at a concentration of 1×10^8 microspheres/ml. Starfire Red™ dye exhibits a broad excitation band and can be excited with Argon or He-Ne lasers, while emitting light in the FL3 channel (685 nm) of a standard flow cytometer (488 nm).

2.2. Buffers and solutions

All buffers and solutions were autoclaved for 20 min at 121°C and 200 kPa pressure. For general buffers and solutions refer to Chapter II 2.1 and Chapter V 2.2.

Table VI.1: Description of buffers and solutions.

Binding Wash buffer (BW buffer)	10 mM Tris/HCl (pH 7.5), 2.0 M NaCl and 1 mM EDTA
BioMag buffer	20 mM Tris (pH 7.8), 1 M NaCl, 1mM EDTA and 0.02% Triton x-100
QD incubation buffer	2% BSA in 50 mM borate with 0.05% sodium azide. Final pH 8.3
50 x Denhardt's mix	1% (w/v) of Ficoll, 1% (w/v) of Polyvinyl pyrrolidone (PVP) and 1% (w/v) of Bovine Serum Albumine (BSA). The solution was filtered using 0.22 µm pore filters and stored at -20°C
Hybridisation buffer	6 x SSC, 0.1% SDS and 1 x Denhardt's mix
Hybridisation wash	0.1 x SSC and 0.1% SDS
Imidazole buffer, 100 mM	0.68 gr of Imidazole dissolved in 100 ml of distilled MilliQ water. pH adjusted to 7 using 1 M NaOH
MES buffer, 100 mM	1.95 gr of 2-(N-morpholino)ethanesulfonic acid dissolved in 100 ml of distilled MilliQ water. pH adjusted to 7 using 1 M HCl

2.3. Molecular procedures

2.3.1. *Deinococcus radiodurans*

D. radiodurans (strain number MQ480) was obtained from the Extremophile Group Microbial Collection (Macquarie University, Australia). *D. radiodurans* was cultured on LA agar plates at 30°C for 48 h (II.2.3) and formed pink colonies on the surface of the plate. Single colonies were picked using sterile toothpicks and transferred to 50 ml of LB broth (II.2.3) followed by incubation overnight at 30°C with shaking. Liquid cultures were analysed by light microscopy prior to DNA extraction.

2.3.2. DNA extraction

Genomic DNA of *D. radiodurans* was obtained using a modified phenol extraction method (D.D. Morris, Ph.D. thesis, University of Auckland, 1998). Enzymes and solutions are listed in Chapter II (Table II.3). One inoculating loop of cells was resuspended in 1 ml of 50 mM Tris/HCl (pH 8) and 150 µl of 0.25 M EDTA (pH 8). With liquid samples, 1 ml of culture was spun at 13,000 rpm for 15 min at 15°C. The pellet was resuspended as before. The mixture was vortexed briefly and incubated at 37°C for 20 min. A portion (120 µl) of Lysozyme (20 mg/ml) and 1.4 µl of Mutanolysin (100 µg/µl) were added and the tubes were mixed by hand and incubated at 50°C for 20 min. After the addition of 70 µl of RNAaseA (10 mg/ml), the mixture was incubated for another 20 min at 37°C. Then 57 µl of protease from *S. griseus* (40 mg/ml) and 70 µl of 10% SDS were added to the mixture, followed by incubation at 50°C for 20 min. The final volume was then adjusted to 5 ml using TE buffer and transferred to 15 ml Phase Lock Gel (PLG) light tubes, followed by the addition of 5 ml of phenol/CIAA (25:24:1). The sample was mixed gently for up to 5 min. The tubes were centrifuged for 5 min at 13,000 rpm, 17°C. The gel separates the DNA content of the cells from the organic and protein contaminants after centrifugation. Subsequently, the aqueous layer was transferred to a fresh PLG tube with the addition of 5 ml phenol/CIAA (25:24:1) followed by another centrifugation step. The aqueous layer subsequently was transferred to a clean PLG light tube with the addition of 1 volume of CIAA (24:1) and centrifuged as above. The final aqueous layer was transferred to a clean 1.5 ml Eppendorf tube and the DNA was precipitated with 1/10

volume of 3 M sodium acetate (pH 5) and 2 volumes of cold absolute EtOH (-20°C). The solution was mixed gently and, after incubation at RT for 30 min, was centrifuged for 1 hr at 5,000 rpm at 4°C. The supernatant was discarded and the pellet washed in 3 ml of 70% EtOH. After a final centrifugation step, the supernatant was discarded, the DNA pellet was air dried, resuspended in 100-250 µl of TE buffer and stored at 4°C. In the event that the DNA had not dissolved after overnight incubation, 200-300 µl TE buffer was added and incubated at 55°C for a further 20 min. This procedure could be repeated up to 3 times. The final DNA obtained from *D. radiodurans* was quantified by gel electrophoresis and spectrophotometry (II.2.6.1).

2.3.3. Amplification and analysis of 16S rDNA of *D. radiodurans*

Primers PB36 and PB38 were used to amplify 16S ribosomal RNA genes of *D. radiodurans* following the standard bacterial PCR protocol (II.2.6.2). They were sequenced by the chain-termination method using BigDye Terminator and the bacterial 16S rDNA-specific primers: 16SR2, PB36, 16SF1 (II.2.6.3). The sequencing reactions were analysed using an ABI-Prism 377 Sequencer (DNA Analysis Facility, Macquarie University, Australia) and the sequenced fragments obtained were assembled and edited using the BioManager workspace of the Australian National Genomic Information Service (ANGIS).

2.3.4. Design of *D. radiodurans* specific oligonucleotide probes

BlastN algorithms megablast and discontinuous megablast searches (<http://www.ncbi.nlm.nih.gov/BLAST/>) were performed on the 16S rDNA sequences obtained from *D. radiodurans* to determine the most closely related species based on the 16S rDNA. This information was used to identify unique regions within *D. radiodurans* for the design of capture and target oligonucleotide probes. Up to 17 different sequences were found to be closely related to *D. radiodurans*. All sequences were aligned and compared using ClustalW (Thompson *et al.* 1994) and ClustalX (Thompson *et al.* 1997).

Oligonucleotides probes were designed for specific experiments based on the 16S rDNA gene sequence of *D. radiodurans* compared to the most closely relative species (Table V.2). All designed probes were purchased from Sigma-Aldrich (Australia).

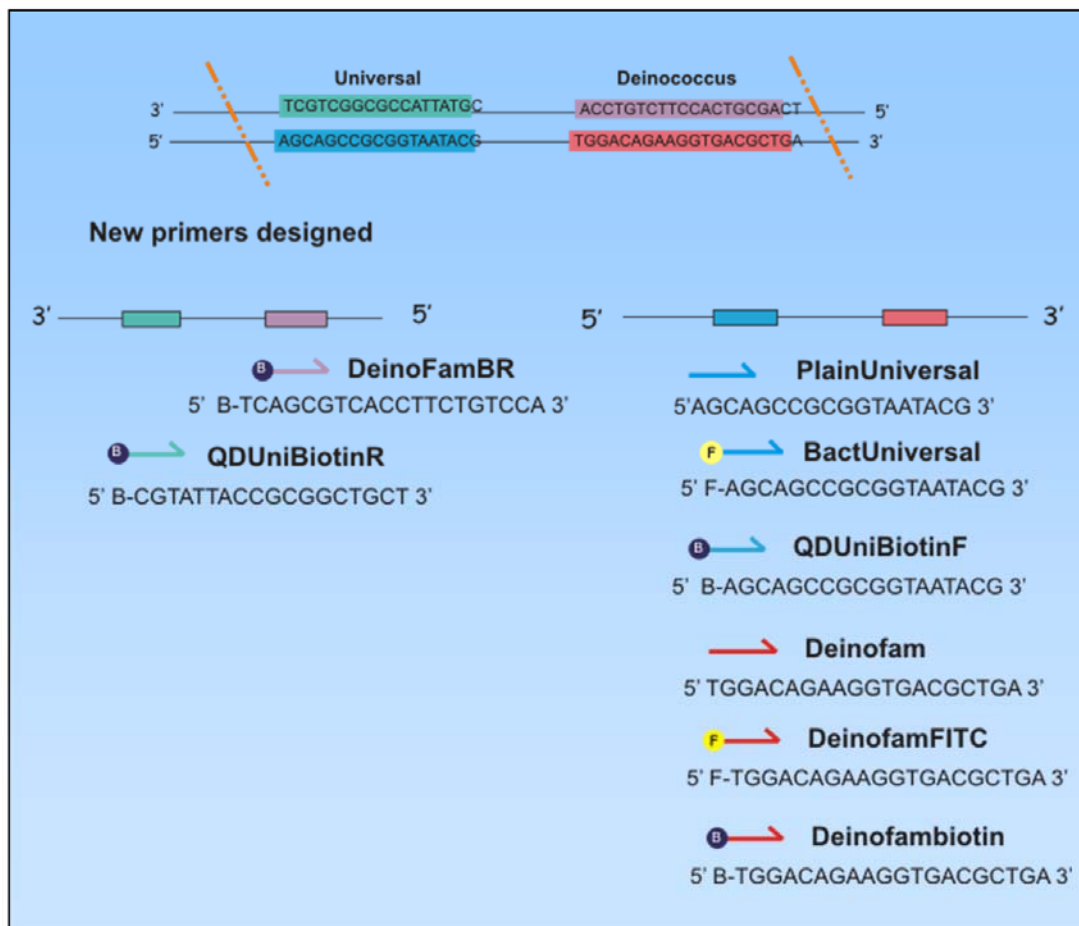


Figure VI.2: Schematic representation of the 16S rDNA gene sequence of *D. radiodurans*. The Universal region belongs to the part of the sequence common to the majority of bacterial species. The Deinococcus region belongs to the part of the sequence unique for *D. radiodurans*. Reverse and forward probes were designed based on the Universal and Deinococcus regions. B = biotin modification. F = FITC modification.

Table V.2: List of probes designed from the 16S rDNA gene sequence of *D. radiodurans*. Specifications: 7 (Biotin), F (Fluorescein), 6THS (Thiol), 1 (Alexa 521nm), 5AmMC12 (Amine followed by 12 carbons).

Name	Sequence
DeinoFamBiotin	7-TGGACAGAAGGTGACGCTGA
QDLinker	7-AAAAAAAAAAA4-6THS
Bactouniversal	5'-Fluorescein-AGCAGCCGCGGTAATACG
DeinoFam	5'-Sulphydryl-TGGACAGAAGGTGACGCTGA
Plainuniversal	AGCAGCCGCGGTAATACG
DeinoFamFITC	F-TCAGCGTCACCTTCTGTCCA
LinkerFITC	7-AAAAAAAAA-F
EukQD	7-ACCAGACTTGCCCTCC
CRY2Cy3	GATATGTCACATTAATTGT
Eub388-QD	7-GCTGCCTCCCGTAGGAGT
Eub388-FITC	F-GCTGCCTCCCGTAGGAGT
QDUniBiotinF	7-AGCAGCCGCGGTAATACG
DeinoFamBR	7-TCAGCGTCACCTTCTGTCCA
QDuniBiotinR	7-CGTATTACCGCGGCTGCT
Bactuni2	F-AGCAGCCGCGGTAATACG
BactuniAlexa	1-AGCAGCCGCGGTAATACG
Deino-Capture680	5AmMC12- TCAGCGTCACCTTCTGTCC

2.3.5. Polymerase chain reaction (PCR)

Polymerase chain reaction (PCR) amplification of 16S ribosomal DNA genes was carried out following the procedures described previously (II.2.6.2). PCR products were checked by gel electrophoresis and spectrophotometry (II.2.6.1).

Specific primers were designed to amplify small sequences within the 16S ribosomal DNA genes of bacterial and archaeal microorganisms selected for detection by the bead-based QD technique.

Table V.3: Bacterial PCR set-up.

<i>Sulfobacillus thermosulfidooxidans</i>		
Forward primer	Sulfo288	GGG AGC TCG CGG CCC ATT A
Reverse primer	EUBR	GCT GCC TCC CGT AGG AGT
PCR size product	127 bp	
PCR product concentration	1 pmol = 76.2 ng	

<i>Acidithiobacillus ferrooxidans</i>		
Forward primer	Thio2	TAA TGC GTA GGA ATC T
Reverse primer	EUBR	GCT GCC TCC CGT AGG AGT
PCR size product	238 bp	
PCR product concentration	1 pmol = 143 ng	

Table VI.4: Archaeal PCR settings.

<i>Ferroplasma acidiphilum</i>		
Forward primer	ASF	CCA GGY CCT ACG GGG CGC A
Reverse primer	FER565R	ACG TTT AAC CTC ACC CGA TC
PCR size product	296 bp	
PCR product concentration	1 pmol = 177 ng	

<i>Sulfolobus metallicus</i>		
Forward primer	ASF	CCA GGY CCT ACG GGG CGC A
Reverse primer	Smet	GAG CTC GGG TCT TTA AGC AG
PCR size product	242 bp	
PCR product concentration	1 pmol = 145 ng	

2.3.6. Gel electrophoresis analysis

Binding of QDs to oligonucleotide target probes was confirmed by gel electrophoresis. In all cases (unless stated otherwise) the gel was prepared as described previously (II.2.6.1). Agarose gels were subjected to electrophoresis for 45 min at 100 V. Samples were mixed

with 2 μ l of loading dye (6 x) and loaded into a 1% agarose gel (w/v) in 1xTBE buffer containing 5 μ g Etbr/100 ml.

2.4. QD-bead complex binding procedures

All binding procedures involving the use of QDs or organic fluorophores were carried out in darkness to avoid exposure to the light. The final products were kept at 4°C in the dark until further analysis, but for not longer than 24 h. Some of the binding procedures were described in Chapter V.2.4.

2.4.1. Washing of paramagnetic beads

Paramagnetic beads were washed before use as described previously (V.2.4.2).

2.4.2. Binding of QD-oligonucleotide amine probe complexes to Dynabeads

Generally, 10 μ l of pre-washed Dynabead stock solution was used for every reaction. Dynabeads were resuspended in the same volume of BioMag buffer as the original portion taken to maintain the concentration of the beads after washing. Generally, 20 μ l of previously prepared QDs-oligonucleotide amine probe complexes (V.2.4.1) were used per reaction and added to the pre-washed Dynabeads. The final volume of the reaction was made up to 100 μ l with BioMag buffer. The solutions were incubated at RT in darkness for 30 min to 1 h with occasional gentle shaking. Dynabeads coated with the QDs-probe complexes were washed up to 3 times with 100 μ l of BioMag buffer. Finally, the beads were resuspended in the desired volume using 10 x PBS, DEPC water or BioMag buffer.

2.4.3. Binding of complementary oligonucleotide probes to Dynabeads

A portion (5 μ l) of pre-washed Dynabeads (10 mg/ml) was transferred into a 1.5 ml Eppendorf tube and resuspended in 200 μ l of BW Buffer. Biotinylated oligonucleotide capture probe, DeinoFamBiotin (100 μ M), was diluted 1:1000 in sterile MilliQ water and used for serial dilutions. A portion (20 μ l) of complementary target probe,

DeinoFamFITC (100 μ M), also diluted 1:1000 in sterile MilliQ water was added to the solution. The hybridisation between the capture and target complementary probes and the binding to the Dynabeads were performed simultaneously (Figure VI.3). The reactions were incubated at 55°C for 1 h with frequent rotation in the dark. After incubation, the reactions were washed 3 times with 100 μ l of BW buffer and resuspended in a final volume of 300 μ l BW buffer. Dynabeads bound to the probes were stored at 4°C in the dark for no more than 24 h.

2.4.4. Binding of biotinylated PCR amplicons to Dynabeads

Generally, a portion (1 μ l) of pre-washed Dynabeads was transferred to 1.5 ml Eppendorf tubes and resuspended in 100 μ l of BW Buffer. Then the appropriate amount of purified biotinylated PCR amplicon from *D. radiodurans* was added to the solution for binding to the Dynabeads. The reactions were incubated at RT for 2 h with rotation or occasional mixing by hand. After incubation, the reactions were washed 3 times with 100 μ l of BW Buffer and resuspended in 200 μ l BW buffer. PCR amplicons bound to Dynabeads were stored in the dark at 4°C for no more than 24 h.

2.5. Capture and detection of genomic DNA bound to Dynabeads

Genomic DNA from *D. radiodurans* was obtained as described previously (VI.2.3). The concentration of gDNA was determined by spectrophotometry (II.2.6.1.2).

2.5.1. Direct capture and reporting of gDNA

Generally, a portion (5 μ l) of washed Dynabeads was transferred into a 1.5 ml Eppendorf tube and resuspended in 100 μ l of BW buffer for each reaction. A portion of the capture probe, DeinoFamBiotin (100 μ M), was added to the reaction. After incubation at RT with rotation or gently mixing during 1 h, Dynabeads bound to the capture probe were washed 3 times using 100 μ l of BW buffer. The first waste fraction was kept for further analysis.

Genomic DNA from *D. radiodurans* was denatured as follows: 5 μ l of gDNA (0.15 μ g/ μ l) was transferred to PCR tubes (0.2 ml). The final volume was made up to 100 μ l

with 95 µl of TE buffer. Genomic DNA then was heated to 99°C for 10 min using a PCR thermo-cycler. Samples were transferred to ice for 1 min to prevent renaturation. Once the gDNA was denatured, it was added to the Dynabeads-capture probe complexes. Hybridisation between the single stranded gDNA and the capture probe was carried out by incubation at 50°C with rotation for 2-6 h. Following hybridisation, samples were washed 3 times with 200 µl of BioMag buffer. The first waste fraction containing unbound gDNA was kept for further analysis. Dynabead-gDNA complexes were then resuspended in 200 µl of BioMag buffer. The gDNA captured on the Dynabeads was labelled using a target oligonucleotide probe (Bactouniversal). A portion (5 µl) of the Bactouniversal probe was added to the samples. Hybridisation between the gDNA captured onto the Dynabeads to the target probe was carried out by incubation at 50°C for 2-6 h with rotation in the dark. Samples were then washed 3 times with 200 µl of BioMag buffer. Finally, hybridised Dynabead complexes were resuspended in 200 µl of BioMag buffer or TE buffer and kept at 4°C in the dark until further analysis.

2.5.2. Indirect capture and reporting of gDNA

This method was modified from Mangiapan *et al.* (Mangiapan *et al.* 1996). Generally, 5 µl of gDNA from *D. radiodurans* was denatured by heating to 99.9°C for 10 min. The denatured gDNA was transferred quickly to ice for 1 to 5 min. Then, a portion of the capture probe (DeinoFamBiotin) was added to the denatured gDNA for hybridisation, and incubated at 60°C for 5 h with rotation. The final volume of the reaction was made up to 100 µl using pre-warmed hybridisation buffer. A portion (5 µl per reaction) of pre-washed Dynabeads was then added to gDNA-capture probe complexes and incubated at 20°C overnight to allow binding between the capture probe and the Dynabeads by the biotin-streptavidin interaction. After binding, the samples were washed 3 times using 100 µl of hybridisation wash buffer. The first waste fraction was kept for further analysis. Dynabeads-gDNA complexes were then resuspended in 150 µl of hybridisation buffer and a portion of target probe (Bactouniversal) was added to each reaction for hybridising the gDNA attached to the Dynabeads. After hybridisation at 50°C for 5 h in the dark with rotation, the final Dynabeads complexes were washed 3 times using 150 µl of WB buffer. The first wash fraction containing the unbound target probe was kept for further analysis.

The final products were resuspended in 100 μ l of BioMag buffer and stored at 4°C until further analyses.

2.5.3. Restriction enzyme digestion of gDNA

The restriction enzyme used to digest the gDNA of *D. radiodurans* was HinP1I (10 units/ μ l) stored at -20°C in glycerol. To set up the reaction, the enzyme was placed on ice. A portion (10-50 μ l) of gDNA was transferred to a fresh 1.5 ml Eppendorf tube. Generally, 40 μ l of gDNA (425 ng/ μ l) was used per reaction. After adding 0.3 μ l of NEbuffer2 (incubation buffer for HinP1I as indicated by the manufacturer) and 0.3 μ l of enzyme, the solution was tapped and quickly spun to remove bubbles. The reaction was incubated at 37°C for 16 h. After incubation, the reaction was stopped by heat inactivation at 65°C for 20 min. The digestion was confirmed by 1% gel electrophoresis, and the restriction digests were stored at 4°C until further analysis. Digested gDNA was then hybridised to Dynabeads either by the direct or indirect method described below.

2.5.3.1. Direct method for capturing digested gDNA

For all reactions, 1 μ l of pre-washed Dynabeads was resuspended in 50 μ l of BioMag buffer. Generally, 3 μ l of the QDUniBiotinF capture probe (1 μ M) was added to the Dynabeads and incubated at RT for 30 min. The Dynabeads-capture probe complexes were then washed 3 times using 100 μ l of BW buffer and resuspended in 50 μ l of BW buffer. A portion (40 μ l) of digested gDNA (425 ng/ μ l) was used for hybridisation to 1 μ l of Dynabeads-capture probe complexes. Digested gDNA was denatured at 99°C for 20 min using a thermo-cycler followed by cold shock on ice for 1 min. Denatured fragments of digested gDNA were then added to Dynabeads-capture probe complexes and hybridised at 55°C for 30 min followed by cold shock on ice for 1 min. The samples were washed and resuspended in 50 μ l of BW buffer. Then, 3 μ l of DeinoFamFITC target probe (1 μ M) was added followed by hybridisation at 55°C for 30 min to target the digested gDNA attached to the Dynabeads. The reaction was stopped by placing the samples on ice for 1 min. The final Dynabeads complexes were washed and resuspended in 200 μ l of TE buffer pH 8 at 4°C, until further analysis.

2.5.3.2. Indirect method for capturing digested gDNA

Digested gDNA from *D. radiodurans* was mixed with 3 μl of the QDUniBiotinF capture probe (1 μM) in 50 μl of BioMag buffer and 1 μl of PCR buffer. Generally, 40 μl of digested gDNA (425 ng/ μl) was used per reaction. The digested gDNA was denatured and hybridised to the capture probe by bringing the solution up to 94°C for 30 s followed by 55°C for 30 s. This step was repeated 15 times using the thermo-cycler. Then, the solutions were placed on ice for 1 min. A portion (1 μl) of pre-washed Dynabeads was added to the gDNA-capture probe complexes and incubated at RT for 30 min followed by a wash step using 100 μl of BioMag buffer and resuspended in 50 μl of BioMag buffer. Then, 3 μl of DeinoFamFITC target probe (1 μM) was added to the solution and incubated at 55°C for 30 min in the dark. After placing the samples on ice for 1 min, the final Dynabeads complexes were washed using 100 μl of BioMag buffer and resuspended in 200 μl of TE buffer pH 8 and kept at 4°C until further analysis.

2.6. Capture and detection of PCR amplicons bound to Dynabeads

PCR amplicons from *D. radiodurans* were obtained as described earlier (VI.2.3.5) using the primers DeinoFamBR (with a biotin modification) and Plainuniversal. PCR amplicons were analysed by 1% gel electrophoresis. The band of the desired size of PCR product (243 bp) was cut out of the gel using a sterile scalpel under a UV lamp, and extracted using a gel extraction kit (Qiagen). The final concentration of the PCR amplicon was measured by spectrophotometry (II.2.6.1.2).

2.6.1. Alkali treatment for denaturation of PCR amplicons

1 μl of pre-washed Dynabeads were transferred to fresh 1.5 ml Eppendorf tubes to a final volume of 50 μl using BioMag buffer. After adding the appropriate amount of biotinylated PCR amplicon, the reactions were incubated at RT for 30 min with rotation. Biotinylated PCR amplicons bound to Dynabeads were washed twice with BW buffer to remove unbound products. The final complexes were resuspended in 50 μl of TE buffer pH 8. The reactions were washed twice using the Dynal MPC™ magnet and resuspended in 50 μl of 0.1 M NaOH for 10 min. After the second wash, the samples were resuspended

in 50 μl of BW buffer. A portion of target probe was added as quickly as possible to the reactions after the last wash. Generally 2-3 μl of 1:100 diluted target probes from stock (100 μM) in sterile MilliQ water was used for hybridisation with the single strands of the PCR amplicon bound to the Dynabeads. The target probes used were: Bactouniversal2, BactouniAlexa and QDUniBiotinF. After incubation at 55°C for 1 h with rotation in the dark, the reactions were put on ice for 30 s. The final Dynabeads complexes were washed as usual and resuspended in 200 μl of BW buffer. The final products were kept at 4°C in the dark until further analysis.

2.6.2. Preparation of target probes modified with QDs

Generally, 2 μl of QD525 (1 μM) were mixed with different concentrations of QDUniBiotinF target probe (1 μM). The volume of the reactions was made up to 50 μl using QDs incubation buffer. The solutions were incubated at 30°C for 30 min in the dark with gentle rotation. It was calculated that all QDUniBiotinF probes would be bound to the QD525 due to the low concentrations used. Therefore, a washing step was not considered to be necessary. The QDs-target probe complexes were kept at 4°C in the dark up to 24 h until further analyses.

2.7. Capture and detection of PCR amplicons bound to QuantumPlex™M beads

2.7.1. Calculations of the saturation point of the QuantumPlex™M beads

A QuantumPlex™M bead contains 7.4×10^7 active carboxylic sites (Bangs Laboratories, pers. comm.). In addition, a single bead binds to 4.6×10^5 oligonucleotides as indicated by the user's manual. From Avogadro's number; 1 mol contains 6.023×10^{23} molecules, hence 1 pmol contains 6.023×10^{11} molecules.

1 μl of QuantumPlex™M beads stock contains 10^6 beads. Therefore, if 1 bead binds 4.6×10^5 oligonucleotides, then 10^6 beads would bind a maximum of 4.6×10^{12} oligonucleotides. The stock solution of the modified oligonucleotide probe was 100 μM .

Therefore, 1 μl of probe stock contained 6.023×10^{13} molecules, which is the number of molecules required to saturate 1 μl of QuantumPlex™M beads. Therefore, probe stocks were diluted 100 times using autoclaved MilliQ water prior to binding to the beads, which resulted in 1 μl of probe (1 μM) containing 6.023×10^{11} molecules.

2.7.2. Preparation of QuantumPlex™M beads bound to the capture probe

The following protocol was modified from Kolarova and Hengerer (Kolarova & Hengerer 1996). Stock solutions of QuantumPlex™M beads were vortexed prior to use to ensure a uniform suspension of beads. Immediately after washing, 1 μl (10^6 beads) of solution was taken from the stock for each conjugation. The beads were washed once with 30 μl imidazole buffer (100 mM) pH 7.0 using the Dynal MPC™ magnet and resuspended in 25 μl of freshly prepared EDC (100 mM). A portion of Deino-Capture680 capture probe (1 μM) was added in the reaction and incubated at 35°C for 2 h with rotation. The reactions were kept away from the light as much as possible. Beads complexes were then washed twice with 100 μl of 3 x SSC buffer containing 0.1% SDS. Finally, the beads were resuspended in 50 μl of PBS (0.01 M) pH 7.4 and stored at 4°C in the dark.

2.7.3. Capturing the non-biotinylated strand of PCR amplicons

PCR reactions were prepared using the forward and reverse primers DeinoFamBR and Plainuniversal, respectively. PCR amplicons were denatured at 99°C for 5 min followed by 95°C for 10 min using the thermo-cycler. Pre-washed QuantumPlex™M beads were resuspended in 25 μl of BioMag buffer and 25 μl of TE buffer pH 8. The denatured PCR amplicons were added to the beads as quickly as possible. The reporter probe, QDuniBiotinR, was added to the solution. After a hybridisation step at 50°C for 1 h with rotation, the beads were washed once and resuspended in 50 μl of BioMag buffer. 0.5 μl of streptavidin R-PE (1 mg/ml) was added to the solution and incubated at 30°C for 30 min with rotation to allow binding between R-PE and the reporter probe, QDuniBiotinR. The beads-PCR amplicon complexes were washed with 30 μl of BW buffer and resuspended in 200 μl of BW buffer. The final product was kept at 4°C in the dark until further analysis.

2.7.4. Evaluation of the bead-based method for the detection of extremophiles

Several DNA signatures from acidophilic thermophilic microorganisms identified from sulphur-rich environments and hydrothermal systems were developed for evaluation of the bead-based QD technique. The microorganisms were bacterial and archaeal sulphur- and iron- oxidisers: *Sulfobacillus thermosulfidooxidans*, *Acidithiobacillus ferrooxidans*, *Sulfolobus metallicus* and *Ferroplasma acidiphilum*.

Microbial strains were purchased from the Deutsche Sammlung von Mikroorganismen und Zellkulturen GmbH (DSMZ, Braunschweig, Germany), except *Sulfolobus metallicus* strain Kra23 that was kindly provided by Dr Ruth Henneberger (Macquarie University, Australia). *Acidithiobacillus ferrooxidans* was cultivated in DSMZ 882 medium at 28°C / 250 rpm. *Ferroplasma acidiphilum* was cultivated in DSMZ 874 medium at 37°C / 250 rpm. *Sulfobacillus thermosulfidooxidans* was cultivated in DSMZ 665 medium at 37°C / 50 rpm and *Sulfolobus metallicus* was cultivated in MAL medium containing 0.05% elemental sulphur and 0.02% yeast extract (Brock *et al.* 1972) at 65°C / 50 rpm. All microbial cultures were grown under aerobic conditions and growth was monitored by light microscopy.

DNA extraction was undertaken as described previously (VI.2.3.2) and PCR amplification was carried out using specific primers for each microorganism as described previously (VI.2.3.5).

Specific capture probes were used to hybridise the PCR amplicon from the different microorganisms and bind it to the QuantumPlex™™ beads. The target probe was designed to hybridise the captured PCR amplicon while labelling with the different fluorophores (Table VI. 5).

Table VI.5: PCR product concentration, capture probe and target probe used per each microorganism.

Microorganism	Concentration of PCR product	Volume of PCR amplicon	Capture probe (10 μ l, 1 μ M)	Target probe (10 μ M, 1 μ M)
<i>Deinococcus radiodurans</i>	55 ng/ μ l	20 μ l	Deino-Capture680	QDuniBiotinR
<i>Sulfobacillus thermosulfidooxidans</i>	363 ng/ μ l	10 μ l	Sulf288A	EUBB
<i>Acidithiobacillus ferrooxidans</i>	10 ng/ μ l	28 μ l	Thio2A	EUBB
<i>Sulfolobus metallicus</i>	39 ng/ μ l	9 μ l	SmetA	ASFRB
<i>Ferroplasma acidiphilum</i>	330 ng/ μ l	14 μ l	FER565A	ASFRB

PCR amplicons were bound to the QuantumPlex™M beads and labelled with the different fluorophores following the protocols described earlier (VI.2.7.3). Negative controls were set up to confirm the binding specificity of the probes and the fluorophores. The controls excluded PCR amplicons in the reaction.

2.8. Flow cytometry

Flow cytometric analyses were undertaken using a BD FACS-Calibur Flow cytometer with the settings and data acquisition described previously (II.2.5.2).

Unlabelled paramagnetic beads were used to set up the system every time before analysis. A fluorescent signal from the samples analysed above the signal observed from unlabelled paramagnetic beads was considered positive.

3. RESULTS

3.1. Optimisation of the binding procedures

3.1.1. Binding of complementary probes to Dynabeads

Complementary oligonucleotide probes were bound to the Dynabeads and analysed by flow cytometry to validate the binding procedures. The maximum and minimum detection limits of complementary probes were determined.

Two complementary oligonucleotide probes were chosen for binding to the Dynabeads: a biotinylated probe (DeinoFamBiotin) was first bound to Dynabeads by the biotin-streptavidin interaction, followed by the hybridisation to the complementary probe modified with FITC (DeinoFamFITC) (VI.2.4.3). Figure VI.3 describes the hybridisation of the complementary probes followed by their binding to the Dynabeads.

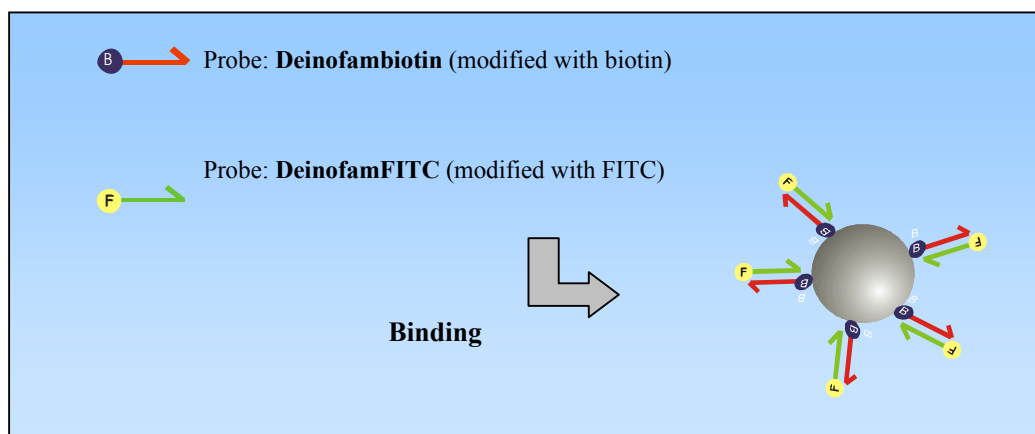


Figure VI.3: Schematic representation of complementary probes bound to the Dynabeads.

Different concentrations of DeinoFamBiotin probe were bound to the Dynabeads (Table VI.6), followed by its hybridisation to the complementary target probe, DeinoFamFITC (VI.2.4.3). The samples were analysed by flow cytometer and the MFI values recorded (Figure VI.4).

Table VI.6: Concentrations of DeinoFamBiotin probe used for binding 5 μ l (10 mg/ml) of Dynabeads.

Sample number	Volume of DeinoFamBiotin	Concentration of DeinoFamBiotin	Molecules per sample
1	0.5 μ l	0.5 pmol	3.01125×10^{11}
2	1 μ l	1 pmol	6.0225×10^{11}
3	2 μ l	2 pmol	1.2045×10^{12}
4	3 μ l	3 pmol	1.806×10^{12}
5	4 μ l	4 pmol	2.409×10^{12}
6	5 μ l	5 pmol	3.011×10^{12}
7	6 μ l	6 pmol	3.6135×10^{12}
8	7 μ l	7 pmol	4.215×10^{12}
9	8 μ l	8 pmol	4.818×10^{12}
10	9 μ l	9 pmol	5.420×10^{12}
11	10 μ l	10 pmol	6.0225×10^{12}
12	11 μ l	11 pmol	6.624×10^{12}
13	12 μ l	12 pmol	7.227×10^{12}
14	13 μ l	13 pmol	7.829×10^{12}
15	14 μ l	14 pmol	8.4313×10^{12}
16	15 μ l	15 pmol	9.033×10^{12}

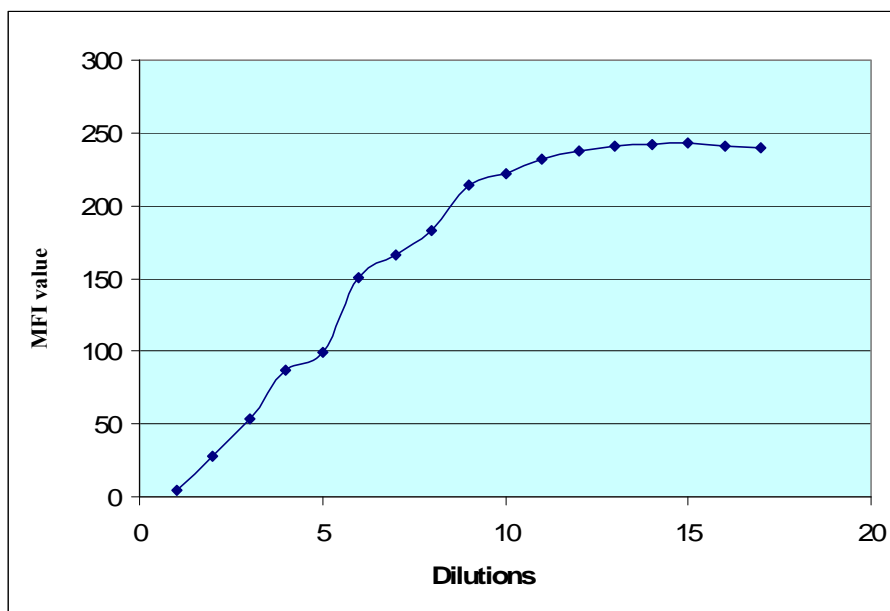


Figure VI.4: Fluorescent intensity measured as MFI values of several concentrations of complementary probes (Table VI.6) bound to Dynabeads as measured by FACS-Calibur flow cytometry.

The complementary target probe DeinoFamFITC was modified with FITC for flow cytometric detection. The increase of the fluorescent signal observed by flow cytometry (Figure VI.4) indicated that both complementary probes have successfully hybridised and bound to the Dynabeads. Only 0.5 pmol of DeinoFamBiotin probe was required to obtain a positive signal by flow cytometry. The saturation point of the Dynabeads was reached when 10 pmol of DeinoFamBiotin probe were added to the binding reactions. The saturation point of Dynabeads was in concordance with the previous results obtained (V.3.3.4). Therefore, it could be inferred that the binding and hybridisation of the two complementary probes on the surface of the Dynabeads did not alter the overall binding capacity of the beads.

Low concentrations of DeinoFamBiotin probe (Table VI.7) were hybridised to the complementary probe followed by their binding to the Dynabeads to determine the minimum detection limit.

Table VI.7: Several concentrations of DeinoFamBiotin probe used for binding to the Dynabeads followed by the hybridisation to the complementary probe, DeinoFamFITC.

Sample number	Volume of DeinoFamBiotin	Concentrations of DeinoFamBiotin	Number of molecular probes per sample
1	0.5 μ l	0.1 pmol	6.02×10^{10}
2	1 μ l	0.2 pmol	1.20×10^{11}
3	2 μ l	0.4 pmol	2.41×10^{11}
4	3 μ l	0.6 pmol	3.61×10^{11}
5	4 μ l	0.8 pmol	4.82×10^{11}
6	5 μ l	1 pmol	6.02×10^{11}
7	6 μ l	1.2 pmol	7.22×10^{11}
8	7 μ l	1.4 pmol	8.43×10^{11}
9	8 μ l	1.6 pmol	9.63×10^{11}
10	9 μ l	1.8 pmol	1.08×10^{12}
11	10 μ l	2 pmol	1.20×10^{12}

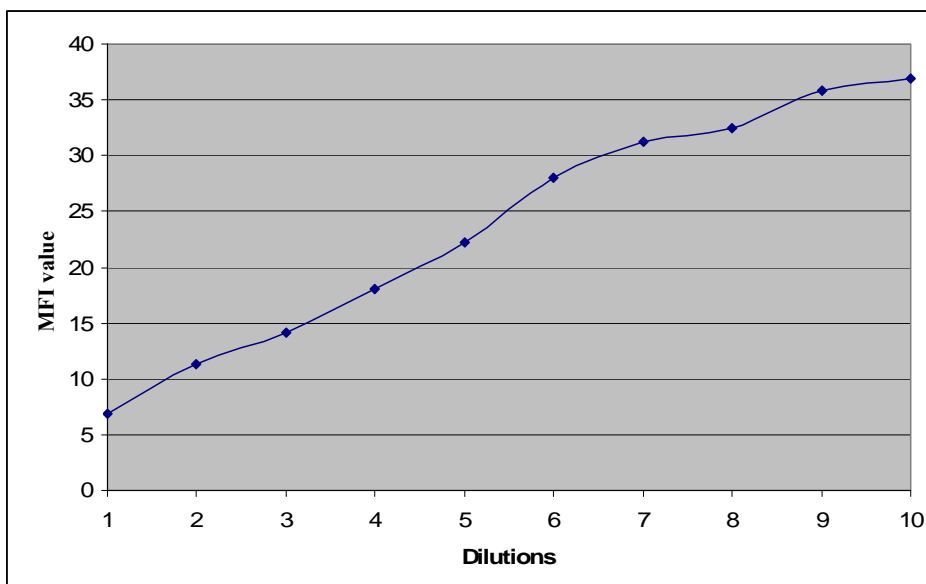


Figure VI.5: Fluorescent intensity measured as MFI values of different concentrations of complementary probes bound to the Dynabeads (Table VI.6).

As expected, increasing concentrations of complementary probe bound to the Dynabeads resulted in an increased fluorescent signal (Figure VI.5). The minimum concentration of the complementary probe bound to Dynabeads necessary to obtain a positive signal by flow cytometry was 1 pmol (Figure VI.5). The minimum and maximum detection limit of the complementary probe bound to the Dynabeads was valuable in verifying their binding capacity.

3.1.2. Binding of biotinylated PCR amplicons to Dynabeads

Two different types of biotinylated PCR amplicons were bound to Dynabeads. The PCR amplicons were hybridised to different target probes labelled either FITC or QD680 for detection by flow cytometry.

The first type of biotinylated PCR amplicons were obtained from the amplification of the gDNA of *D. radiodurans* using the specific primers Bactouniversal and DeinoFamBR, modified with FITC and biotin respectively. Consequently, the resulting PCR amplicon was modified with biotin at one end and FITC at the other end. The biotin modification was used for binding to the Dynabeads while FITC provided the fluorescence signal required for detection by flow cytometry (Figure VI.6).

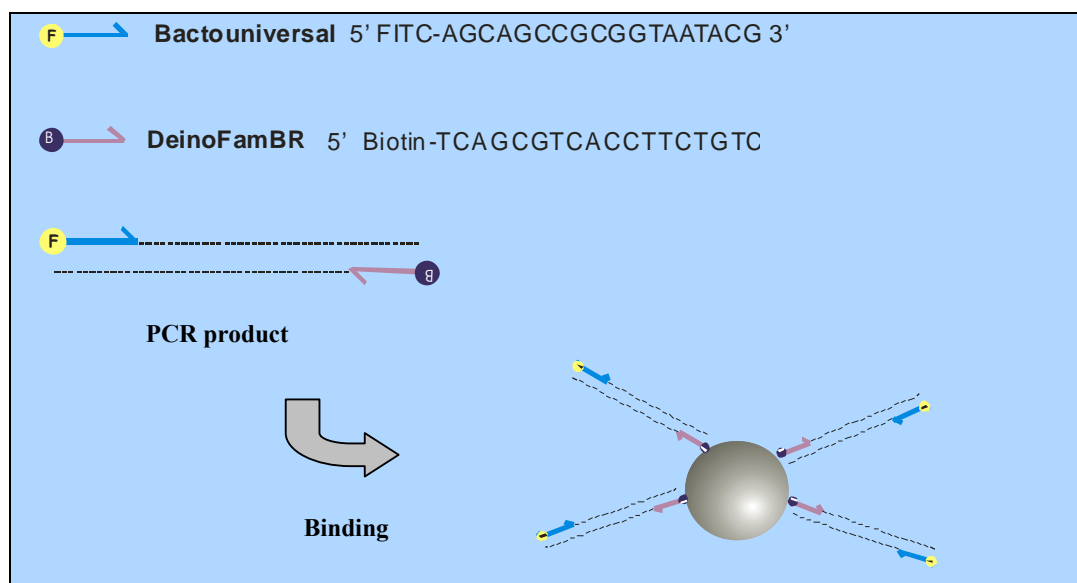


Figure VI.6: Schematic representation of PCR amplicon modified with biotin and FITC bound to Dynabeads.

The second type of PCR amplicons was obtained using the primers QDUniBiotinF and DeinoFamBR, both modified with biotin. The amplicon produced was consequently modified with biotin at both ends to allow binding to Dynabeads at one end and, binding to QD680 to the other of the PCR amplicon, by the biotin-streptavidin interaction (Figure VI.7).

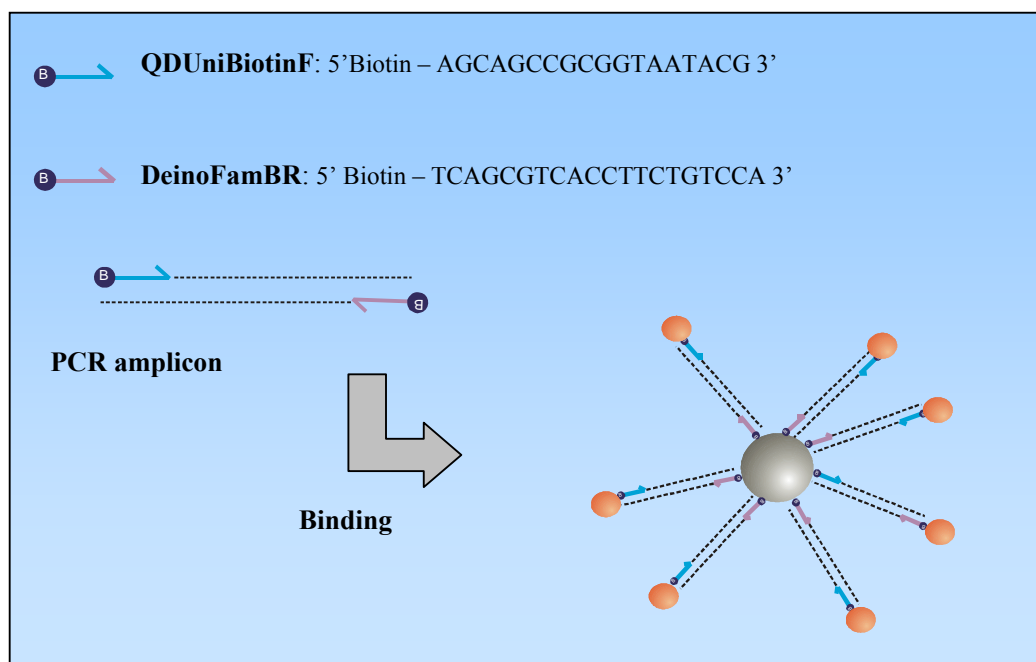


Figure VI.7: Schematic representation of the biotinylated PCR amplicons labelled with QD680 bound to Dynabeads.

As discussed earlier, the binding capacity of Dynabeads was 2 pmol of biotinylated probe per 1 μl (10mg/ml) of Dynabeads. The appropriate concentration of PCR amplicons required to bind the Dynabeads was calculated based on their size. Both types of PCR amplicons were 243 bp. 1 pmol of 243 bp dsDNA corresponds to 0.160 μg (nucleic acid data from www.neb.com). Therefore, the amount of PCR that would saturate the beads would be 0.32 μg (2 pmol).

The concentration of the PCR amplicon modified with FITC was 24 ng/ μl . Therefore, 13.3 μl of PCR amplicon was estimated to reach the saturation point of 1 μl Dynabeads (2 pmol). Three different concentrations of PCR amplicons modified with FITC were bound to the Dynabeads: Sample 1 (1 pmol, 6.65 μl), Sample 2 (2 pmol, 13.3 μl) and Sample 3 (4 pmol, 26.6 μl). The data was analysed on a histogram displaying FL1 (green) fluorescence (Figure VI.8).

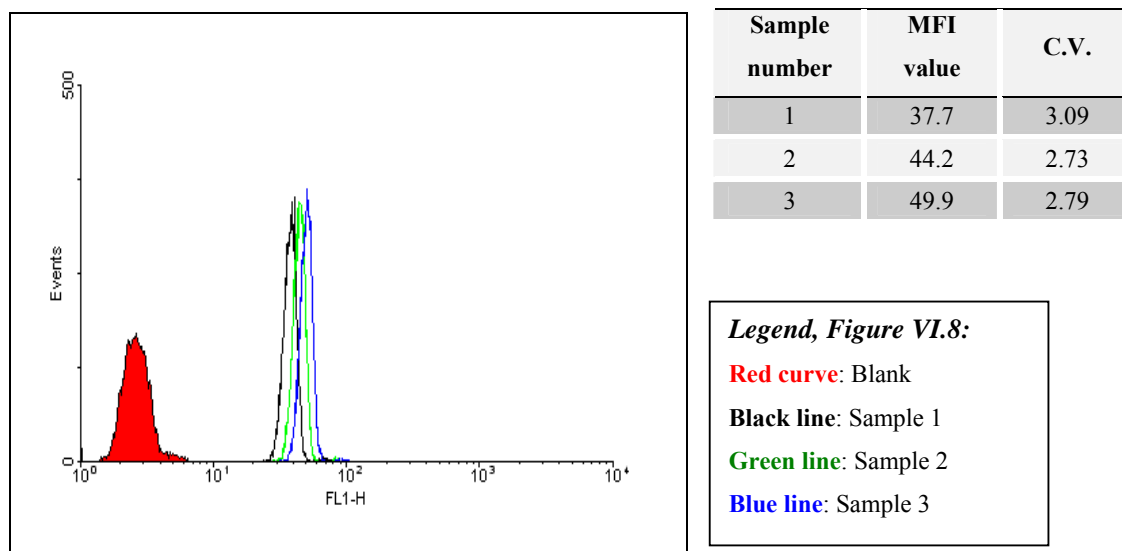


Figure VI.8: Biotinylated PCR amplicons modified with FITC bound to Dynabeads. X-axis: fluorescent signal detected in the FL1 channel. Y-axis: number of counts per sample. MFI value: Geomean C.V.: Coefficient of variation

All the samples analysed showed a significant fluorescent signal above the blank (Figure VI.8), indicating the success of the binding procedures and detection. The highest fluorescent signal was obtained when 4 pmol of PCR amplicon were used to bind the Dynabeads (Figure VI.8, blue line).

In contrast, PCR amplicons modified with biotin were obtained at a concentration of 26 ng/ μ l. Three concentrations of biotinylated PCR amplicons were bound to the Dynabeads: Sample 1 (1 pmol, 6.15 μ l), Sample 2 (2 pmol, 12.3 μ l) and Sample 3 (4 pmol, 24.6 μ l) bound to 1 μ l (10 mg/ml) of Dynabeads per sample. The bound PCR amplicons were labelled with QD680 (1 μ l, 1 μ M) and analysed on a histogram displaying FL3 (red) fluorescence (Figure VI.9). The maximum emission of QD680 was at 680 nm which was detected in the FL3 channel of the flow cytometer.

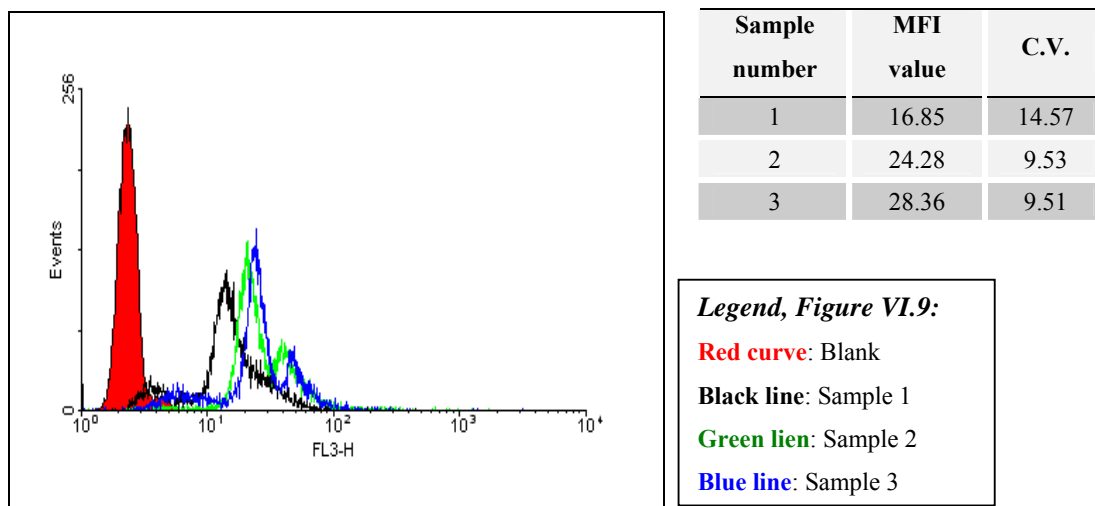


Figure VI.9: Flow cytometric analysis. Histogram of biotinylated PCR amplicons labelled with QD680 bound to the Dynabeads. X-axis: fluorescent signal detected in the FL3 channel. Y-axis: number of counts per sample. MFI value: Geomean C.V.: Coefficient of variation

As expected, all samples showed a significant increase of fluorescence above the blank (Figure VI.9). The results confirmed the successful binding of the PCR amplicons labelled with QD680 to the Dynabeads. However, the population of fluorescent Dynabeads appeared to be spread along the histogram (Figure VI.9) instead of forming a narrow fluorescent peak as found when labelling the PCR amplicons with FITC (Figure VI.8). This result indicated that agglomeration of the Dynabeads had occurred which may have been due to the QDs. The highest fluorescent signal was obtained when 4 pmol of PCR amplicon was bound to the Dynabeads (Figure VI.9, blue line), as occurred when labelling with FITC.

3.1.3. Buffers and incubation times

Several buffers and incubation times were tested in an attempt to reduce agglomeration of the Dynabeads when working with QDs.

The buffers tested were: BioMag buffer, Dynabeads buffer, TE buffer pH 8 and HYB buffer (6 x SSC, 0.1 % SDS and 1 x Denhardt's mix). Incubation times varied from 1 h to overnight. For these experiments, 1 µl of Dynabeads was bound to 1 pmol (6.15 µl) of biotinylated PCR amplicons (Figure VI.8) followed by labelling with QD680 (1µl, 2µM) and analysed on a bivariate dot-plot of SSC versus FL3 (Figure VI.10).

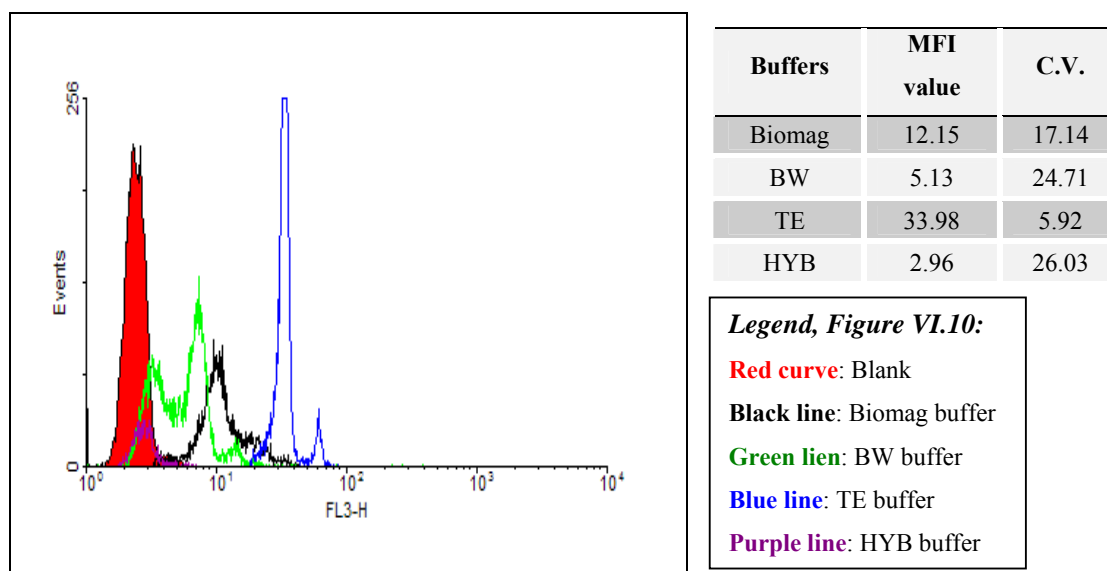


Figure VI.10: Histogram of biotinylated PCR amplicons labelled with QD680 bound to Dynabeads using different hybridisation buffers. X-axis: fluorescent signal detected in the FL3 channel. Y-axis: number of counts per sample. Observed was a significant increase in MFI when TE buffer was used for hybridisation.

MFI value: Geomean

C.V.: Coefficient of variation

Flow cytometric analysis revealed that agglomeration of the Dynabeads occurred under all hybridisation conditions tested (Figure VI.10). TE buffer showed the best result with higher fluorescent intensity measured as MFI values (MFI: 32.61, CV: 3.59) and less agglomeration than the other buffers tested: BioMag buffer (MFI: 10.46, CV: 11.05), Dynabeads buffer (MFI: 6.61, CV: 11.22) and HYB buffer (MFI: 2.79, CV: 19.05). It was

observed also that long periods of incubation increased the degree of agglomeration of the Dynabeads. One to two hours of incubation was found to provide the best results.

3.2. Bead-based QDs technique for DNA detection

3.2.1. Detection of gDNA bound to Dynabeads

The gDNA of *D. radiodurans* was used to optimise and validate the bead-based QDs technique. Two oligonucleotide probes were used to capture and target the gDNA on the Dynabeads' surface. The capture probe (DeinoFamBiotin) had a biotin modification while the target probe (Bactouniversal) had a FITC modification. Both probes were able to hybridise the gDNA of *D. radiodurans*. After hybridisation, the capture probe was able to bind the gDNA to the Dynabeads while the target probe provided the fluorescence for detection by flow cytometry (Figure VI.11).

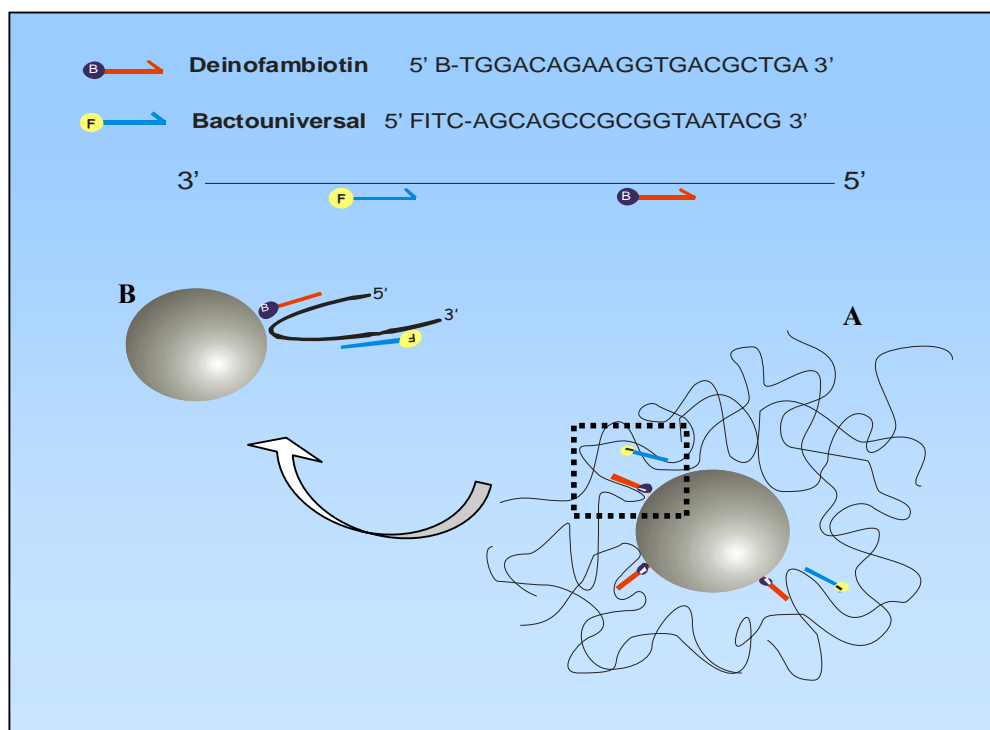


Figure VI.11: A: Speculative schematic representation of the hybridisation of the capture and target probe to gDNA from *D. radiodurans* bound to Dynabeads. B: Enlarged detail of a single strand of gDNA bound to Dynabeads. The gDNA may have been forced to fold in order to allow hybridisation to the probes.

Two different methods for hybridising to the probes to the gDNA were tested: a direct method where the capture probe was bound to the Dynabeads prior to hybridisation to the pre-denatured gDNA (VI.2.5.1), and an indirect method where the denatured gDNA was hybridised to the capture probe before binding to the Dynabeads (VI.2.5.2). After the binding of the gDNA to the Dynabeads, both methods used the target probe to label the gDNA. The data was analysed on histogram exhibiting FL1 (green) fluorescence (Figure VI.12).

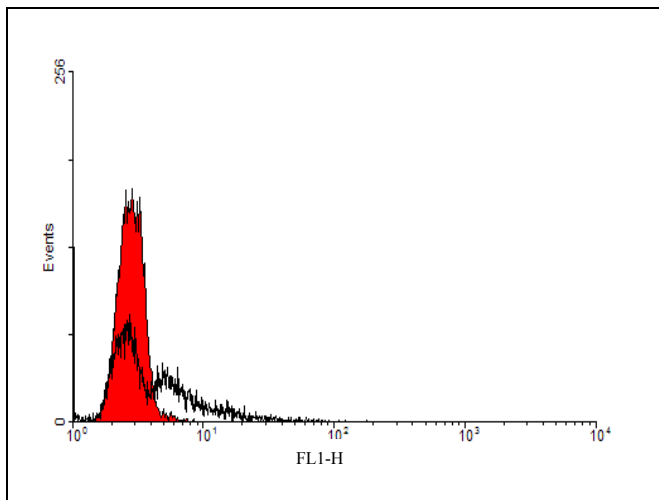


Figure VI.12: Flow cytometric analysis. Histogram of the Dynabeads bound to gDNA of *D. radiodurans* labelled with FITC by the direct method. X-axis: fluorescent signal detected in the FL1 channel. Y-axis: number of counts per sample

Legend, Figure VI.12:

- Red curve:** Blank
- Black line:** gDNA of *D. radiodurans* bound to the Dynabeads labelled with FITC

Dynabeads bound to gDNA of *D. radiodurans* labelled with FITC by both methods did not show fluorescence above the negative control, indicating failure of the binding procedures (Figure VI.12). Different buffers and incubation times were tested in an attempt to avoid improve the binding capacity (data not shown). However, none of the modifications tested improved the fluorescent signal of the beads.

3.2.2. Detection of digested gDNA bound to Dynabeads

The gDNA of *D. radiodurans* was digested enzymatically to obtain smaller fragments of DNA for binding to the Dynabeads in an attempt to facilitate hybridisation to the capture and target probes and avoid agglomeration issues.

Molecular analyses of two different restriction enzymes were carried out to find their recognition sites on the gDNA of *D. radiodurans* (Figure VI.13). HinP1I was selected as

the restriction enzyme as it resulted in digestion at eight different sites along the 16S rDNA gene sequence, leaving the hybridisation sites of the probes available for subsequent capture and target probe hybridisation.

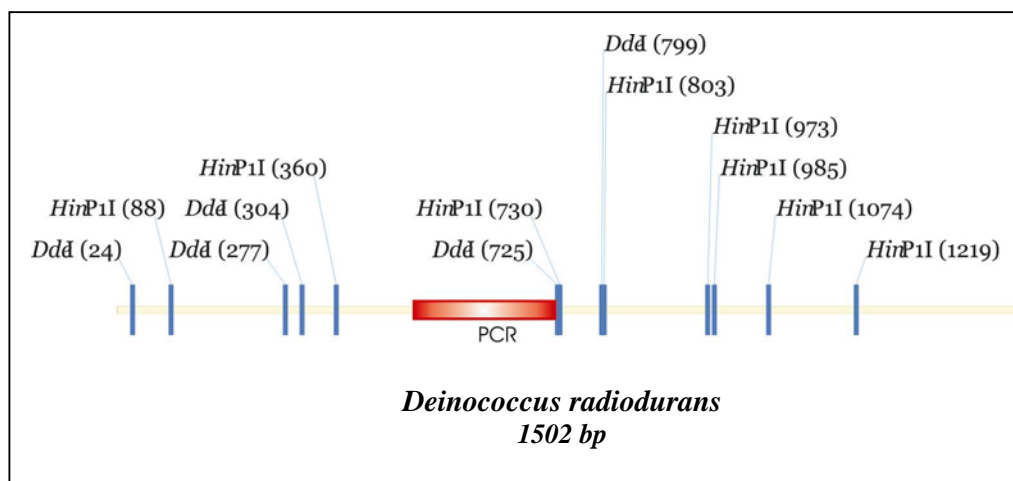


Figure VI.13: Schematic representation of the 16S rRNA sequence of *D. radiodurans* and the recognition sites of two restriction enzymes: *HinP1I* and *DdeI*. The red rectangle indicates the hybridisation sites of the capture and target probe and it represents the hypothetical segment of the sequence that would be amplified by PCR if the probes were used as primers.

The size of the DNA segment containing the hybridisation sites of the capture and target probes were 370 bp. The capture probe (QDUniBiotinF) had a biotin modification for binding to Dynabeads, while the target probe (DeinoFamFITC) had a FITC modification for labelling of digested DNA, enabling detection by flow cytometry. The hybridisation sites of both probes were aligned one after the other along the 16S rDNA gene sequence of *D. radiodurans* (Figure VI.14), preventing DNA hairpin formation or other artefacts.

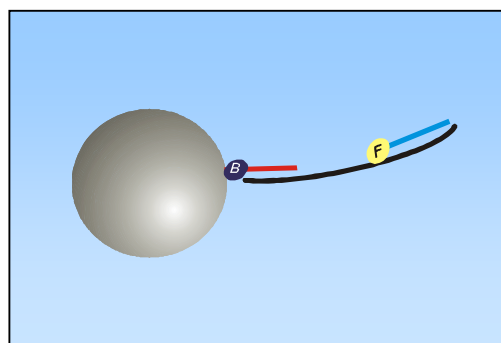


Figure VI.14: Schematic representation of the hybridisation sites of the capture probe (QDunibiotinF) and the target probe (DeinofamFITC) on the digested DNA of *D. radiodurans*.

Two different methods to denature the digested DNA and hybridise it to the probes were tested. The direct binding procedure was based on binding the capture probe to the Dynabeads prior to hybridisation to the digested DNA, while the indirect method was based on the hybridisation of the capture probe to the digested DNA, prior to binding to the Dynabeads. After binding to the Dynabeads, both methods used a target probe to hybridise the digested DNA and labelled it with FITC.

Flow cytometric analysis revealed negative results for both hybridisation methods tested. Spectrophotometric analysis performed on the waste fractions obtained during the binding procedures revealed a highly fluorescent signal (data not shown). These results indicated that the target probe (DeinoFamFITC) did not hybridise to the digested DNA remaining in the waste fraction, or the digested DNA was not captured by the Dynabeads.

3.2.3. Detection of biotinylated PCR amplicons bound to Dynabeads

PCR amplicons obtained from the amplification of the 16S rDNA gene sequence of *D. radiodurans* using specific primers were used to develop and optimise the bead-based QD technique for DNA detection.

The PCR amplicons were biotinylated at one end to allow direct binding to the Dynabeads and avoid the need for a capture probe (Figure VI.15). After denaturation of the PCR amplicons, the biotinylated PCR strand was bound to the Dynabeads and hybridised to a target probe modified either with FITC, Alexa Fluor 488, QD525 or QD585 (Table VI.8).

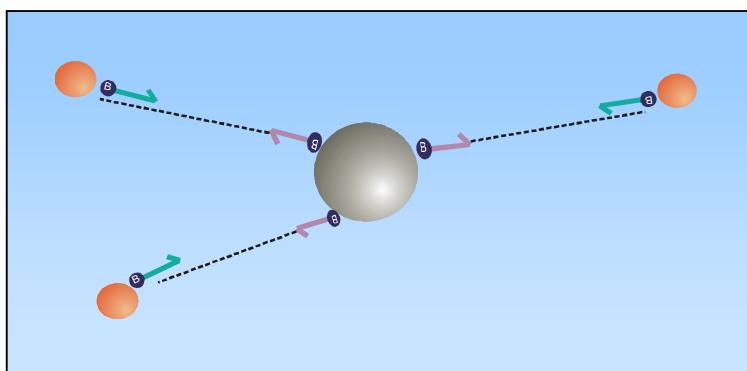


Figure VI.15: Schematic representation of the bead-based QD technique to detect biotinylated PCR products labelled with a target probe modified with a fluorophore.

Table VI.8: Target probes used to label the biotinylated single strand of the PCR amplicon bound to Dynabeads.

Capture	Target probe	Fluorophore modification
Biotinylated PCR product	BactoUni2	FITC
	Bactouniversal2	FITC
	BactouniAlexa	Fluor Alexa 488
	QDUniBiotinF	QD525 or QD585

PCR amplification of *D. radiodurans* gDNA was carried out using DeinoFamBR as a forward primer and Plainuniversal as the reverse primer. The concentration of PCR product obtained was 34 ng/ μ l. Several methods for hybridising the biotinylated PCR amplicons to the target probes and binding to the Dynabeads were tested (Appendix IV). However, none of those methods were successful.

Biotinylated PCR amplicons labelled with QD525, FITC and Alexa Fluor 488 (Table VI.9) following alkaline treatment and bound to the Dynabeads were analysed on a histogram displaying FL1 (green) fluorescence (Figure VI.16). The maximum emission of QD525 was at 525 nm which was detected in the FL1 channel of the flow cytometer.

Table VI.9: Biotinylated PCR amplicons labelled with the specific target probe (modified FITC, Alexa and QD525) by the alkaline treatment followed by binding to Dynabeads.

Sample number	Biotinylated PCR amplicon (210 μ M)	Dynabeads (10 mg/ml)	Target probe (1 μ M)
1	5 μ l	1 μ l	3 μ l QDUniBiotinF (QD525, 1 μ M)
2	5 μ l	1 μ l	6 μ l QDUniBiotinF (QD525, 1 μ M)
3	5 μ l	1 μ l	10 μ l QDUniBiotinF (QD525, 1 μ M)
4	5 μ l	1 μ l	15 μ l QDUniBiotinF (QD525, 1 μ M)
5	5 μ l	1 μ l	2 μ l Bactouniversal (FITC)
6	5 μ l	1 μ l	2 μ l BactouniAlexa (Alexa Fluor 488)

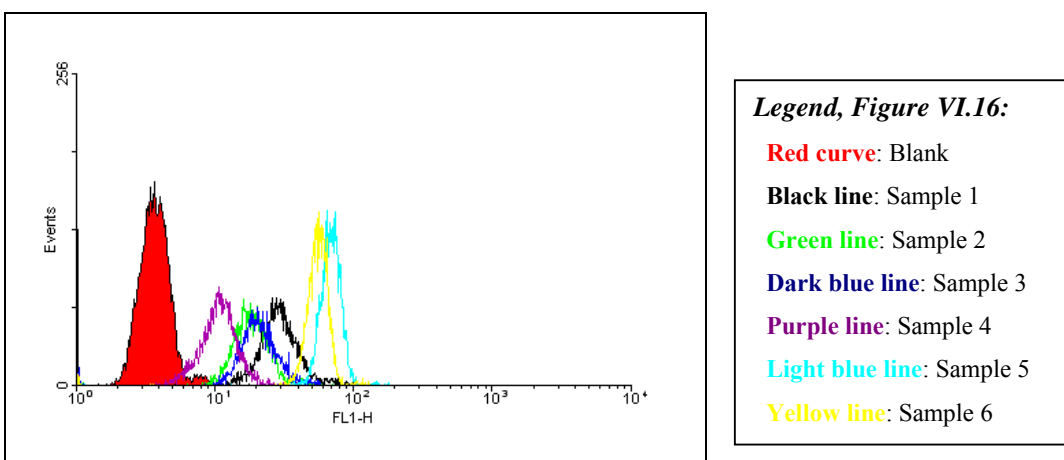


Figure VI.16: Flow cytometric analysis. Histogram of biotinylated PCR amplicons labelled with FITC, Alexa Fluor 488 and new QD525 by the alkaline treatment bound to Dynabeads. X-axis: fluorescent signal detected in the FL1 channel. Y-axis: number of counts per sample.

Table VI.10: MFI values (Geomean) and C.V. (coefficient of variation) of the different samples of labelled biotinylated PCR amplicons bound to the Dynabeads (Table VI.9).

Sample number	MFI value	C.V.
Blank	3.66	16.84
1	29.10	8.87
2	18.28	8.82
3	20.95	9.53
4	10.70	12.86
5	68.83	3.81
6	55.55	4.05

All the samples analysed were positive, exhibiting a fluorescent signal above background (Figure VI.16). The positive fluorescence indicated successful hybridisation of the biotinylated PCR amplicons to the target probes and their subsequent binding to the Dynabeads. The yellow line indicates the fluorescent signal of the biotinylated PCR amplicons labelled with Alexa Fluor 488, while the light blue line indicated the biotinylated PCR amplicons labelled with FITC. The MFI values from FITC (MFI: 68.83) were higher than Fluor Alexa 488 (MFI: 55.55). Despite the successful binding and detection of the PCR amplicons with QD525, the fluorescent signal obtained from all the samples was lower than FITC and Alexa Fluor 488 (Table VI.9). QD525 bound to the lowest concentration of target probe (sample 1) gave the highest MFI values (29.10) compared to the other QD samples.

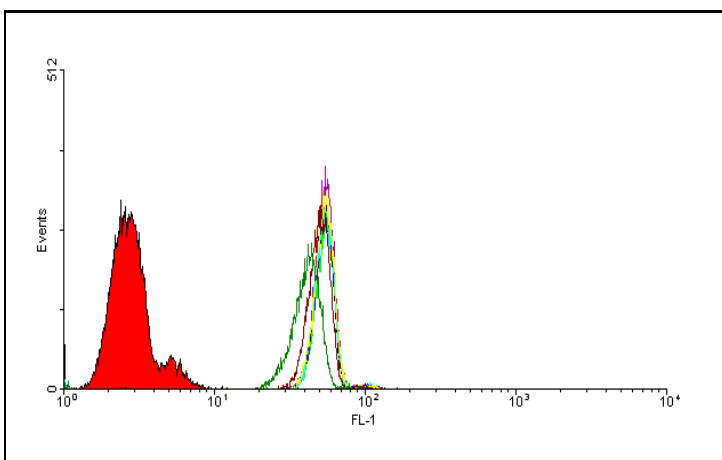
3.2.4. Fluorescent intensity of QDs versus organic dyes

Flow cytometry can accurately measure the fluorescent intensity of a given sample as it is directly proportional to the amount of fluorochrome present. The fluorescent intensity of FITC and QD525 labelling the single strand of biotinylated PCR amplicons bound to the Dynabeads was quantified and compared based on their MFI values.

Several concentrations of both target probes, Bactouniversal2 (modified with FITC) and QDUniBiotinF (bound to QD525) (Table VI.11), were used to compare the fluorescent intensities of the two fluorochromes, following analysis by the bead-based method. Two sets of samples were set up. First biotinylated PCR amplicon were labelled with different concentrations of Bactouniversal target probe modified with FITC and their MFI values were analysed and recorded. Secondly, the same amounts of biotinylated PCR amplicon as used before were labelled with different concentrations of QDUniBiotinF target probe bound to QD525 and their MFI values were recorded. The MFI values of both sets of samples were then plotted against the concentration of fluorophore to labelled the biotinylated PCR amplicon used in each hybridisation, either FITC or QD525 (Figure VI.19).

Table VI.11: Biotinylated PCR amplicons labelled with different concentrations of Bactouniversal target probe and QDUniBiotinF target probe (bound to QD525) bound to Dynabeads

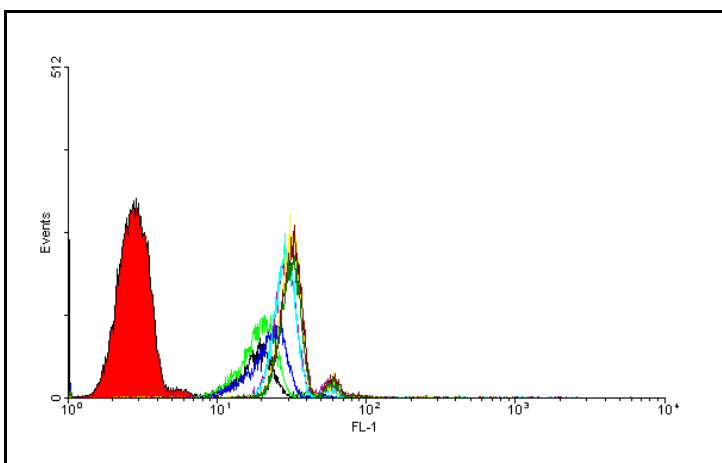
Sample number	Biotinylated PCR amplicon (320 μ M)	Dynabeads (10 mg/ml)	Bactouniversal2 (0.1 μ M)	QDUniBiotinF (1 μ M, QD525)
1	5 μ l	1 μ l	10 μ l	3 μ l (1 μ M)
2	5 μ l	1 μ l	9 μ l	2 μ l (1 μ M)
3	5 μ l	1 μ l	8 μ l	1 μ l (1 μ M)
4	5 μ l	1 μ l	7 μ l	10 μ l (0.1 μ M)
5	5 μ l	1 μ l	6 μ l	9 μ l (0.1 μ M)
6	5 μ l	1 μ l	5 μ l	8 μ l (0.1 μ M)
7	5 μ l	1 μ l	4 μ l	7 μ l (0.1 μ M)
8	5 μ l	1 μ l	3 μ l	6 μ l (0.1 μ M)



Legend, Figure VI.17:

- Red curve:** Blank
- Black line:** Sample 1
- Green line:** Sample 2
- Dark blue line:** Sample 3
- Purple line:** Sample 4
- Light blue line:** Sample 5
- Yellow line:** Sample 6
- Brown line:** Sample 7
- Dark green line:** Sample 8

Figure VI.17: Flow cytometric analysis. Histogram of biotinylated PCR amplicons labelled with different concentrations of Bactouniversal2 target probe (modified with FITC) (Table VI.11). X-axis: fluorescent signal detected in the FL1 channel. Y-axis: number of counts per sample.



Legend, Figure VI.18:

- Red curve:** Blank
- Black line:** Sample 1
- Green line:** Sample 2
- Dark blue line:** Sample 3
- Purple line:** Sample 4
- Light blue line:** Sample 5
- Yellow line:** Sample 6
- Brown line:** Sample 7
- Dark green line:** Sample 8

Figure VI.18: Flow cytometric analysis. Histogram of biotinylated PCR amplicons labelled with different concentrations of QDUniBiotinF (bound to QD525) (Table VI.11) bound to Dynabeads. X-axis: fluorescent signal detected in the FL1 channel. Y-axis: number of counts per sample.

Following analysis by FCM, both FITC and QD525 resulted in positive fluorescent signals above background (Figures VI.17 and VI.18). The MFI values from each sample were recorded for comparative purposes and plotted against the concentration of fluorophore used to label the biotinylated PCR amplicons as shown in Table VI.11 (Figure VI.19).

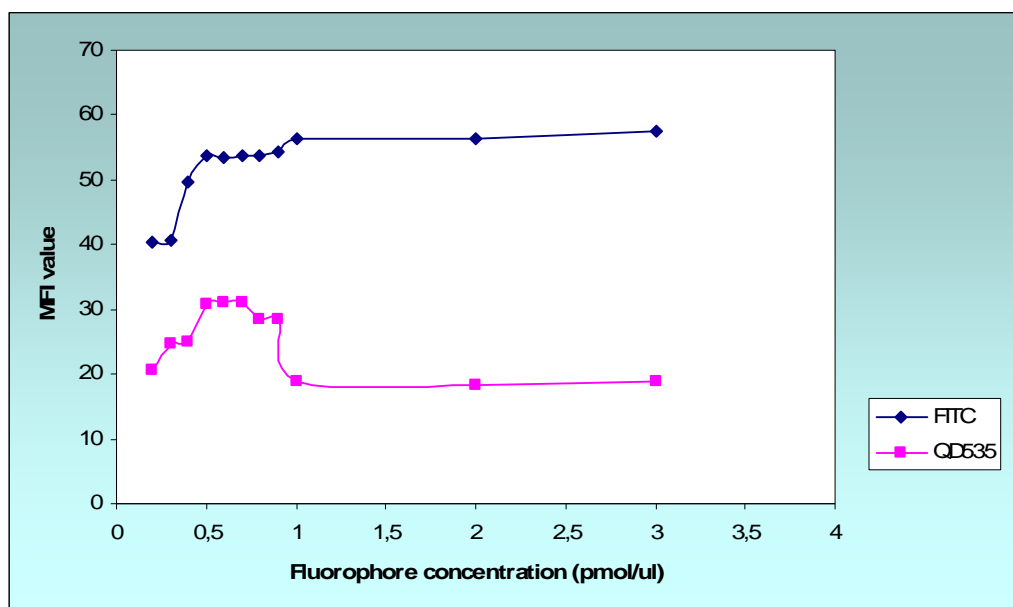


Figure VI.19: Fluorescent intensity measured as the MFI value of biotinylated PCR amplicons labelled with different concentrations of Bactouniversal2 (FITC) and QDUniBiotinF (QD525) bound to Dynabeads.

The MFI values obtained from the bead-based technique when using FITC as a fluorophore were 2-fold higher than when using QDs under the same concentration and experimental conditions (Figure VI.19). The fluorescent signal increased with increasing concentration of FITC until it reached its saturation point at 1 pmol (Figure VI.17 black line and Figure VI.19). However, it was observed that the fluorescent signal of the samples labelled with QD525 decreased after the saturation point was reached at 0.5 pmol.

3.2.5. Detection of PCR amplicons with QuantumPlex™M beads

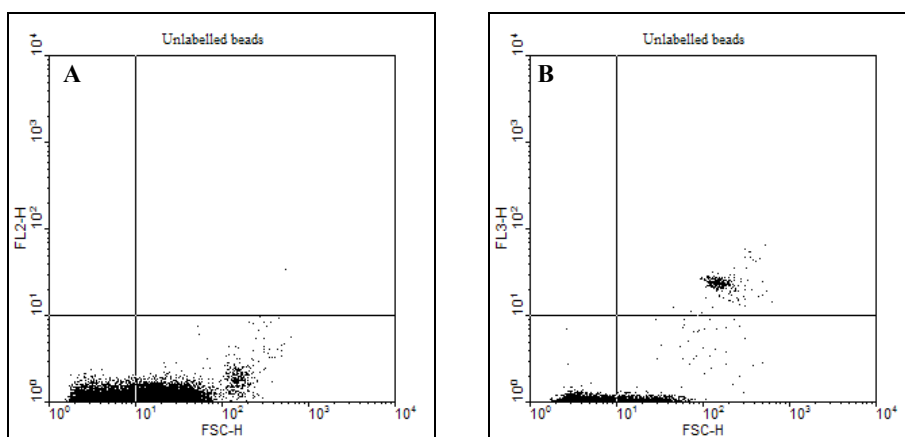
QuantumPlex™M beads are super-paramagnetic microspheres encoded with different intensities of Starfire Red (emission at 578 nm). The beads were functionalised with carboxyl (COOH) groups on their surface, permitting conjugation to amine compounds. QuantumPlex™M beads were selected to avoid any possible non-specific binding of the biotinylated probes and PCR amplicons with the beads, as they were not able to interact with the carboxyl groups of the beads.

QuantumPlex™ beads were used in a similar fashion as Dynabeads. They were used as a platform to capture PCR amplicons from *D. radiodurans* for their labelling and detection with different fluorophores. PCR amplicons were obtained using the primers DeinoFamBR and Plainuniversal. The capture probe used to hybridise the PCR amplicons while binding the beads was Deino-Capture probe. The target probe (QDuniBiotinR) was bound to R-PE (R-Phycoerythrin) which is a dye molecule with a maximum emission at 578 nm.

PCR amplicons were bound to the beads followed by labelling with R-PE (Table VI.12). Two negative controls were set up to confirm the binding specificity of the probes and dyes: one control did not include PCR amplicons in the reaction and the second control used PCR amplicons from *E. coli* instead of *D. radiodurans*. All data was analysed on bivariate dotplots of SSC versus FL2 (PE fluorescence) and SSC versus FL3 (red bead fluorescence) (Figure VI.20).

Table VI.12. PCR amplicons labelled with R-PE bound to QuantumPlex™ beads.

Sample numbers	PCR amplicon (55 ng/μl)	QuantumPlex™ beads (1x10 ⁸ beads/ml)	Deino-Capture (1 μM)	QDuniBiotinR (1 μM)	R-PE (1mg/ml)
1	5 μl	1 μl	1 μl	10 μl	0.5 μl
2	12 μl	1 μl	3 μl	10 μl	0.5 μl
3	20 μl	1 μl	5 μl	10 μl	0.5 μl
4	28 μl	1 μl	7 μl	10 μl	0.5 μl



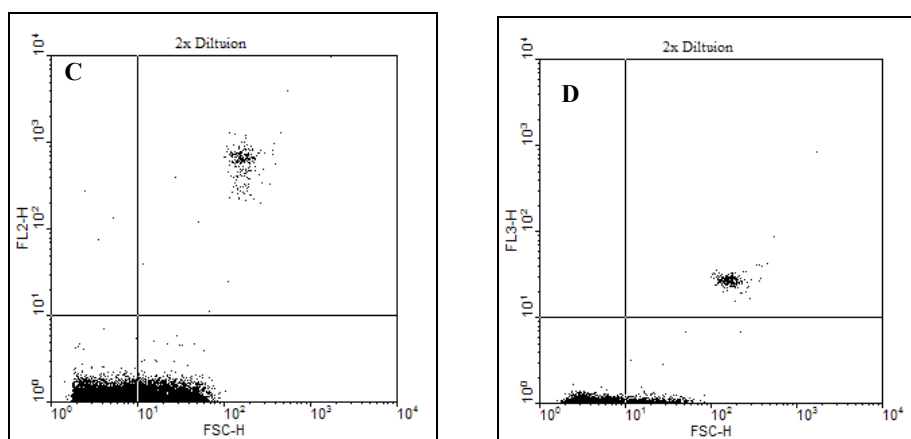


Figure VI.20: Flow cytometric analysis of PCR amplicons labelled with R-PE bound to QuantumPlex™™ beads. Bivariate dot-plots defining log FL2 or FL3 channel (y-axis) versus log SSC channel (x-axis). A: Unlabelled QuantumPlex™™ beads on the FL2 channel. B: Unlabelled QuantumPlex™™ beads on the FL3 channel. C: Sample 2 (Table VI.12) on the FL2 channel. D: Sample 3 (Table VI.12) on the FL3 channel.

Table VI.13: MFI values (Geomean) and C.V. (coefficient of variation) of the different samples of PCR amplicons labelled with R-PE bound to the QuantumPlex™™ beads (Table VI.12).

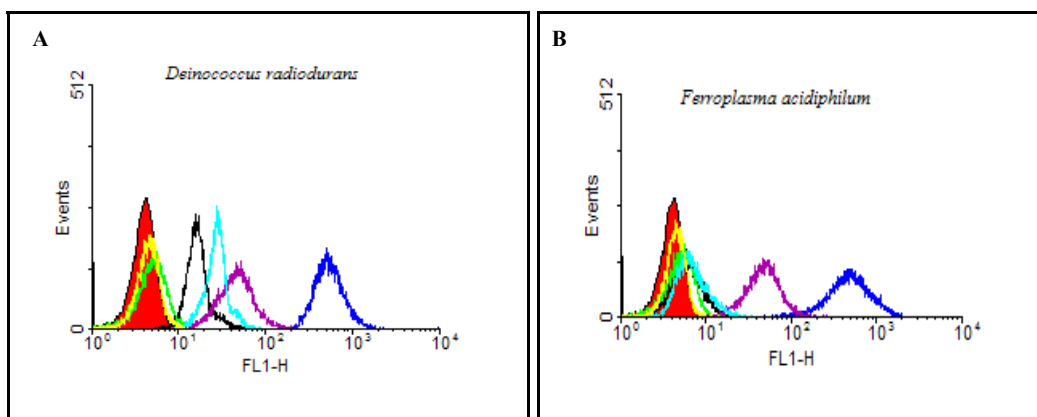
Sample number	MFI value	C.V.
Blank	1.04	47.82
1	292.05	3.64
2	676.49	2.50
3	911.32	2.26
4	1329.36	2.01

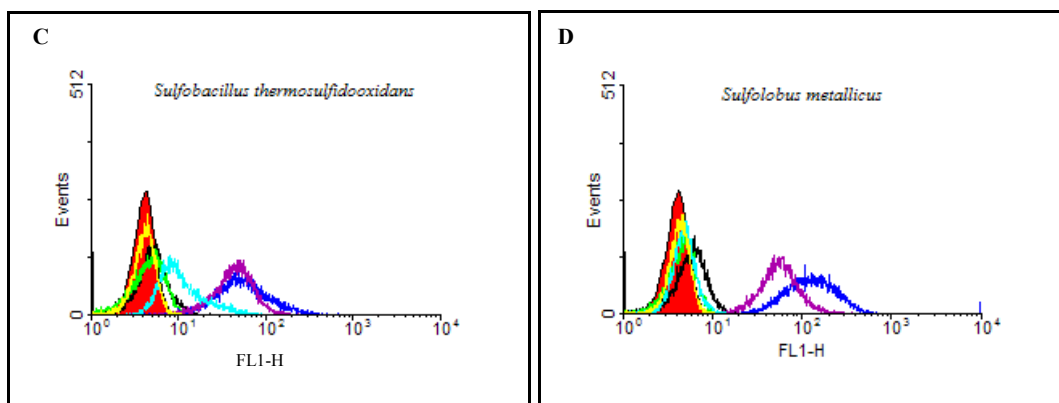
Unlabelled QuantumPlex™™ beads had an inherent red dye which could be observed in the FL3 channel of the flow cytometer (Figure VI.20, B). Cross-talk from the QuantumPlex™™ beads to the FL2 channel was not observed (Figure VI.20, A). The fluorescent signal of the PCR amplicons bound to QuantumPlex™™ beads labelled with R-PE was above background for all samples tested (Figure VI.20, C), indicating the successful binding procedure and hybridisation. The fluorescent intensity measured as the MFI values revealed an increment of the fluorescence while increasing the concentration of PCR amplicons bound to the beads (Table VI.13). Cross-talk of R-PE to the FL3 channel was not observed (Figure VI.20, D). The potential use of QuantumPlex™™ beads as a platform for the bead-based technique to detect DNA was confirmed as a result of successful binding without agglomeration issues.

3.2.6. Detection of bacterial and archaeal DNA with QuantumPlex™M beads

PCR amplicons from different bacterial and archaeal microorganisms were bound to QuantumPlex™M beads and labelled with different fluorophores. Capture and target probes varied between microorganisms (Table VI.5). The fluorophores used to label the PCR amplicons were FITC (1 mg/ml), Alexa Fluor 488 (1 mg/ml), R-PE (1 mg/ml), QD525 (1 µM) and QD585 (1 µM). All fluorophores were modified with streptavidin to allow binding to the biotinylated target probe.

PCR amplicons were obtained from *Deinococcus radiodurans*, *Sulfobacillus thermosulfidooxidans*, *Acidithiobacillus ferrooxidans*, *Sulfolobus metallicus* and *Ferroplasma acidiphilum*. PCR amplicons were bound to the QuantumPlex™M beads and labelled with the different fluorophores following the protocols described earlier (VI.2.6.3). Negative controls were set up to confirm the binding specificity of the probes and the fluorophores. The controls excluded PCR amplicons in the reaction. Data was analysed on histograms displaying FL1 (green) or FL2 (orange) fluorescence (Figures VI.21 and VI.22).



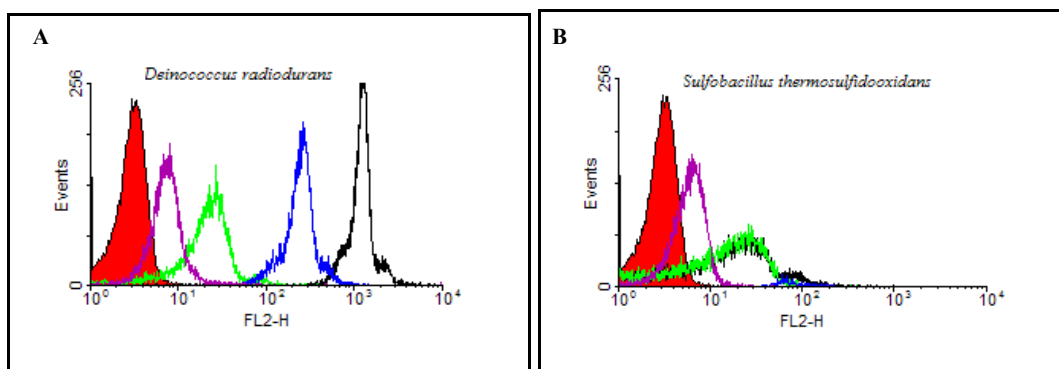


Legend, Figure VI.21:

- Red curve:** Blank
- Black line:** FITC
- Green line:** Negative control of FITC
- Blue line:** Alexa Fluor 488
- Purple line:** Negative control of Alexa Fluor 488
- Light blue line:** QD525
- Yellow line:** Negative control of QD525

Figure VI.21: Flow cytometric analysis. Histograms of PCR amplicons from different microorganisms labelled with 1 μ l of FITC, Fluor Alexa 488 and QD525 bound to QuantumPlex™. X-axis: fluorescent signal detected in the FL1 channel. Y-axis: number of counts per sample. A: *D. radiodurans*. B: *F. acidiphilum*. C: *S. thermosulfidooxidans*. D: *S. metallicus*.

The fluorescent signal of the negative control of Alexa Fluor 488 appeared above the blank for all the microorganisms tested, indicating non-specific binding of the fluorophores to the beads (Figure VI.21). Only *D. radiodurans* labelled with FITC, Alexa Fluor 488 and QD525 gave positive signals above background (Figure VI.21, A). The detection of PCR amplicons from the rest of the microorganisms remained negative when labelling with FITC and QD525. Alexa Fluor 488 gave positive signals above the negative control for all microorganisms tested except for *S. thermosulfidooxidans*.



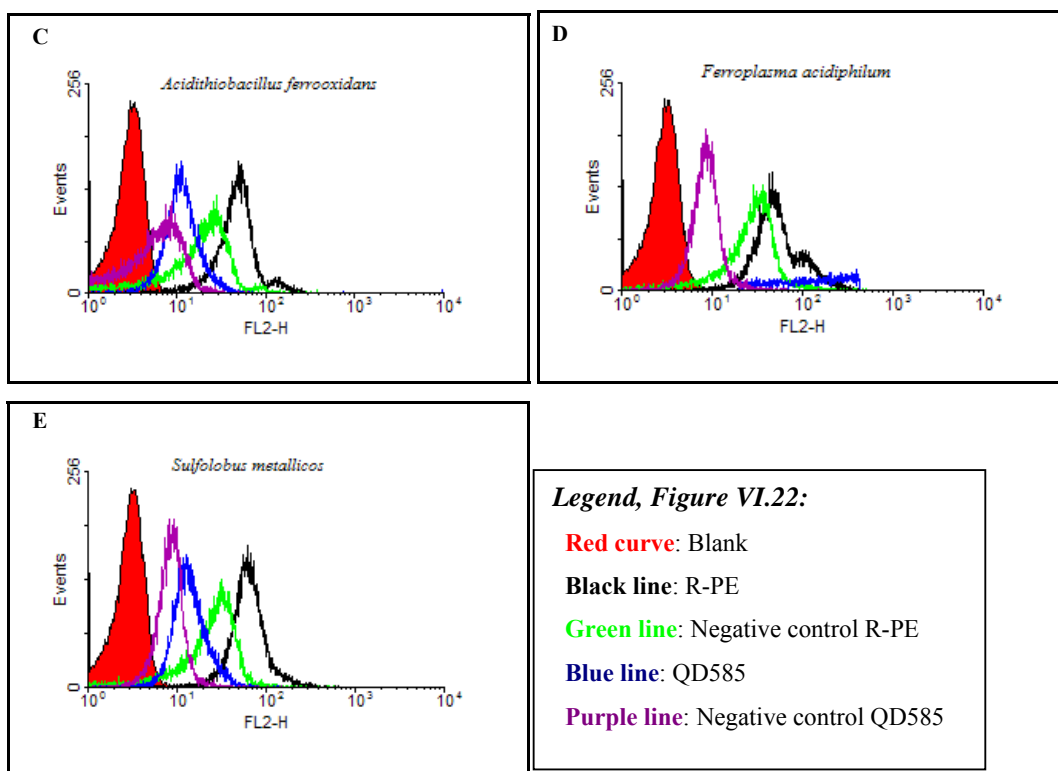


Figure VI.22: Flow cytometric analysis. Histograms of PCR amplicons from different microorganisms labelled with R-PE and QD585 bound to QuantumPlex™M beads. X-axis: fluorescent signal detected in the FL2 channel. Y-axis: Number of counts per sample. A: *D. radiodurans*. B: *S. thermosulfidooxidans*. C: *A. ferrooxidans*. D: *F. acidiphilum*. E: *S. metallicus*.

Fluorescent signal above the blank and the negative control was observed from the PCR amplicons of all microorganisms labelled with both R-PE and QD585 except for *S. thermosulfidooxidans*, where R-PE did not exhibit signal above the negative control (Figure VI.22). *Deinococcus radiodurans*, *Acidithiobacillus ferrooxidans* and *Sulfolobus metallicus* histograms had similar patterns. The reason for the lack of fluorescent signal from the PCR amplicon of *Sulfobacillus thermosulfidooxidans* could not be identified. PCR amplification of *S. thermosulfidooxidans* and hybridisation procedures were undertaken under the same experimental conditions as the other PCR amplicons.

Table VI.14: Fluorescent intensity measurements based on MFI values of each fluorophore labelling the PCR amplicons of the different microorganisms.
CV: coefficient of variation.

Microorganisms	FITC	Alexa Fluor 488	QD525	R-PE	QD585
<i>D. radiodurans</i>	16.47 (CV: 10.58)	545.59 (CV: 5.79)	27.20 (CV: 8.84)	1203.13 (CV: 3.73)	245.74 (CV: 6.40)
<i>Control of D. radiodurans</i>	6.74 (CV: 14.37)	56.69 (CV: 11.19)	6.73 (CV: 17.67)	22.60 (CV: 11.47)	8.08 (CV: 20.83)
<i>S. thermosulfidooxidans</i>	5.12 (CV: 21.31)	54.93 (CV: 15.39)	9.24 (CV: 17.82)	19.57 (CV: 20)	78.02 (CV: 7.16)
<i>Control of S. thermosulfidooxidans</i>	4.66 (CV: 25.52)	48.82 (CV: 13.33)	5.78 (CV: 11.96)	19.12 (CV: 19.66)	5.88 (CV: 20.88)
<i>A. ferrooxidans</i>	5.72 (CV: 19.27)	158.84 (CV: 9.20)	6.52 (CV: 18.57)	47.11 (CV: 8.51)	11.26 (CV: 14.39)
<i>Control of A. ferrooxidans</i>	4.49 (CV: 21.14)	53.72 (CV: 10.39)	4.15 (18.49)	22.07 (CV: 14.30)	7.51 (CV: 19.63)
<i>S. metallicus</i>	5.99 (CV: 17.95)	126.20 (CV: 10.92)	4.89 (CV: 16.89)	63.95 (CV: 7.18)	13.33 (CV: 11.65)
<i>Control of S. metallicus</i>	4.66 (CV: 18.94)	56.76 (CV: 9.57)	4.35 (CV: 15.43)	30.12 (CV: 10.22)	8.52 (CV: 12.57)
<i>F. acidiphilum</i>	5.95 (CV: 19.93)	502.32 (CV: 7.99)	6.63 (CV: 17.43)	46.61 (CV: 8.43)	712.78 (CV: 7.75)
<i>Control of F. acidiphilum</i>	5.15 (CV: 19.41)	78.96 (CV: 8.46)	4.48 (CV: 16.31)	31.56 (CV: 9.59)	13.43 (CV: 10.99)

The MFI values of every fluorophore labelling the PCR amplicon of *D. radiodurans* were significantly higher than their respective controls (Table VI.14). R-PE (MFI: 1203) exhibited significantly higher levels of fluorescence than QD585 (MFI: 245.74) under the same experimental conditions. In addition, Alexa Fluor 488 (MFI: 545.59) was found to have superior fluorescence than FITC and QD525 when labelling the PCR amplicon of *D. radiodurans*. Only QD585 (MFI: 712.78) exhibited higher fluorescence levels than R-PE (MFI: 46.61) when labelling the PCR amplicon of *F. acidiphilum*. All the microorganisms were able to be detected when using R-PE and QD585 as fluorophores, both being detectable in the FL2 channel of the flow cytometer, while only Fluor Alexa 488 detectable in the FL1 channel gave significant detection above the control.

4. DISCUSSION

4.1. Optimisation of the bead-based technique for DNA detection

A constant problem encountered during the experimental work of this part of this thesis was the agglomeration of the beads. Agglomeration occurred when QDs bound to the probes were attached to the Dynabeads (Figure VI.9). By comparison very little aggregation was observed when using organic fluorophores (Figure VI.8). As discussed in Chapter V, salt concentration, pH and cations influence the fluorescence and agglomeration of the QDs. In addition, under ideal conditions, the relation between the biotinylated molecules and the QDs functionalised with streptavidin groups should be 1:1. However, a single QD contains approximately 7 active streptavidin groups on its surface. Therefore, up to 7 biotinylated molecules could be attached to a single QD, which may result in agglomeration when forming the complexes between QDs and biotinylated molecules.

Several strategies were tested to avoid multiple binding of QDs to biotinylated molecules. Biocytin was used to reduce the number of active sites on the QDs (Appendix IV). Biocytin is a biotin complex from yeast that interacts with the streptavidin functional group of the QDs, inactivating them. In addition, it was calculated the appropriate concentration of biotinylated probes necessary to be bound to the QDs in order that only one biotinylated molecule would be bound to one QD (Appendix IV). However, agglomeration issues did not decrease with any method tested. It has been suggested that oligonucleotide-derivatised QDs form free carboxylic acid groups on the QD surface, allowing non-specific binding to target cells, making them far less useful than conventional organic fluorophore probes and contributing to agglomeration issues (Jamieson *et al.* 2007). There is no technique which consistently allows preparation of QDs with control over the ratio of biomolecules per QD and their orientation on the

surface, representing difficulties of reproducibility and aggregation of the QDs (Mattoussi *et al.* 2000).

The fluorescent emission of QDs was found to decrease when their concentration bound to beads increases (Figures VI.16 and VI.17). Agglomeration of the QDs and their close proximity potentially may lead to quenching and blinking effects (Speckman *et al.* 2002). The strength of quenching is affected by the interparticle distance, and with short interparticle distances additional non-radiative interactions affect the quenching of the QDs (Jamieson *et al.* 2007). The magnetic properties of the beads may also cause quenching of the QDs due to internal atomic forces caused by the magnetic field (Fortina *et al.* 2005).

It was established that functional groups of the QDs can dissociate from the surface of the surface after 6 months of storage, losing their binding capacity (Appendix IV). Several reports have described other problems associated with aged QDs such as quenching and blinking (Chung *et al.* 2007). The issues associated with aged QDs may reduce their potential for biological and commercial applications.

4.2. The bead-based QD technique for DNA detection

The aim of the bead-based technique was to target and detect specific sequences of DNA from environmental samples using QDs as a reporter fluorophore. *D. radiodurans* was used as a control microorganism to validate the procedures for the bead-based QD technique. Two different methods to detect genomic DNA of *D. radiodurans* were developed. However, in both cases the binding of gDNA to the Dynabeads resulted in significant agglomeration of the beads (Figure VI.12). The size of the gDNA may have played an important role in the binding procedure. Long segments of DNA may self-hybridise, lowering efficiency and preventing the hybridisation to the capture and target probes, resulting in agglomeration (Figure VI.11).

The hybridisation sites of the capture and target probes also may have influenced the binding of the gDNA to the Dynabeads. These sites were relatively close to each other. As a result, the single strand of gDNA bound to the Dynabeads may have been forced to make a loop around the bead in order to allow hybridisation with both probes (Figure

VI.11). This may have formed hairpins or artefacts on the gDNA, preventing the successful hybridisation to the molecular probes and increasing the agglomeration issues (Figure VI.12). Although the gDNA was enzymatically digested and cut it into smaller fragments in an attempt to avoid non-specific hybridisation of the DNA and agglomeration of the beads, the digested gDNA also was not detectable by the bead-based technique (VI.3.2.2). Several reasons may explain this lack of detection. First, single strands of gDNA could easily re-hybridise to each other during the procedure, preventing access by the probes. A second explanation could be the low concentration of target DNA fragments. The lack of these copies of gDNA could have been a potential limiting factor for their detection. As determined earlier, the detection limit of Dynabeads was 1 pmol of biotinylated probe modified with the fluorophores. Therefore, if the gDNA capture on the Dynabeads did not reach the minimum detection limit, a positive result would not have been detected by flow cytometry.

The bead-based assay was modified to detect amplified DNA. PCR amplicons of *D. radiodurans* using specific primers resulted in small sequences of 243 bp. The PCR amplicons were biotinylated at one end in order to facilitate the binding to the beads without the need of a capture probe. The target probe (modified with FITC, Alexa Fluor 488 or biotin) was used to label the single strand of the PCR bound to the Dynabeads (Figure VI.15). The three fluorophores successfully targeted the PCR amplicons detectable by flow cytometry (Figure VI.16). Therefore, the bead-based technique was able to detect amplified sequences of DNA.

QuantumPlex™ beads were used in an attempt to avoid potential artefacts and non-specific binding of the capture and target probes to the beads, as they were functionalised with carboxyl groups which can not interact with the biotin or streptavidin groups from the molecular probes and fluorophores.

After obtaining positive binding of PCR amplicons of *D. radiodurans* using QuantumPlex™ beads (Figure VI.20), the technique was used to detect several PCR amplicons from different extremophiles. These microorganisms were acidophilic sulphur- and iron-oxidisers bacterial and archaeal species normally found in sulphur-rich environments such as volcanically-active hydrothermal systems. These species were

selected for detection by the bead-based technique as they were closely related representatives from those found in the sediments of White Island (Chapter IV). Amplified DNA from several extremophiles was detected by the bead-based QDs technique using QuantumPlex™ beads. The PCR amplicons were labelled with FITC, Alexa Fluor 488, QD525, R-PE and QD585 using specific target probes for each microorganism. Negative controls showed a fluorescent signal above background, indicating non-specific binding of the fluorophores to the beads (Figures VI.21 and VI.22).

It has been reported that the surface of magnetic polystyrene particles are generally hydrophobic (Grüttner *et al.* 2001). Hydrophobic surfaces bind strongly to any molecule that has a hydrophobic character, including proteins and nucleic acids. The fluorophores were functionalised with streptavidin. Therefore, the fluorophores may have bound non-specifically to the QuantumPlex™ beads due to the hydrophobic character of the streptavidin groups. Despite the non-specific binding of the fluorophores to the surface of the beads, in most cases it was possible to distinguish the fluorescent emission of the samples from the negative control except for *Sulfobacillus thermosulfidooxidans* that did not show a positive signal with any of the fluorophores tested except Alexa Fluor 488 (Table VI.14). It may be speculated that the lack of fluorescent signal detection of *S. thermosulfidooxidans* was caused by the integrity of the PCR amplicon rather than the unsuccessful binding of the probes. As discussed in Chapter IV, PCR amplicons may be affected by different factors introducing artefacts or bias in the PCR amplicon during the amplification step due to primer mismatches, annealing temperature or number of amplification cycles (Reysenbach *et al.* 1992). Possible artefacts may have altered the recognition sites of the probes inhibiting the hybridisation.

QuantumPlex™ beads were a suitable platform for the bead-based technique, allowing the detection of amplified sequences of DNA from different microorganisms, while reducing the agglomeration issues. QDs were a suitable fluorophore for labelling the DNA sequences. However, the fluorescent signal of the QDs appeared to be inferior to the signal of organic dyes for this technique (Table VI.14). Several factors may have influenced the fluorescent signal of the QDs when using them as fluorophores for biological applications, as observed in preliminary experiments. In addition, differences in

fluorescence detection of the same fluorophores for the different microorganisms may be caused by the difference in the size of the PCR amplicons.

The bead-based technique was aimed to detect the key microbial species of White Island using QDs as fluorophores. Although the technique was able to detect amplified DNA sequences of several acidophiles, the technique was not tested with environmental DNA from White Island or DNA extracted from the enrichment cultures. The difficulties encountered during the development of the technique limited the full application and characterisation in this study. If time permitted, the bead-based technique would have been fully evaluated further in environmental samples.

4.3. Fluorescence detection of QDs versus organic dyes

The fluorescent intensity of the QDs has been described to be higher than conventional organic fluorophores (Zhang *et al.* 2007). However, the results obtained in this thesis indicated the opposite. MFI values of PCR amplicons labelled with FITC and QD525 at the same concentration and analysed under the same experimental conditions revealed that FITC was 2-fold brighter than QD525 (Figure VI.19).

Similar contradictory results have appeared in the literature recently. In 2005, it was reported that QD525 streptavidin conjugates were 100-times more sensitive than FITC-streptavidin for the detection of *E. coli* when analysed by flow cytometry (Hahn *et al.* 2005), while other reports indicated that the fluorescence intensity of QDs was up to 35-times less than that of organic fluorophores (Ferrari & Bergquist 2007). The lack of consistent results found in the literature could be attributed to the different methodologies used and the quality and integrity of the QDs. As discussed previously, parameters such as pH, temperature, salt and cations concentration, and some buffers have a crucial role in the quantum yield and photo-stability of the QDs. The quality of the QDs is also crucial to obtain a constant fluorescent emission and photo-stability. Although many improvements have been made in the synthesis of the QDs in the last few years, the optical behaviour is susceptible to batch-to-batch variations. Small defects in the core of the QDs may have major effects on the quantum yield and photo-stability.

Fluorescence quantification between different fluorophores is not an easy task (Wang *et al.* 2002). Most methods used to quantify the fluorescence from unknown samples are based on converting the MFI values obtained by flow cytometry into Molecules of Equivalent Soluble Fluorochrome (MESF) units (Schwartz *et al.* 2002). The MESF unit corresponds to the fluorescent intensity of a given number of pure fluorochrome molecules in solution. However, a quantitative method to compare the fluorescence intensity of FITC to QD525 could not be determined by (MESF) units. Despite the fact that both fluorophores were detectable in the same channel of the flow cytometer and have the same emission wavelength, they do not excite at the same wavelength and do not have the same quantum efficiency, resulting in significantly different fluorescence emissions.

The fluorescence signal (FS) associated with a sample that passes through a cytometer is given by: $FS = I_0 \Omega \varepsilon \phi N f$, where ' I_0 ' is the laser intensity, ' Ω ' is the detection efficiency, ' ε ' is the molecular extinction coefficient, ' ϕ ' is the quantum yield, ' N ' is the number of fluorophores on the cell, and ' f ' is the fraction of the total fluorescence emission spectrum passed by the optics which defines the fluorescence channel (Gaigalas *et al.* 2005). Therefore, a comparison of fluorescence intensity of samples labelled with FITC and QDs under the same laser intensity and detection efficiency in the same fluorescence channel could be determined by $\varepsilon_{QD} \phi_{QD} N_{QD} f_{QD} = \varepsilon_{FITC} \phi_{FITC} N_{FITC} f_{FITC}$. However, this equation could not be calculated for comparative purposes as many of the factors were unknown.

An alternative method to calculate the fluorescence intensity of the QDs from unknown samples would be by measuring the fluorescence of QDs in solution by fluorometry and generation of a standard curve. Then, the fluorescence of unknown samples could be plotted on the standard curve to obtain the number of molecules in solution or MESF units (Schwartz *et al.* 2004). However, a comparison of the MESF values obtained from the QDs and FITC would not be accurate due to their differences in optical properties.

4.4. QDs and FISH

The possibility of targeting microbial cells using QDs and FISH was investigated for its potential for identification by flow cytometry (Appendix I). The combination of FISH with flow cytometry represents a useful tool for identification and estimation of

abundance of different members of a mixed microbial community (Wallner *et al.* 1993). In addition, isolation of microorganisms from complex communities has been successfully carried out with FISH in combination with cell sorting (Kalyuzhnaya *et al.* 2006).

FISH is a known technique for culture-independent studies for the detection and identification of microorganisms either directly from their natural environment or from enrichment cultures (DeLong *et al.* 1989; Amann *et al.* 1990a; Amann *et al.* 1990b). As discussed in Chapter IV, the success and effectiveness of traditional FISH is influenced by several different factors (Zwirgmaier 2005). Cell detection can be limited due to a strong background from debris or autofluorescence, specifically in environmental samples where minerals have a strong non-specific binding to the fluorescent probes (Bertaux *et al.* 2007). Signal intensities also vary depending on the accessibility of rRNA for the probes, the low ribosomal content of the cells or insufficient permeabilisation of cell walls using standard fixation protocols (Amann *et al.* 1995).

Modified QDs with molecular probes were tested as a fluorescent label for FISH, to overcome some of the limitations of the technique when using conventional fluorophores (Appendix I). It was postulated that the QDs would increase the fluorescent signal allowing detection above the debris and auto-fluorescent background. However, several problems were encountered when using QDs as fluorophore probes for FISH. First, the QDs showed non-specific binding to the surface of the microscope slide. The slides were prepared with 0.1% PEI (Polyethylemine). It has been reported that PEI forms chelation complexes with heavy metal compounds and has an affinity to a wide range of substrates including polymers (Wang & Gao 1999). Commercially-available QDs are coated with an organic polymer. Therefore, the non-specific binding could be due to the interaction of PEI with the QDs. A non-conventional technique using Eppendorf tubes instead of microscope slides was developed in an attempt to avoid non-specific binding. In this case, QDs were observed to be attached to the membranes of the microorganisms instead of hybridising to the RNA from the organisms.

It has been reported that QDs can be used useful for labelling and imaging cytoplasmatic proteins. These techniques deliver QDs into the cells by invasive approaches such as microinjection (Dubertret *et al.* 2002), cationic lipid-based reagents (Jaiswal & Simon

2004), or conjugation to membrane-permeable peptides (Mattheakis *et al.* 2004). However, the size and chemical nature of the QDs inhibit the diffusion through the membrane of microorganisms as compared to conventional dyes such as FITC. The final size of the functionalised QD modified with molecular probes can reach up to 100 nm, making it too big to reach targets within cellular compartments or multi-component molecular complexes (Alivisatos *et al.* 2005; Fortina *et al.* 2005). QDs can be conjugated to several biomolecules which hinder both the mobility of the QDs and the functionality of the conjugated target unless the active sites of the QDs are reduced. Non-invasive approaches for the efficient intracellular delivery and dispersal of QDs remain to be investigated.

In addition, several concerns about the toxicity of QDs for biological applications have been reported recently (Dubertret *et al.* 2002; Medintz *et al.* 2005). Cytotoxicity of QDs has been observed in a large number of *in vitro* studies, affecting cell growth and viability (Chen & Gerion 2004; Kirchner *et al.* 2005; Lovric *et al.* 2005). Although the reasons are still unknown for their possible toxicity, it has been postulated that the core of the QDs can be degraded, including desorption of free Cd ions (Derfus *et al.* 2004) and the generation of free radicals (Clarke *et al.* 2006).

4.5. Summary

PCR amplicons were successfully detected by the bead-based QD technique when using paramagnetic beads as a platform and a blue light excitation source. However, the semiconductor properties of QDs potentially lead to difficulties in their application as fluorophores due to agglomeration and quenching issues described here.

Despite the low fluorescent signal of QDs compared to organic dyes used for the bead-based technique in this study, it is anticipated that the use of a UV laser instead of a blue laser would magnify this signal significantly, making QDs a powerful and superior fluorophore. As determined earlier, the fluorescent intensity of the QDs could be up to four times higher when using UV light than blue light. Therefore, it is suggested that the bead-based QD technique could be useful for the study of environmental samples where the microorganism or DNA of interest may be fluorescing too low to be detected by blue lasers.

The biological applications of the QDs may be reduced due to their large size relative to current fluorophores that prevents the access and labelling at a molecular level in microbial cells. However, the results found in this thesis have shown that QDs have the potential to be used in flow cytometric techniques leading to future new applications.

Chapter VII. Concluding remarks

CONCLUDING REMARKS

The general aim of this thesis was to study the microbial diversity from the hydrothermal systems of White Island using conventional techniques such as molecular-based analyses and culture-dependent techniques, as well as novel techniques based on QDs.

The results presented in this thesis provide the first description of the microbial communities from sediments of White Island. A survey of the microbial diversity was conducted using culture-dependent techniques based on a sediment-extract medium followed by molecular-based and phylogenetic analyses to describe the enriched microorganisms grown, revealing that the environments analysed harbour a variety of acidophilic bacterial and archaeal species (Chapter IV.3).

The development of a medium based upon the use of sediment-extract provided the essential nutrients and trace elements required for successful microbial growth. This extract mimicked the natural conditions of White Island sediments, and resulted in the enrichments of Archaea previously undetected in the hydrothermal systems of White Island, as well as a variety of acidophilic and thermophilic bacterial species. Considering the low pH, high temperatures and high contents of sulphur and iron present in White Island, it was not surprising to identify sulphur-oxidising and sulphur-reducing organisms such as *Sulfobacillus*, *Acyclobacillus* and *Acidiphilum* species from the sediments. Moreover, *Alicyclobacillus sp.* and *Sulfobacillus sp.* have been previously found growing in consortia. This result was not unexpected as these species are known to interact together in acidic geothermal habitats and artificial acidic environments (Okibe & Johnson 2004). *A. acidocaldarius* and *S. acidophilus* were isolated into pure cultures using a new agarose-based solid medium supplemented with sediment-extract (Chapter IV.3.4).

High concentrations of minerals and particles present in the sediment-extract combined with the low pH represented significant difficulties for the various analyses, such as DNA extraction and especially for the fluorescence detection of enriched microorganisms. High

levels of non-specific background fluorescence, caused by mineral structures and detrital particles present in the sediment-extract observed during microscopic visualisation of cells, caused inconclusive cell counts (Chapter IV.3.5). However, while the presence of detritus hampered detection, the presence of sediment particles may have conferred a substantial advantage for the cultivation of environmental microorganisms over conventional media as it provided not only the essential nutrients for their growth, but also the physical support for their associated microbial interactions.

Thermophilic acidophiles are associated with geothermal activities in volcanic regions and mining activities (Johnson 1998; Norris *et al.* 2000). Currently, there are over 200 species of thermophiles and acidophiles recognised from many habitats (Stetter 1999a; Stetter 1999b; Gonzalez-Toril *et al.* 2003; Chaban *et al.* 2006; Hallberg *et al.* 2006). However, the microbial diversity of hydrothermal systems and bioleaching environments with conditions comparable to White Island have been reported to be low (Burton & Norris 2000; Dopson & Lindstrom 2004; Henneberger 2008). The high temperatures, low levels of organic carbon and the high acidity decreases the number of species capable of growth in such extreme habitats (Bond *et al.* 2000b). The research undertaken during this thesis has increased the number of known acidophiles by enriching and culturing novel acidophilic and thermophilic strains (Chapter IV. 3.3).

In future studies, additional novel strains and species may be isolated from the samples or enrichment cultures already obtained. Techniques such as dilution to extinction, or novel approaches like the use of membranes or chambers to isolate microorganisms from their community (Janssen *et al.* 2002; Kaeberlein *et al.* 2002), would improve the number of isolates from White Island.

Phylogenetic placement by 16S rDNA gene sequences obtained from the enriched cultures suggested that the resident microorganisms of White Island are involved in the cycling of sulphur and iron, as they were closely related to previously described sulphur-oxidising microorganisms such as *Acidiphilum* and *Sulfobacillus* species (Chapter IV.4.2). However, closely related species can vary in their substrate usage and most metabolic pathways are not restricted to single branches of the 16S rRNA phylogenetic trees (Wagner *et al.* 1998). Consequently, further studies are required to prove the existence of

such cycles, such as the analyses of metabolic genes involved in sulphur- and iron-metabolism from the enriched microorganisms (Friedrich *et al.* 2001).

The microbial diversity of White Island was also aimed to be analysed using a novel technique based on QDs. The bead-based QD technique for DNA detection was developed as a tool able to detect the key microbial species from specific habitats. The technique involved flow cytometry detection of analyte DNAs hybridised to capture probes on the surface of paramagnetic beads. QDs were used as a reporter fluorophore that hybridised the captured DNAs.

Organic molecules and fluorophores traditionally have been used as fluorescent labels for *in vitro* and *in vivo* biological applications, despite their non-optimal optical properties and photochemical instability (Ballou 2005). However, the use of QDs for bioanalytical applications has great potential for spectral multiplexing assays and bead-based techniques in flow cytometry.

Spectral multiplexing or multicolour detection typically is performed at a single excitation wavelength and discriminates between different fluorescent labels based on their emission wavelength (Chan *et al.* 2002). Organic fluorophores have broad emission bands that limit their applications for multicolour signalling at single excitation wavelengths (Spiro *et al.* 2002; Morgan *et al.* 2004). New methods for multiplexing assays make use of FRET to increase the spectral separation of absorption and emission from the donor to the acceptor dye (Sapford *et al.* 2006). FRET-based multiplexing strategies enable automated DNA sequencing and robust multiplex diagnostic methods for detection of PCR products (Sapford *et al.* 2006). Organic dyes have many limitations for FRET applications due to their optical properties. However, QDs would be ideal candidates for spectral multiplexing at a single excitation wavelength because of their unique flexibility in excitation and their narrow and symmetric emission bands which allow colour discrimination and simultaneous detection and quantification of several different analytes (Jaiswal *et al.* 2003; Menditz *et al.* 2005).

There is a need to develop more rapid, sensitive and accurate methods for detecting specific DNA sequences in environmental samples (Spiro *et al.* 2000). A variety of

molecular methods have been used for microbial profiling such as oligonucleotide microarrays (Liu & Zhu 2005). However, bead-based methods for multiplex identification and quantification of DNA sequences using flow cytometry have resulted in superior performance compared to oligonucleotide microarrays (Spiro & Lowe 2002). Bead methods normally are based on microscopic polystyrene spheres coded with varying amounts of fluorophores to create different barcodes. The beads then are modified with a capture probe that allows hybridisation of fluorescent DNA sequences from the sample and then analysed by flow cytometry (Cai *et al.* 2000; Spiro *et al.* 2000; Taylor *et al.* 2001). Although these techniques have opened the door to new applications in multiplex technology and the improvement of rapid detection and quantification of specific DNAs, their detection threshold is a critical issue. The DNA extracted from microbial communities in environmental samples can be too low to be detected with these techniques. It has been suggested that the detection limit in bead-based techniques can be improved by increasing the efficiency of probe-target hybridisation (Chandler *et al.* 2000) and/or by increasing the signal-to-noise ratio for fluorescence detection (Lowe *et al.* 2004). Several studies have focussed on improving the sensitivity of fluorescence measurements by increasing the signal-to-noise ratio for the labelling of captured DNA on the surface of fluorescent beads, for example by labelling the DNA molecule with high amounts of fluorophores (Wang *et al.* 1998; Lowe *et al.* 2004). Although the use of these techniques is promising, they are complicated to execute and still require a PCR step to allow detection of low concentration of DNA in the unknown samples (Lowe *et al.* 2004).

It has been postulated that the use of QDs instead of dendrimers or other fluorophores to label the DNA molecules from environmental samples would overcome the signal-to-noise issue and improve the detection. Microsphere embedded with QDs have been used in previous studies as a platform for multiplexed assays such as those for single nucleotide polymorphisms (SNP) genotyping (Xu *et al.* 2003; Cao *et al.* 2006; Wang *et al.* 2006). Encoded microspheres with different ratios of QDs were hybridised to fluorescently-labelled PCR amplicons for flow cytometric detection. Despite the successful detection of SNP genotypes using encoded microspheres with QDs, several issues still remained such as spectral overlapping, fluorescence intensity variations, and control ratio of QDs incorporated into the beads (Xu *et al.* 2003).

The general technique developed in this thesis was designed to target specific sequences of environmental DNA for detection by flow cytometry. Following the extraction of gDNA from the environmental microbial communities, pre-designed oligonucleotide probes that matched the desired segments of DNA were applied to capture the DNA on paramagnetic beads. To avoid overlapping issues in encoded microspheres and increase the signal-to-noise detection of the captured DNA, QDs were used as a target fluorophore.

The results obtained in this thesis reported many optical anomalies occurring with the QDs such as quenching and possible blinking that lowered the fluorescent signal compared to organic dyes such as FITC (Figure VI.19). The spectroscopic and optical properties of QDs are dependent on their size distribution, shape, and surface defects, and subtle differences in their preparation can lead to basic spectroscopic and property variations (Danek *et al.* 1996; Norris & Bawendi 1996a; Dabbousi *et al.* 1997; Kuno *et al.* 1997). Commercial QDs are not spectroscopically standardised and their characterisation has not yet been completed and their properties can be influenced by details of their synthetic history (Tonti *et al.* 2004; Wu *et al.* 2007b). Moreover, the results obtained in this thesis revealed that quantum yield of the QDs is highly dependant on the excitation source, with a 4-fold decrease in fluorescent intensity at short excitation wavelengths such as blue light (Figures V.5 and V.6). Other parameters such as pH, temperature and ionic buffers were also found to compromise the photo-stability of the QDs (Chapter V.4.1). The dependence of the quantum yield of the QDs to these factors was found to reduce the fluorescence emission by 2-fold compared to organic dyes (Figure VI.19).

Numerous biological applications of the QDs have been reported in the literature due to multiplexed imaging, photo-stability and superior optical properties of the QDs compared with currently-used imaging molecules (Jamieson *et al.* 2007). However, many of those applications have not yet been solved as the QD behaviour has yet to be fully standardised. As discussed, many significant problems remain in their production that still need to be addressed in order to make a considered judgment on the applications into which they can be incorporated, such as cell imaging, drug delivery and microbial detection (Chen 2008).

The bead-based technique was initially developed to detect gDNA of *D. radiodurans*. Despite every attempt, high agglomeration of the beads, probably due to the long length of the DNA, led to the lack of detection of the gDNA by flow cytometry (Chapter VI.3.2.1). Therefore, amplification of small DNA segments was also necessary in this technique to avoid such issues. PCR amplicons of *D. radiodurans* were successfully detected by the bead-based technique (Chapter VI.3.2.3). However, detection of multiple PCR amplicons from different extremophiles was found to be a more difficult task (Chapter VI. 3.2.6). Selection of specific target and capture probes was crucial to target the desired amplified sequence from the different microorganisms. In addition, size and number of copies of the PCR amplicons may also have influenced the detection rate.

Despite the difficulties encountered when working with QDs, this thesis describes a bead-based flow cytometric method for QDs that it is highly sensitive despite being excited by lasers that do not allow QDs to perform to their highest capacity. It is anticipated that the use of this technique when using UV light excitation sources, instead of blue excitation, would increase the signal of the QDs up to four times. This increase in emission would improve the detection limit of the QDs, becoming more powerful fluorophores than conventional organic dyes. The development of this technique would have then important implications for the study of environmental samples where microorganisms of interest need to be detected from the background debris.

QDs were also examined as a fluorophore probe for fluorescent *in situ* hybridisation assays (Appendix I). Many reports have shown an important role for QDs for cell imaging and detection such as imaging of cytoplasmic proteins (Chan *et al.* 2005). However, the use of QDs as a fluorophore for FISH to detect microbial cells was not successful in this thesis (Appendix I). Despite permeabilisation, the pore size of the microbial cell wall did not allow the diffusion of the QDs as they do in mammalian tissues (Alivisatos *et al.* 2005; Michalet *et al.* 2005). The large size of QDs relative to current fluorophores reduces their ability to access and label cellular molecules (Pinaud *et al.* 2006). Therefore, non-invasive approaches for the efficient intracellular delivery of QDs into microbial cells remain to be investigated. Alternatively, QDs modified with antibodies could be used to target specific receptors on the cell wall of the microorganism to label them, instead of labelling intracellular structures or molecules, avoiding the use of invasive approaches.

In summary, this work represents the first description of the microbial diversity of the hydrothermal sediments of White Island, improving the knowledge base of microbial life in acidic environments. The development of a novel technique based on QDs to investigate the microbial diversity in extreme environments such as White Island was initiated. Although the technique could successfully detect specific sequences of DNA, its application in environmental samples still remains. Several optical and physical characteristics of the QDs still require to be standardised for further developments of the technique. However, the outcomes of this thesis set the basis for a bead-based technique for DNA detection using QDs that potentially has significant advantages over other traditional techniques such as high detection speed, sensitivity and specificity to screen environmental microbial diversity.

Appendices

APPENDIX I: QDs as a fluorophore probe for FISH

Fluorescence *in situ* hybridisation was used to target fixed *E. coli* cells using probes modified with QDs. Biotinylated probes, EUB388 and EUK502 (II.2.6.4.1), were modified with QD680 and used as hybridisation probes.

Conventional FISH analyses were performed using microscope slides, while a non-conventional technique was used to replace the microscopy slides with Eppendorf tubes.

1. Conventional FISH technique

Microscope slides were prepared as described previously (II.2.6.4.2) and coated with 0.1% PEI (Polyethylemine) to allow fixation of the sample onto the slide. The hybridisation probes utilised were EUB388 labelled with FITC as a control and EUB388 labelled with red quantum dots (QD680). Hybridisation procedures and conditions were described in II.2.6.4.

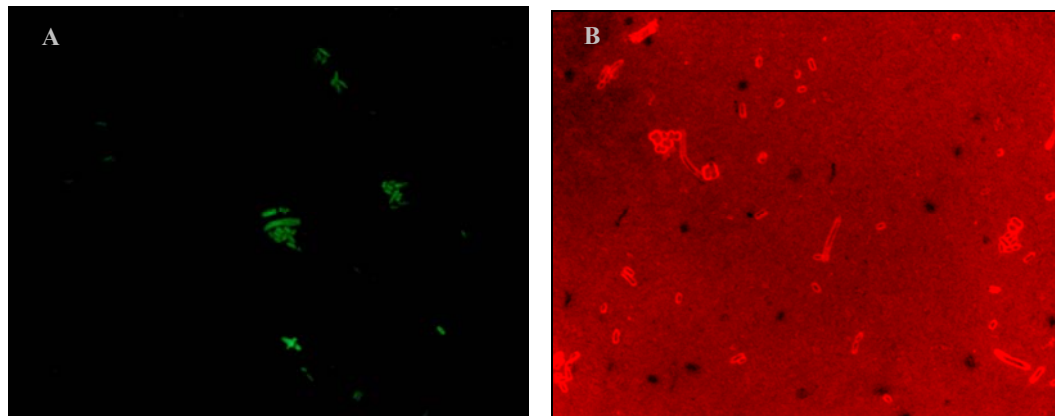


Figure 1.1: Fluorescent *in situ* hybridisation on *E. coli* cells examined under UV light excitation by epi-fluorescence microscopy. A: *E. coli* labelled with EUB388-FITC. B: *E. coli* labelled with EUB388-QD680.

EUB388-FITC was used as a positive control to verify the efficiency of the hybridisation. In each case, the positive control resulted in bright green fluorescent signal from the cells (Figure 1.1, A). However, EUB388 labelled with QD680 did not hybridise to *E. coli* cells (Figure 1.1., B). Non-specific binding of QDs was observed to occur on the microscopy

slide surface and around the outside of the cells as indicated by the red fluorescence observed on the slide.

2. Non-conventional FISH technique

To avoid the non-specific binding by the QDs onto the surface of the microscope slides, FISH procedures were modified. Microfuge tubes were used instead of microscopy slides during the hybridisation and washing steps (II.2.6.4.6). Three oligonucleotide probes were used: EUB338 modified with FITC, EUB338 modified with QD680 and EUK502 modified with QD680.

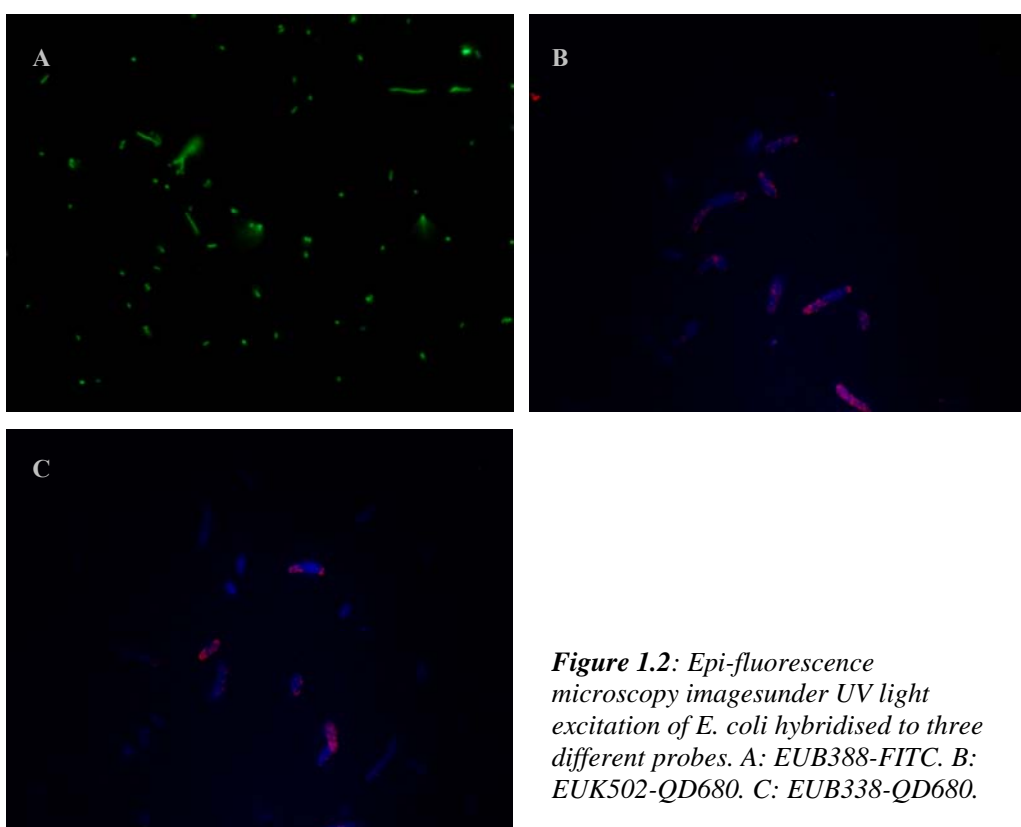


Figure 1.2: Epi-fluorescence microscopy images under UV light excitation of *E. coli* hybridised to three different probes. A: EUB338-FITC. B: EUK502-QD680. C: EUB338-QD680.

EUB338-FITC was used as a positive control. The control verified positive hybridisation by the EUB338-FITC as observed by the green stain of the bacteria (Figure 1.2, A). Although QDs did not bind to the microscopy slide as observed previously (Figure 1.1, B), non-specific binding to the cell wall of the bacteria was observed. QD680 have red fluorescence emission which was observed forming clusters on the cell wall of the microorganisms (Figure 1.2, B and C). The bacterial cells appeared in blue due to natural

autofluorescence of the microorganisms under UV light excitation. It was concluded that the QDs-modified FISH probes did not penetrate the permeabilised membrane of the bacteria.

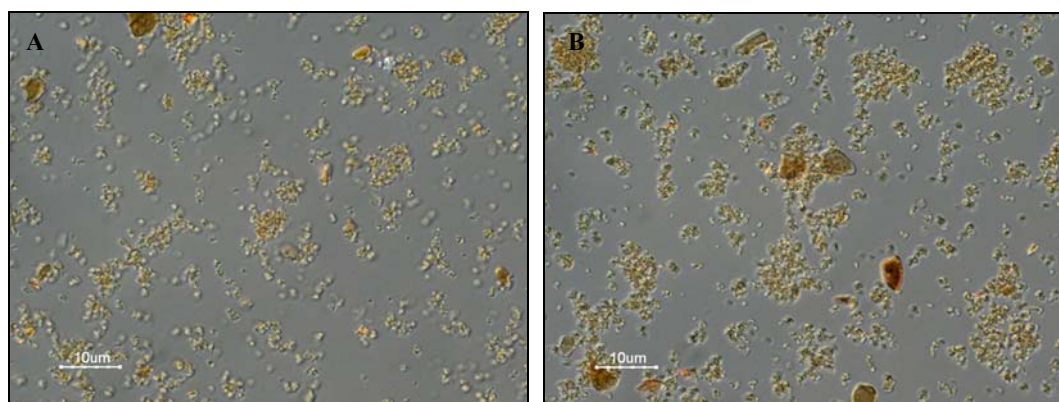
A discussion of QDs as a fluorophore for FISH can be found in Chapter VI. 4.4.

APPENDIX II: BioMag beads

BioMag streptavidin super-paramagnetic particles of 1.6 microns in size functionalised with streptavidin (Polysciences Inc., Australia) were tested as a platform for binding QD-probe complexes.

BioMag beads were provided in a stock solution of 50 mg/ml. They were resuspended by gently shaking the vial to obtain a homogeneous suspension. A portion (5 μ l) of BioMag beads was transferred to a fresh 1.5 ml Eppendorf tube. The beads were washed as described previously (V.2.4.2). 100 μ l of Hops-Yellow QDs (4 nmol/ml) were bound to 25 μ l (0.1 mM) of QDLinker probe (a poly A oligonucleotide probe modified with biotin at the 3' end and a thiol group at the 5' end) as described previously (V.2.4.1). A portion (10 μ l) of QD-oligo complexes was mixed with BioMag beads. The sample was then incubated at RT for 10 min with occasional gentle mixing. The solution was washed to remove unbound QDs-oligo complexes using the Dynal MPC™ magnet and 1 x WB buffer (V 2.2). Washed BioMag beads labelled with QDs-oligo complexes finally were resuspended in 10xPBS and stored at 4°C in darkness.

The success of the binding was confirmed by epi-fluorescence microscopy (II.2.4.2.2) and by flow cytometer (II.2.5.2).



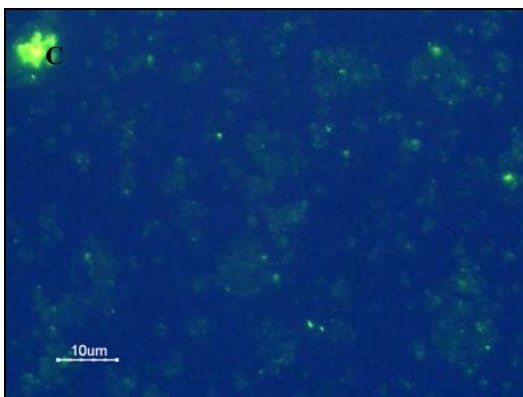


Figure 2.1: Epi-fluorescence microscopy images of unlabeled BioMag beads and QDs-oligo complexes bound to beads A: DIC image of unlabelled BioMag beads. B: DIC image of BioMag beads bound to QDs-oligo complexes. C: BioMag beads bound to QDs-oligo complexes under UV excitation.

The shape, size and auto-fluorescence of unlabelled BioMag beads were confirmed by epi-fluorescence microscopy (Figure 2.1, A). Unlabelled BioMag beads naturally agglomerated, forming small clusters even after vigorous shaking (Figure 2.1., B). BioMag beads were characterised for not showing autofluorescence background under UV excitation. BioMag beads after binding to the QDs-oligo complexes appeared to form larger clusters (Figures 2.1, B and C).

The incubation time during the binding step could have influenced the binding and the observed agglomeration of the QD-bead complexes. Several modifications to the protocol were performed on the binding of QD-oligo complexes to BioMag beads in an attempt to avoid agglomeration issues. BW buffer (V.2.2) was substituted with BioMag buffer (V.2.2) and the final binding product was resuspended in DEPC-treated water instead of 10xPBS. The incubation time was varied between 15 min to 30 min. The samples were then analysed by epi-fluorescence microscopy and flow cytometry. Agglomeration of the beads was observed under all the binding conditions tested, indicating that the agglomeration was not caused by either the buffers or incubation time (data not shown). The most probable explanation appeared to be the physical shape and size of the beads. BioMag beads have an irregular shape which may have facilitated agglomeration which increased after binding to the QDs.

APPENDIX III: Hops-Yellow QDs

Hops-Yellow QDs were bound to Dynabeads using an intermediate linker (QDLinker) following the procedures previously described (V.2.4.1 and V.2.4.3). QDLinker was conjugated to the Hops-Yellow by the amine group while binding the Dynabeads by the biotin-streptavidin interaction. The final binding product was checked by epi-fluorescence microscopy (II.2.4.2.2) and flow cytometry (II.2.5.2)

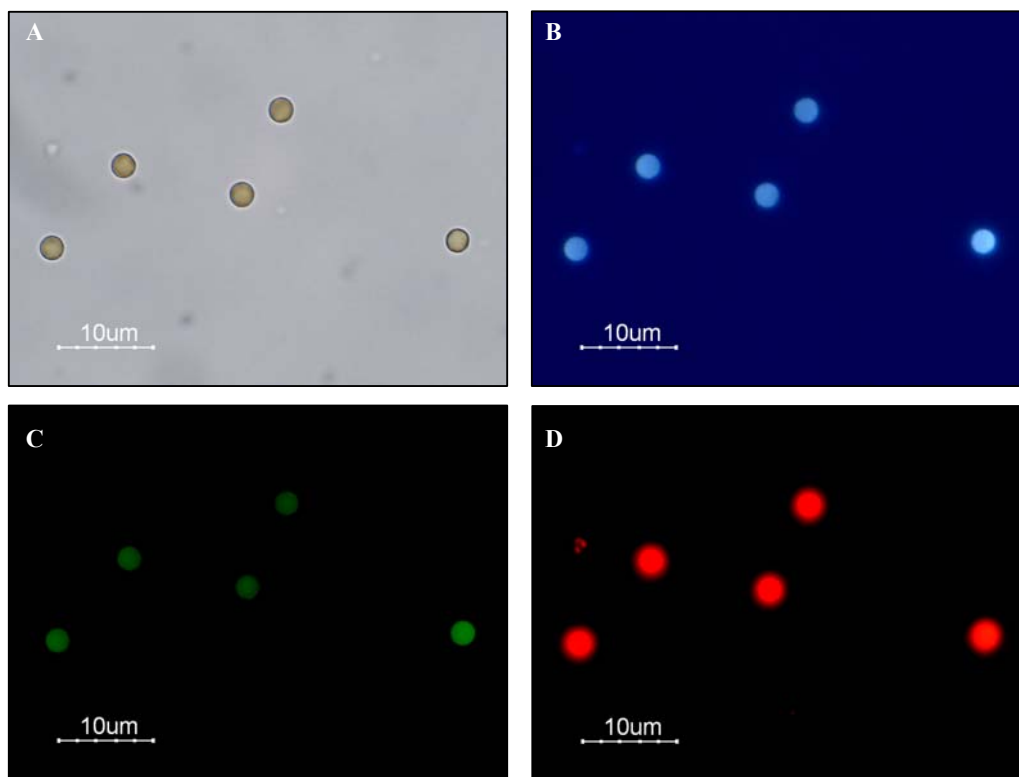


Figure 3.1: Background autofluorescence of unlabeled Dynabeads under epi-fluorescence microscopy. A: DIC. B: UV excitation. C: Blue excitation. D: Green excitation.

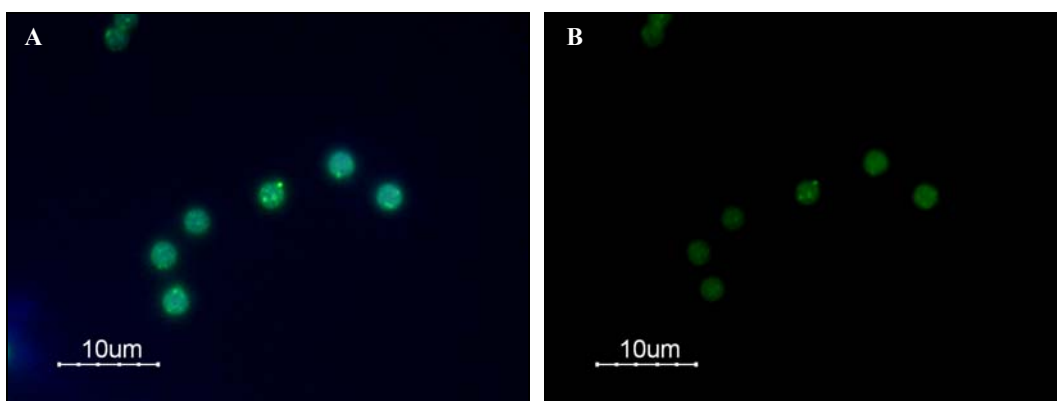


Figure 3.2: *Dynabeads bound to Hops-Yellow QDs visualised by epi-fluorescence microscopy. A: UV excitation. B: Blue excitation.*

Unlabelled Dynabeads showed autofluorescence background under all the excitation sources examined (Figure 3.1). Hops-Yellow QDs exhibited green emission. The autofluorescence of the Dynabeads (Figure 3.1) did not appear to influence the fluorescent signal of the Hops-Yellow QDs after binding (Figure 3.2). A shift in colour of the Dynabeads from blue to green after binding to Hops-Yellow QDs could be observed under the UV excitation (Figure 3.2). However, Hops-Yellow QDs were found to form clusters on the surface of the Dynabeads.

The following buffers were tested during the incubation step for binding of Dynabeads to Hops-Yellow QDs-oligo complexes: BW buffer, BioMag buffer, SDS buffer and a new buffer containing 10 mM Tris/HCl and 1 mM EDTA (V.2.2). Several incubation times were tested from 30 min to 12 h. Despite every attempt to avoid agglomeration of the QDs on the surface of the Dynabeads, the agglomeration did not decrease (data not shown).

APPENDIX IV: Methods for detection of PCR amplicons bound to the Dynabeads

Different methods were tested for the detection of biotinylated PCR amplicons (VI.2.3) of *D. radiodurans* bound to Dynabeads.

1. Methods

1.1. Direct method for labelling PCR amplicons

For all reactions, 5 μ l of pre-washed Dynabeads were resuspended in 5 μ l of BioMag buffer. Then, 8 different amounts of the biotinylated PCR product from 0.21 to 14.7 pmol were added to the reactions and incubated at RT for 30 min with rotation. After binding, Dynabeads were washed 3 times using 100 μ l of BW buffer (V.2.2.) and resuspended in 200 μ l of BW buffer. PCR amplicons bound to the Dynabeads were denatured by heat at 95°C for 10 min in the water bath. 1 μ l of the BactoUni2 target probe (100 μ M) was added to the samples, followed by further incubation at 50°C for 10 min in the dark. After hybridisation, the beads were washed 3 times using 100 μ l of BW buffer and were finally resuspended in 200 μ l of BioMag buffer until further analysis.

1.2. Indirect method for labelling PCR amplicons

A portion (30 μ l) of PCR amplicon (120 ng/ μ l) was mixed with 2 μ l (100 μ M) of target probes. Three different target probes were used per binding reaction: Bactouniversal2, BactouniAlexa and QDUniBiotinF. The solutions were heated to 95°C for 10 min using the thermo-cycler to denature the PCR product, followed by 50°C for 5 min for hybridisation of the capture DNA strand to the target probe. After hybridisation, the reactions were placed on ice to stop further hybridisation. Pre-washed Dynabeads (5 μ l per reaction) were added to the PCR reactions and incubated at 30 min at RT with rotation to allow binding of biotinylated strands of the PCR amplicon. After the binding step,

Dynabeads were washed 3 times using 100 μ l of BW buffer and resuspended in 200 μ l of BW buffer and kept at 4°C until further analysis.

1.3. Detection of PCR amplicons with QD525

A portion (5 μ l) of Qdots™ 525 (2 μ M) was mixed with 1 μ l of QDUniBiotinF probe (100 μ M). The final volume of the reaction was made up to 200 μ l using TE buffer pH 8. After incubation at RT for 1 h in the dark with gentle rotation, excess probe was washed away using Microcon filter devices YM-100 following the user's manual. The waste fraction was kept for further analysis. QD535 labelled probes were resuspended in a final volume of 100 μ l TE buffer pH 8. 30 μ l of PCR amplicon (120 ng/ μ l) was denatured by heat at 95°C for 10 min. The denatured PCR product was then placed at 50°C for 2 min. QDs-oligo complexes were added to the reaction for hybridisation to the PCR amplicon at 50°C for 10 min. Then, the PCR amplicons were bound to Dynabeads as described in the direct method (Appendix IV 1.1)

1.4. Blocking the active sites of the QDs with biocytin

Biocytin is a water-soluble biotin that can be used to reduce the number of functional sites of the QDs by binding to streptavidin. A single QD contained approximately 7 streptavidin groups on its surface. The number of active sites of a solution of QDs was calculated using Avogadro's number. The concentration of the QDs was 2 μ M, which is equal to 2 pmol/ μ l. 2 pmol of the solution of the QDs contained 1.2045×10^{12} QDs. Each QD had 7 active sites. Therefore, 2 pmol of QDs in solution had 8.43×10^{12} active sites. The concentration of the biocytin was 4 μ M (4 pmol/ μ l). Therefore, in theory, 14 pmol (3.5 μ l) of biocytin would block all the active sites of 1 μ M (1 μ l) of QD525 streptavidin conjugates. Different concentrations of biocytin were used to block QD525 prior to binding to the oligonucleotides. They were: 2 pmol (0.5 μ l), 6 pmol (1.5 μ l), 10 pmol (2.5 μ l) and 14 pmol (3.5 μ l). 1 μ l of QD525 (2 μ M) was mixed with the different biocytin concentrations in 50 mM of QD incubation buffer. After incubation at 30°C for 20 min in the dark, the reactions were washed using Microcon filter devices YM-100. The final volume was made up to 400 μ l using BW buffer. 2 μ l of QDUniBiotinF probe (1 μ M) was

then added to the samples. After incubation at 30°C for 10 min in the dark, the QDs-oligo complexes were stored in the dark at 4°C until hybridisation to the PCR amplicons.

2. Results

2.1. Direct method for labelling PCR amplicons

The direct method for labelling PCR amplicons was based on binding biotinylated PCR amplicons directly to the Dynabeads followed by heat denaturation to separate the two strands of PCR. The target probe (BactoUni2) was added for hybridisation to the biotinylated PCR strands bound to Dynabeads.

The reactions were analysed by flow cytometry (data not shown). None of the samples tested showed fluorescent signal above the blank, indicating that the hybridisation procedures were not successful using the direct method.

2.2. Indirect method for labelling PCR amplicons

The indirect method for labelling PCR amplicons was based on denaturing the PCR amplicons followed by hybridisation to the target probe prior to capture by binding to the Dynabeads. Three different target probes were used for labelling the biotinylated strand: Bactouniversal2 (modified with FITC), BactouniAlexa (modified with Alexa Fluor 488) and QDUniBiotinF (modified with biotin). The target probe QDUniBiotinF was used as a linker to label the PCR amplicons with QD525. The reactions were analysed on a dot-plot of FL1 (green fluorescence) versus SSC (Figure 4.1).

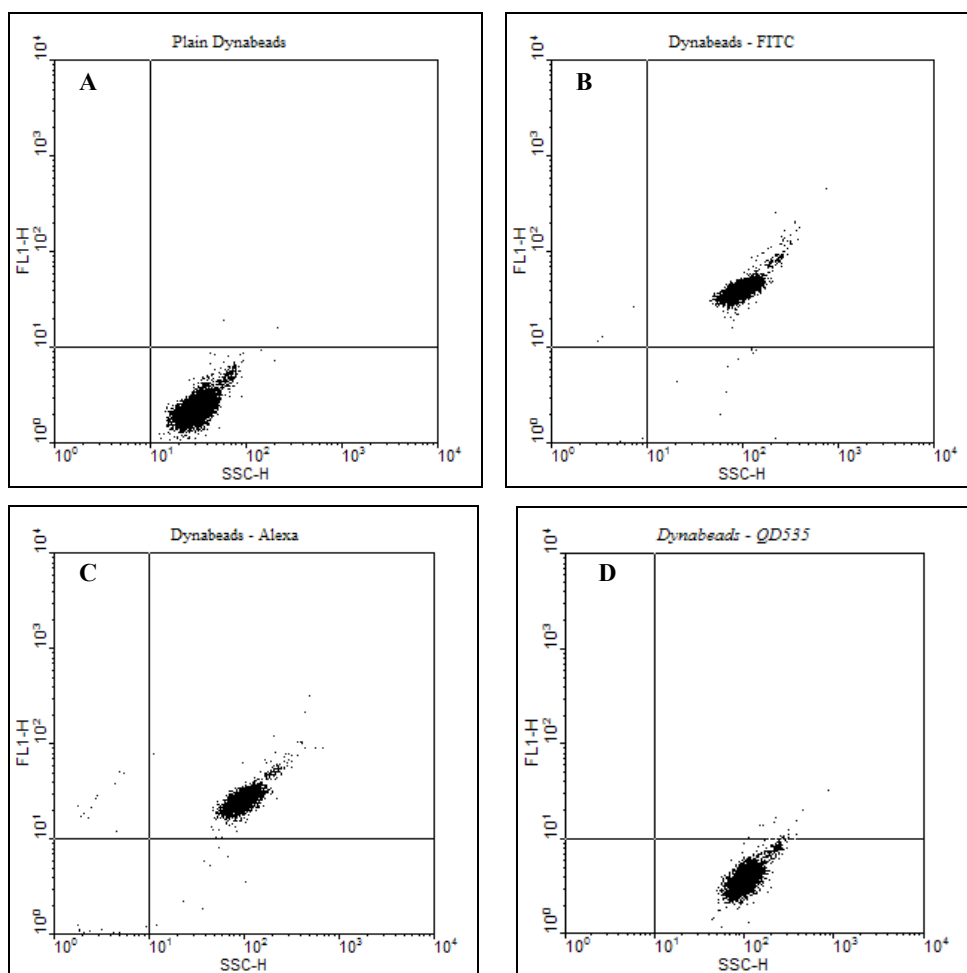


Figure 4.1: Flow cytometric analysis of biotinylated single strands of PCR amplicons labelled with FITC, Alexa Fluor 488 and QD535 bound to Dynabeads. Bivariate dot-plots defining log FL1 channel (y-axis) versus log SSC channel (x-axis). A: Unlabelled Dynabeads. B: *Bactouniversal2*. C: *BactouniAlexa*. D: *QDUniBiotinF* (target probe bound to QD525).

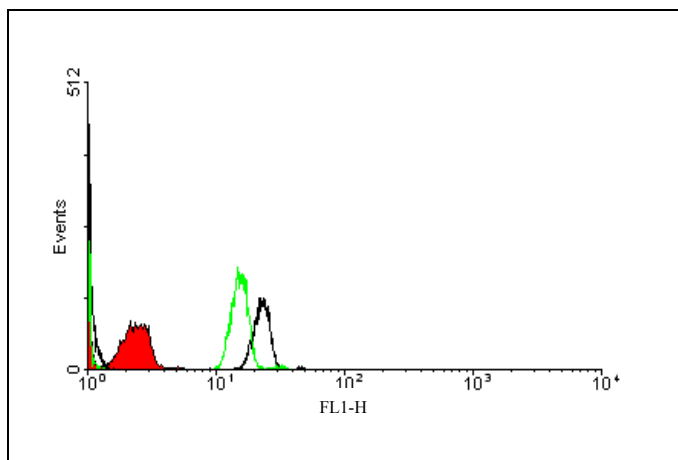


Figure 4.2: Flow cytometric analysis. Histogram of biotinylated single strands of PCR amplicons labelled to FITC and Alexa Fluor 488 bound to Dynabeads. X-axis: fluorescent signal detected in the FL1 channel. Y-axis: number of counts per sample.

Legend, Figure 4.2:

- Red curve:** Blank
- Green line:** Alexa Fluor 488

The biotinylated single strand of the PCR amplicons labelled with FITC and Alexa Fluor 488 bound to Dynabeads gave positive fluorescent signals above the blank, indicating successful capture and detection (Figures 4.1 and 4.2). However, Dynabeads labelled with QD525 did not show fluorescence above the blank value (Figure 4.1, D). Dynabeads labelled with FITC showed the higher fluorescence levels than Fluor Alexa 488 (Figure 4.2).

2.3. Blocking the active sites of the QDs with biocytin

QD525 have approximately 7 functional groups (streptavidin) on their surface. It may be possible that the target probe saturates the QD525 functional groups, preventing the hybridisation to the single strand of biotinylated PCR amplicons. For that reason, the number of functional groups of QD525 was reduced by blocking of free biotin groups with biocytin. After the blocking step, QD525 were bound to the target probe (QDUniBiotinF) for hybridisation and reporting of successfully captured single strands of PCR product (Table 4.1). Samples were analysed on a histogram displaying FL1 (green) fluorescence (Figure 4.3).

Table 4.1: Biotinylated PCR amplicons labelled with FITC, Alexa Fluor 488 and QD535 blocked with biocytin bound to Dynabeads.

Sample number	Biotinylated PCR amplicon (210 μM)	Dynabeads (10 mg/ml)	Target probe (1 μM)	Biocytin (4 μM)
1	5 μ l	1 μ l	2 μ l BactouniAlexa (Alexa Fluor 488)	-
2	5 μ l	1 μ l	2 μ l Bactouniversal (FITC)	-
3	5 μ l	1 μ l	2 μ l QDUniBiotinF (QD535, 1 μ M)	0.5 μ l (2 pmol)
4	5 μ l	1 μ l	2 μ l QDUniBiotinF (QD535, 1 μ M)	1.5 μ l (6 pmol)
5	5 μ l	1 μ l	2 μ l QDUniBiotinF (QD535, 1 μ M)	2.5 μ l (10 pmol)
6	5 μ l	1 μ l	2 μ l QDUniBiotinF (QD535, 1 μ M)	3.5 μ l (14 pmol)

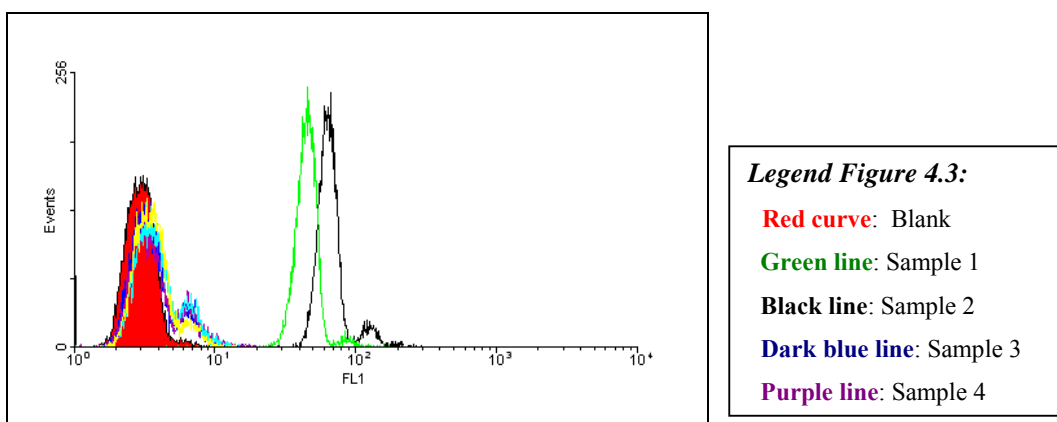


Figure 4.3: Histogram data analysis of biotinylated PCR amplicons labelled with FITC, Alexa Fluor 488 and QD525 blocked with biocytin bound to Dynabeads (Table 4.1). X-axis: fluorescent signal detected in the FL1 channel. Y-axis: number of counts per sample.

As occurred with the indirect method tested, biotinylated PCR amplicons labelled with FITC and Alexa Fluor 488 gave positive signals above the blank, while none of the samples labelled with QD525 were positive remaining with similar fluorescent signal as the blank (Figure 4.3).

2.4. Modifications in the binding procedures

Several modifications were tested in order to obtain successful hybridisation of the target probe modified with QD525 to the biotinylated strand of PCR amplicon. The PCR amplicon was denaturing by the alkali treatment (VI.2.6.1).

- The hybridisation time was increased from 10 min to 1 h to allow the binding of the QD525 to the target probe following hybridisation to the biotinylated strand of PCR bound to the Dynabeads (Appendix IV.1.1)
- The hybridisation temperature for the target probe was increased from 50°C to 60°C.
- PCR amplicons were denatured by an alkaline treatment instead of using heat (VI.2.6.4). The alkaline treatment allowed the denaturation of the PCR amplicons after their binding to Dynabeads without losing the efficiency of the biotin-streptavidin interaction. The alkaline treatment also facilitated the washing step of the non-biotinylated strand of PCR by using a magnet.

- Low concentrations of target probe (QDUniBiotinF) were bound with QD525 in a ratio 1:1 (one target probe per one QD).

3. Discussion

Analysis of reactions by flow cytometry indicated positive binding of the biotinylated PCR amplicons to the streptavidin-Dynabeads and successful hybridisation by the target probes modified with FITC and Alexa Fluor 488, for all the methods tested except by the direct method (Appendix IV.2.1). The direct method employed heat to denature the PCR amplicon after it was bound to the Dynabeads. The binding of the biotinylated PCR amplicon to the Dynabeads was made by the interaction of the biotin group of the PCR amplicon to the streptavidin group of the Dynabeads. Streptavidin is a protein that can be denatured at temperatures above 70°C. Dynabeads were subjected to temperatures up to 95°C in the methods tested. Therefore, it could be inferred that the streptavidin was also denatured during this step, losing its ability to bind the biotinylated PCR amplicon in the direct method.

The biotinylated single strand of the PCR amplicons bound to Dynabeads labelled with QD525 did not show fluorescence above background under any of the procedures employed, while PCR amplicons labelled with FITC and Alexa Fluor 488 resulted in fluorescent signals above the background, indicating a positive hybridisation (Figures 4.2 and 4.3). This result indicated successful binding of the target probes to the PCR amplicons and demonstrated the successful compatibilities of the technique and the procedures when using conventional fluorophores. However, all the modifications of the binding procedures tested (Appendix IV 2.4) resulted in no positive hybridisation of the QD525 to PCR amplicons.

The lack of fluorescent signal from the PCR amplicons labelled with QD525 compared to the positive results obtained when using FITC and Alexa Fluor 488 led to the hypothesis that the functional groups of the QDs (streptavidin) might dissociate from their surface after long periods of storage. QD525 used for these experiments were over 6 months old. Therefore, fresh QDs were purchased and the experiments repeated obtaining positive fluorescent signals from the QDs (Figure VI.16). It was established that the binding

procedures initially designed for the detection of biotinylated PCR amplicons were appropriate and all the modifications were not required.

APPENDIX V: Publications and conference proceedings

1. Publications

Ibáñez-Peral R., Bergquist P.L., Walter M.R., Gibbs M., Goldys E.M. and Ferrari B. (2008). Potential use of quantum dots in flow cytometry. Submitted in the International Journal of Molecular Sciences.

Ibáñez-Peral R., Ferrari B., Walter M.R. and Bergquist P.L. (2008). Cultivation of thermo-acidophilic microorganisms from volcanically-active sediments of White Island, New Zealand. Submitted in Extremophiles.

Leuko., F. Goh., **Ibáñez-Peral R.**, Burns B.P., Walter M.R. and Neilan B.A. (2007). Lysis efficiency of standard DNA extraction methods for *Halococcus spp.* in an organic rich environment (2007). Extremophiles 12: 301-308

2. Conference proceedings

Ibáñez-Peral R., Ferrari B., Walter M.R. and Bergquist P.L. (2006). Culturing the “unculturable”: Microbial communities from New Zealand’s most active volcano. *FEMS 2006*, Madrid, Spain.

Ibáñez-Peral R., Ferrari B., Gibbs M., Walter M.R. and Bergquist P.L. (2005). Quantum dots, Smart Nanocrystals in the Study of Thermophilic Microbial Diversity. *Thermophiles 05*, Gold Coast, Australia.

Ibáñez-Peral R., Ferrari B., and Bergquist P.L. (2005). Applying quantum dots to environmental microbiology. *Analysis of microbial cell at the single cell level conference*, Simmering, Austria.

Butterworth P., **Ibáñez-Peral R.**, Walter M.R., Bergquist P.L., Morgan H. and Anitori R. (2005). Sulfur-metabolizing Thermophiles in the White Island Hydrothermal Systems. *Thermophiles 05*, Gold Coast, Australia.

Ferrari B., Stoner K., **Ibáñez-Peral R.** and Bergquist, P.L. (2005). Applying fluorescence technologies to environmental waste water samples. *ASM 2005*, Canberra, Australia.

Ferrari B., **Ibáñez-Peral R.**, Gengos M. and Bergquist P.L. (2005). Novel pathogen detection strategies for the environment. *Analysis of microbial cell at the single cell level conference*, Simmering, Austria

Ibáñez-Peral R., Bergquist P.L., Walter M.R. and Ferrari B. (2004) Real time analysis of biodiversity in extreme environments. *Australian society for microbiology, annual scientific conference*, Sydney, Australia. Oral presentation

References

- Abrams B. & Dubrovsky T.** (2007) Quantum dots in flow cytometry. *Methods Mol Biol* 374: 185-203
- Acinas S.G., Sarma-Rupavtarm R., Klepac-Ceraj V. & Polz M.F.** (2005) PCR-induced sequence artifacts and bias: insights from comparison of two 16S rRNA clone libraries constructed from the same sample. *Appl Environ Microbiol* 71: 8966-8969
- Aislabie J.M., K. Chhour, D.J. Saul, S. Miyauchi, J. Ayton, Paetzold R.F. & Balks M.R.** (2006) Dominant bacteria in soils of Marble Point and Wright Valley, Victoria Land, Antarctica *Soil Biol Biochem* 38: 3041-3056
- Akerman M.E., Chan W.C.W., Laakkonen P., Bhatia S.N. & Ruoslahti E.** (2002) Nanocrystals targeting *in vivo*. *PNAS* 99: 12617-12621
- Aldana J., Wang Y.A. & Peng X.** (2001) Photochemical instability of CdSe nanocrystals coated by hydrophilic thiols. *J Am Chem Soc* 123: 8844-8850
- Alef K.** (1995) Nutrients, sterilization, aerobic and anaerobic culture techniques. In: *Methods in Applied Soil Microbiology and Biochemistry*. Eds. Alef K. and Nannipieri P., London, Academy Press: 124-129
- Algar W.R. & Krull U.J.** (2007) Towards multi-colour strategies for the detection of oligonucleotide hybridization using quantum dots as energy donors in fluorescence resonance energy transfer (FRET). *Anal Chim Acta* 581: 193-201
- Alivastos A.P.** (1996) Semiconductor Clusters, nanocrystals, and quantum dots. *Science* 271: 933-937
- Alivisatos A.P., Gu W. & Larabell C.** (2005) Quantum dots as cellular probes. *Annu Rev Biomed Eng* 7: 55-76
- Alm E.W., Oerther D.B., Larsen N., Stahl D.A. & Raskin L.** (1996) The oligonucleotide probe database. *Appl Environ Microbiol* 62: 3557-3559
- Altschul S.F., Madden T.L., Schaffer A.A., Zhang J., Zhang Z., Miller W. & Lipman D.J.** (1997) Gapped BLAST and PSI-BLAST: a new generation of protein database search programs. *Nucleic Acids Res* 25: 3389-3402
- Allwood A.C., Walter M.R., Kamber B.S., Marshall C.P. & Burch I.W.** (2006) Stromatolite reef from the early Archaean era of Australia. *Nature* 441: 714-718
- Amann R., Ludwig T. & Schleifer K.H.** (1992) Identification and *in situ* detection of individual cells. *FEMS Microbiol Lett* 100: 45-50
- Amann R. & Ludwig W.** (2000) Ribosomal RNA-targeted nucleic acid probes for studies in microbial ecology. *FEMS Microbiol Rev* 24: 555-565
- Amann R.I., Binder B.J., Olson R.J., Chisholm S.W., Devereux R. & Stahl D.A.** (1990a) Combination of 16S rRNA-targeted oligonucleotide probes with flow cytometry for analyzing mixed microbial populations. *Appl Environ Microbiol* 56: 1919-1925
- Amann R.I., Krumholz L. & Stahl D.A.** (1990b) Fluorescent-oligonucleotide probing of whole cells for determinative, phylogenetic, and environmental studies in microbiology. *J Bacteriol* 172: 762-770
- Amann R.I., Ludwig W. & Schleifer K.H.** (1995) Phylogenetic identification and *in situ* detection of individual microbial cells without cultivation. *Microbiol Rev* 59: 143-169
- Anitori R.P. & Bergquist P.L.** (2006). *A simple, agar-based method for culturing environmental microbes*. Paper presented at the ISME-11 - 11th International Symposium on Microbial Ecology, Vienna

- Anitori R.P., Trott C., Saul D.J., Bergquist P.L. & Walter M.R.** (2002) A culture-independent survey of the bacterial community in a radon hot spring. *Astrobiology* 2: 255-270
- Arya H., Kaul Z., Wadhwa R., Taira K., Hirano T. & Kaul S.C.** (2005) Quantum dots in bio-imaging: Revolution by the small. *Biochem Biophys Res Commun* 329: 1173-1177
- Atkinson T., Cairns S., Cowan D.A., Danson M.J., Hough D.W., Johnson D.B., Norris P.R., Raven N., Robinson C., Robson R. & Sharp R.J.** (2000) A microbiological survey of Montserrat Island hydrothermal biotopes. *Extremophiles* 4: 305-313
- Azzazy H.M., Mansour M.M. & Kazmierczak S.C.** (2007) From diagnostics to therapy: prospects of quantum dots. *Clin Biochem* 40: 917-927
- Bacelar-Nicolau P. & Johnson D.B.** (1999) Leaching of pyrite by acidophilic heterotrophic iron-oxidizing bacteria in pure and mixed cultures. *Appl Environ Microbiol* 65: 585-590
- Bada J.L., Fegley B., Jr., Miller S.L., Lazcano A., Cleaves H.J., Hazen R.M. & Chalmers J.** (2007) Debating evidence for the origin of life on Earth. *Science* 315: 937-939; author reply 937-939
- Bagwe R.P., Zhao X. & Tan W.** (2003) Bioconjugated luminescent nanoparticles for biological applications. *J Disp Sci Technol* 24: 453-464
- Bailey R.E. & Nie S.** (2003) Alloyed semiconductor quantum dots: tuning the optical properties without changing the particle size. *J Am Chem Soc* 125: 7100-7106
- Baker B.J. & Banfield J.F.** (2003) Microbial communities in acid mine drainage. *FEMS Microbiol Ecol* 44: 139-152
- Baker G.C. & Cowan D.A.** (2004) 16S rDNA primers and the unbiased assessment of thermophile diversity. *Biochem Soc Trans* 32: 218-221
- Baker G.C., Gaffar S., Cowan D.A. & Suharto A.R.** (2001) Bacterial community analysis of Indonesian hot springs. *FEMS Microbiol Lett* 200: 103-109
- Baker G.C., Smith J.J. & Cowan D.A.** (2003) Review and re-analysis of domain-specific 16S primers. *J Microbiol Methods* 55: 541-555
- Ballou B.** (2005) Quantum dot surfaces for use *in vivo* and *in vitro*. *Curr Top Dev Biol* 70: 103-120
- Ballou B., Lagerholm B.C., Ernst L.A., Bruchez M.P. & Waggoner A.S.** (2004) Noninvasive imaging of quantum dots in mice. *Bioconjugate Chem* 15: 79-86
- Barns S.M., Delwiche C.F., Palmer J.D. & Pace N.R.** (1996) Perspectives on archaeal diversity, thermophily and monophyly from environmental rRNA sequences. *Proc Natl Acad Sci USA* 93: 9188-9193
- Barns S.M., Fundyga R.E., Jeffries M.W. & Pace N.R.** (1994) Remarkable archaeal diversity detected in a Yellowstone National Park hot spring environment. *Proc Natl Acad Sci USA* 91: 1609-1613
- Bartscht K., Cypionka H. & Overmann J.** (1999) Evaluation of cell activity and of methods for the cultivation of bacteria from natural lake community. *FEMS Microbiol Ecol* 28: 249-259
- Bayer E.A. & Wilcheck M.** (1980) The use of the avidin-biotin complex as a tool in molecular biology. *Methods Biochem Anal* 26: 1-45
- Bell P.J., Sunna A., Gibbs M.D., Curach N.C., Nevalainen H. & Bergquist P.L.** (2002) Prospecting for novel lipase genes using PCR. *Microbiology* 148: 2283-2291

Bergquist P.L., Gibbs M.D., Morris D.D., Thompson D.R., Uhl A.M. & Daniel R.M. (2001) Hyperthermophilic xylanases. *Methods Enzymol* 330: 301-319

Bergquist P.L., Love D.R., Croft J.E., Streiff M.B., Daniel R.M. & Morgan W.H. (1987) Genetics and potential biotechnological applications of thermophilic and extremely thermophilic micro-organisms. *Biotechnol Genet Eng Rev* 5: 199-244

Bergquist P.L., Te'o V.S., Gibbs M.D., Cziferszky A.C., De Faria F.P., Azevedo M.O. & Nevalainen K.M. (2002) Production of recombinant bleaching enzymes from thermophilic microorganisms in fungal hosts. *Appl Biochem Biotechnol* 98-100: 165-176

Bertaux J., Gloger U., Schmid M., Hartmann A. & Scheu S. (2007) Routine fluorescence *in situ* hybridization in soil. *J Microbiol Methods* 69: 451-460

Bhatia U., Robison K. & Gilbert W. (1997) Dealing with database explosion: a cautionary note. *Science* 276: 1724-1725

Bintrim S.B., Donohue T.J., Handelsman J., Roberts G.P. & Goodman R.M. (1997) Molecular phylogeny of Archaea from soil. *Proc Natl Acad Sci USA* 94: 277-282

Black P.M. (1970) Observations on White Island Volcano, New Zealand. *Bull Volcanol* 34: 158-167

Blöchl E., Burggraf S. & Fiala G. (1995) Isolation, taxonomy and phylogeny of hyperthermophilic microorganisms. *World J Microbiol Biotechnol* 11: 9-16

Blöchl E., Rachel R., Burggraf S., Hafenbradl D., Jannasch H.W. & Stetter K.O. (1997) *Pyrolobus fumarii*, gen. and sp. nov., represents a novel group of archaea, extending the upper temperature limit for life to 113 degrees C. *Extremophiles* 1: 14-21

Bloem J., Veninga M. & Shepherd J. (1995) Fully automatic determination of soil bacterium numbers, cell volumes, and frequencies of dividing cells by confocal laser scanning microscopy and image analysis. *Appl Environ Microbiol* 61: 926-936

Bogdanova T.I., Tsaplina I.A., Kondrat'eva T.F., Duda V.I., Suzina N.E., Melamud V.S., Tourova T.P. & Karavaiko G.I. (2006) *Sulfobacillus thermotolerans* sp. nov., a thermotolerant, chemolithotrophic bacterium. *Int J Syst Evol Microbiol* 56: 1039-1042

Boldt K., Bruns O.T., Gaponik N. & Eychmuller A. (2006) Comparative examination of the stability of semiconductor quantum dots in various biochemical buffers. *J Phys Chem B Condens Matter Mater Surf Interfaces Biophys* 110: 1959-1963

Bond P.L., Druschel G.K. & Banfield J.F. (2000a) Comparison of acid mine drainage microbial communities in physically and geochemically distinct ecosystems. *Appl Environ Microbiol* 66: 4962-4971

Bond P.L., Smriga S.P. & Banfield J.F. (2000b) Phylogeny of microorganisms populating a thick, subaerial, predominantly lithotrophic biofilm at an extreme acid mine drainage site. *Appl Environ Microbiol* 66: 3842-3849

Bosecker K. (1997) Bioleaching metal solubilization by microorganisms. *FEMS Microbiol Rev* 20: 591-604

Bragger J.M., Daniel R.M., Coolbear T. & Morgan H.W. (1989) Very stable enzymes from extremely thermophilic Archaeobacteria and Eubacteria. *Appl Microbiol Biotechnol* 31: 556-561

Brand B.C., Amann R.I., Steinert M., Grimm D. & Hacker J. (2000) Identification and *in situ* detection of intracellular bacteria in the environment. *Subcell Biochem* 33: 601-624

- Brewer W.H.** (1866) Note on the organisms of the geysers of California. *Am J Sci* 92: 429
- Bridge T.A.M. & Johnson D.B.** (1998) Reduction of soluble iron and reductive dissolution of ferric iron-containing minerals by moderately thermophilic iron-oxidizing bacteria. *Appl Environ Microbiol* 64: 2181-2186
- Britten V. & Murphy J.** (1986) Cell sorting by continuous flow cytometry. *Parasitol Today* 2: 85-87
- Brock T.D.** (1978) *Thermophilic microorganisms and life at high temperatures*, Springer, Berlin Heidelberg
- Brock T.D., Brock K.M., Belly R.T. & Weiss R.L.** (1972) Sulfolobus: a new genus of sulfur-oxidizing bacteria living at low pH and high temperature. *Arch Mikrobiol* 84: 54-68
- Brosius J., Palmer M.L., Kennedy P.J. & Noller H.F.** (1978) Complete nucleotide sequence of a 16S ribosomal RNA gene from *Escherichia coli*. *Proc Natl Acad Sci USA* 75: 4801-4805
- Bruchez M., Moronne M., Gin P., Weiss S. & Alivisatos A.P.** (1998) Semiconductor nanocrystals as fluorescent biological labels. *Science* 281: 2013-2016
- Bruchez M.P.** (2005) Turning all the lights on: quantum dots in cellular assays. *Curr Opin Chem Biol* 9: 533-537
- Bruns A., Hoffelner H. & Overmann J.** (2003) A novel approach for high throughput cultivation assays and the isolation of planktonic bacteria. *FEMS Microbiol Ecol* 45: 161-171
- Burggraf S., Mayer T., Amann R.I., Schadhauer S., Woese C.R. & Stetter K.O.** (1994) Identifying members of the domain archaea with rRNA-targeted oligonucleotide probes. *Appl Env Microbiol* 60
- Burton N.P. & Norris P.R.** (2000) Microbiology of acidic, geothermal springs of Montserrat: environmental rDNA analysis. *Extremophiles* 4: 315-320
- Butterworth P.R., Ibáñez-Peral R., Walter M.R. & Bergquist P.** (2005). *Sulfur metabolizing thermophiles in the White Island hydrothermal systems*. Paper presented at the Poster presentation. Thermophiles 05, Sept 18-22. Gold Coast, Australia
- Cai H., White P.S., Torney D., Deshpande A., Wang Z., Keller R.A., Marrone B. & Nolan J.P.** (2000) Flow cytometry-based minisequencing: a new platform for high-throughput single-nucleotide polymorphism scoring. *Genomics* 66: 135-143
- Caldwell D.E., Korber D.R. & Lawrence J.R.** (1992) Imaging of bacterial cells by fluorescence exclusion using scanning confocal laser microscopy. *J Microbiol Methods* 15: 249-261
- Cao Y.C., Huang Z.L., Liu T.C., Wang H.Q., Zhu X.X., Wang Z., Zhao Y.D., Liu M.X. & Luo Q.M.** (2006) Preparation of silica encapsulated quantum dot encoded beads for multiplex assay and its properties. *Anal Biochem* 351: 193-200
- Caracciolo A.B., Grenni P., Ciccoli R., Di Landa G. & Cremisini C.** (2005) Simazine biodegradation in soil: analysis of bacterial community structure by *in situ* hybridization. *Pest Manag Sci* 61: 863-869
- Caruge J.M., Chan Y.T., Sundar V., Eisler H.J. & M.G. B.** (2004) Transient photoluminescence and simultaneous amplified spontaneous emission from multiexciton states in CdSe quantum dot. *Phys Rev B* 70: 085316

- Cavicchioli R., Siddiqui K.S., Andrews D. & Sowers K.R.** (2002) Low-temperature extremophiles and their applications. *Curr Opin Biotechnol* 13: 253-261
- Chaban B., Ng S.Y. & Jarrell K.F.** (2006) Archaeal habitats-from the extreme to the ordinary. *Can J Microbiol* 52: 73-116
- Chalmers N.I., Robert J. Palmer J., Du-Thumm L., Sullivan R., Shi W. & Kolenbrander P.E.** (2007) Use of quantum dot luminescent probes to achieve single-cell resolution of human oral bacteria in biofilms. *Appl Environ Microbiol* 73: 630-636
- Chan P., Yuen T., Ruf F., Gonzalez-Maeso J. & Sealfon S.C.** (2005) Method for multiplex cellular detection of mRNAs using quantum dot fluorescent in situ hybridization. *Nucleic Acids Res* 33: e161
- Chan W.C., Maxwell D.J., Gao X., Bailey R.E., Han M. & Nie S.** (2002) Luminescent quantum dots for multiplexed biological detection and imaging. *Curr Opin Biotechnol* 13: 40-46
- Chan W.C.W. & Nie S.** (1998) Quantum dot bioconjugates for ultrasensitive nonisotopic detection. *Science* 281: 2016-2018
- Chandler D.P., Stults J.R., Anderson K.K., Cebula S., Schuck B.L. & Brockman F.J.** (2000) Affinity capture and recovery of DNA at femtomolar concentrations with peptide nucleic acid probes. *Anal Biochem* 283: 241-249
- Chattopadhyay P.K., Price D.A., Harper T.F., Betts M.R., Yu J., Gostick E., Perfetto S.P., Goepfert P., Koup R.A., De Rosa S.C., Bruchez M.P. & Roederer M.** (2006) Quantum dot semiconductor nanocrystals for immunophenotyping by polychromatic flow cytometry. *Nat Med* 12: 972-977
- Chen F.Q. & Gerion D.** (2004) Fluorescent CdSe/ZnS nanocrystal-peptide conjugates for long-term, nontoxic imaging and nuclear targeting in living cells. *Nano Lett* 4: 1827-1832
- Chen L., Brugger K., Skovgaard M., Redder P., She Q., Torarinsson E., Greve B., Awayez M., Zibat A., Klenk H.P. & Garrett R.A.** (2005) The genome of *Sulfolobus acidocaldarius*, a model organism of the Crenarchaeota. *J Bacteriol* 187: 4992-4999
- Chen W.** (2008) Nanoparticle fluorescence based technology for biological applications. *J Nanosci Nanotechnol* 8: 1019-1051
- Christoffel D.A.** (1989) Variations in magnetic field intensity at White Island volcano related to the 1976-82 eruption sequence. *NZ Geol Surv Bull* 103: 109-118
- Chung I., Witkoskie J.B., Zimmer J.P., Cao J. & Bawendi M.G.** (2007) Extracting the number of quantum dots in a microenvironment from ensemble fluorescence intensity fluctuations. *Phys Rev B* 75: 045311
- Chyba C. & Phillips C.** (2001) Possible ecosystems and the search for life on Europa. *Proc Natl Acad Sci USA* 98: 801-804
- Clark R.H.** (1970) Volcanic activity on White Island, Bay of Plenty, 1966-69. Part I: Chronology and crater floor level changes. *NZ J Geol Geophys* 13: 565-574
- Clark R.H. & Otway P.M.** (1989) Deformation monitoring associated with the 1976-82 White Island eruption sequence. *NZ Geol Surv Bull* 103: 69-84
- Clarke S.J., Hollmann C.A., Zhang Z., Suffern D., Bradforth S.E., Dimitrijevic N.M., Minarik W.G. & Nadeau J.L.** (2006) Photophysics of dopamine-modified quantum dots and effects on biological systems. *Nat Mater* 5: 409-417

Cleaves H.J., 2nd & Chalmers J.H. (2004) Extremophiles may be irrelevant to the origin of life. *Astrobiology* 4: 1-9

Cole J.R., Chai B., Marsh T.L., Farris R.J., Wang Q., Kulam S.A., Chandra S., McGarrell D.M., Schmidt T.M., Garrity G.M. & Tiedje J.M. (2003) The Ribosomal Database Project (RDP-II): previewing a new autoaligner that allows regular updates and the new prokaryotic taxonomy. *Nucleic Acids Res* 31: 442-443

Cole J.W. (1981) Genesis of lavas of the Taupo volcanic zone, North Island New Zealand. *J Volcanol Geotherm Res* 10: 317-337

Cole J.W. & Nairn I.A. (1975) Catalogue of the active volcanoes of the world including Solfatara fields. Part 22: New Zealand. *International Association of Volcanology and Chemistry of the Earth's Interior*, Naples

Cole J.W., Thordarson T. & Burt R.M. (2000) Magma origin and evolution of White Island (Whakaari) volcano, Bay of Plenty, New Zealand. *J Petrol* 2: 867-895

Cannon S.A. & Giovannoni S.J. (2002) High-throughput methods for culturing microorganisms in very-low-nutrient media yield diverse new marine isolates. *Appl Environ Microbiol* 68: 3878-3885

Coolbear T., Daniel R.M., Cowan D.A. & Morgan H.W. (1988) Proteases from extreme thermophiles. *Ann N Y Acad Sci* 542: 279-281

Coolbear T., Daniel R.M. & Morgan H.W. (1992) The enzymes from extreme thermophiles: bacterial sources, thermostabilities and industrial relevance. *Adv Biochem Eng Biotechnol* 45: 57-98

Cowan D. (2000) Use your neighbour's genes. *Nature* 407: 466-467

Cowan D.A. (1992) Enzymes from thermophilic Archaeobacteria: current and future applications in biotechnology. *Biochem Soc Symp* 58: 149-169

Cowan D.A. (2004) The upper temperature for life - where do we draw the line? *Trends Microbiol* 12: 58-60

Cowan D.A., Daniel R.M. & Morgan H.W. (1987) The specific activities of mesophilic and thermophilic proteinases. *Int J Biochem* 19: 741-743

Cowan D.A., Russell N.J., Mamais A. & Sheppard D.M. (2002) Antarctic Dry Valley mineral soils contain unexpectedly high levels of microbial biomass. *Extremophiles* 6: 431-436

Crut A., Geron-Landre B., Bonnet I., Bonneau S., Desbiolles P. & Escude C. (2005) Detection of single DNA molecules by multicolor quantum-dot end-labeling. *Nucleic Acids Res* 33: e98

Curtis T.P. & Sloan W.T. (2004) Prokaryotic diversity and its limits: microbial community structure in nature and implications for microbial ecology. *Curr Opin Microbiol* 7: 221-226

Curtis T.P. & Sloan W.T. (2005) Exploring microbial diversity - a vast below. *Science* 309: 1331-1333

Dabbousi B.O., Rodriguez-Viejo J., Mikulec F.V., Heine J.R., Mattoussi H., Ober R., Jensen K.F. & Bawedi M.G. (1997) (CdSe)ZnS Core-Shell Quantum dots: Synthesis and characterization of a size series of highly luminescent nanocrystallites. *J Phys Chem B* 101: 9463-9475

Dahan M., Levi S., Luccardini C., Rostaing P., Riveau B. & Triller A. (2003) Diffusion dynamics of glycine receptors revealed by single-quantum dot tracking. *Science* 302: 442-445

- Daims H., Nielsen J.L., Nielsen P.H., Schleifer K.H. & Wagner M.** (2001a) *In situ* characterization of *Nitrospira*-like nitrite-oxidizing bacteria active in wastewater treatment plants. *Appl Environ Microbiol* 67: 5273-5284
- Daims H., Ramsing N.B., Schleifer K.H. & Wagner M.** (2001b) Cultivation-independent, semiautomatic determination of absolute bacterial cell numbers in environmental samples by fluorescence *in situ* hybridization. *Appl Environ Microbiol* 67: 5810-5818
- Danek M., Jensen K.F., Murray C.B. & Bawendi M.G.** (1996) Synthesis of luminescent thin-film CdSe/ZnSe quantum dot composites using CdSe quantum dots passivated with an overlayer of ZnSe. *Chem Matter* 8: 173-180
- Darland G. & Brock T.D.** (1971) *Bacillus acidocaldarius* sp. nov., an acidophilic thermophilic spore-forming bacterium. *J Gen Microbiol* 76: 9-15
- Davies P.** (2001) The origin of life. I: When and where did it begin? *Sci Prog* 84: 1-16
- Davis K.E., Joseph S.J. & Janssen P.H.** (2005) Effects of growth medium, inoculum size, and incubation time on culturability and isolation of soil bacteria. *Appl Environ Microbiol* 71: 826-834
- Delehanty J.B., Medintz I.L., Pons T., Brunel F.M., Dawson P.E. & Mattoussi H.** (2006) Self-assembled quantum dot-peptide bioconjugates for selective intracellular delivery. *Bioconjug Chem* 17: 920-927
- DeLeo P.C., Baveye P. & Ghiorse W.C.** (1997) Use of confocal laser scanning microscopy on soil thin-sections for improved characterization of microbial growth in unconsolidated soils and aquifer materials. *J Microbiol Methods* 30: 193-203
- DeLong E.F.** (2001) A phylogenetic perspective on hyperthermophilic microorganisms. *Methods Enzymol* 330: 3-24
- DeLong E.F.** (2002) Microbial population genomics and ecology. *Curr Opin Microbiol* 5: 520-524
- DeLong E.F. & Pace N.R.** (2001) Environmental diversity of Bacteria and Archaea. *Syst Biol* 50: 470-478
- DeLong E.F. & Taylor L.T.** (1999) Visualization and enumeration of marine planktonic Archaea and Bacteria by using polyribonucleotide probes and fluorescent *in situ* hybridization. *Appl Environ Microbiol* 65: 5554-5563
- DeLong E.F., Wickham G.S. & Pace N.R.** (1989) Phylogenetic stains: ribosomal RNA-based probes for the identification of single cells. *Science* 243: 1360-1363
- Derfus A.M., Chan W.C.W. & Bhatia S.N.** (2004) Probing the cytotoxicity of semiconductor quantum dots. *Nano Lett* 4: 11-18
- DeRose P.C. & Kramer G.W.** (2005) Bias in the absorption coefficient determination of a fluorescent dye, standard reference material 1932 fluorescein solution. *J Luminescence* 113: 314-320
- Des Marais D.J., Allamandola L.J., Benner S.A., Boss A.P., Deamer D., Falkowski P.G., Farmer J.D., Hedges S.B., Jakosky B.M., Knoll A.H., Liskowsky D.R., Meadows V.S., Meyer M.A., Pilcher C.B., Nealson K.H., Spormann A.M., Trent J.D., Turner W.W., Woolf N.J. & Yorke H.W.** (2003) The NASA Astrobiology Roadmap. *Astrobiology* 3: 219-235
- Des Marais D.J. & Walter M.R.** (1999) Astrobiology: Exploring the origins, evolution, and distribution of life in the universe. *Annu Rev Syst* 30: 397-420

- Devasia P., Natarajan K.A., Sathyanarayana D.N. & Rao G.R.** (1993) Surface chemistry of *Thiobacillus ferrooxidans* relevant to adhesion on mineral surfaces. *Appl Environ Microbiol* 59: 4051-4055
- Devereux R. & Boddy L.** (1993) Phylogeny of sulfate-reducing bacteria and a perspective for analyzing their natural communities. In: *The sulfate-reducing bacteria: contemporary perspectives*. Eds. Odom J.M. and Singleton R., Springer-Verlag, New York: 131-160
- Devereux R., Delaney M., Widdel F. & Stahl D.A.** (1989) Natural relationships among sulfate-reducing Eubacteria. *J Bacteriol* 171: 6689-6695
- Diaby N., Dold B., Pfeifer H.R., Holliger C., Johnson D.B. & Hallberg K.B.** (2007) Microbial communities in a porphyry copper tailings impoundment and their impact on the geochemical dynamics of the mine waste. *Environ Microbiol* 9: 298-307
- Donachie S.P., Christenson B.W., Kunkel D.D., Malahoff A. & Alam M.** (2002) Microbial community in acidic hydrothermal waters of volcanically active White Island, New Zealand. *Extremophiles* 6: 419-425
- Doolittle W.F.** (2000) The nature of the universal ancestor and the evolution of the proteome. *Curr Opin Struct Biol* 10: 355-358
- Dopson M., Baker-Austin C., Koppineedi P.R. & Bond P.L.** (2003) Growth in sulfidic mineral environments: metal resistance mechanisms in acidophilic micro-organisms. *Microbiology* 149: 1959-1970
- Dopson M. & Lindstrom E.B.** (2004) Analysis of community composition during moderately thermophilic bioleaching of pyrite, arsenical pyrite, and chalcopyrite. *Microb Ecol* 48: 19-28
- Douglas S. & Douglas D.D.** (2001) Structural and geomicrobiological characteristics of a microbial community from a cold sulfide spring *Geomicrobiol* 18: 401-422
- Druschel G.K., Baker B.J., Gihring T.M. & Banfield J.F.** (2004) Acid mine drainage biogeochemistry at Iron Mountain, California. *Geochem. Trans.* 5: 13-32
- Dubertret B.** (2005) Quantum dots: DNA detectives. *Nat Mater* 4: 797-798
- Dubertret B., Skourides P., Norris D.J., Noireaux V., Brivanlou A.H. & Libchaber A.** (2002) *In vivo* imaging of quantum dots encapsulated in phospholipid micelles. *Science* 298: 1759-1762
- Dufresne S., Bousquet J., Boissinot M. & Guay R.** (1996) *Sulfobacillus disulfidooxidans* sp. nov., a new acidophilic, disulfide-oxidizing, gram-positive, spore-forming bacterium. *Int J Syst Bacteriol* 46: 1056-1064
- Edgar R., McKinsty M., Hwang J., Oppenheim A.B., Fekete R.A., Giulian G., Merrill C., Nagashima K. & Adhya S.** (2006) High-sensitivity bacterial detection using biotin-tagged phage and quantum-dot nanocomplexes. *Proc Natl Acad Sci USA* 103: 4841-4845
- Edmond J., L'Haridon S., Corre E., Forterre P. & Prieur D.** (2003) *Thermococcus gammatolerans* sp. nov., a hyperthermophilic archaeon from deep-sea hydrothermal vent that resists to ionizing radiation. *Int J Syst Evol Microbiol* 53: 847-851
- Edwards K.J., Bond P.L., Gihring T.M. & Banfield J.F.** (2000) An archaeal iron-oxidizing extreme acidophile important in acid mine drainage. *Science* 287: 1796-1799
- Eilers H., Pernthaler J., Glockner F.O. & Amann R.** (2000) Culturability and *in situ* abundance of pelagic bacteria from the North Sea. *Appl Environ Microbiol* 66: 3044-3051

Elshahed M.S., Senko J.M., Najjar F.Z., Kenton S.M., Roe B.A., Dewers T.A., Spear J.R. & Krumholz L.R. (2003) Bacterial diversity and sulfur cycling in a mesophilic sulfide-rich spring. *Appl Environ Microbiol* 69: 5609-5621

Evanko D. (2006) Bioluminescent quantum dots. *Nat Methods* 3: 240-241

Farrelly V., Rainey F.A. & Stackebrandt E. (1995) Effect of genome size and *rrn* gene copy number on PCR amplification of 16S rRNA genes from a mixture of bacterial species. *Appl Environ Microbiol* 61: 2798-2801

Farris M.H. & Olson J.B. (2007) Detection of *Actinobacteria* cultivated from environmental samples reveals bias in universal primers. *Lett Appl Microbiol* 45: 376-381

Felske A., Wolterink A., van Lis R., de Vos W.M. & Akkermans A.D.L. (1999) Searching for predominant soil bacteria: 16S rDNA cloning versus strain cultivation. *FEMS Microbiol Ecol* 30: 137-145

Fernández-Remolar D., Gómez-Elvira J., Gómez F., Sebastian E., Martín J., Manfredi J.A., Torres J., Kesler C.G. & Amils R. (2004) The Tinto River, an extreme acidic environment under control of iron, as an analog of the *Terra Meridiani* hematite site of Mars. *Plan Space Sci* 52: 239-248

Ferrari B.C. & Bergquist P.L. (2007) Quantum dots as alternatives to organic fluorophores for *Cryptosporidium* detection using conventional flow cytometry and specific monoclonal antibodies: lessons learned. *Cytometry A* 71: 265-271

Ferrari B.C., Binnerup S.J. & Gillings M. (2005) Microcolony cultivation on a soil substrate membrane system selects for previously uncultured soil bacteria. *Appl Environ Microbiol* 71: 8714-8720

Ferrari B.C., Oregaard G. & Sorensen S.J. (2004) Recovery of GFP-labeled bacteria for culturing and molecular analysis after cell sorting using a benchtop flow cytometer. *Microbiol Ecol* 48: 239-245

Ferrari B.C., Tujula N., Stoner K. & Kjelleberg S. (2006) Catalyzed reporter deposition-fluorescence *in situ* hybridization allows for enrichment-independent detection of microcolony-forming soil bacteria. *Appl Environ Microbiol* 72: 918-922

Ferrari B.C., Vesey G., Davis K.A., Gauci M. & Veal D. (2000) A novel two-color flow cytometric assay for the detection of *cryptosporidium* in environmental water samples. *Cytometry* 41: 216-222

Ferreira A.C., Nobre M.F., Moore E., Rainey F.A., Battista J.R. & da Costa M.S. (1999) Characterization and radiation resistance of new isolates of *Rubrobacter radiotolerans* and *Rubrobacter xylanophilus*. *Extremophiles* 3: 235-238

Fierer N., Bradford M.A. & Jackson R.B. (2007) Toward an ecological classification of soil bacteria. *Ecology* 88: 1354-1364

Fierer N. & Jackson R.B. (2006) The diversity and biogeography of soil bacterial communities. *Proc Natl Acad Sci USA* 103: 626-631

Fishbain S., Dillon J.G., Gough H.L. & Stahl D.A. (2003) Linkage of high rates of sulfate reduction in Yellowstone hot springs to unique sequence types in the dissimilatory sulfate respiration pathway. *Appl Environ Microbiol* 69: 3663-3667

Foght J., Aislabie J., Turner S., Brown C.E., Ryburn J., Saul D.J. & Lawson W. (2004) Culturable bacteria in subglacial sediments and ice from two Southern Hemisphere glaciers. *Microb Ecol* 47: 329-340

Ford T.C. & Rickwood D. (1982) Formation of isotonic Nycodenz gradients for cell separations. *Anal Biochem* 124: 293-298

- Fortina P., Kricka L.J., Surrey S. & Grodzinski P.** (2005) Nanobiotechnology: the promise and reality of new approaches to molecular recognition. *Trends Biotechnol* 23: 168-173
- Fox G.E., Stackebrandt E., Hespell R.B., Gibson J., Maniloff J., Dyer T.A., Wolfe R.S., Balch W.E., Tanner R.S., Magrum L.J., Zablen L.B., Blakemore R., Gupta R., Bonen L., Lewis B.J., Stahl D.A., Luehrsen K.R., Chen K.N. & Woese C.R.** (1980) The phylogeny of prokaryotes. *Science* 209: 457-463
- Franchi M., Bramanti E., Marassi Bonzi L., Luigi Orioli P., Vettori C. & Gallori E.** (1999) Clay-nucleic acid complexes characteristics and implications for the preservation of genetic material in primeval habitats. *Origins Life Evol B* 29: 297-315
- Friedrich C.G., Bardischewsky F., Rother D., Quentmeier A. & Fischer J.** (2005) Prokaryotic sulfur oxidation. *Curr Opin Microbiol* 8: 253-259
- Friedrich C.G., Rother D., Bardischewsky F., Quentmeier A. & Fischer J.** (2001) Oxidation of reduced inorganic sulfur compounds by bacteria: emergence of a common mechanism? *Appl Environ Microbiol* 67: 2873-2882
- Frohlich J. & Konig H.** (2000) New techniques for isolation of single prokaryotic cells. *FEMS Microbiol Rev* 24: 567-572
- Frostegard A., Courtois S., Ramisse V., Clerc S., Bernillon D., Le Gall F., Jeannin P., Nesme X. & Simonet P.** (1999) Quantification of bias related to the extraction of DNA directly from soils. *Appl Environ Microbiol* 65: 5409-5420
- Fry J.C.** (1990) Direct methods and biomass estimation. *Methods Microbiol* 22: 41-85
- Fulwyler M.J.** (1980) Flow cytometry and cell sorting. *Blood Cells* 6: 173-184
- Furnes H., Banerjee N.R., Muehlenbachs K., Staudigel H. & de Wit M.** (2004) Early life recorded in archean pillow lavas. *Science* 304: 578-581
- Fuseler K., Krekeler D., Sydow U. & Cypionka H.** (1996) A common pathway of sulfide oxidation by sulphate-reducing bacteria. *FEMS Microbiol Lett* 144: 129-134
- Gaigalas A.K., Wang L., Schwartz A., Marti G.E. & vogt R.F.** (2005) Quantitating fluorescence intensity from fluorophore: Assignment of MESF values. *J Res Natl and Technol* 110: 101-114
- Gans J., Wolinsky M. & Dunbar J.** (2005) Computational improvements reveal great bacterial diversity and high metal toxicity in soil. *Science* 309: 1387-1390
- Gao M.Y., Kirstein S., Mohwald H., Rogach A., Kornowski A. & Eychmuller A.** (1998) Strongly photoluminescent CdTe nanocrystals by proper surface modification. *J Phys Chem B* 102: 8360-8363
- Gao X., Cui Y., Levenson R.M., Chung L.W.K. & Nie S.** (2004) *In vivo* cancer targeting and imaging with semiconductor quantum dots. *Nat Biotechnol* 22: 969-976
- Gao X. & Nie S.** (2003) Doping mesoporous materials with multicolor quantum dots. *J Phys Chem B* 107: 11575-11578
- Gao X. & Nie S.** (2004) Quantum dot-encoded mesoporous beads with high brightness and uniformity: rapid readout using flow cytometry. *Anal Chem* 76: 2406-2410
- Garon E.B., Marcu L., Luong Q., Tcherniantchouk O., Crooks G.M. & Koeffler H.P.** (2007) Quantum dot labeling and tracking of human leukemic, bone marrow and cord blood cells. *Leuk Res* 31: 643-651

- Gehrke T., Telegdi J., Thierry D. & Sand W.** (1998) Importance of extracellular polymeric substances from *Thiobacillus ferrooxidans* for bioleaching. *Appl Environ Microbiol* 64: 2743-2747
- Gerday C., Aittaleb M., Bentahir M., Chessa J.P., Claverie P., Collins T., D'Amico S., Dumont J., Garsoux G., Georgette D., Hoyoux A., Lonhienne T., Meuwis M.A. & Feller G.** (2000) Cold-adapted enzymes: from fundamentals to biotechnology. *Trends Biotechnol* 18: 103-107
- Gerion D., Parak W.J., Williams S.C., Zanchet D., Michael C.M. & Alivisatos A.P.** (2002) Sorting fluorescent nanocrystals with DNA. *J Am Chem Soc* 124: 7070-7074
- Giepmans B.N., Deerinck T.J., Smarr B.L., Jones Y.Z. & Ellisman M.H.** (2005) Correlated light and electron microscopic imaging of multiple endogenous proteins using quantum dots. *Nat Methods* 2: 743-749
- Giggenbach W.F.** (1986). *The use of gas chemistry in delineating the origin of fluids discharged over the Taupo Volcanic Zone*. Paper presented at the Proc. Symp. V, Int. Volcanol. Congr., Auckland, New Zealand
- Giggenbach W.F.** (1987) Redox processes governing the chemistry of fumarolic gas discharges from White Island, New Zealand. *Appl Geochem* 2: 143-161
- Giggenbach W.F. & Sheppard D.S.** (1989) Variations in the temperature and chemistry of White Island fumarole discharges 1972-85. *NZ Geological Survey Bulletin* 103: 119-126
- Goff F. & Janik C.J.** (2000) Geothermal systems. In: *Encyclopedia of volcanoes*. Ed. Sigurdsson H., Academic Press, San Diego: 817-834
- Goldman E.R., Balighaian E.D., Mattoussi H., Kuno M., Mauro J.M., Tran P.T. & Anderson G.P.** (2002) Avidin: A natural bridge for quantum dot-antibody conjugates. *J Am Chem Soc* 124: 6378-6382
- Golovacheva R.S. & Karavaiko G.I.** (1978) *Sulfobacillus*, a new genus of thermophilic sporulating bacteria. *Mikrobiologiya* 47: 815-822
- Gomez-Alvarez V., King G.M. & Nusslein K.** (2007) Comparative bacterial diversity in recent Hawaiian volcanic deposits of different ages. *FEMS Microbiol Ecol* 60: 60-73
- Gonzalez-Toril E., Llobet-Brossa E., Casamayor E.O., Amann R. & Amils R.** (2003) Microbial ecology of an extreme acidic environment, the Tinto River. *Appl Environ Microbiol* 69: 4853-4865
- Green B.D. & Keller M.** (2006) Capturing the uncultivated majority. *Curr Opin Biotechnol* 17: 236-240
- Groenewald W.H., Gouws P.A. & Witthuhn R.C.** (2008) Isolation and identification of species of *Alicyclobacillus* from orchard soil in the Western Cape, South Africa. *Extremophiles* 12: 159-163
- Grüttner C., Rudershausen S. & Teller J.** (2001) Improved properties of magnetic particles by combination of different polymer materials as particle matrix. *J Magnet Magnet Mater* 225: 1-7
- Gyure R.A., Konopka A., Brooks A. & Doemel W.** (1987) Algal and bacterial activities in acidic (pH 3) strip mine lakes. *Appl Environ Microbiol* 53: 2069-2076
- Gyure R.A., Konopka A., Brooks A. & Doemel W.** (1990) Microbial sulfate reduction in acidic (pH 3) strip mine lakes. *FEMS Microbiol Ecol* 73: 193-202
- Habicht K.S. & Canfield D.E.** (1996) Sulphur isotope fractionation in modern microbial mats and the evolution of the sulphur cycle. *Nature* 382: 342-343

- Haeckel E.** (1866) *Generelle morphologie der organismen: Allgemeine grundzuge der organischen formenwissenschaft, mechanisch begrundet durch die von Charles Darwin reformierte descendenz-Theorie*, 1 & 2, Georg Reimer: Berlin
- Hahn M.A., Tabb J.S. & Krauss T.D.** (2005) Detection of single bacterial pathogens with semiconductor quantum dots. *Anal Chem* 77: 4861-4869
- Hallberg K.B., Coupland K., Kimura S. & Johnson D.B.** (2006) Macroscopic streamer growths in acidic, metal-rich mine waters in North Wales consist of novel and remarkably simple bacterial communities. *Appl Environ Microbiol* 72: 2022-2030
- Hallberg K.B. & Johnson D.B.** (2001) Biodiversity of acidophilic prokaryotes. *Adv Appl Microbiol* 49: 37-84
- Hallmann R., Friedrich A., Koops H.P., Pommerening-Roser A., Rohde K., Zeeneck C. & Sand W.** (1992) Physiological characteristics of *Thiobacillus ferrooxidans* and *Leptospirillum ferrooxidans* and physicochemical factors influence microbial metal leaching. *Geomicrobiol J* 10: 193-206
- Han M., Gao X., Su J.Z. & Nie S.** (2001) Quantum-dot-tagged microbeads for multiplexed optical coding of biomolecules. *Nat Biotechnol* 19: 631-635
- Hanaki K.-i., Momo A., Oku T., Komoto A., Maenosono S., Yamaguchi Y. & Yamamoto K.** (2003) Semiconductor quantum dot/albumin complex is a long-life and highly photostable endosome marker. *Biochem Biophys Res Comm* 302: 496-501
- Hedderich R., Klimmek O., Kröger A., Dirmeier R., Keller M. & Stetter K.O.** (1999) Anaerobic respiration with elemental sulfur and with disulfides. *FEMS Microbiol Rev* 22: 353-381
- Henneberger R.** (2008) *The microbial diversity and ecology of selected andesitic hydrothermal environments*, Ph.D. thesis. Macquarie University, Australia
- Henneberger R., Moissl C., Amann T., Rudolph C. & Huber R.** (2006) New insights into the lifestyle of the cold-loving SM1 euryarchaeon: natural growth as a monospecies biofilm in the subsurface. *Appl Environ Microbiol* 72: 192-199
- Herrera A. & Cockell C.S.** (2007) Exploring microbial diversity in volcanic environments: a review of methods in DNA extraction. *J Microbiol Methods* 70: 1-12
- Hess B.C., Okhrimenko I.G., Davis R.C., Stevens B.C., Schulzke Q.A. & Wright K.C.** (2001) Surface transformation and photoinduced recovery in CdSe nanocrystals. *Phys Rev Lett* 86: 3132-3135
- Hetzer A., Morgan H.W., McDonald I.R. & Daughney C.J.** (2007) Microbial life in Champagne Pool, a geothermal spring in Waiotapu, New Zealand. *Extremophiles* 11: 605-614
- Hines M.A. & Guyot-Sionnest P.** (1996) Synthesis and characterization of strongly luminescing ZnS-capped CdSe nanocrystals. *J Phys Chem* 100: 468-471
- Hoheisel W., Colvin V.L., Johnson C.S. & Alivisatos A.P.** (1994) Threshold for quasi-continuum absorption and reduced luminescence efficiency in CdSe nanocrystals. *J Chem Phys* 101: 8455-8460
- Horejsh D., Martini F., Poccia F., Ippolito G., Caro A.D. & Capobianchi M.R.** (2005) A molecular beacon, bead-based assay for the detection of nucleic acids by flow cytometry. *Nucleic Acids Res* 33: e13
- Horikoshi K.** (1990) Genetic applications of alkaliphilic microorganisms. *FEMS Microbiol Rev* 6: 279-286

- Hoshino A., Fujioka K., Oku T., Nakamura S., Suga M., Yamaguchi Y., Suzuki K., Yasuhara M. & Yamamoto K.** (2004a) Quantum dots targeted to the assigned organelle in living cells. *Microbiol Immunol* 48: 985-994
- Hoshino A., Hanaki K.-i., Suzuki K. & Yamamoto K.** (2004b) Applications of T-lymphoma labeled with fluorescent quantum dots to cell tracing markers in mouse body. *Bioch Biophys Res Comm* 314: 46-53
- Houghton B. & Naira I.** (1991) The 1976-1982 Strombolian and phreatomagmatic eruptions of White Island, New Zealand: eruptive and depositional mechanisms at a "wet" volcano. *Bull Volcanol* 54: 25-49
- Houghton B.F. & Nairn I.A.** (1989a) The 1976-82 eruption sequence at White Island volcano, Bay of Plenty, New Zealand. *NZ Geol Surv Bull* 103: 1-136
- Houghton B.F. & Nairn I.A.** (1989b) The phreatomagmatic and Strombolian eruption events at White Island volcano 1976-82: eruption narrative. *NZ Geol Surv Bull* 103: 13-23
- Houghton B.F. & Nairn I.A.** (1989c) A model for the 1976-82 phreatomagmatic and Strombolian eruption sequence at White Island volcano, New Zealand. *NZ Geol Surv Bull* 103: 127-136
- Houghton B.F., Nairn I.A. & Scott B.J.** (1989) Phreatomagmatic and Strombolian eruptive activity at White Island volcano 1976-82: deposits and depositional mechanisms. *NZ Geol Surv Bull* 103: 35-56
- Houghton B.F., Scott B.J., Nairn I.A. & Wood C.P.** (1983) Cyclic variation in eruption products, White Island volcano, New Zealand 1976-1979. *NZ J Geol Geophys* 26: 213-216
- Howarth M., Takao K., Hayashi Y. & Ting A.Y.** (2005) Targeting quantum dots to surface proteins in living cells with biotin ligase. *Proc Natl Acad Sci USA* 102: 7583-7588
- Huber G. & Stetter K.O.** (2000) Thermoplasmatales. In: *The Prokaryotes: An evolving electronic resource for the microbiological community*. Ed. Dworkin M., Springer-Verlag, New York
- Huber H., Burggraf S., Mayer T., Wyszchony I., Rachel R. & Stetter K.O.** (2000a) *Ignicoccus* gen. nov., a novel genus of hyperthermophilic, chemolithoautotrophic Archaea, represented by two new species, *Ignicoccus islandicus* sp nov and *Ignicoccus pacificus* sp nov. *Int J Syst Evol Microbiol* 50: 2093-2100
- Huber R., Huber H. & Stetter K.O.** (2000b) Towards the ecology of hyperthermophiles: biotopes, new isolation strategies and novel metabolic properties. *FEMS Microbiol Rev* 24: 615-623
- Huber H., Hohn M.J., Rachel R., Fuchs T., Wimmer V.C. & Stetter K.O.** (2002) A new phylum of Archaea represented by a nanosized hyperthermophilic symbiont. *Nature* 417: 63-67
- Huber T., Faulkner G. & Hugenholtz P.** (2004) Bellerophon: a program to detect chimeric sequences in multiple sequence alignments. *Bioinformatics* 20: 2317-2319
- Hugenholtz P., Goebel B.M. & Pace N.R.** (1998a) Impact of culture-independent studies on the emerging phylogenetic view of bacterial diversity. *J Bacteriol* 180: 4765-4774
- Hugenholtz P., Pitulle C., Hershberger K.L. & Pace N.R.** (1998b) Novel division level bacterial diversity in a Yellowstone hot spring. *J Bacteriol* 180: 366-376
- Hurst A.W., Rickerby P.C., Scott B.J. & Hashimoto T.** (2004) Magnetic field changes on White Island, New Zealand, and the value of magnetic changes for eruption forecasting. *J Volcanol Geoth Res* 136: 53-70
- Ibrahim S.F. & van den Engh G.** (2003) High-speed cell sorting: fundamentals and recent advances. *Curr Opin Biotechnol* 14: 5-12

- Ibrahim S.F. & van den Engh G.** (2007) Flow cytometry and cell sorting. *Adv Biochem Eng Biotechnol* 106: 19-39
- Jackson C.R., Roden E.E. & Churchill P.F.** (1998) Changes in bacterial species composition in enrichment cultures with various dilutions of inoculum as monitored by denaturing gradient gel electrophoresis. *Appl Environ Microbiol* 64: 5046-5048
- Jaiswal J.K., Goldman E.R., Mattoussi H. & Simon S.M.** (2004) Use of quantum dots for live cell imaging. *Nat Methods* 1: 73-78
- Jaiswal J.K., Mattoussi H., Mauro J.M. & Simon S.M.** (2003) Long-term multiple color imaging of live cells using quantum dot bioconjugates. *Nat Biotechnol* 21: 47-51
- Jaiswal J.K. & Simon S.M.** (2004) Potentials and pitfalls of fluorescent quantum dots for biological imaging. *Trends Cell Biol* 14: 497-504
- Jamieson T., Bakhshi R., Petrova D., Pocock R., Imani M. & Seifalian A.M.** (2007) Biological applications of quantum dots. *Biomaterials* 28: 4717-4732
- Janssen P.H., Schuhmann A., Morschell E. & Rainey F.A.** (1997) Novel Anaerobic ultramicrobacteria belonging to the *Verrucomicrobiales* lineage of bacterial descent isolated by dilution culture from anoxic rice paddy soil. *Appl Environ Microbiol* 63: 1382-1388
- Janssen P.H., Yates P.S., Grinton B.E., Taylor P.M. & Sait M.** (2002) Improved culturability of soil bacteria and isolation in pure culture of novel members of the division *Acidobacteria*, *Actinobacteria*, *Proteobacteria* and *Verrucomicrobia*. *Appl Environ Microbiol* 68: 2391-2396
- Johnson D.B., Kelso W.I. & Jenkins D.A.** (1979) Bacterial streamer growth in a disused pyrite mine. *Environ. Pollut.* 18: 107-118
- Johnson D.B. & McGinnes S.** (1991) Ferric iron reduction by acidophilic heterotrophic bacteria. *Appl Environ Microbiol* 57: 207-211
- Johnson D.B., McGinness S. & Ghauri M.A.** (1993) Biogeochemical cycling of iron and sulfur in leaching environments. *FEMS Microbiol Rev* 11: 63-70
- Johnson D.B. & Rang L.** (1993) Effects of acidophilic protozoa on populations of metal-mobilising bacteria during the leaching of pyritic coal. *J Gen Microbiol* 139: 1417-1423
- Johnson D.B.** (1995) Selective solid media for isolation and enumerating acidophilic bacteria. *J Microbiol Methods* 23: 205-218
- Johnson D.B. & Roberto F.F.** (1997) Heterotrophic acidophiles and their roles in the bioleaching of sulfide minerals. In: *Biomining: Theory, microbes and industrial processes*. Eds. Rawlings D.E., Springer-Verlag/Landes Bioscience, Georgetown, TX.: 259-280
- Johnson D.B.** (1998) Biodiversity and ecology of acidophilic microorganisms. *FEMS Microbiol Ecol* 27: 307-317
- Johnson D.B.** (2001) Importance of microbial ecology in the development of new mineral technologies. *Hydrometallurgy* 59: 147-157
- Johnson D.B., Body D.A., Bridge T.A.M., Bruhn D.F. & Roberto F.F.** (1998) Biodiversity of acidophilic moderate thermophiles isolated from two sites in Yellowstone National Park, and their role in the dissimilatory oxido-reduction of iron. In: *Biodiversity, ecology and evolution of thermophiles in Yellowstone National Park*. Eds. Reysenbach A.L. and Mancinelli R., Plenum Press, New York

- Johnson D.B. & Hallberg K.B.** (2003) The microbiology of acidic mine waters. *Res Microbiol* 154: 466-473
- Johnson D.B., Okibe N. & Hallberg K.B.** (2005) Differentiation and identification of iron-oxidizing acidophilic bacteria using cultivation techniques and amplified ribosomal DNA restriction enzyme analysis. *J Microbiol Methods* 60: 299-313
- Johnson D.B., Okibe N. & Roberto F.F.** (2003) Novel thermo-acidophilic bacteria isolated from geothermal sites in Yellowstone National Park: physiological and phylogenetic characteristics. *Arch Microbiol* 180: 60-68
- Johnson D.B., Stallwood B., Kimura S. & Hallberg K.B.** (2006) Isolation and characterization of *Acidicaldus organivorus*, gen. nov., sp. nov.: a novel sulfur-oxidizing, ferric iron-reducing thermo-acidophilic heterotrophic Proteobacterium. *Arch Microbiol* 185: 212-221
- Jones B.E., Grant W.D., Duckworth A.W. & Owenson G.G.** (1998) Microbial diversity of soda lakes. *Extremophiles* 2: 191-200
- Jorgensen B.B.** (1982) Ecology of the bacteria of the sulfur cycle with special reference to anoxic-oxic interface environments. *Philos Trans R Soc Lond* 298: 543-561
- Jorgensen B.B.** (1994) Sulfate reduction and thiosulfate transformations in a cyanobacterial mat during a dial oxygen cycle. *FEMS Microbiol Ecol* 13: 303-312
- Jorgensen B.B., Isaksen M.F. & Jannasch H.W.** (1992) Bacterial sulfate reduction above 100°C in deep-sea hydrothermal vent sediments. *Science* 258: 1756-1757
- Kabata H., Kurosawa O., Arai I., Washizu M., Margaron S.A., Glass R.E. & Shimamoto N.** (1993) Visualization of single molecules of RNA polymerase sliding along DNA. *Science* 262: 1561-1563
- Kaerberlein T., Lewis K. & Epstein S.S.** (2002) Isolating "uncultivable" microorganisms in pure culture in a simulated natural environment. *Science* 296: 1127-1129
- Kalyuzhnaya M.G., Zabinsky R., Bowerman S., Baker D.R., Lidstrom M.E. & Chistoserdova L.** (2006) Fluorescence in situ hybridization-flow cytometry-cell sorting-based method for separation and enrichment of type I and type II methanotroph populations. *Appl Environ Microbiol* 72: 4293-4301
- Kamekura M.** (1998) Diversity of extremely halophilic bacteria. *Extremophiles* 2: 289-295
- Kampani K., Quann K., Ahuja J., Wigdahl B., Khan Z.K. & Jain P.** (2007) A novel high throughput quantum dot-based fluorescence assay for quantization of virus binding and attachment. *J Virol Methods* 141: 125-132
- Karavaiko G.I., Bogdanova T.I., Tourova T.P., Kondrat'eva T.F., Tsaplina I.A., Egorova M.A., Krasil'nikova E.N. & Zakharchuk L.M.** (2005) Reclassification of '*Sulfobacillus thermosulfidooxidans* subsp. *thermotolerans*' strain K1 as *Alicyclobacillus tolerans* sp. nov. and *Sulfobacillus disulfidooxidans*. *Int J Syst Evol Microbiol* 55: 941-947
- Kashefi K. & Lovley D.R.** (2003) Extending the upper temperature for life. *Science* 301: 5635
- Kashefi K.** (2004) Response to Cowan: The upper temperature for life - where do we draw the line?. *Trends in Microbiol* 12: 60-61
- Kawashima T., Amano N., Koike H., Makino S., Higuchi S., Kawashima-Ohya Y., Watanabe K., Yamazaki M., Kanehori K., Kawamoto T., Nunoshiba T., Yamamoto Y., Aramaki H., Makino K. &**

- Suzuki M.** (2000) Archaeal adaptation to higher temperatures revealed by genomic sequence of *Thermoplasma volcanium*. *Proc Natl Acad Sci USA* 97: 14257-14262
- Keller M. & Zengler K.** (2004) Tapping into microbial diversity. *Nat Rev Microbiol* 2: 141-150
- Kelly D.P.** (1982) Biochemistry of the chemolithotrophic oxidation of inorganic sulphur. *Philos Trans R Soc Lond B Biol Sci* 298: 499-528
- Kelly D.P., Shergill J.K., Lu W.P. & Wood A.P.** (1997) Oxidative metabolism of inorganic sulfur compounds by bacteria. *Antonie Van Leeuwenhoek* 71: 95-107
- Kelly D.P.** (1999) Thermodynamic aspects of energy conservation by chemolithotrophic sulfur bacteria in relation to the sulfur oxidation pathways. *Arch Microbiol* 171: 219-229
- Khanna M. & Stotzky G.** (1992) Transformation of *Bacillus subtilis* by DNA bound on montmorillonite and effect of DNase on the transforming ability of bound DNA. *Appl Environ Microbiol* 58: 1930-1939
- Kim S., Lim Y.T., Soltesz E.G., Grand A.M.D., Lee J., Nakayama A., Parker J.A., Mihaljevic T., Laurence R.G., Dor D.M., Cohn L.H., Bawendi M.G. & Frangioni J.V.** (2004) Near-infrared fluorescent type II quantum dots for sentinel lymph node mapping. *Nat Biotechnol* 22: 93-97
- Kinnunen P.H. & Puhakka J.A.** (2004) Characterization of iron- and sulphide mineral-oxidizing moderately thermophilic acidophilic bacteria from an Indonesian auto-heating copper mine waste heap and a deep South African gold mine. *J Ind Microbiol Biotechnol* 31: 409-414
- Kinnunen P.H., Robertson W.J., Plumb J.J., Gibson J.A., Nichols P.D., Franzmann P.D. & Puhakka J.A.** (2003) The isolation and use of iron-oxidizing, moderately thermophilic acidophiles from the Collie coal mine for the generation of ferric iron leaching solution. *Appl Microbiol Biotechnol* 60: 748-753
- Kirchner C., Liedl T., Kudera S., Pellegrino T., Munoz Javier A., Gaub H.E., Stolze S., Fertig N. & Parak W.J.** (2005) Cytotoxicity of colloidal CdSe and CdSe/ZnS nanoparticles. *Nano Lett* 5: 331-338
- Kirk J.L., Beaudette L.A., Hart M., Moutoglou P., Klironomos J.N., Lee H. & Trevors J.T.** (2004) Methods of studying soil microbial diversity. *J Microbiol Methods* 58: 169-188
- Klappenbach J.A., Saxman P.R., Cole J.R. & Schmidt T.M.** (2001) rrndb: The ribosomal RNA operon copy number database. *Nucleic Acids Res* 29: 181-184
- Klepner R.L. & Pratt J.R.** (1994) Use of fluorochromes for direct enumerations of total bacteria in environmental samples: Past and present *Microbiol Rev* 58: 603-615
- Kletzin A., Urich T., Muller F., Bandejas T.M. & Gomes C.M.** (2004) Dissimilatory oxidation and reduction of elemental sulfur in thermophilic archaea. *J Bioenerg Biomembr* 36: 77-91
- Kloepfer J.A., Mielke R.E., Wong M.S., Nealson K.H., Stucky G. & Nadeau J.L.** (2003) Quantum dots as strain- and metabolism-specific microbiological labels. *Appl Environ Microbiol* 69: 4205-4213
- Knoblauch C., Jorgensen B.B. & Harder J.** (1999) Community size and metabolic rates of psychrophilic sulfate-reducing bacteria in Arctic marine sediments. *Appl Environ Microbiol* 65: 4230-4233
- Kolarova H. & Hengerer B.** (1996) Preparation of magnetic oligo (dT) particles. *Biotechniques* 20: 196-198
- Krsek M. & Wellington E.M.** (1999) Comparison of different methods for the isolation and purification of total community DNA from soil. *J Microbiol Methods* 39: 1-16

- Kuno M., Lee J.K., Dabbousi B.O., Mikulec F.V. & Bawedi M.G.** (1997) The band edge luminescence of surface modified CdSe nanocrystallites: Probing the luminescing state. *J. Chem. Phys* 106: 9869-9882
- Küsel K., Roth U. & Drake H.L.** (2002) Microbial reduction of Fe(III) in the presence of oxygen under low pH conditions. *Environ Microbiol* 4: 414-421
- Küsel K., Roth U., Trinkwalter T. & Peiffer S.** (2001) Effect of pH on the anaerobic microbial cycling of sulfur in mining-impacted freshwater lake sediments. *Environ Exper Bot* 46: 213-223
- Kvist T., Ahring B.K. & Westermann P.** (2007) Archaeal diversity in Icelandic hot springs. *FEMS Microbiol Ecol* 59: 71-80
- Kvist T., Mengewein A., Manzei S., Ahring B.K. & Westermann P.** (2005) Diversity of thermophilic and non-thermophilic Crenarchaeota at 80 degrees C. *FEMS Microbiol Lett* 244: 61-68
- Lane D.J.** (1991) 16S/23S rRNA sequencing. In: *Nucleic acid techniques in bacterial systematics*. Eds. Stackebrandt E. and Goodfellow M., John Wiley & Sons: 115–175
- Lane D.J., Arthur P. Harrison J., Stahl D., Pace B., Giovannoni S.J., Olsen G.J. & Pace N.R.** (1992) Evolutionary relationships among sulfur- and iron-oxidizing Eubacteria. *J Bacteriol* 174: 269-278
- Langdahl B.R. & Ingvorsen K.** (1997) Temperature characteristics of bacterial iron solubilisation and ¹⁴C assimilation in naturally exposed sulfide ore material at Citronen Fjord, Greenland (83°N). *FEMS Microbiol Ecol* 23: 275-283
- Lazaroff N., Sigal W. & Wasserman A.** (1982) Iron oxidation and precipitation of ferric hydroxysulfates by resting *Thiobacillus ferrooxidans* cells. *Appl Environ Microbiol* 43: 924-938
- Leadbetter J.R.** (2003) Cultivation of recalcitrant microbes: cells are alive, well and revealing their secrets in the 21st century laboratory. *Curr Opin Microbiol* 6: 274-281
- Leatherdale C.A., Woo W.K., Mikulec F.V. & Bawendi M.G.** (2002) On the absorption cross section of CdSe nanocrystal quantum dots. *J Phys Chem B* 106: 7619-7622
- Lee L.Y., Ong S.L., Hu J.Y., Ng W.J., Feng Y., Tan X. & Wong S.W.** (2004) Use of semiconductor quantum dots for photostable Immunofluorescence labeling of *cryptosporidium parvum*. *App Environ Microbiol* 70: 5732-5736
- Lenaerts J., Lappin-Scott H.M. & Porter J.** (2007) Improved fluorescent *in situ* hybridization method for detection of bacteria from activated sludge and river water by using DNA molecular beacons and flow cytometry. *Appl Environ Microbiol* 73: 2020-2023
- Lettl A., Langkramer O. & Lochman V.** (1981) Dynamics of oxidation of inorganic sulphur compounds in upper soil horizons of spruce forests. *Folia Microbiol (Praha)* 26: 24-28
- Li H., Yang M., Zhang Y., Yu T. & Kamagata Y.** (2006) Nitrification performance and microbial community dynamics in a submerged membrane bioreactor with complete sludge retention. *J Biotechnol* 123: 60-70
- Li Y., Dick W.A. & Tuovinen O.H.** (2004) Fluorescence microscopy for visualization of soil microorganisms-a review. *Biol Fert Soils* 39: 301-311
- Liang R.Q., Li W., Li Y., Tan C.Y., Li J.X., Jin Y.X. & Ruan K.C.** (2005) An oligonucleotide microarray for microRNA expression analysis based on labeling RNA with quantum dot and nanogold probe. *Nucleic Acids Res* 33: e17

- Lidke D.S. & Arndt-Jovin D.J.** (2004) Imaging takes a quantum leap. *Physiology* 19: 322-325
- Lidke D.S., Nagy P., Heintzmann R., Arndt-Jovin D.J., Post J.N., Grecco H.E., Jares-Erijman E.A. & Jovin T.M.** (2004) Quantum dot ligands provide new insights into erbB/HER receptor-mediated signal transduction. *Nat Biotechnol* 22: 198-203
- Lim Y.T.** (2003) Selection of quantum dot wavelengths for biomedical assays and imaging. *Mol Imaging* 2: 50-64
- Liu T.C., Huang Z.L., Wang H.Q., Wang J.H., Li X.Q. & Zhao Y.D.** (2006) Temperature-dependent photoluminescence of water-soluble quantum dots for a bioprobe. *Anal Chim Acta* 559: 120-123
- Liu W.T. & Zhu L.** (2005) Environmental microbiology-on-a-chip and its future impacts. *Trends Biotechnol* 23: 174-179
- Lochhead A.G. & Chase F.E.** (1943) Qualitative studies of soil microorganisms: v. nutritional requirements of the predominant bacterial flora. *Soil Sci* 55: 185-196
- Loessner M.J., Rees C.E., Stewart G.S. & Scherer S.** (1996) Construction of luciferase reporter bacteriophage A511::luxAB for rapid and sensitive detection of viable *Listeria* cells. *Appl Environ Microbiol* 62: 1133-1140
- Lopez-Archilla A.I., Gerard E., Moreira D. & Lopez-Garcia P.** (2004) Macrofilamentous microbial communities in the metal-rich and acidic River Tinto, Spain. *FEMS Microbiol Lett* 235: 221-228
- Lopez-Archilla A.I., Marin I. & Amils R.** (2001) Microbial community composition and ecology of an acidic aquatic environment: The Tinto River, Spain. *Microbiol Ecol* 41: 20-35
- Losekann T., Knittel K., Nadalig T., Fuchs B., Niemann H., Boetius A. & Amann R.** (2007) Diversity and abundance of aerobic and anaerobic methane oxidizers at the Haakon Mosby Mud Volcano, Barents Sea. *Appl Environ Microbiol* 73: 3348-3362
- Lovric J., Bazzi H.S., Cuie Y., Fortin G.R., Winnik F.M. & Maysinger D.** (2005) Differences in subcellular distribution and toxicity of green and red emitting CdTe quantum dots. *J Mol Med* 83: 377-385
- Lowe M., Spiro A., Zhang Y.-Z. & Getts R.** (2004) Multiplexed, particle-based detection of DNA using flow cytometry with 3D dendrimers for signal amplification. *Cytometry A* 60A: 135-144
- Ludwig W., Strunk O., Westram R., Richter L., Meier H., Yadhukumar, Buchner A., Lai T., Steppi S., Jobb G., Forster W., Brettske I., Gerber S., Ginhart A.W., Gross O., Grumann S., Hermann S., Jost R., Konig A., Liss T., Lussmann R., May M., Nonhoff B., Reichel B., Strehlow R., Stamatakis A., Stuckmann N., Vilbig A., Lenke M., Ludwig T., Bode A. & Schleifer K.H.** (2004) ARB: a software environment for sequence data. *Nucleic Acids Res* 32: 1363-1371
- Madsen E.L.** (2005) Identifying microorganisms responsible for ecologically significant biogeochemical processes. *Nat Rev Microbiol* 3: 439-446
- Mahtab R., Sealey S.M., Hunyadi S.E., Kinard B., Ray T. & Murphy C.J.** (2007) Influence of the nature of quantum dot surface cations on interactions with DNA. *J Inorg Biochem* 101: 559-564
- Mangiapan G., Vokurka M., Schouls L., Cadranel J., Lecossier D., van Embden J. & Hance A.J.** (1996) Sequence capture-PCR improves detection of mycobacterial DNA in clinical specimens. *J Clin Microbiol* 34: 1209-1215
- Manna L., Scher E.C., Li L.S. & Alivisatos A.P.** (2002) Epitaxial growth and photochemical annealing of graded CdS/ZnS shells on colloidal CdSe nanorods. *J Am Chem Soc* 124: 7136-7145

Manning H.L. (1975) New media for isolating iron-oxidizing and heterotrophic acidophilic Bacteria from acid mine drainage. *Appl Microbiol* 30: 1010-1016

Mansson A., Sundberg M., Balaz M., Bunk R., Nicholls I.A., Omling P., Tagerud S. & Montelius L. (2004) In vitro sliding of actin filaments labelled with single quantum dots. *Biochem Biophys Res Comm* 314: 529-534

Marsh T.L. (1999) Terminal restriction fragment length polymorphism (T-RFLP): an emerging method for characterizing diversity among homologous populations of amplification products. *Curr Opin Microbiol* 2: 323-327

Mattheakis L.C., Dias J.M., Choi Y.-J., Gong J., Bruchez M.P., Liu J. & Wang E. (2004) Optical coding of mammalian cells using semiconductor quantum dots. *Anal Biochem* 327: 200-208

Mattoussi H., Mauro J.M., Goldman E.R., Anderson G.P., Sundar V.C., Mikulec F.V. & Bawedi M.G. (2000) Self-assembly of CdSe-ZnS quantum dot bioconjugates using an engineered recombinant protein. *J Am Chem Soc* 122: 12142-12150

McCaig A.E., Glover L.A. & Prosser J.I. (1999) Molecular analysis of bacterial community structure and diversity in unimproved and improved upland grass pastures. *Appl Environ Microbiol* 65: 1721-1730

McGinness S. & Johnson D.B. (1992) Grazing of acidophilic bacteria by a flagellate protozoan. *Microbiol Ecol* 23: 75-86

McHale R.H., Stapleton P.M. & Bergquist P.L. (1991) Rapid preparation of blood and tissue samples for polymerase chain reaction. *Biotechniques* 10: 20, 22-23

Medintz I.L., Clapp A.R., Brunel F.M., Tiefenbrunn T., Uyeda H.T., Chang E.L., Deschamps J.R., Dawson P.E. & Mattoussi H. (2006) Proteolytic activity monitored by fluorescence resonance energy transfer through quantum-dot-peptide conjugates. *Nat Mater* 5: 581-589

Medintz I.L., Uyeda H.T., Goldman E.R. & Mattoussi H. (2005) Quantum dot bioconjugates for imaging, labelling and sensing. *Nat Mater* 4: 435-446

Meyer-Dombard D.R., Shock E.L. & Amend J.P. (2005) Archaeal and bacterial communities in geochemically diverse hot springs of Yellowstone National Park, USA. *Geobiology* 3: 211-277

Michalet X., Pinaud F., Lacoste T.D., Dahan M., Bruchez M.P. & Alivastos A.P. (2001) Properties of fluorescent semiconductor nanocrystals and their applications to biological labeling. *Single Molec* 2: 261-276

Michalet X., Pinaud F.F., Bentolila L.A., Tsay J.M., Doose S., Li J.J., Sundaresan G., Wu A.M., Gambhir S.S. & Weiss S. (2005) Quantum dots for live cells, *in vivo* imaging, and diagnostics. *Science* 307: 538-544

Miller D.N., Bryant J.E., Madsen E.L. & Ghiorse W.C. (1999) Evaluation and optimization of DNA extraction and purification procedures for soil and sediment samples. *Appl Environ Microbiol* 65: 4715-4724

Miquel P. (1888) Monographie d'un bacilli vivant au delá de 70 centigrades. *Ann Micrographie* 1: 3-10

Miteva V.I., Sheridan P.P. & Brenchley J.E. (2004) Phylogenetic and physiological diversity of microorganisms isolated from a deep Greenland glacier ice core. *Appl Environ Microbiol* 70: 202-213

Moira R.Y. (1975) Psychrophilic bacteria. *Bacteriol Rev* 39: 144-167

- Moissl C., Rudolph C., Rachel R., Koch M. & Huber R.** (2003) *In situ* growth of the novel SM1 euryarchaeon from a string-of-pearls-like microbial community in its cold biotope, its physical separation and insights into its structure and physiology. *Arch Microbiol* 180: 211-217
- Mongillo M.A. & Wood C.P.** (1995) Thermal infrared mapping of White Island volcano, New Zealand. *J Volcan Geoth Research* 69: 59-71
- Montegrossi G., Tassi F., Vaselli O., Buccianti A. & Garofalo K.** (2001) Sulfur species in volcanic gases. *Anal Chem* 73: 3709-3715
- Moon V., Bradshaw J., Smith R. & de Lange W.** (2005) Geotechnical characterization of stratocone crater wall sequences, White Island Volcano, New Zealand *Eng Geol* 81: 146-178
- Morgan E., Varro R., Sepulveda H., Ember J.A., Apgar J., Wilson J., Lowe L., Chen R., Shivraj L., Agadir A., Campos R., Ernst D. & Gaur A.** (2004) Cytometric bead array: a multiplexed assay platform with applications in various areas of biology. *Clinical Immunol* 110: 252-266
- Moter A. & Gobel U.B.** (2000) Fluorescence *in situ* hybridization (FISH) for direct visualization of microorganisms. *J Microbiol Methods* 41: 85-112
- Murray C.B., Kagan C.R. & Bawendi M.G.** (2000) Synthesis and characterization of monodisperse nanocrystals and close-packed nanocrystals assemblies. *Annu Rev Mater Sci* 30: 545-610
- Nairn I.A. & Houghton B.F.** (1989) Formation of collapse craters and morphological changes in the main crater of White Island volcano during the 1976-82 eruption sequence. *NZ Geol Surv Bull* 103: 25-34
- Nercessian O., Prokofeva M., Lebedinski A., L'Haridon S., Cary C., Prieur D. & Jeanthon C.** (2004) Design of 16S rRNA-targeted oligonucleotide probes for detecting cultured and uncultured archaeal lineages in high-temperature environments. *Environ Microbiol* 6: 170-182
- Niederberger T.D., Gotz D.K., McDonald I.R., Ronimus R.S. & Morgan H.W.** (2006) *Ignisphaera aggregans* gen. nov., sp. nov., a novel hyperthermophilic crenarchaeote isolated from hot springs in Rotorua and Tokaanu, New Zealand. *Int J Syst Evol Microbiol* 56: 965-971
- Niederberger T.D., McDonald I.R., Hacker A.L., Soo R.M., Barrett J.E., Wall D.H. & Cary S.C.** (2008) Microbial community composition in soils of Northern Victoria Land, Antarctica. *Environ Microbiol: in press.*
- Nies D.H.** (1999) Microbial heavy-metal resistance. *Appl Microbiol Biotechnol* 51: 730-750
- Nisbet E.G. & Sleep N.H.** (2001) The habitat and nature of early life. *Nature* 409: 1083-1091
- Nishi Y., Sherburn S., Scott B.J. & Sugihara M.** (1996) High-frequency earthquakes at White Island volcano, New Zealand: insights into the shallow structure of a volcano-hydrothermal system. *J Volcanol Geother Research* 72: 183-197
- Norris P.R.** (1990) Acidophilic bacteria and their activity in mineral sulfide oxidation. In: *Microbial Mineral Recovery*. Eds. Ehrlich H.L. and Brierley C.L., McGraw-Hill, New York, NY: 3-27
- Norris D.J. & Bawendi M.G.** (1996a) Measurement and assignment of the size-dependent optical spectrum in CdSe quantum dots. *Phys Rev B Condens Matter* 53: 16338-16346
- Norris P.R., Clark D.A., Owen J.P. & Waterhouse S.** (1996b) Characteristics of *Sulfobacillus acidophilus* sp. nov. and other moderately thermophilic mineral sulphide-oxidizing bacteria. *Microbiology* 141: 775-783

- Norris P.R., Burton N.P. & Foulis N.A.** (2000) Acidophiles in bioreactor mineral processing. *Extremophiles* 4: 71-76
- Norris T.B., Wraith J.M., Castenholz R.W. & McDermott T.R.** (2002) Soil microbial community structure across a thermal gradient following a geothermal heating event. *Appl Env Microbiol* 68: 6300-6309
- Okibe N. & Johnson D.B.** (2004) Biooxidation of pyrite by defined mixed cultures of moderately thermophilic acidophiles in pH-controlled bioreactors: significance of microbial interactions. *Biotechnol Bioeng* 87: 574-583
- Olsen G.J., Lane D.J., Giovannoni S.J. & Pace N.R.** (1986) Microbial ecology and evolution: A ribosomal RNA approach. *Ann Rev Microbiol* 40: 337-365
- Osborne C.A., Galic M., Sangwan P. & Janssen P.H.** (2005) PCR-generated artefact from 16S rRNA gene-specific primers. *FEMS Microbiol Lett* 248: 183-187
- Otsuka Y., Hanaki K., Zhao J., Ohtsuki R., Toyooka K., Yoshikura H., Kuratsuji T., Yamamoto K. & Kirikae T.** (2004) Detection of *Mycobacterium bovis* Bacillus Calmette-Guerin using quantum dot immuno-conjugates. *Jpn J Infect Dis* 57: 183-184
- Ozkan M.** (2004) Quantum dots and other nanoparticles: what can they offer to drug discovery? *Drug Discov Today* 9: 1065-1071
- Pace N.R.** (1997) A molecular view of microbial diversity and the biosphere. *Science* 276: 734-740
- Page S. & Burns R.G.** (1991) Flow cytometry as a means of enumerating bacteria introduced into soil. *Soil Biol Biochem* 23: 1025-1028
- Palleroni N.J.** (1997) Prokaryotic diversity and the importance of culturing. *Antonie Van Leeuwenhoek* 72: 3-19
- Parak W.J. & Pellegrino T.** (2005) Labelling of cells with quantum dots. *Nanotechnology* 16: R9-R25
- Parker C.D. & Prisk J.** (1953) The oxidation of inorganic compounds of sulphur by various sulphur bacteria. *J Gen Microbiol* 8: 344-364
- Patel G.B. & Sprott G.D.** (1999) Archaeobacterial ether lipid liposomes (archaeosomes) as novel vaccine and drug delivery systems. *Crit Rev Biotechnol* 19: 317-357
- Pernthaler A., Pernthaler J. & Amann R.** (2002) Fluorescence *in situ* hybridization and catalyzed reporter deposition for the identification of marine bacteria. *Appl Environ Microbiol* 68: 3094-3101
- Pernthaler J., Pernthaler A. & Amann R.** (2003) Automated enumeration of groups of marine picoplankton after fluorescence *in situ* hybridization. *Appl Environ Microbiol* 69: 2631-2637
- Pikuta E.V., Hoover R.B. & Tang J.** (2007) Microbial extremophiles at the limits of life. *Crit Rev Microbiol* 33: 183-209
- Pinaud F., Michalet X., Bentolila L.A., Tsay J.M., Doose S., Li J.J., Iyer G. & Weiss S.** (2006) Advances in fluorescence imaging with quantum dot bio-probes. *Biomaterials* 27: 1679-1687
- Pinkel D. & Steen H.B.** (1982) Simple methods to determine and compare the sensitivity of flow cytometers. *Cytometry* 3: 220-223

- Porter J., Deere D., Hardman M., Edwards C. & Pickup R.W.** (1997) Go with the flow - use of flow cytometry in environmental microbiology. *FEMS Microbiol Ecol* 24: 93-101
- Poulsen L.K., Ballard G. & Stahl D.A.** (1993) Use of rRNA fluorescence *in situ* hybridization for measuring the activity of single cells in young and established biofilms *Appl Environ Microbiol* 59: 1354-1360
- Prescott L.M., Harley J.P. & Klein D.A.** (1996) The diversity of the microbial world. In: *Microbiology*. Eds. Prescott L.M., Harley J.P. and Klein D.A., WCB Publishers, Dubuque, Iowa
- Pronk J.T. & Johnson D.B.** (1992) Oxidation and reduction of iron by acidophilic bacteria. *Geomicrobiol. J.* 10: 153-171
- Pronk J.T., Meijer W.M., Hazeu W., van Dijken J.P., Bos P. & Kuenen J.G.** (1991) Growth of *Thiobacillus ferrooxidans* on formic acid. *Appl Environ Microbiol* 57: 2057-2062
- Qu L. & Peng X.** (2002) Control of photoluminescence properties of CdSe nanocrystals in growth. *J Am Chem Soc* 124: 2049-2055
- Raj H.D., Duryee F.L., Deeney A.M., Wang C.H., Anderson A.W. & Elliker P.R.** (1960) Utilization of carbohydrates and amino acids by *Micrococcus radiodurans*. *Can J Microbiol* 6: 289-298
- Rappe M.S., Connon S.A., Vergin K.L. & Giovannoni S.J.** (2002) Cultivation of the ubiquitous SAR11 marine bacterioplankton clade. *Nature* 418: 630-633
- Rappe M.S. & Giovannoni S.J.** (2003) The uncultured microbial majority. *Annu Rev Microbiol* 57: 369-394
- Rawlings D.E.** (2005) Characteristics and adaptability of iron- and sulfur-oxidizing microorganisms used for the recovery of metals from minerals and their concentrates. *Microb Cell Fact* 4: 13
- Reysenbach A.L. & Cady S.L.** (2001) Microbiology of ancient and modern hydrothermal systems. *Trends Microbiol* 9: 79-86
- Reysenbach A.L., Giver L.J., Wickham G.S. & Pace N.R.** (1992) Differential amplification of rRNA genes by polymerase chain reaction. *Appl Environ Microbiol* 58: 3417-3418
- Reysenbach A.L., Longnecker K. & Kirshtein J.** (2000) Novel bacterial and archaeal lineages from an *in situ* growth chamber deployed at a Mid-Atlantic Ridge hydrothermal vent. *Appl Environ Microbiol* 66: 3798-3806
- Rieger S., Kulkarni R.P., Darcy D., Fraser S.E. & Koster R.W.** (2005) Quantum dots are powerful multipurpose vital labeling agents in zebrafish embryos. *Dev Dyn* 234: 670-681
- Riegler J. & Nann T.** (2004) Application of luminescent nanocrystals as labels for biological molecules. *Anal Bioanal Chem* 10.1007: s00216-00004-02706-y
- Ritchie N.J., Schutter M.E., Dick R.P. & Myrold D.D.** (2000) Use of length heterogeneity PCR and fatty acid methyl ester profiles to characterize microbial communities in soil. *Appl Environ Microbiol* 66: 1668-1675
- Rodriguez-Valera F., Juez G. & Kushner D.J.** (1983) *Halobacterium mediterranei* spec. nov., a new carbohydrate-utilizing extreme halophile. *Syst Appl Microbiol* 4: 369-381
- Roederer M.** (2001) Spectral compensation for flow cytometry: visualization artifacts, limitations, and caveats. *Cytometry* 45: 194-205

- Roh C., Villatte F., Kim B.G. & Schmid R.D.** (2006) Comparative study of methods for extraction and purification of environmental DNA from soil and sludge samples. *Appl Biochem Biotechnol* 134: 97-112
- Rohwerder T., Gehrke T., Kinzler K. & Sand W.** (2003) Bioleaching review part A: progress in bioleaching: fundamentals and mechanisms of bacterial metal sulfide oxidation. *Appl Microbiol Biotechnol* 63: 239-248
- Roling W.F., Ortega-Lucach S., Larter S.R. & Head I.M.** (2006) Acidophilic microbial communities associated with a natural, biodegraded hydrocarbon seepage. *J Appl Microbiol* 101: 290-299
- Rondon M.R., Goodman R.M. & Handelsman J.** (1999) The Earth's bounty: assessing and accessing soil microbial diversity. *Tibtech* 17: 403-409
- Rossello-Mora R. & Amann R.** (2001) The species concept for prokaryotes. *FEMS Microbiol Rev* 25: 39-67
- Rossetti R. & Brus L.** (1982) Electron-hole recombination emission as a probe of surface chemistry in aqueous CdS colloids. *J Phys Chem* 86: 4470-4472
- Rothschild L.J.** (1990) Earth analogs for Martian life. Microbes in evaporites, a new model system for life on Mars. *Icarus* 88: 246-260
- Rothschild L.J.** (2007) Extremophiles: defining the envelope for the search for life in the universe. In: *Planetary systems and the origin of life*. Eds. Pudritz R., Higgs P. and Stone J., Cambridge, Astrobiology: 111-134
- Rothschild L.J. & Mancinelli R.L.** (2001) Life in extreme environments. *Nature* 409: 1092-1101
- Rowe O.F., Sanchez-Espana J., Hallberg K.B. & Johnson D.B.** (2007) Microbial communities and geochemical dynamics in an extremely acidic, metal-rich stream at an abandoned sulfide mine (Huelva, Spain) underpinned by two functional primary production systems. *Environ Microbiol* 9: 1761-1771
- Rudolph C., Wanner G. & Huber R.** (2001) Natural communities of novel Archaea and Bacteria growing in cold sulfurous springs with a string-of-pearls-like morphology. *Appl Environ Microbiol* 67: 2336-2344
- Rusch A. & Amend J.P.** (2004) Order-specific 16S rRNA-targeted oligonucleotide probes for (hyper)thermophilic archaea and bacteria. *Extremophiles* 8: 357-366
- Sait M., Hugenholtz P. & Janssen P.H.** (2002) Cultivation of globally distributed soil bacteria from phylogenetic lineages previously only detected in cultivation-independent surveys. *Environ Microbiol* 4: 654-666
- Sand W., Gehrke T., Hallmann R. & Schippers A.** (1995) Sulfur chemistry, biofilm, and the (in)direct attack mechanism - critical evaluation of bacterial leaching. *Appl Microbiol Biotechnol* 43: 961-966
- Sapsford K.E., Bert L. & Medintz I.L.** (2006) Materials for fluorescence resonance energy transfer analysis beyond traditional donor-acceptor combinations. *Angew. Chem. Int. Edn* 45: 4562-4588
- Saul D.J., Reeves R.A., Morgan H.W. & Bergquist P.L.** (1999) *Thermus* diversity and strain loss during enrichment. *FEMS Microbiol Ecol* 30: 157-162
- Saul D.J., Rodrigo A.G., Reeves R.A., Williams L.C., Borges K.M., Morgan H.W. & Bergquist P.L.** (1993) Phylogeny of twenty *Thermus* isolates constructed from 16S rRNA gene sequence data. *Int J Syst Bacteriol* 43: 754-760

- Scarth A.** (1994) *Volcanoes*, London, UCL Press Limited
- Scott B.J., Houghton B.F. & Wilson C.J.M.** (1995) Surveillance of New Zealand volcanos. *Tepha* 14: 12-17
- Schleifer K.H.** (2004) Microbial diversity: facts, problems and prospects. *Syst Appl Microbiol* 27: 3-9
- Schleper C., Puehler G., Holz I., Gambacorta A., Janekovic D., Santarius U., Klenk H.P. & Zillig W.** (1995) *Picrophilus* gen. nov., fam. nov.: a novel aerobic, heterotrophic, thermoacidophilic genus and family comprising archaea capable of growth around pH 0. *J Bacteriol* 177: 7050-7059
- Schleper C., Pühler G., Klenk H.P. & Zillig W.** (1996) *Picrophilus ashimae* and *Picrophilus torridus* fam. nov., sp., two species of hyperacidophilic, thermophilic, heterotrophic, aerobic Archaea. *Int J Syst Bacteriol* 46: 814-816
- Schmidt-Nielsen S.** (1902) Ueber einige psychrophile Mikroorganismen und ihr Vorkommen. *Zentralblatt für Bakteriologie, Parasitenkunde, Infektionskrankheiten und Hygiene, Abteilung 9*: 145-147
- Scholten J.C., Joye S.B., Hollibaugh J.T. & Murrell J.C.** (2005) Molecular analysis of the sulfate reducing and archaeal community in a meromictic soda lake (Mono Lake, California) by targeting 16S rRNA, *mcrA*, *apsA*, and *dsrAB* genes. *Microbiol Ecol* 50: 29-39
- Schönhuber W., Fuchs b., Juretschko S. & Amann R.** (1997) Improved sensitivity of whole-cell hybridization by the combination of horseradish peroxidase-labeled oligonucleotides and tyramide signal amplification. *Appl Environ Microbiol* 63: 3268-3273
- Schopf J.W.** (2006) Fossil evidence of Archaean life. *Philos Trans R Soc Lond B Biol Sci* 361: 869-885
- Schrenk M.O., Kelley D.S., Delaney J.R. & Baross J.A.** (2003) Incidence and diversity of microorganisms within the walls of an active deep-sea sulfide chimney. *Appl Environ Microbiol* 69: 3580-3592
- Schwartz A., Gaigalas A.K., Wang L., Marti G.E., Vogt R.F. & Fernandez-Repollet E.** (2004) Formalization of the MESF unit of fluorescence intensity. *Cytometry B Clin Cytom* 57: 1-6
- Schwartz A., Marti G.E., Poon R., Gratama J.W. & Fernández-Repollet E.** (1998) Standardizing flow cytometry: A classification system of fluorescence standards used for flow cytometry. *Cytometry* 33: 106-114
- Schwartz A., Wang L., Early E., Gaigalas A.K., Zhang Y., Marti G.E. & vogt R.F.** (2002) Quantitating fluorescence intensity from fluorophore: The definition of MESF assignment. *J Res Natl and Technol* 107: 83-91
- Segerer A.H., Burggraf S., Fiala G., Huber G., Huber R., Pley U. & Stetter K.O.** (1993) Life in hot springs and hydrothermal vents. *Orig Life Evol Biosph* 23: 77-90
- Shane P., Sikes E.L. & Guilderson T.P.** (2006) Tephra beds in deep-sea cores off northern New Zealand: implications for the history of Taupo Volcanic Zone, Mayor Island and White Island volcanoes. *J Volcanol Geother Research* 154: 276-290
- Shapiro H.M.** (1977) Fluorescent dyes for differential counts by flow cytometry: does histochemistry tell us much more than cell geometry? *J Histochem Cytochem* 25: 976-989
- Shapiro H.M.** (1986) Technical developments in flow cytometry. *Hum Pathol* 17: 649-651
- Shapiro H.M.** (1993) Cell Measurement. *Science* 260: 1533

- Shapiro H.M.** (2000) Microbial analysis at the single-cell level: tasks and techniques. *J Microbiol Methods* 42: 3-16
- Shapiro H.M.** (2001) Principles of data acquisition and display. *Methods Cell Biol* 63: 149-167
- Shapiro H.M.** (2004) The evolution of cytometers. *Cytometry A* 58: 13-20
- Shapiro H.M., Perlmutter N.G. & Stein P.G.** (1998) A flow cytometer designed for fluorescence calibration. *Cytometry* 33: 280-287
- Sharma P., Brown S., Walter G., Santra S. & Moudgil B.** (2006) Nanoparticles for bioimaging. *Adv Colloid Interface Sci* 123-126: 471-485
- Shiohara A., Hoshino A., Hanaki K.-i., Suzuki K. & Yamamoto K.** (2004) On the cyto-toxicity caused by quantum dots. *Microbiol Immunol* 48: 669-675
- Shock E.L.** (1996) Hydrothermal systems as environments for the emergence of life. *Ciba Found Symp* 202: 40-52; discussion 52-60
- Sievert S.M., Ziebis W., Kuever J. & Sahm K.** (2000) Relative abundance of Archaea and Bacteria along a thermal gradient of a shallow-water hydrothermal vent quantified by rRNA slot-blot hybridization. *Microbiology* 146 (Pt 6): 1287-1293
- Silverman M.P.** (1967) Mechanism of bacterial pyrite oxidation. *J Bacteriol* 94: 1046-1051
- Simbahan J., Drijber R. & Blum P.** (2004) Alicyclobacillus vulcanalis sp. nov., a thermophilic, acidophilic bacterium isolated from Coso Hot Springs, California, USA. *Int J Syst Evol Microbiol* 54: 1703-1707
- Simkin T.** (1993) Terrestrial volcanism in space and time. *Ann Rev Earth Pl Sc* 21: 427-452
- Simkin T. & Siebert L.** (2000) Earth's volcanoes and eruptions: an overview. In: *Encyclopedia of Volcanoes*. Ed. Sigurdsson H., Academic Press: 249-261
- Simmons S. & Norris R.** (2002) Acidophiles of saline water at thermal vents of Vulcano, Italy. *Extremophiles* 6: 201-207
- Simon N., LeBot N., Marie D., Partensky F. & Vaultot D.** (1995) Fluorescent *in situ* hybridization with rRNA-targeted oligonucleotide probes to identify small phytoplankton by flow cytometry. *Appl Environ Microbiol* 61: 2506-2513
- Singleton D.R., Furlong M.A., Rathbun S.L. & Whitman W.B.** (2001) Quantitative comparisons of 16S rRNA gene sequence libraries from environmental samples. *Appl Environ Microbiol* 67: 4374-4376
- Smith A.M. & Nie S.** (2004) Chemical analysis and cellular imaging with quantum dots. *Analyst* 129: 672-677
- Smith J.J., Tow L.A., Stafford W., Cary C. & Cowan D.A.** (2006) Bacterial diversity in three different Antarctic cold desert mineral soils. *Microbiol Ecol* 51: 413-421
- So M.K., Xu C., Loening A.M., Gambhir S.S. & Rao J.** (2006) Self-illuminating quantum dot conjugates for *in vivo* imaging. *Nat Biotechnol* 24: 339-343
- Speckman D.M., Jennings T.L., LaLumondiere S.D. & Moss S.C.** (2002) Quenching phenomena in water-soluble CdSe/ZnS Quantum dots. *Mat. Res. Soc. Symp. Proc.* 704: 269-274

- Spiegelman D., Whissell G. & Greer C.W.** (2005) A survey of the methods for the characterization of microbial consortia and communities. *Can J Microbiol* 51: 355-386
- Spiro A. & Lowe M.** (2002) Quantification of DNA sequences in environmental PCR products by a multiplexed, bead-based method. *Appl Environ Microbiol* 68: 1010-1013
- Spiro A., Lowe M. & Brown D.** (2000) A bead-based method for multiplexed identification and quantitation of DNA sequences using flow cytometry. *Appl Environ Microbiol* 66: 4258-4265
- Stahl D.A. & Amann R.** (1991) Development and application of nucleic acid probes. In: *Nucleic acid techniques in bacterial systematics*. Eds. E. S. and M. G., Wiley, Chichester: 205-248
- Stender H., Lund K., Petersen K.H., Rasmussen O.F., Hongmanee P., Miorner H. & Godtfredsen S.E.** (1999) Fluorescence *in situ* hybridization assay using peptide nucleic acid probes for differentiation between tuberculous and nontuberculous *mycobacterium* species in smears of *mycobacterium* cultures. *J Clin Microbiol* 37: 2760-2765
- Stetter K.O.** (1989) Extremely thermophilic chemolithoautotrophic Archaeobacteria. In: *Autotrophic Bacteria*. Eds. Schlegel H.G. and Bowien H.G., Science Technical Publications, Madison, WI: 167-176
- Stetter K.O.** (1996) Hyperthermophilic prokaryotes. *FEMS Microbiol Rev* 18: 149-158
- Stetter K.O.** (1999a) Extremophiles and their adaptation to hot environments. *FEBS Letters* 452: 22-25
- Stetter K.O.** (1999b) Hyperthermophiles: isolation, classification, and properties. In: *Extremophiles. Microbial life in extreme environments*. Eds. Horikoshi K. and Grant W.D., Wiley & Sons, Inc., New York
- Stevenson B.S., Eichorst S.A., Wertz J.T., Schmidt T.M. & Breznak J.A.** (2004) New strategies for cultivation and detection of previously uncultured microbes. *Appl Environ Microbiol* 70: 4748-4755
- Stumm W. & Morgan J.J.** (1981) *Aquatic chemistry: an Introduction emphasizing chemical equilibria in natural waters*, Wiley. New York, USA
- Su X.L. & Li Y.** (2004) Quantum dot biolabeling coupled with immunomagnetic separation for detection of *Escherichia coli* O157:H7. *Anal Chem* 76: 4806-4810
- Sugita M. & Tenjin Y.** (1993) The application of confocal laser scanning microscopy (CLSM) in cell biology. *Nippon Rinsho* 51: 1108-1113
- Sukhanova A., Devy J., Venteo L., Kaplan H., Artemyev M., Oleinikov V., Klinov D., Pluot M., Cohen J.H. & Nabiev I.** (2004) Biocompatible fluorescent nanocrystals for immunolabeling of membrane proteins and cells. *Anal Biochem* 324: 60-67
- Sunna A. & Bergquist P.L.** (2003) A gene encoding a novel extremely thermostable 1,4-beta-xylanase isolated directly from an environmental DNA sample. *Extremophiles* 7: 63-70
- Suzuki M.T. & Giovannoni S.J.** (1996) Bias caused by template annealing in the amplification of mixtures of 16S rRNA genes by PCR. *Appl Environ Microbiol* 62: 625-630
- Suzuki M.T., Rappé M.S., Haimberger Z.W., Winfield H., Adair N., Ströbel J. & Giovannoni S.J.** (1997) Bacterial diversity among small-unit rRNA gene clones and cellular isolates from the same seawater sample. *Appl Environ Microbiol* 63: 983-989
- Svenning M.M., Warttinen I., Hestnes A.G. & Binnerup S.J.** (2003) Isolation of methane oxidising bacteria from soil by use of a soil substrate membrane system. *FEMS Microbiol Ecol* 44: 347-354

Symonds R.B., Rose W.I., Bluth G. & Gerlach T.M. (1994) Volcanic gas studies: methods, results, and applications. In: *Volatiles in magmas: Mineralogical society of America reviews in mineralogy*. Eds. Carroll M.R. and Holloway J.R.: 1-66

Takai K. & Horikoshi K. (1999) Genetic diversity of archaea in deep-sea hydrothermal vent environments. *Genetics* 152: 1285-1297

Takai K., Inagaki F., Nakagawa S., Hirayama H., Numoura T., Sako Y., Nealson K.H. & Horikoshi K. (2003) Isolation and phylogenetic diversity of members of previously uncultivated Proteobacteria in deep-sea hydrothermal fields. *FEMS Microbiol Lett* 218: 167-174

Tanner M.A., Goebel B.M., Dojka M.A. & Pace N.R. (1998) Specific ribosomal DNA sequences from diverse environmental settings correlate with experimental contaminants. *Appl Environ Microbiol* 64: 3110-3113

Taylor C.B. (1951) Nature of the factor in soil-extract responsible for bacterial growth-stimulation. *Nature* 168: 115-116

Taylor J.D., Briley D., Nguyen Q., Long K., Iannone M.A., Li M.S., Ye F., Afshari A., Lai E., Wagner M., Chen J. & Weiner M.P. (2001) Flow cytometric platform for high-throughput single nucleotide polymorphism analysis. *Biotechniques* 30: 661-666, 668-669

Taylor J.R., Fang M.M. & Nie S. (2000) Probing specific sequences in single DNA molecules with bioconjugated fluorescent nanoparticles. *Anal Chem* 72: 1979-1986

Temple K.L. & Colmer A.R. (1951) The autotrophic oxidation of iron by a new bacterium, *thiobacillus ferrooxidans*. *J Bacteriol* 62: 605-611

Thompson J.D., Gibson T.J., Plewniak F., Jeanmougin F. & Higgins D.G. (1997) The CLUSTAL_X windows interface: flexible strategies for multiple sequence alignment aided by quality analysis tools. *Nucleic Acids Res* 25: 4876-4882

Thompson J.D., Higgins D.G. & Gibson T.J. (1994) CLUSTAL W: improving the sensitivity of progressive multiple sequence alignment through sequence weighting, position-specific gap penalties and weight matrix choice. *Nucleic Acids Res* 22: 4673-4680

Tillett D. & Neilan B.A. (2000) Xanthogenate nucleic acid isolation from cultured and environmental cyanobacteria. *J Phycol* 35: 1-8

Tonti D., Mourik F.v. & Chergui M. (2004) On the excitation wavelength dependence of the luminescence yield of colloid CdSe quantum dots. *Nano Lett* 4: 2483-2487

Trask B., van den Engh G., Landegent J., Wal N.J. & van der Ploeg M. (1985) Detection of DNA sequences in nuclei in suspension by in situ hybridization and dual beam flow cytometry. *Science* 230: 1401-1403

Trask B., van den Engh G., Pinkel D., Mullikin J., Waldman F., van Dekken H. & Gray J. (1988) Fluorescence *in situ* hybridization to interphase cell nuclei in suspension allows flow cytometric analysis of chromosome content and microscopic analysis of nuclear organization. *Hum Genet* 78: 251-259

Tringe S.G., von Mering C., Kobayashi A., Salamov A.A., Chen K., Chang H.W., Podar M., Short J.M., Mathur E.J., Detter J.C., Bork P., Hugenholtz P. & Rubin E.M. (2005) Comparative metagenomics of microbial communities. *Science* 308: 554-557

- True L.D. & Gao X.** (2007) Quantum dots for molecular pathology: their time has arrived. *J Mol Diagn* 9: 7-11
- Tsai S.H., Selvam A. & Yang S.S.** (2007) Microbial diversity of topographical gradient profiles in Fushion forest soils of Taiwan. *Ecol Res* 22: 814-824
- Tully E., Hearty S., Leonard P. & O'Kennedy R.** (2006) The development of rapid fluorescence-based immunoassays, using quantum dot-labelled antibodies for the detection of *Listeria monocytogenes* cell surface proteins. *Int J Biol Macromol* 39: 127-134
- Van Dalen J.P., Ahsmann W.B. & van Duijn P.** (1970) A method for the determination of the molar extinction coefficient of structure-linked chromophores. *Histochem J* 2: 329-342
- Van den Engh G.** (1993) New applications of flow cytometry. *Curr Opin Biotechnol* 4: 63-68
- Van den Engh G. & Stokdijk W.** (1989) Parallel processing data acquisition system for multilaser flow cytometry and cell sorting. *Cytometry* 10: 282-293
- Vargas M., Kashefi K., Blunt-Harris E.L. & Lovley D.R.** (1998) Microbiological evidence for Fe(III) reduction on early Earth. *Nature* 395: 65-67
- Veal D.A., Deere D., Ferrari B., Piper J. & Attfield P.V.** (2000) Fluorescence staining and flow cytometry for monitoring microbial cells. *J Immunol Methods* 243: 191-210
- Ventosa A. & Nieto J.J.** (1995) Biotechnological applications and potentialities of halophilic microorganisms. *World J Microbiol Biotechnol* 11: 85-94
- Vives-Rego J., Lebaron P. & Caron G.N.-v.** (2000) Current and future applications of flow cytometry in aquatic microbiology. *FEMS Microbiol Rev* 24: 429-448
- Wagner M., Horn M. & Daims H.** (2003) Fluorescence *in situ* hybridisation for the identification and characterisation of prokaryotes. *Curr Opin Microbiol* 6: 302-309
- Wagner M., Roger A.J., Flax J.L., Brusseau G.A. & Stahl D.A.** (1998) Phylogeny of dissimilatory sulfite reductases supports an early origin of sulfate respiration. *J Bacteriol* 180: 2975-2982
- Walter M.R.** (1983) Archean stromatolite: Evidence of the Earth's earliest benthos. In: *The earth's earliest biosphere: Its origin and evolution*. Ed. Schopf J.W., Princeton, Princeton University Press: 187-213
- Walter M.R. & Des Marais D.J.** (1993) Preservation of biological information in thermal spring deposits: developing a strategy for the search for fossil life on Mars. *Icarus* 101: 129-143
- Wallner G., Amann R. & Beisker W.** (1993) Optimizing fluorescent *in situ* hybridization with rRNA-targeted oligonucleotide probes for flow cytometric identification of microorganisms. *Cytometry* 14: 136-143
- Wallner G., Erhart R. & Amann R.** (1995) Flow cytometric analysis of activated sludge with rRNA-targeted probes. *Appl Environ Microbiol* 61: 1859-1866
- Wang H.Q., Li Y.Q., Wang J.H., Xu Q., Li X.Q. & Zhao Y.D.** (2008) Influence of quantum dot's quantum yield to chemiluminescent resonance energy transfer. *Anal Chem Acta* 610: 68-73
- Wang H.Q., Liu T.C., Cao Y.C., Huang Z.L., Wang J.H., Li X.Q. & Zhao Y.D.** (2006) A flow cytometric assay technology based on quantum dots-encoded beads. *Anal Chim Acta* 580: 18-23

- Wang J. & Gao L.** (1999) Adsorption of polyethylenimine on nanosized zirconia particles in aqueous suspensions. *J Colloid Interface Sci* 216: 436-439
- Wang J., Jiang M., Nilsen T.W. & Getts R.** (1998) Dendritic nucleic acid probes for DNA biosensors. *J Am Chem Soc* 120: 8281-8282
- Wang L., Gaigalas A.K., Abbasi F., Marti G.E., Vogt R.F. & Schwartz A.** (2002) Quantitating fluorescence intensity from fluorophores: Practical use of MESF values. *J Res Natl tand Technol* 107: 339-353
- Ward D.M., Weller R. & Bateson M.M.** (1990a) 16S rRNA sequences reveal numerous uncultured microorganisms in a natural community. *Nature* 344: 63-65
- Ward D.M., Weller R. & Bateson M.M.** (1990b) 16S rRNA sequences reveal uncultured inhabitants of a well-studied thermal community. *FEMS Microbiol Rev* 6: 105-115
- Wardell L.J., Kyle P.R., Dumbar N. & Christenson B.** (2001) White Island volcano, New Zealand: carbon dioxide and sulfur dioxide emission rates and melt inclusion studies. *Chem Geol* 177: 187-200
- Watnick P. & Kolter R.** (2000) Biofilm, city of microbes. *J Bacteriol* 182: 2675-2679
- Weng J. & Ren J.** (2006) Luminescent quantum dots: a very attractive and promising tool in biomedicine. *Curr Med Chem* 13: 897-909
- Weng J., Song X., Li L., Qian H., Chen K., Xu X., Cao C. & Ren J.** (2006) Highly luminescent CdTe quantum dots prepared in aqueous phase as an alternative fluorescent probe for cell imaging. *Talanta* 70: 397-402
- West J.L. & Halas N.J.** (2003) Engineered nanomaterials for biophotonics applications: improving sensing, imaging, and therapeutics. *Annu Rev Biomed Eng* 5: 285-292
- White D.E., Muffler L.J.P. & Truesdell A.H.** (1971) Vapour-dominated hydrothermal systems compared with hot-water systems. *Econ Geol* 66: 75-97
- Whitman W.B., Coleman D.C. & Wiebe W.J.** (1998) Prokaryotes: the unseen majority. *Proc Natl Acad Sci USA* 95: 6578-6583
- Wichlacz P.L., Unz R.F. & Langworthy T.A.** (1986) *Acidiphilium angustum* sp. nov., *Acidiphilium facilis* sp. nov., and *Acidiphilium rubrum* sp. nov.; acidophilic heterotrophic bacteria from acidic coal mine drainage. *Int J Syst Bacteriol* 36: 197-201
- Williard D.M., Carillo L.L., Jung J. & Orden A.V.** (2001) CdSe-ZnS quantum dots as resonance energy transfer donors in a model protein-protein binding assay. *Nano Lett* 1: 469-474
- Wisotzkey J., Jurtshuk P., Fox G., Deinhard G. & Poralla K.** (1992) Comparative sequence analyses on the 16S rRNA (rDNA) of *Bacillus acidocaldarius*, *Bacillus acidoterrestris*, and *Bacillus cycloheptanicus* and proposal for creation of a new genus, *Alicyclobacillus* gen. nov. *Int J Syst Evol Microbiol* 42: 263-269
- Woese C.R. & Fox G.E.** (1977) Phylogenetic structure of the prokaryotic domain: the primary kingdoms. *Proc Natl Acad Sci USA* 74: 5088-5090
- Woese C.R.** (1987) Bacterial evolution. *Microbiol Rev* 51: 221-271
- Woese C.R.** (1998) The universal ancestor. *PNAS* 95: 6854-6859
- Woese C.R.** (2002) On the evolution of cells. *PNAS* 99: 8742-8747

- Woese C.R., Kandler O. & Wheelis M.L.** (1990) Towards a natural system of organisms: proposal for the domains Archaea, Bacteria, and Eucarya. *Proc Natl Acad Sci USA* 87: 4576-4579
- Wood J.C.S.** (1998) Fundamental flow cytometer properties governing sensitivity and resolution. *Cytometry* 33: 260-266
- Wu X., Liu H., Liu J., Haley K.N., Treadway J.A., Larson J.P., Ge N., Peale F. & Bruchez M.** (2003) Immunofluorescent labeling of cancer marker Her2 and other cellular targets with semiconductor quantum dots. *Nat Biotechnol* 21: 41-46
- Wu Y., Campos S.K., Lopez G.P., Ozbun M.A., Sklar L.A. & Buranda T.** (2007a) The development of quantum dot calibration beads and quantitative multicolor bioassays in flow cytometry and microscopy. *Anal Biochem* 364: 180-192
- Wu Y., Lopez G.P., Sklar L.A. & Buranda T.** (2007b) Spectroscopic characterization of streptavidin functionalized quantum dots. *Anal Biochem* 364: 193-203
- Xiao Y. & Barker P.E.** (2004) Semiconductor nanocrystal probes for human metaphase chromosomes. *Nucleic Acids Res* 32: e28
- Xu H., Sha M.Y., Wong E.Y., Uphoff J., Xu Y., Treadway J.A., Truong A., O'Brien E., Asquith S., Stubbins M., Spurr N.K., Lai E.H. & Mahoney W.** (2003) Multiplex SNP genotyping using the Qbead™ system: a quantum dot-encoded microsphere-based assay. *Nucleic Acids Res* 31
- Yamamoto S., Manabe N., Fujioka K., Hoshino A. & Yamamoto K.** (2007) Visualizing vitreous using quantum dots as imaging agents. *IEEE Trans Nanobio* 6: 94-98
- Yang H., Holloway P.H. & Santra S.** (2004) Water-soluble silica-overcoated CdS:Mn/ZnS semiconductor quantum dots. *J Chem Phys* 121: 7421-7426
- Yang L. & Li Y.** (2005) Quantum dots as fluorescent labels for quantitative detection of *Salmonella typhimurium* in chicken carcass wash water. *J Food Prot* 68: 1241-1245
- Yang L. & Li Y.** (2006) Simultaneous detection of *Escherichia coli* O157:H7 and *Salmonella typhimurium* using quantum dots as fluorescence labels. *Analyst* 131: 394-401
- Yokota A., Fujii T. & Goto K.** (2007) *Alicyclobacillus, thermophilic acidophilic bacilli*, Springer, Berlin Heidelberg
- Yu D., Wang Z., Liu Y., Jin L., Cheng Y., Zhou J. & Cao S.** (2007) Quantum dot-based pH probe for quick study of enzyme reaction kinetics. *Enzyme Mol Technol* 41: 127-132
- Zengler K., Toledo G., Rappé M., Elkins J., Mathur E.J., Short J.M. & Keller M.** (2002) Cultivating the uncultured. *PNAS* 99: 15681-15686
- Zhang C.Y., Yeh H.C., Kuroki M.T. & Wang T.H.** (2005) Single-quantum-dot-based DNA nanosensor. *Nat Mater* 4: 826-831
- Zhang H., Zhou Z., Yang B. & Gao M.Y.** (2003) The influence of carboxyl groups on the photoluminescence of mercaptocarboxylic acid-stabilized CdTe nanoparticles. *J Phys Chem B* 107: 8-13
- Zhang L.W., Yu W.W., Colvin V.L. & Monteiro-Riviere N.A.** (2008) Biological interactions of quantum dot nanoparticles in skin and in human epidermal keratinocytes. *Toxicol Appl Pharmacol* in press

- Zhang Y., Kaji N., Tokeshi M. & Baba Y.** (2007) Nanobiotechnology: quantum dots in bioimaging. *Expert Rev Proteomics* 4: 565-572
- Zhelev Z., Jose R., Nagase T., Ohba H., Bakalova R., Ishikawa M. & Baba Y.** (2004) Enhancement of the photoluminescence of CdSe quantum dots during long-term UV-irradiation: privilege or fault in life science research? *J Photochem Photobiol B* 75: 99-105
- Zhong W. & Cai Z.** (2004) Methods for studying soil microbial diversity. *Ying Yong Sheng Tai Xue Bao* 15: 899-904
- Zhou D., Piper J.D., Abell C., Klenerman D., Kang D.J. & Ying L.** (2005) Fluorescence resonance energy transfer between a quantum dot donor and a dye acceptor attached to DNA. *Chem Commun (Camb)*: 4807-4809
- Zhou Z., Pons M.N., Raskin L. & Zilles J.L.** (2007) Automated image analysis for quantitative fluorescence in situ hybridization with environmental samples. *Appl Environ Microbiol* 73: 2956-2962
- Zhu L., Ang S. & Liu W.-T.** (2004) Quantum dots as a novel immunofluorescent detection system for *Cryptosporidium parvum* and *Giardia lamblia*. *Appl Environ Microbiol* 70: 597-598
- Zimmermann J., Ludwig W. & Schleifer K.H.** (2001) DNA polynucleotide probes generated from representatives of the genus *Acinetobacter* and their application in fluorescence *in situ* hybridization of environmental samples. *Syst Appl Microbiol* 24: 238-244
- Zuckerandl E. & Pauling L.** (1965) Molecules as documents of evolutionary history. *J Theoret Biol*: 357-366
- Zwirgmaier K.** (2005) Fluorescence *in situ* hybridisation (FISH)-the next generation. *FEMS Microbiol Lett* 246: 151-158